CHARACTERISING THE ROLE OF TRIM16 IN DIFFERENTIATION, PROLIFERATION AND TUMOUR DEVELOPMENT IN NEUROBLASTOMA

By Jessica Lilian Bell

This thesis is submitted in fulfilment of the requirements for the degree of Doctor of Philosophy at the University of New South Wales

Children's Cancer Institute Australia for Medical Research

School of Women's and Children's Health, Faculty of Medicine

University of New South Wales

Australia

2012

ORIGINALITY STATEMENT

'I hereby declare that this submission is my own work and to the best of my knowledge it contains no materials previously published or written by another person, or substantial proportions of material which have been accepted for the award of any other degree or diploma at UNSW or any other educational institution, except where due acknowledgement is made in the thesis. Any contribution made to the research by others, with whom I have worked at UNSW or elsewhere, is explicitly acknowledged in the thesis. I also declare that the intellectual content of this thesis is the product of my own work, except to the extent that assistance from others in the project's design and conception or in style, presentation and linguistic expression is acknowledged.'

Signed ..... Jessica Bell .....

Date ..... 12th January 2012 .....

This thesis is dedicated to my loving parents Geoffrey and Lisa Bell

CONTENTS

LIST OF TABLES

LIST OF FIGURES

ABSTRACT

Neuroblastoma is the most common solid tumour in childhood and represents a significant 15% of all cancer deaths in children. Retinoids are used in the conventional treatment of several human cancers, including neuroblastoma. Retinoids are essential for normal differentiation processes, and can induce terminal differentiation of cancer cells with minimal side-effects. TRIM16, a member of the RING B-box coiled-coil (RBCC)/Tripartite Motif (TRIM) protein family, is a positive transcriptional regulator of the retinoid anti-cancer signal. This characteristic led to the hypothesis that TRIM16 regulates cell proliferation and differentiation in neuroblastoma. This thesis examines TRIM16's role in neuroblastoma proliferation and tumour development, and also investigates the function of TRIM16's putative protein domains.

TRIM16 overexpression was shown to decrease neuroblastoma proliferation *in vitro.* Significantly, overexpression of TRIM16 in a neuroblastoma xenograft mouse model also decreased tumour growth. Additionally, overexpression of TRIM16 enhanced retinoid-induced differentiation *in vitro*. This indicated a role of TRIM16 in neuroblastoma cell differentiation. Immunohistochemical staining in a transgenic neuroblastoma mouse model revealed that tumour cells have weak cytoplasmic TRIM16 expression compared with strong nuclear TRIM16 staining in newly differentiated ganglia cells. Furthermore, *in vitro*, immunofluorescence studies showed that strong nuclear expression of TRIM16 is also seen during the G1 cell cycle phase of synchronised neuroblastoma cells. Significantly, knockdown of TRIM16 affected several G1 cell cycle phase regulatory proteins including downregulation of p27 and Cyclin D1. Furthermore, domain deletion mutants demonstrated that TRIM16's B-boxes were required for *in vivo* ubiquitin binding and its coiled-coil domain conferred TRIM16 homodimerisation ability. Moreover, TRIM16 also heterodimerised with other

TRIM proteins; MID1, PML and TRIM24. Most importantly, both TRIM16's nuclear localisation and growth inhibition traits were attributed to a region linking the coiled-coil and B30.2 domains of TRIM16.

Taken together, this research strongly indicates that nuclear localisation of the TRIM16 protein is required for its role in neuroblastoma proliferation and differentiation. Furthermore, this study provides compelling evidence that TRIM16 is a novel regulator of differentiation and proliferation in neuroblastoma and is a potential tumour suppressor.

ABBREVIATIONS

4-HPR	Fenretinide
AA	Amino acid
Ab	Antibody
AP	Aphidicolin
APL	Acute promyelocytic leukaemia
ATP	Adenosine 5’-triphosphate
ATDC	Ataxia telangiectasia group D-complementing/TRIM29
B1	B-box1 protein domain
B30.2	B30.2/SPRY or RFP protein domain
bHLH	Basic-helix-loop-helix DNA binding protein
BrdU	5-bromo-2'-deoxyuridine
bp	Base pairs
cAMP	Cyclic AMP
CC	Coiled-coil protein domain
CD2	Cluster of differentiation 2
CDK	Cyclin-dependent kinase
cDNA	Complementary deoxyribonucleic acid
CHX	Cycloheximide
COG	Children Oncology Group
CRA	13-*cis*-retinioc acid
CRABP	Cellular retinol binding protein
d	Day
DAB	3,3-diaminobenzidine
DAPI	4,6-diamidino-2-phenylindole
DMEM	Dulbecco’s modified eagle’s medium
DNA	Deoxyribonucleic acid
dNTP	Deoxynucleoside triphosphate
DTT	1,4-Dithiothreitol
EBBP	Estrogen-responsive B-box protein/TRIM16
EFP	Estrogen-responsive finger protein/TRIM25
EGF	Epidermal growth factor
ELISA	Enzyme-linked immunosorbent assay
ERK	Extracellular signal-regulated kinase
EV	Empty vector
FGF	Fibroblast growth factor
G418	Geneticin
GD2	Chimeric anti-disialoganglioside
GFP	Green fluorescence protein
g_n	Standard gravity/g-force
h	Hour
HA	Human influenza haemagglutinin protein tag
HDAC	Histone deacetylase
IHC	Immunohistochemistry

IL-2	Interleukin-2
INRGSS	The International Neuroblastoma Risk Group Staging System
Kb	Kilobase
KDa	Kilodalton
LB	Luria broth
MG132	N-(benzyloxycarbonyl)leucinylleucinylleucinalZ-Leu-Leu-Leu-al
MIBG	^{131}I-metaiodobenylguanidine
MID1	Midline-1/TRIM18
miRNA	MicroRNA
mRNA	Messenger RNA
NES	Nuclear export signal
NGF	Nerve growth factor
NLS	Nuclear localisation signal
NRBM	Nuclear receptor binding motif
N.S.	Not significant
NZ	Nocodazole
PBS	Phosphate buffered saline
PML	Promyelocytic leukaemia gene/protein
pRb	Retinoblastoma tumour suppressor protein
RA	All-*trans*-retinoic acid
RAR	Retinoic acid receptor
RARβ	Retinoic acid receptor beta
RARE	Retinoid acid response element
RET	Rearranged during transfection
RFP	RET finger protein/TRIM27
RING	Really interesting new gene protein domain
RNA	Ribonucleic acid
RT-PCR	Reverse transcriptase polymerase chain reaction
SAHA	Vorinostat (rINN) or suberoylanilide hydroxamic acid
STAT	Signal transducer and activator of transcription
TBST	Tris-Buffered Saline with 0.5% Tween20
TGF-β	Transforming growth factor beta
TH	Tyrosine hydroxylase
TRIM	Tripartite motif
TRK/Trk	Tyrosine kinase receptor
Ub	Ubiquitin
wt	Wildtype
α	Alpha/anti-
β2M	Beta-2-microglobulin

PUBLICATIONS AND PRESENTATIONS

The following publications have arisen from this thesis:

Jessica L. Bell, Alena Malyukova, Maria Kavallaris, Glenn M. Marshall, Belamy B. Cheung. The linker domain of TRIM16 is required for its nuclear localisation in neuroblastoma. *Manuscript in preparation*

Jessica L. Bell*, Alena Malyukova*, Jessica K. Holien, Jessica Koach Michael W. Parker, Maria Kavallaris, Glenn M. Marshall & Belamy B. Cheung. TRIM16 acts as an E3 ubiquitin ligase and can heterodimerize with other TRIM family Members. ***Plos One*** 7: e37470 ** denotes shared first authorship*

Cheung BB, Koach J, Tan O, Kim P, **Bell JL**, D'andreti C, Sutton S, Malyukova A, Sekyere E, Norris M, Haber M, Kavallaris M, Cunningham AM, Proby C, Leigh I, Wilmott JS, Cooper CL, Halliday GM, Scolyer RA, Marshall GM. The retinoid signalling molecule, TRIM16, is repressed during squamous cell carcinoma skin carcinogenesis in vivo and reduces skin cancer cell migration in vitro. ***The Journal of Pathology***. 2012 Feb;226(3):451-62.

Glenn M. Marshall, **Jessica L. Bell**, Jessica Koach, Owen Tan, Patrick Kim, Alena Malyukova, Wayne Thomas, Eric O. Sekyere, Tao Liu, Anne M. Cunningham, Vivienne Tobias, Murray D. Norris, Michelle Haber, Maria Kavallaris and Belamy B. Cheung. TRIM16 acts as a tumour suppressor by inhibitory effects on cytoplasmic vimentin and nuclear E2F1 in neuroblastoma cells. ***Oncogene***. 2010 29, 6172–6183.

Anna Raif, Glenn M. Marshall, **Jessica L Bell**, Jessica Koach, Owen Tan, Wayne Thomas, Eric Sekyere, Murray Norris, Michelle Haber, Maria Kavallaris and Belamy B Cheung. The estrogen-responsive B box protein (EBBP) restores retinoid sensitivity in retinoid-resistant cancer cells via effects on histone acetylation. ***Cancer Letters.*** 2009; 277: 82–90.

J.L. Bell, B.B. Cheung, C. D'Andreti, J. Koach, A. Raif, W.D. Thomas, M. Norris, M. Haber, M. Kavallaris and G.M. Marshall. The role of the estrogen-responsive B box protein (EBBP) in cancer. ***European Journal of Cancer Supplements.*** Volume 6, Issue 9, July 2008, Page 95 *Abstract only*

The following conference presentations have arisen from this thesis:

Jessica L. Bell, Alena Malyukova, Maria Kavallaris, Glenn M. Marshall and Belamy B. Cheung. TRIM16 has a role in neuroblastoma differentiation and proliferation via dynamic nuclear localization**. Seeing is Believing, Heidelberg, GERMANY 2011**

Jessica L. Bell, Alena Malyukova, Maria Kavallaris, Glenn M. Marshall and Belamy B. Cheung. TRIM16 has a role in neuroblastoma differentiation and proliferation via dynamic nuclear localization. **Lorne Cancer Conference, Victoria, 2011**

Jessica L. Bell, Alena Malyukova, Maria Kavallaris, Glenn M. Marshall and Belamy B. Cheung. TRIM16 has a role in neuroblastoma differentiation and proliferation via dynamic nuclear localization. **Tow Prize 2010. Sydney, ORAL PRESENTATION**

Jessica L. Bell, Glenn M. Marshall, Maria Kavallaris and Belamy B. Cheung The estrogen-responsive B box protein (EBBP/TRIM16) has a role in both differentiation and tumorigenicity in neuroblastoma. **ASMR NSW, Sydney, 2010**.

Jessica L. Bell, Maria Kavallaris, Glenn M. Marshall and Belamy B. Cheung. The estrogen-responsive B box protein (EBBP/TRIM16) is a novel regulator of differentiation and tumorigenicity in neuroblastoma. **Lowy Cancer Symposium, Sydney, 2010**

Jessica L. Bell, Belamy B. Cheung, Jessica Koach, Murray Norris, Michelle Haber, Maria Kavallaris, Anne M. Cunningham and Glenn M. Marshall. The estrogen-responsive B box protein (EBBP/TRIM16) is a potential tumour suppressor which modulates vimentin protein in neuroblastoma cancer cells. **ASMR NSW, Sydney, 2009.**

Jessica L. Bell, Belamy B. Cheung, Jessica Koach, Wayne D. Thomas, Eric Sekyere, Murray Norris, Michelle Haber, Maria Kavallaris and Glenn Marshall. The estrogen-responsive B box protein (EBBP/TRIM16) is a novel tumour suppressor and down-regulates MYCN and Vimentin protein expression in human cancer cells**. Lorne Cancer, Victoria, 2009.**

Jessica L. Bell, Belamy B. Cheung, Carla D'Andreti, Jessica Koach, Anna Raif, Wayne D.Thomas, Murray Norris, Michelle Haber, Maria Kavallaris and Glenn M. Marshall. The role of estrogen-responsive B box protein (EBBP) as a tumour suppressor gene. **Faculty of Medicine Poster Day. UNSW, Sydney 2008.**

J.L. Bell, B.B. Cheung, C. D'Andreti, J. Koach, A. Raif, W.D. Thomas, M. Norris, M. Haber, M. Kavallaris and G.M. Marshall. The role of the estrogen-responsive B box protein (EBBP) in cancer. **The European Association for Cancer Research 20th Meeting. Lyon, FRANCE 2008.**

ACKNOWLEDGMENTS

I wish to thank my supervisors Dr. Belamy Cheung and Prof. Maria Kavallaris for their wisdom and patience throughout my candidature. This thesis would not have been possible without their support and understanding in challenging times. Also, I would like to acknowledge Prof. Glenn Marshall (program head of the Molecular Carcinogenesis Program) who supported and influenced research on TRIM16. I would like to acknowledge the critical funding received from the National Health and Medical Research Council in the form of the Biomedical PhD scholarship (2008-2011).

In my years at CCIA, there have been many that have helped me on my journey. I would like to thank the members of the Molecular Carcinogenesis Program. Particular mention must go to; Andrew Bohlkan, Carla D'Andreti, Tanya Dwarte, Joanna Keating, Jessica Koach, Selena Kuljaka and Alena Malyukova.

I would also like to thank other staff members of CCIA: animal house personnel, Scientific Services team, IT team and my after-hours companions. Also, Jayne Murray and Sela Po'uha for specialised training, advice and their extensive knowledge. Moira Clay for advice and confidence, and Sarah Meachem for editing and support.

Thanks to all my friends for trivia nights, morning/afternoon teas, postcards from the blue and putting things in perspective. Also, to Maximilian Elz for hearing about everything, and being patient and supportive.

Finally, a big thanks to my family. To my parents and grandparents, who always fostered my curiosity and independent thinking. My sisters Stephanie and Natalie for sharing de-stressing weekend breakfasts, friendship and support. Nick for his hugs and eternal cuteness.

CHAPTER 1

INTRODUCTION

1.1 Introduction

Neuroblastoma is a disease which represents the most common solid tumour in infants [1]. Even with current treatment regimes, less than 50% of neuroblastoma patients experience long term survival. Although neuroblastoma cell differentiation is not well understood, it is believed to be mediated by changes in the G1 cell cycle phase components [2]. Retinoid compounds are strong differentiating agents which are essential in vertebrate development and homeostasis [3]. Retinoids can also induce differentiation of neuroblastoma cells via G1 cell cycle phase arrest [4,5]. Importantly, retinoids are also exploited clinically and used in minimal residual disease neuroblastoma as differentiation therapy, aiming to curb inappropriate cancer cell division through cell maturation [6,7].

In 2006, our research group identified the scantly studied gene, tripartite motif 16 (TRIM16), as a positive transcriptional regulator of the retinoic acid receptor β gene (RARβ) [8]. RARβ is a tumour suppressor in neuroblastoma, and is also a key component of the retinoid differentiation signal, which is currently utilised in anti-cancer therapies [3]. Importantly, TRIM16 is a member of a large protein family, which has established roles in cancer, differentiation and cell cycle regulation, among other attributes [9]. Due to the nature of TRIM16's interaction with the RARβ gene and its structural similarity to other tumour suppressor genes, I undertook research to address TRIM16's role in neuroblastoma cell proliferation, differentiation and tumorigenicity.

This chapter will firstly review the current literature on neuroblastoma tumorigenesis. Secondly, the factors involved in retinoid-induced differentiation will be discussed. Finally, the retinoid pathway enhancer, TRIM16 will be discussed within the context of its more widely studied TRIM protein family members.

1.2 Childhood neuroblastoma

Neuroblastoma is an embryonal malignancy, usually arising from neuroblast cells of the adrenal medulla [1,10-13]. At the time of diagnosis, approximately half of patients have highly aggressive disease, with tumours growing rapidly and forming metastasis to the bone, liver, skin and/or lymph tissue. The prognosis for such patients is poor. Even with advances in current treatments, only about half of such cases achieve long-term survival. More importantly, however, the enigma of neuroblastoma is the high rate of natural spontaneous regression of the disease without treatment [12,14]

1.2.1 Incidence and aetiology

Neuroblastoma is the most common extra-cranial solid tumour in infancy, accounting for up to 10% of all childhood cancers and a significant 15% of all childhood cancer deaths [10,12]. In New South Wales, Australia, the incidence of neuroblastoma is 2 cases per 100,000 live births [15]. This is comparable to other regions such as Europe and The United States of America. However, in Japan after mass screening of urine for catecholamine metabolites (a significant marker of neuroblastoma disease) was introduced the country's rate of diagnosis almost doubled [16,17]. This strongly supports the presence of 'in situ' neuroblastoma in infants, a phenomenon first described in 1963 by Beckwith and Perrin [18]. Beckwith and Perrin observed a 40 times higher incidence of neuroblastoma in developing embryos than quantified in the live birth rate incidence. It is probable that mass screening of urine, identifies individuals who will not go on to develop clinical disease. Moreover, it suggests that neuroblastoma develops as a result of a failure for the induction of specific developmental controls and programed cell death in neuronal cells, however, the mechanisms of the process of cell regression or pathological persistence remain unclear.

With ‘in situ’ neuroblastoma in mind, it is relevant to note that the incidence of neuroblastoma is weighted towards infants in their first year of life, which constitute 40% of diagnoses [10]. The median age of diagnosis is only 18 months, with, 75% of cases diagnosed before 5 years of age and 98% before 10 years of age. Generally, younger patients have a better prognosis depending on other known risk factors.

There is a small subset of patients with an inherited predisposition to neuroblastoma [19]. Their disease is typically characterised by multi-focal primary tumours, diagnosed at an early age. This heritability has been mapped to the short arm of chromosome 16. The majority of neuroblastoma cases are considered sporadic and are also unaffected by environmental factors [20]. That being stated, the lack of information as to the cause of neuroblastoma leaves open the possibility that the current philosophy could be tested with future approaches and improved research technologies.

1.2.2 Clinical presentation and disease stage

Neuroblastoma displays extremely different clinical phenotypes [10,21,22]. Neuroblastoma arises from sympathetic nerve cells and thus tumours initially develop within components of the sympathetic nervous system. Two thirds of cases develop in the abdomen (of these 40% arise in the adrenal gland), 25% in the abdominal sympathetic ganglion, 15% in the ganglia of the thorax, 5% in the cervical region and 5% in the pelvis. Symptoms of neuroblastoma include weight loss, fever, bruising, bone pain, lumps in the abdomen, neck, or chest, and bulging eyes or dark circles around the eyes. Obviously, the site of the primary tumour and presence of metastases will influence the compression and pathology of surrounding tissues. Metastasis of neuroblastoma involves the bone marrow in 56% of cases [23].

Ultrasound, x-ray, magnetic resonance imaging and radiolabeled meta-iodobenzylguanidine are some of the methods used to diagnose and characterise the extent of neuroblastoma disease [24] Tumour excision, biopsy and bone marrow aspiration all allow for staging of the tumour. Immunohistochemistry studies are used by pathologists to confirm the neural origin of the tumour, using cell morphology and tissue structure [25]. Neuroblastoma is generally heterogeneous tissue containing microscopic foci of small cells with dense hyperchromatic nuclei (neuroblasts), areas of eosinophic material and stroma. Protein markers such as vimentin, neuron-specific enolase and S100 are used to distinguish neuroblastoma from other tumour types of similar morphology.

The clinical stage of neuroblastoma at diagnosis is critical in the prediction of patient outcome and will determine the mode of treatment the patient will receive. Various classifying systems have evolved with increased knowledge of neuroblastoma. One of the first staging systems was developed by Evans in 1971 [26]. This system defined the importance of tumours across the midline of the patient (IVS group) and of metastatic/advanced disease. Shimada introduced the use of a combination of age at diagnosis and histology [25]. Histology was used to classify patients according to the degree of cellular differentiation, cell division, degeneration of nuclei and proportion of stroma cells. This staging was followed by the Paediatric Oncology Group (as described by Hayes in 1983) and other protocols [27,28]. The International Neuroblastoma Staging System (INSS) was established to produce a system that was uniform and allowed for better comparison of research studies and protocols, and ultimately benefit patients [27,29]. This classification system used tumour stage, age, MYCN gene amplification status, Shimada histopathology and DNA ploidy to determine the patient's risk group and treatment. This system had 5 stages (1, 2A, 2B, 3, 4, 4S) with stage 4

being the most high-risk for patients. The INSS, although a major improvement to neuroblastoma management, was ultimately a postsurgical staging system, which carried a major disadvantage for a disease where a proportion of patients do not undergo surgery.

Recently, a new system, called The International Neuroblastoma Risk Group Staging System (INRGSS) has been successfully trialled and will shortly (if not already) be adopted internationally, based on clinical criteria and image-defined risk factors (IDRFs) which can be used prior to surgery [30]. A brief summary of the new staging system is presented in Table 1.1. Stage L1 is in the low risk grouping, with a localised tumour, while L2 has an intermediate risk and Stage M has a high risk, involving distant metastasis. Alternatively, MS usually has a favourable outcome. In typical MS neuroblastoma, rapid tumour proliferation suddenly stops and starts to regress spontaneously. Recommendations on treatment are not part of this publication, as this policy aims to produce a defined system globally and thus allow proper evaluation and comparison of treatment regimes.

Table 1.1 The International Neuroblastoma Risk Group Staging System

Adapted from Monclair, Brodeur et al. 2009 [30].

Stage	Description	Risk
L1	Localised tumour not involving vital structures as defined by the list of image-defined risk factors and confined to one body compartment	Low
L2	Locoregional tumour with presence of one or more image-defined risk factors	Intermediate
M	Distant metastatic disease (except stage MS)	High
MS	Metastatic disease in children younger than 18 months with metastases confined to skin, liver, and/or bone marrow	Low

1.2.3 Biological prognostic indicators

1.2.3.1 MYCN

The significance of the amplification of MYCN in neuroblastoma is made clear by its inclusion in the INSS risk groupings. N-Myc is the protein encoded by the MYCN gene. Several experimental studies demonstrate the independent power of N-Myc to initiate tumorigenesis in primary cells, cell lines, and genetically engineered mice [31-35]. MYCN amplification is not unique to neuroblastoma and can be present in other cancers such as retinoblastoma, Wilm's tumour, glioma, small cell carcinoma and breast cancer [36-39]. Approximately 25% of patients with neuroblastoma exhibit amplification of the MYCN locus, the distal short arm of chromosome 2 (2p24). MYCN amplification is significantly associated with poor prognosis and rapid tumour progression [31]. *In vitro* studies show N-Myc can act to drive unrestricted proliferation [40,41] but also can inhibit differentiation [42]. Alternatively, the loss of N-Myc expression not only inhibits cell growth [43-45], but also accelerates differentiation [46].

N-Myc interacts with many proteins and especially interacts with gene promoters as a transcription factor. For instance, N-Myc regulates the transcriptional expression of MDM2, the inhibitor of p53 and a crucial regulator of cell cycle progression [47], focal adhesion kinase, which regulates cell survival [48], and cellular RA-binding protein II, which functions in cell motility [49]. Thus, N-Myc has the ability to influence the majority of significant cellular processes in neuroblastoma and is involved in disease aggression.

1.2.3.2 Trk Family

Abnormal gene expression of another family of oncogenes can also indicate neuroblastoma outcome. The *trk* gene family are known to influence the behaviour of

neuroblastoma tumours [50,51]. They are specifically expressed in neuronal precursor cells. They regulate cell survival, proliferation, death, invasiveness, angiogenesis genomic stability and differentiation, generally by interaction with nerve growth factor ligands [50-53]. In neuroblastoma, a high level of TrkA protein is associated with a favourable outcome. Interestingly, retinoid treatment, often used in minimal residual disease neuroblastoma, increases TrkA and other related receptors [54]. High TrkA expression is also associated with younger patient age, lower stage of disease and absence of MYCN amplification [55,56]. Additionally, the 4S tumour stage, which often regresses spontaneously, also shows high levels of TrkA. In contrast, TrkB is highly associated with MYCN amplification and poor prognosis [57].

1.2.3.3 Neuroblastoma associated chromosomal genetics

Neuroblastoma has many types of genetic aberrations apart from ploidy and MYCN alterations [10,58]. MYCN amplification is strongly associated with 1p36 deletion and poor outcome, with up to 95% of MYCN amplified tumours having this deletion [58-62]. Occasionally, 1p36 is also deleted in MYCN non-amplified tumours. However, this deletion may indicate progression of a tumour rather than overall survival in patients [63]. There are several genes and microRNAs that make 1p deletion advantageous to Myc driven cancer such as L-myc, Brain Specific Angiogenesis Inhibitor 2, Castor Homolog 1 Zinc finger, Chromodomain Helicase DNA binding protein 5 [59,62,64-66].

Another common genetic abnormality is trisomy 17q, which is associated with both poor and good prognosis [67]. It appears that the 17p13-17q21 region is highly expressed in 4S neuroblastoma, whereas stage 4 tumours acquire 17q21-q25 fragments. Several genes have been identified as having a promoting role in neuroblastoma in the 17q-q25 region. Gene candidates in the gained 17q21-25 region include the anti-

apoptotic protein, Survivin [68], Topoisomerase II [69], nm23-H1 and nm-H2 [70-72]. Recently, a novel non-coding RNA, ncRAN, was significantly associated with poor patient outcome [73].

11q allelic loss is not associated with MYCN amplification but is associated with high-risk disease [59,74,75]. It occurs in 20% of primary tumours and 50% of advanced stage neuroblastoma, when MYCN is not amplified. Chromosomal changes to 11q are late in tumour development and associated with advanced disease and older age. Therefore, 11q status may prove to be a useful predictor of outcome and risk of relapse in the subset of patients without MYCN amplification [76].

1.2.3.4 RNA expression profiles

With improvements in technology, subsets of neuroblastoma are becoming more defined and outperforming historical methods of neuroblastoma risk assessment at predicting clinical outcome. Recent studies (discussed below) have shown that mRNAs and miRNAs have a role in the pathogenesis of various diseases and in cancer relevant cell processes such as proliferation, apoptosis and differentiation. An interesting aspect of this work is the disparity of results, as depending on the platform and analysis, different RNA identifiers are elucidated. Therefore thorough validations need to confirm results gained by this method.

There are several mRNA expression studies in neuroblastoma to date. Schramm *et al.* [77] have been able to achieve a prediction rate of 80% for clinical outcome by analysing 39 mRNAs. In comparison, using the same cohort of patients, conventional risk determination gives only a 64% prediction rate of patient survival. Surprisingly, 32 of the genes have not been previously identified as important in neuroblastoma. MYCN status and TrkA expression did associate with some of the mRNA expressions. Another

more recent study using 933 neuroblastoma samples (significantly more powerful than most studies) was able to identify 42 robust prognostic genes [78]. Not surprisingly, this list contains MYCN, NTRK1, NME1, CADM1, FYN, ODC1, and WSB1. This led to prediction of outcome in over 90% of patients. This vast improvement on extensive previous studies was attributed to the comparison of data from 4 different cross platform studies.

Two recent studies into the miRNA expression profiles in neuroblastoma have demonstrated that miRNA profiling alone is an effective and feasible method of grouping patients [79,80]. MiRNAs can be either oncogenic or tumour suppressive in certain cases [79]. An interesting trend is the global downregulation of miRNAs observed in advanced stage neuroblastoma. Lin and colleagues [79] have identified 27 miRNAs that can clearly distinguish high and low risk clinical groupings. Furthermore, mRNA expression of 2 miRNA processing components Dicer and Drosha also have a significant impact on patient risk with high expression. In fact, a prediction accuracy above 82% was obtained by combining the analysis of both miRNA and mRNA biomarkers. This demonstrates that using a combination of RNA expression types is a powerful prognostic tool in neuroblastoma.

Another study by Schulte et al. [80] used miRNA expression differences alone to predict patient clinical outcome. The analysis of 40 miRNAs produced a significant 89% accurate prediction of clinical outcome. Interestingly, 35 of these miRNAs were differentially expressed depending on MYCN status, with 6 being influenced by TrkA expression. Notably, the MYCN-induced miR92 is downregulated in tumours highly expressing the low risk marker TrkA. For this methodology, it appears the biomarkers used are just another method to quantify the same tumour biologies already identified

by historical protein biomarkers. However, the novel miR545-5p was highlighted as having the highest importance in neuroblastoma outcome, but to date little is known about this miRNA.

Although many of the RNA biomarkers discussed above are independent of conventional risk markers (MYCN status or TrkA expression), many RNAs are still indicative of these historical prognostic factors. The power of these novel RNAs was only highly significant when used within expression profiles and not as independent markers. Follow up research is required to determine the biological significance of these RNAs. Also, further research should determine the robustness of using a particular profile of markers across other patient cohorts and analysis platforms.

1.2.4 Experimental models of neuroblastoma

1.2.4.1 In vitro models

Sufficient *in vitro* and *in vivo* models are required for the development of novel anti-neuroblastoma drugs and for greater understanding of the initiation and development of neuroblastoma. To date, cell culture models using human or mouse cells have been used for pre-clinical validation of drugs as well as facilitating new insights into the initiation and biology of neuroblastoma.

There are many human neuroblastoma cell lines. They vary in morphology and genetic mutations, often reflecting those changes seen in the clinic [81-84]. However, most are derived from the most malignant and aggressive tumours, which correlate with the ability of these cells to be passaged indefinitely *in vitro.* Also, some cell lines have mutations which are unusual in primary neuroblastoma tissues, presumably which assist *in vitro* passaging. For example, the p53 tumour suppressor gene is commonly mutated in neuroblastoma cell lines, but only rarely in the primary tissue [85,86].

Cell lines can be grouped according to their differentiation potential [81-84]. There are 'I' type or intermediate cells (e.g. IMR-32 and BE2C) which can be differentiated towards a Schwann cell or neuronal cell type depending on the differentiation drug. 'I' type cells tend to be more tumorigenic and aggressive, which could be reflective of their neuronal stem cell attributes. 'N' type cells can only be differentiated towards a neuronal phenotype (e.g. SH-SY5Y), typified by neurite outgrowth (which can be quantified as an indicator of differentiation). 'S' type cells, differentiate toward a Schwann cell type (e.g. SHEP). When differentiated, these cells become flatter and longer in morphology. There are also mouse (Neuro-2a) and rat (B104) cell lines derived from spontaneous tumours in animal models. One advantage of using cell lines is that they are relatively easy to maintain, commercially available and can be used for mechanistic *in vitro* work and high through-put screening of drugs. However, cell lines do not facilitate the study of clinically relevant diverse interactions within the host, such as immune response and angiogenesis.

1.2.4.2 In vivo models

Xenograft mouse models allow the use of human derived cell lines in a murine host to test the toxicity and efficacy of treatment regimes [10,87]. Generally, in immuno-compromised mice, cancer cell lines can be grown subcutaneously, allowing easy access for measurements of tumour growth. Cells can also be injected intravenously in an effort to better replicate metastatic disease. This is more relevant to high-risk neuroblastoma, but estimating tumour growth in this model is difficult [88]. Orthotopic xenograft models which inject cells into the adrenal medulla are an attempt to better replicate the disease in humans, as the adrenal gland of the kidneys is involved with the majority of neuroblastoma cases [89,90].

Although xenograft models come closer to the human disease compared with cell lines, animal models of spontaneously arising tumours are arguably closer to clinical disease [33,34,91,92]. One neuroblastoma transgenic mouse model uses the powerful MYCN as a conditionally expressed transgene, under the tyrosine hydroxylase (TH) promoter. This leads to MYCN overexpression in neural crest progenitor cells and subsequent tumour initiation. In these mice, the neuroblastoma tumours are localised to para-spinous ganglia. The resulting tumours stain for neuroblastoma markers; NSE and S100, and contain neuroblasts (small blue round cells) and large ganglia cells, in a similar morphology as seen in human histology. Interestingly, the resulting tumours also have various chromosomal aberrations similar to those documented in human neuroblastoma, further proving the closeness of this animal model to the human disease [33-35]. The fact that MYCN expression alone is sufficient for tumorigenesis again highlights MYCN's role in the initiation and progression of neuroblastoma and that it is not just an indicator of disease status. The major limitation of the TH-MYCN mouse model is that N-Myc is expressed in all cells of the tumour and studies into how non-MYCN driven tumours develop *in vivo* or respond to therapy cannot be accessed. Also, the final stages of disease in the mouse do not follow that seen in human cases [93].

One study using the TH-MYCN mouse model performed by our research group demonstrated that tumours arise from neuroblast hyperplasia cells that persisted in 100% of the MYCN homozygous mice by 6.5 weeks of age [92]. Alternatively, in the wildtype mice, these areas of hyperplasia did not persist to form tumours and instead regressed. This study also highlights that this model can be used to study factors in neuroblastoma development. Significantly, the wildtype hyperplasia regression is reminiscent of the observations by Beckwith and Perrin of '*in situ*' neuroblastoma as discussed above in section 1.2.1 [18].

1.2.5 Neuroblastoma treatments

1.2.5.1 Current treatment approaches

Neuroblastoma treatment is based on the risk grouping as determined by stage and other prognostic factors [7,12,25,29,30]. Low-risk and intermediate-risk have a good probability of being cured, whereas high-risk neuroblastoma may be difficult to cure. Five types of treatment are currently used; surgery, chemotherapy, radiotherapy, biologic/biogenic and observation (recently reviewed in [94,95]).

Low-risk patients are typically observed or have their tumours removed followed by an observation period [96]. In high-risk patients, chemotherapy is the mainstay of treatment. Induction therapy allows the tumour/s to shrink and become avascular, allowing safer removal of the tumour [7]. Then usually over a 21 day period, consolidation chemotherapy eradicates any residual disease. The standard chemotherapeutic agents used in neuroblastoma treatment are cyclophosphamides, vincristine, doxorubicin, cisplatin, carboplatin and etoposide [7,97-99]. Some induction regimes also include isosfamide and topotecan. High dose therapy is often followed by stem cell reinfusion to reconstitute the bone marrow which has been damaged by the therapy [12]. Irradiation therapy can be used to target any remaining primary tumour. Retinoid therapy is given at the end of conventional therapy cycles to treat minimal residual disease [6,7].

The clinical benefits of 13-*cis*-retinoic acid (CRA) treatment was first shown in 1999 in a landmark clinical trial by the Children's Cancer Group, where the drug was used after chemotherapy [7]. Even though some resistance to this therapy is apparent, use of CRA is now part of standard front line therapy. Retinoid therapy exerts growth inhibitory and differentiation effects on the minimal residual disease cells through its

interaction with retinoid receptors (discussed in 1.4). Drug dosage and mass of the tumour have a large effect on the usefulness of retinoids, and currently they are not useful on large tumours [7,100,101].

1.2.5.2 Emerging treatment approaches

A recent study demonstrates that a more defined risk grouping system leads to a more accurate use of intense therapies [102]. In brief, intermediate patients who would normally be given intense treatments, received less intense therapies and were monitored for a clinical response during therapy. The reduction in chemotherapy duration did not lead to a significant decrease in patient survival, but presumably would lead to reduced side effects in these patients. This challenges current protocols and indicates the current staging system and drug protocols need to be re-visited to improve patient long-term outcomes.

The holy grail of neuroblastoma research would be to develop a drug to stimulate regression of disease [94,95]. Given the great need for new neuroblastoma therapies there are several targets and approaches towards the development of new neuroblastoma drugs. A few promising developments are highlighted below.

Immunotherapy is in theory more specific than conventional chemotherapy. To date, the most effective immunotherapy in neuroblastoma is CD2 (cluster of differentiation 2) antibodies. CD2 is expressed in 100% of neuroblastoma cells regardless of age or stage and therefore is a good molecular target [103]. Monoclonal antibodies directed against this molecular target kill tumour cells through both complement and cell-mediated lysis. This process is enhanced by IL-2 and granulocyte-macrophage-colony stimulating factor [104]. Ch14.18 is the next generation of CD2

antibodies with less immunogenic properties. However, this therapy appears to be more appropriate for use with minimal residual disease [105].

Since neuroblastoma tumours are usually radiosensitive, another way to improve treatment is to incorporate ^{131}I-metaiodobenylguanidine (MIBG) [106]. MIBG is selectively taken up by norepinephrine receptors and can be used when the tumour is definable with MIBG scans. This treatment achieves the highest response rate with relapsed neuroblastoma. A European trial has also demonstrated that it can be added to conventional induction therapy [107]. In future, radiosensitisers such as suberoylanilide hydroxamic acid (SAHA) or irinotecan could also be used together with MIBG. Additionally, chimeric anti-disialoganglioside (GD2) antibody 3F8 is an alternative method to effectively deliver radiation to the tumour cells and has been clinically trailed [108,109].

One antimitotic agent that has recently shown huge promise is MLN8237, an Aurora Kinase A inhibitor. In the Paediatric Pre-clinical Testing Program, this drug induced complete response in three of four neuroblastoma models [110]. The *in vivo* activity observed against the neuroblastoma panel far exceeded that observed for standard agents used clinically and supports the expedited clinical development of MLN8237, in childhood cancer. As a consequence of this research, there is a Phase I trial underway.

Biological therapy uses substances that occur naturally in the body as treatments. The retinoid, CRA is well tolerated as a single agent and part of the standard neuroblastoma treatment protocol. [7,100,101]. However, CRA is not potent enough for frontline use and resistance can occur, and therefore its activity can theoretically be improved upon. One particularly promising agent, Fenretinide (4-HPR) is a synthetic

retinoid developed to improve the efficacy of retinoid drugs by increasing neuroblastoma cytotoxicity, in part by increasing intracellular levels of ceramide [111,112]. Retinoids are a prime example of a differentiation therapy approach to cancer treatment [113].

1.2.6 Differentiation Therapy

Differentiation therapy aims to force the cancer cell to resume the process of maturation [114]. Although differentiation therapy does not kill the majority of cancer cells, it inhibits their growth and allows the application of more conventional therapies (such as chemotherapy) to eradicate the malignant cells. Differentiation agents tend to have less toxicity than conventional cancer treatments.

The first differentiation agent utilised was all-*trans*-retinoic acid (RA) in the treatment of acute promyelocytic leukaemia (APL) [115,116]. APL can result from various chromosomal translocations and inversions. In the majority of cases, a translocation between chromosome 15 and 17 is particularly responsive to retinoid treatment. This translocation causes a fusion of the promyelocytic leukaemia (PML) gene (tumour suppressor) and the retinoic acid receptor alpha (RARα) gene (myeloid differentiation regulator). This translocation produces a fusion protein PML/RARα which arrests cells at the promyelocytic stage, blocking terminal differentiation and proliferation control of promyelocytes leading to leukaemia. Patients with PML/RARα fused APL are treated with RA in combination with other drugs such as anthrcycline and this causes the leukaemia cells to differentiate, leading to remission in up to 90% of cases [117]. As previously discussed (1.2.5.1), a derivative of RA, CRA is used as a treatment for minimal residual disease in neuroblastoma. This demonstrates retinoids are widely used as differentiating agents.

1.2.6.1 Rationale for differentiation therapy in neuroblastoma

Differentiation therapy in neuroblastoma is based on the hypothesis that neuroblastoma cells are arrested at an immature or less differentiated state, and thus lack the ability to control their own growth, and so multiply at an abnormally fast rate [113,114]. Differentiation therapy is an approach to the treatment of advanced or aggressive neuroblastoma in which the cancer cells are treated so that they can resume the process of maturation and differentiation into mature cells. In the case of neuroblastoma, evidence suggests that the cancer cells are stem cell-like and have failed to undergo appropriate differentiation or deletion, as outlined below.

Firstly, it has been shown that in sub-pathological neuroblastoma, a self-rescue through natural spontaneous differentiation processes occurs frequently. This is evident in the mass screening in Japan which resulted in an over-diagnosis of neuroblastoma and also observed *in situ* neuroblastoma [17,18]. Furthermore, using disease tracking, a model of neuroblastoma showed natural regression of pre-cancer tissue [92].

Secondly, less aggressive neuroblastoma correlates with the most differentiated cell morphologies and the expression profiles of differentiated cell types. Histology studies performed by neurobiologists have shown high expression of TrkA and p75 in the differentiated sympathetic ganglion (where neuroblastoma often arises) [92]. These same receptors are associated with predicted good prognosis in neuroblastoma individuals [50,55,56]. Furthermore, molecular mechanisms and pathway studies link neuroblastoma outcome and factors involved in neural development/differentiation. The more aggressive neuroblastoma tissues and cells have a less differentiated phenotype than that of tumours from younger/low risk individuals [13,50,51,118]. These studies have been re-confirmed through mRNA and miRNA expressions, which show similar

differentiation pathways to be more highly activated in low-risk individuals. [65,76,79,80]

Thirdly, the major oncogenic factor MYCN's expression and gene copy number is a significant factor in allocating risk to patients [31,32,46,48,59,119-121]. Significantly, MYCN is also an important regulating factor in neuron development, proliferation and differentiation (refer 1.2.3).

Lastly, the successful use of differentiating agents such as CRA in neuroblastoma indicates that the cancer cells are less differentiated than normal tissue [7,94,101,102,122].

These factors support the use and development of differentiating therapies in neuroblastoma. Although differentiation therapies have been in use for decades, the specific activity of retinoids in minimal residual disease neuroblastoma is not fully known [122].

The limitation of differentiation therapies in general is that drugs developed may lead to improper differentiation in non-malignant cells responsible for cell renewal and homeostasis. Specific differentiation of tumour cells is therefore the goal of drug development.

1.3 Neuronal differentiation and cell cycle regulation

Differentiation and the cell cycle are functionally linked processes. Cell cycle arrest is required for neuronal differentiation, and differentiation in neuroblastoma usually occurs via arrest at the G1 phase of cell cycle [2]. There is evidence demonstrating that several key components of cell cycle progression also play a major role in neural cell specification and differentiation by interaction with extrinsic and intrinsic factors. Neural crest-derived progenitor cells are committed to a specific fate, but they undergo several divisions before they exit the cell cycle [123]. The differentiation to their final identity may happen as late as their last cell division. Terminally differentiated neural cells are eventually arrested in G0 (having left the cell cycle).

1.3.1 G1 cell cycle arrest

The G1/S transition is the key step for cell cycle progression and is mediated by Cyclin D proteins and CDK4/CDK6 complexes which operate at mid-G1, then cyclin E/CDK2 which operate late in G1 [124-127]. One key substrate of these complexes is pRb, which when phosphorylated on serine and threonine residues during G1, results in the liberation of E2F proteins and then the subsequent entry into S phase and transcription of S phase genes. The Ink4 family including p15, p16, p18 and p19 and the Cip/Kip family including p21, p27 and p57 can inhibit the progression to S phase via inhibition of CDK kinase activity.

1.3.1.1 Neuronal cell cycle progression

A study by Fergerson and colleagues [128] demonstrated that when mouse neuronal progenitor cells were infected with CDK2 or CDK4/6 and had overexpression of these genes, the cells were arrested in cell cycle. When Rb was knocked-out in this system, CDK4/6 activity was dependant on the Rb pathway, whereas CDK2 activity was not.

When the pRb mediated cell cycle progression is perturbed, neurons apoptose, likely by a p53 mediated pathway [129,130]. Additionally, it is known that N-Myc can bind pRb [131], and when N-Myc is well expressed, in a development situation N-Myc stimulates G1/S progression, ventral migration and neural differentiation [132].

1.3.1.2 N-Myc in the cell cycle

Activation of Myc can stimulate the cyclin E/CDK2 kinase complex which then pushes cells through the G1/S checkpoint. Repression of N-Myc may be required for cell cycle arrest differentiation [133]. Furthermore, in the context of neuroblastoma, N-Myc has also been shown to be essential for the survival of sympathetic neurons, specifically during cell cycle progression after mitosis and in protection from apoptosis caused by aberrant cell cycle re-entry [134].

1.3.1.3 p27 in neuroblastoma differentiation

Another component of cell cycle regulation that has a role in neuron differentiation is p27. p27 is highly expressed in post-mitotic neurons [135]. p27 expression also strictly correlates with both neuronal differentiation *in vitro* and with retinoid treatment (causing cells to both differentiate and induce further p27 expression)[136]. In the absence of p27, N2a-beta neuroblastoma cells fail to differentiate by tri-iodothyronine treatment, therefore p27 is a critical component in neuroblastoma development. Significantly, one study has also shown that high p27 protein expression is a positive prognostic factor in neuroblastoma, independent of MYCN (Bergman [137]. p27 is generally active in the nucleus, however, in breast cancer the localisation of p27 can be disrupted by phosphorylation, de-activating its nuclear location signal, which results in inappropriate cell cycle progression and tumorigenesis [138]. This is just one example of the localisation importance of many cell cycle regulators [2,139-143].

1.4 Retinoid signalling and differentiation

Retinoids are chemical derivatives of vitamin A and are essential throughout life [3,144]. These compounds play a critical role in a vast array of biological processes, including cell growth, differentiation, development, metabolism, apoptosis, immunity and activation of tumour suppressor genes. Significantly, retinoid differentiation therapy has been shown to cause cell cycle arrest at G1 in the cell cycle of neuroblastoma cells [5,145]. Pharmacologically active retinoids are currently used in both conventional and trial cancer treatments in several human cancers, including childhood neuroblastoma [3]. Low expression of retinoid receptors is a common feature of several cancers [3,146-149]. Understanding the mechanisms by which retinoid signalling pathways are induced, may lead to novel cancer drug discoveries and an increase in retinoid drug efficacy in cancer.

1.4.1 Retinoid function

The ancient Egyptians first identified that vitamin A rich foods such as liver could cure night blindness, yet it was not until 1913 that the structures of Beta-carotene and retinol were determined by Paul Karrer [150,151]. From the 1930s to 1960s work on the function of retinoids focused on retinoid deficiency diseases and haemostasis processes. The importance of vitamin deficiency in embryonal development was first described by Hale in 1937 (cited in [152]), where pregnant dams fed a diet deficient in vitamin A had offspring with severe malformations. Retinoid deficiency has led to observations of defects in the embryonic hindbrain development, embryonal patterning, heart, vascular system, ocular, urogenital and respiratory systems. The elimination of retinoids in the rat, mouse, or quail either by genetic or dietary means is lethal in early embryogenesis, whereas an excess of retinoids also leads to embryonal pathology at similar sites to

those seen in deficiency models [153-157]. This indicates that there is a delicate 'juggling act' in regards to retinoid function in homeostasis and development.

In the 1980s and 1990s several endogenous isomers of retinoids were identified and described in human plasma and serum including all-*trans* retinoic acid (RA) [158], 9-*cis* retinoic acid and 13-*cis* retinoic acid (CRA) [159,160]. In mammals, the most predominate and biologically active retinoids are all-*trans* retinoic acid and 9-*cis* retinoic acid [161]. RA is naturally present in the embryonal forebrain, limb buds and spinal cord [162] and in the adult tissues of the central and peripheral nervous system and other tissues such as the liver, where it is metabolised. Experimental evidence suggests that retinoids affect gene expression directly through both activation and repression of target gene transcription and by interfering with different signal transduction pathways [163,164].

Today, retinoids are used in medicine primarily because of their effects on epithelial cell growth [3,114]. Retinoids are used to treat skin disorders such as acne, sun damaged skin and psoriasis as well as in cancer treatment protocols [165-167]. Synthetic retinoids have been developed to act more efficiently and selectively for medical purposes such as acitretin which is used in the treatment of psoriasis, as it acts to induce keratinocyte differentiation. Another synthetic retinoid, bexarotene is specifically selective for retinoid X receptors, as opposed to the retinoic acid nuclear receptors [168]. It is currently used as an oral antineoplastic agent for cutaneous T cell lymphoma [169], and lung cancer [170].

1.4.2 Use of retinoids in cancer therapy

In 1967, U. Saffiotti first published on the anti-carcinogenic effects of vitamin A [171]. Despite early disappointing clinical responses to vitamin A and beta-carotene, research

during the 1990s clearly demonstrated that retinoic acid and other vitamin A derivatives were effective in treating human cancers [150]. Acute promyelocytic leukaemia (refer 1.2.6), particular head and neck cancers and minimal residual disease neuroblastoma have been successfully treated with retinoids [3,7,113,172,173]. In the case of head and neck cancers, retinoid therapy results have been mixed, possibly due to the genotypes of individuals in the trials [174]. However, successful treatment of cancer was found to lead to adverse side effects. Furthermore, resistance to retinoids was observed and this remains a significant issue in the oncology clinic.

Retinoids decrease the expression of h-TERT, N-Myc and increase p27 protein expression among other changes in the cell which correspond to G1/G0 arrest [5,145,175,176]. The receptors of retinoids (members of the nuclear receptor family) respond to retinoid treatment at the transcriptional level and have a significant effect on response to retinoid therapies; however, they also effect neuroblastoma clinical outcome independently [3,164].

1.4.3 Nuclear receptors

In 1987, P. Chambon [177] and R.M. Evans [178], and their respective colleagues discovered the nuclear retinoid receptors. These receptors were found to bind retinoid and lead to the activation or suppression of retinoid target genes or regulate signal transduction pathways [179]. This discovery was essential for the continuing research into the role of retinoids in development and differentiation, and retinoids' relevance in cancer treatment and cancer biology.

Nuclear receptors are transcription factors that are essential for embryonic development, maintenance of differentiated cell type, metabolism, proliferation and apoptosis [3,144,179-185]. Deregulation of their pathways can lead to disease and drugs

have been successfully used to inhibit their function. For example, Tamoxifen is used to inhibit the estrogen receptor in breast cancers [186,187]. Dexamethasone is used against the glucocorticoid receptor in inflammatory diseases and leukaemia [188]. Interestingly, only 24 of the 48 nuclear receptors have known ligands [183].

Most nuclear receptors adhere to a specific domain structure, which can form monomers, and homo/heterodimers which act as functional DNA binding complexes (outlined in [144]). The N terminal domain is isoform specific and is termed activation function 1 (AF1) (A/B domains). The C domain has the DNA binding capability. The D domain is a variable hinge domain, linking the C and E domains. The E domain (AF-2) has very strong dimerisation potential and can bind hormone/ligand and other interacting proteins. The F domain is at the C-terminus. Ligand binding generally induces a confirmation change in the protein and transport to the nucleus. The holo-positioning of the E domain (Helix 12) allows for interaction with short LxxLL motifs called the Nuclear Receptor Binding Motif (NRBM/Nuclear receptor box) [189].

Paralogous genes that originated by gene duplications are characteristic of vertebrates [182,190]. They have evolved for fine-tuned function and homeostatic equilibrium, for example there are two estrogen receptors, α and β, and these show distinct biochemical function and tissue expression inhibition [191-193]. Estrogen signalling is a balancing act between α and β, with estrogen receptor β activating gene factors, and α supressing β and causing growth. Similarly, three paralogues exist for the retinoic acid receptor RARα, RARβ and RARγ [3,179,194].

1.4.4 Retinoid receptors

RARs and RXRs exhibit structurally homologous and functionally conserved DNA-binding domains and also specifically the DNA region of the Retinoic Acid Response

Element (RARE)/Retinoic X Response Element (RXRE) [3,194,195]. This sequence is crucial for sequence recognition and aids dimerisation. In contrast to other nuclear receptors, the ligand binding domain pockets in the RARs can adapt to different retinoids, bending to accommodate them. RARs and RXRs can heterodimerise and homodimerise at the promoter region of several genes. Most of these receptors have varying isoforms, leading to a further level of functional complexity. Retinoid binding of the receptors leads to disassociation of co-repressors and recruitment of co-activators, which either have intrinsic histone acetyltransferase (HAT) activity or associate with HATs. This HAT function subsequently leads to decondensation of chromatin, facilitating gene transcription [196,197].

1.4.5 RARβ as a tumour suppressor gene

The human RARβ gene has three isoforms: β1, β2, and β4 [198,199]. The biologically active RARβ2 isoform is under the regulatory control of the P2 promoter which contains a high affinity RA-responsive element RARE [3,200]. The RARE is associated with the transcriptional promotion of RARβ2 by RA in a variety of cells.

RARβ has induced expression after retinoid treatment and is a crucial part of the retinoid anti-cancer signal [201-203]. Also, RARβ is a tumour suppressor gene in several tissues [3,149,204-206]. RARβ2 is a candidate tumour suppressor gene in myelofibrosis, with epigenetic changes being amongst the most significant determinants of RARβ2 gene activity in myeloid metaplasia patients [207].

Tumour suppressors are regularly downregulated by methylation of their promoter regions, usually at the CpG islands leading to decreased transcription of the gene [208]. Various studies have shown that this occurs for RARβ in multiple cancer types, including colon cancer [209], melanoma [210], oesophageal squamous sell

carcinoma [211], lung cancer [212] and in both primary and metastatic tissues of the breast [213,214].

1.4.6 RARβ in neuroblastoma

In vitro overexpression of RARβ induces profound growth inhibition independent of retinoid treatment, and increases retinoid sensitivity [149]. Furthermore, high levels of RARβ transcription lead to favourable patient prognosis. Comparable to the effect of RA on neuroblastoma cells, RARβ overexpression (independent of retinoid treatment) causes G0/G1 cell cycle arrest, and consequently also causes decreased tumorigenicity in nude mice. Interestingly, N-Myc overexpressing neuroblastoma cell lines, inhibit retinoid responsiveness, whereas overexpression of RARβ is able to improve the response of N-Myc amplified cell lines [215]. This highlights the 'cross-talk' between the retinoid response and N-Myc driven tumour promotion.

The significant effect of RARβ expression in neuroblastoma has led to greater research into mechanisms to restore or activate the retinoid pathway through RARβ in cells where RARβ repression has occurred. Our research group has published work whereby the TRIM protein, TRIM16 was shown to bind the RARE promoter and reverse RARβ repression [8,216].

1.5 Tripartite motif (TRIM) proteins

There have been countless publications on individual TRIM (tripartite motif) family members in the context of cancer. Several of these genes interact with the nuclear receptors and their signalling pathways. TRIM16 is a lesser known TRIM protein that shares a similar structure to tumour suppressors and oncogenes within its protein family (Table 1.2).

1.5.1 Structural domains of TRIM proteins

The TRIM family (or RBCC family) of proteins are defined by the presence of the tripartite motif for which they are named [9]. Structural similarities of TRIM proteins are highly conserved throughout vertebrate evolution [9,217-219]. Typically, this motif consists from the N- to C-terminus of a really interesting new gene (RING) finger domain, one or two B-box domains, a coiled-coil domain and the more variable C-terminal domains such as B30.2 (the most common in humans), NHL and TSS-PHD-BROMO. Strikingly, the order and spacing of domains is highly conserved, indicating a similarity in biochemical action and yet a difference in biological niche activity.

The RING and B-box domains are both cysteine-rich and bind zinc atoms, indicating possible interaction with other proteins, as well as DNA and RNA. The RING finger domain frequently processes E3 ubiquitin-ligase activity and can transfer ubiquitin to RING proteins as well as heterologous substrates [9,220]. Considering the large numbers of B-box domains in TRIM and other proteins, there is limited information about their function. The B-box2 domain of TRIM5α is known to be essential for retrovirus restriction via increasing protein self-association [221-223].

Interestingly, a vast majority of functionally studied TRIM proteins are known to homodimerise; TRIM1, 3, 5, 6, 8, 9, 10, 11, 18, 19, 21, 23, 24, 25, 26, 27, 28, 29, 30,

31, 32 and the coiled-coil domain was necessary and sufficient for the homodimerisation in the majority of cases studied [9,224,225]. The coiled-coil domain is also potentially required for the TRIM protein involvement in high molecular weight protein complexes. In some cases, TRIM proteins interact with other TRIM family members. TRIM24 is known to bind PML and RET finger protein RFP (RFP/TRIM27) through the B-box and part of the coiled-coil domain [226]. Midline-1 (MID1/TRIM18) and RFP can also heterodimerise [9,224,225]. The extent of functional interactions amongst TRIMs is yet to be fully characterised.

The B30.2/SPRY (or RFP-like) domain is present in approximately 150 human genes [227] and was first described in 1993 as being a domain of the human class I major histocompatibility complex region [228]. Mutations to this domain have been shown to impact on retroviral restriction in the case of TRIM5α [229,230], but also feature in Opitz syndrome (MID1) [231,232] and familial Mediterranean fever (Pyrin) [233]. The B30.2 domain has also been identified as essential for some ligand binding interactions, such as the interaction of xanthine dehydrogenase with butyrophilin [234].

Table 1.2 TRIM proteins relevant to cancer

MD = Muscular dystrophy, C = Cytoplasmic, B = Bodies, Mito = Mitochondrial, N = Nuclear, MT=Microtubules, Sk = Cytoskeletal

Name	Cellular function	Associated disease	Localisation	RING, B30.2/SPRY, B-box, DAPN, Coiled-coil, NHL, COS-Fibronectin type-III, TSS-PHD-Bromo
TRIM5 (RNF88)	Restriction of HIV-1 infection		C CB	
TRIM10 (HERF1)	Role in erythropoiesis		C	
TRIM16 (EBBP)	Keratinocyte differentiation		C	
TRIM18 (Midline-1)	Regulation of microtubule dynamics	Opitz syndrome type I	C MT	
TRIM19 (PML)	Apoptosis, senescence, restriction of viral infection	APL cancer	NB	
TRIM20 (MEFV/Pyrin)	Regulation of inflammation through cytoskeleton interactions	Familial mediterranean fever	Sk C,N	
TRIM21 (52 kDa Ro protein1)	E3 ubiquitin-protein ligase, T-cell activation, cell cycle progression		CB C,N	
TRIM24 (TIF1-alpha)	Epigenetic control of transcription	Fusion oncoprotein	C	
TRIM25 (EFP)	Regulation of cell cycle progression, acts as an E3 ligase in ubiquitination		C	
TRIM27 (Zinc finger protein RFP)	transcriptional repressor, Induces apoptosis , cell proliferation	Thyroid cancer	C N	
TRIM29 (ATDC)	Radio-resistance, transcription factor, carcinogenesis	Ataxia tel-angiectasia	C	
TRIM31 (C6orf13, RNF)	Regulator of Src-induced anchorage independent cell growth		C Mito	
TRIM32 (HT2A)	Mediates the HIV-1 Tat protein in vivo	Limb-girdle MD type 2H, Bardet-Biedl syndrome type 11	CB	
TRIM33 (TIF1-gamma)	E3 ubiquitin-protein ligase, control of cell proliferation	Thyroid cancer	NB	
TRIM35 (HLS5)	Induces apoptosis		C,N	
TRIM36 (RBCC728, RNF98)	E3 ubiquitin-protein ligase , chromosome segregation , cell cycle regulation		C Sk	

1.5.2 Roles of TRIM proteins

On last count, there are over 70 TRIM proteins in the human genome. TRIMs have been implicated in a diverse range of processes, including development, cell growth, differentiation, innate immune function, human disease and cancer [9,225].

Several TRIM proteins have a role in balancing self-renewal and differentiation in mammals, ultimately leading to roles in cancer [9]. PML and potentially TRIM 8, 10, 16 24, 32, 35, 36 have a role in tumour suppression. More interesting is the ability of TRIM24 and PML to form oncogenic fusion proteins through chromosomal mutations. Conversely, proteins such as TRIM27, TRIM28, ATDC and TRIM31 are positively associated with alimentary canal tumours.

1.5.3 Tumour suppressor TRIM proteins

1.5.3.1 PML (Acute Promyelocytic Leukaemia Protein)

PML is probably the most discussed TRIM protein. It has a RING domain, two B-boxes with a coiled-coil domain, and a unique C-terminal region which includes the PML nuclear localisation signal [235,236]. As its name suggests, PML was first described in 1991 due to its involvement in the chromosomal translocations that causes the majority of acute promyelocytic leukaemia (APL) [237]. PML is able to promote apoptosis and inhibit cell growth, amongst other tumour suppression characteristics [236,238-240].

The most noted feature of PML is its involvement with more than 50 other proteins in large protein complexes called PML nuclear bodies (also known as ND10 and PODs) which are involved in transcription, cell cycle regulation, chromatin organisation and cell survival [236,238,240,241]. These structures are absent in PML -/- primary cells, but can be restored with the addition of exogenous PML [242-244], suggesting that PML has a crucial role in sequestering proteins into these bodies. PML

bodies can form in response to stress stimuli and interestingly the formation of these bodies is also indicative of a patient's response to anti-APL drugs, such as retinoids and arsenic trioxide [245-248].

Many TRIM proteins including the tumour suppressor PML, are highly expressed during the G1 phase of the cell cycle [140,249]. PML's nuclear bodies are associated with growth inhibition, forming during G1 and partitioning during mitosis. Furthermore, these bodies have been shown to co-localise with TRIM16 after retinoid treatment [8].

Loss of PML expression is involved in several human cancers. [239]. Analysis of tumour and normal tissue microarrays (TTMs) demonstrated that mRNA levels of PML rarely changed. In contrast, PML protein expression was reduced or abolished in prostate adenocarcinomas, colon adenocarcinomas, breast carcinomas, lung carcinomas, lymphomas, CNS tumours, and germ cell tumours. However, there was no reduction of PML expression in thyroid or adrenal carcinomas. Interestingly, loss of PML protein expression was associated with tumour progression in prostate cancer to an invasive carcinoma ($P < 0.001$), and in breast cancer with lymph node metastasis ($P = 0.01$), and with high grade CNS grade tumours ($P = 0.003$).

Surprisingly, PML knockout mice have a normal phenotype, but they do have increased tumour incidence when challenged with carcinogens [250]. This work suggests that PML's role can be compensated for by other genes under 'normal' conditions and that, potentially, its anti-tumorigenic role is essential in challenged or stressed cells. PML knockout mice crossed with a K-Ras transgenic lung cancer mouse model results in offspring with an increased lung cancer burden and display a higher histological grade and decreased tumour p21 and p16 protein expression [251].

In fact, PML has been found to interact with HDACs 1, 2, 3 and 7, which strongly indicates it functions in transcription [252]. Mammalian Homologues of Drosophila Seven in Absentia (SIAHs) are able to target several factors involved in cell growth and tumorigenesis for degradation. Fanelli and colleagues found that TRIM5, TRIM9, TRIM21 and PML are degraded by mSIAH-2 overexpression via the TRIM coiled-coil domain [253]. SIAH-1 is a transcriptional target of p53, but not induced by p53 or its stress response. This work highlights the interactivity of TRIM proteins within critical cell pathways.

P53 is the target of mutation in 50% of all human cancers and is a tumour suppressor which mediates cell cycle and apoptosis [254]. Interestingly, PML is a p53 target gene that also acts downstream of p53 to facilitate its anti-proliferative and apoptotic effects [255]. In PML bodies induced by ultraviolet radiation, PML can directly interact with p53 and also binds and sequests to the nuclear bodies, the p53 regulator Mdm2 [246]. These proteins also form temporal trimeric complexes. This shows PML and its nuclear bodies to have a role in p53 stability and response to stress.

PML is known to interact with c-Myc and mediate Myc function [256-258]. PML also functions in Myc controlled pathways such as differentiation and cell cycle control. PML isoform 4, which has a truncated C terminal was found to specifically destabilise c-Myc [256]. There are more than 11 isoforms of PML, of which the majority are nuclear and involved in the formation of PML bodies [259]. Cytoplasmic PML is induced by the pluripotent cytokine TGF-β and is also a critical regulator of TGF-β via binding to smad2/3. This research illustrates that isoforms of TRIM proteins are able to have interacting roles that lead to multiple and often different outcomes.

A novel characteristic of PML is the common mutation event in leukaemia which leads to a dominant-negative oncogenic fusion protein [260]. PML and PML-Retinoic acid receptor alpha (PML-RARα) fusion proteins have an antagonistic effect on each other and PML-RARα has opposing effects on Retinoblastoma protein (Rb) [261-263]. PML protein and PML body formation is correlated with neuroblastoma retinoid-induced differentiation [264,265]. After retinoid treatment, PML bodies are formed possibly through mediation of the signal regulated kinase (ERK).

It is clear that PML has an important role in transcriptional regulation but also that it is able to interact with several key cancer regulating proteins, and with tissue specific genes and proteins. Because of PML's tumour suppressor attributes, the screening of compounds to find those capable of stabilising PML or localising with PML in PML bodies could be beneficial in finding novel cancer drugs.

Another well characterised TRIM protein, TRIM24 is also able to form onco-fusion proteins in a similar manner to PML.

1.5.3.2 TRIM24 (Transcription intermediary factor 1-alpha /TIF1α)

TRIM24 total knockout mice are viable and fertile [266,267]. However, at 9 months these mice develop hepatocarcinoma. This is due to failure of the liver cells to execute proper cell cycle withdrawal during the transition to adult cells, a process which is dependent on the retinoid signalling pathways. This was demonstrated by the crossing of TRIM24 knockout mice with RARα knockout mice and the consequent block in cancer formation. TRIM24 is therefore a liver-specific tumour suppressor by attenuating RARα-mediated transcription.

As with PML, TRIM24 also interacts with wildtype p53 [268]. Allton and colleagues have found that TRIM24 ubiquitinates and negatively regulates p53. TRIM24 and p53 were found in interact through immunoprecipitation experiments. In a breast cancer cell line (MCF-7) knockdown of TRIM24 caused an increase in p53 stability. Conversely, overexpression of TRIM24 reduced the half-life of p53, an effect which was amplified by Doxorubicin induced stress. However, surprisingly, TRIM24 knockdown did not influence the expression level of p53 target genes. One aspect of this research to consider is that the TRIM24 siRNA appears to target mostly the heavy isoform of TRIM24, whereas the immunoprecipitation experiments display the lighter TRIM24 isoform as binding to p53, although this trend is not discussed in their paper. The interaction of TRIM24 with p53 is interesting but further research needs to be done to clarify TRIM24's role in cancer.

TRIM24 interacts with several nuclear receptors including estrogen, retinoic X receptor and co-localises with PML bodies [269,270]. It often interacts as a co-activator of PML body target genes. Like the nuclear receptors TRIM24 interacts with, TRIM24 may have tissue specific roles in development and homeostasis.

1.5.4 Oncogenic TRIM proteins as markers of aggressive cancer and cell cycle deregulation

1.5.4.1 RFP (RET finger protein/TRIM27)

Not all TRIM oncogenic fusion proteins involve tumour suppressor genes. Like PML, RFP can form a fusion onco-protein, with the RET proto-oncogene (where RET is an abbreviation for "rearranged during transfection") and RFP was originally identified through this association [271]. An interesting mouse model (metallothionein-1/RFP-RET) uses this oncoprotein to produce spontaneous melanoma which progresses to

metastasis in a step-wise progression [272]. This demonstrates the oncogenic potential of un-regulated RFP-RET. Significantly, RFP has been shown to affect cancer cells through mutations and cellular interactions in transcription, cell cycle and also cell movement, illustrating a varied role of RFP in cancer, as discussed below.

RFP has also been shown to be significantly associated with colon cancer. Overall survival of 112 patients with colon carcinomas was stratified by RFP expression, using Kaplein-Myer survival graphs, of which 70/112 tissues were RFP positive, conferring RFP to be unfavourable [273]. Additionally, RFP expression was shown to be unfavourable in endometrial cancer [274]. In this study, 57/119 endometrial tumours showed positive RFP staining and RFP expression predicted both poor overall survival and progression free survival. One characteristic of RFP's role in aggressive cancer may be its influence on migration and invasion, which are impaired by specific siRNA knockdown of RFP in HEC50 and HeLa endometrial cancers cell lines as well as MDA-MB-231 breast cancer cells. However, cell proliferation during RFP knockdown was only decreased in HeLa cells.

RFP has been found to have different nuclear/cytoplasmic distributions depending on the cell type, with myeloma cells having high cytoplasmic expression and hepatocytes and neurons having nuclear expression [275]. RFP is also expressed in both breast cancer and non-cancer breast cell lines and has been shown to interact and modulate the estrogen receptor alpha in breast cancer cell lines [276].

There have been several studies into the molecular mechanism of RFP, as discussed below. RFP has been shown to bind Scaffold attachment factor B1 which interacts with the transcriptional machinery and RNA polymerase II [277], and is a known co-repressor of the estrogen receptor [181,278]. Importantly, RFP knockdown

resulted in the downregulation of the estrogen receptor target genes, Cyclin D1 and another nuclear receptor, the progesterone receptor. RFP physically interacts with the tumour suppresser Rb protein and inhibits gene transcription activation by Rb [279]. Furthermore, histone deacetylase (HDAC1) and RFP interact and HDAC1 is required for the association of RFP with the transcription factor NF-YC on the TBP-2 promoter [273]. Another study highlights RFP's repressor abilities, showing RFP to inhibit transcriptional activation by bHLH transcription factors (SCL, E47, MyoD and mASH-1) via its B-box and first coiled-coil domains. Since this repression was HDACi sensitive, it is possible that RFP recruits HDAC and/or polycomb proteins for bHLH interactions. The above interactions point heavily towards RFP involvement in transcriptional control of cell cycle in conjunction with nuclear receptor function.

1.5.4.2 TRIM28 (TIFβ/KAP1)

TRIM28 was originally identified as a co-repressor of the Kruppel-associated box-domain-containing zinc finger proteins [280,281]. Homozygous deletion in knockout mouse models produce embryonic lethality at E5.5, demonstrating a crucial role for TRIM28 in development [282].

TRIM28 has been associated with many cancers but those of the gut are most commonly reported. Yokoe and colleagues have shown that specific siRNA interference of TRIM28 decreased gastric cancer cell proliferation *in vitro* [283]. More significantly, high transcript expression of TRIM28 in gastric cancer was found to be a predictor of patient survival. Another study demonstrated the clinical significance of TRIM28, as it was identified as a serum marker of colorectal cancer in a screen of antibody profiles in patients [284]. A protein array was used to identify cancer-associated proteins from sex- and age-matched sets for 43 patients. Metastases kill more people than the primary

cancers themselves, and in a search for novel breast cancer metastasis-associated proteins, TRIM28 was identified to be deregulated in a protein expression profile screen (ITRAC-based LC/MS/MS) [285]. IHC analysis of human primary invasive ductal carcinoma tumours and lymph node metastasis tissues confirmed an increase in TRIM28 expression in 17/44 cases.

Relative to other TRIM proteins the mechanism of action of TRIM28 has been well studied. TRIM28 is known to interact and regulate many components of transcriptional regulation as discussed below. TRIM28 is an essential component of two chromatin remodelling and histone deacetylase complexes, N-CoR1 and NuRD [286,287], and directly interacts with the histone methyltransferase SETDB1, which methylates histone 3 [288]. TRIM28 also binds heterochromatin protein (HP) 1, which is also involved in histone modification [289]. TRIM28 also binds to the E2F1 transcription factor in a retinoblastoma protein (pRb)-independent fashion and inhibits E2F1 activity [290]. TRIM28 induces E2F1-HDAC1 complex formation and inhibits E2F1 acetylation. Furthermore, TRIM28 was identified as Mdm2-binding protein and shown to form a complex with Mdm2 and p53 [291]. Moreover, TRIM28-mediated gene silencing involves the recruitment of the histone deacetylase complex (HDAC) [286,287,292]. Thus TRIM28 is involved in many significant transcriptional pathways.

TRIM28 has also been shown to interact with STAT1, 3, 4 and 6 which are all important regulators of proliferation, differentiation and immune response [293,294]. STAT3 is constitutively activated in several cancers [295]. Interestingly, TRIM28 is rapidly phosphorylated following DNA damage and localises to the DNA lesions [296] where it becomes an essential component of heterochromatic DNA double strand repair

[297]. This demonstrates that TRIM28 not only binds and regulates DNA structure but is also involved in DNA repair, a characteristic associated with self-renewal genes.

TRIM28 may also be an important mouse embryonic stem cell self-renewal transcription factor [298]. This is relevant to cancer as regulatory networks of self-renewal have been hypothesised to be active in cancer. Interestingly, TRIM28 was highly expressed in stem cells and embryonic tissue and after its knockdown a differentiated phenotype was induced (as indicated by a decrease in alkaline phosphatase staining cells and an induction in differentiation markers). Four factors were found to significantly co-occupy the putative gene promoters of 326 genes. TRIM28 and Cnot3 were found to co-occupy with the known pluripotent gene proteins; Zfx and the oncogenic c-Myc. This module of proteins was found to target cell cycle, cell death and cancer pathways. Another study confirms this line of hypothesis showing that TRIM28 promotes the pluripotent state of mouse ES cells [299]. Critically, mechanistic studies show that phosphorylated TRIM28 is a critical modification for TRIM28's pluripotent transcriptional activity and inhibits neural differentiation [298].

1.5.4.3 ATDC (Ataxia-telangiectasia group D/TRIM29)

ATDC was first described as a candidate gene associated with the genetic disorder ataxia-telangiectasia [300]. Ataxia-telangiectasia affects the brain and immune system, and is associated with an increased risk of cancer. ATDC is normally expressed in the placenta, lung, thymus, prostate, testis, and colon [301]. There is no expression in skeletal muscle, heart, brain, ovary and small intestine. ATDC is located at chromosome 11q23, and whilst it lacks the RING domain, it has 2 B-boxes, a coiled-coil domain and a large C terminal domain that is yet to be characterised.

Like other oncogenic TRIM proteins, ATDC is associated with alimentary canal cancers. In gastric cancer, for example, ATCD has been identified as a marker for lymph-node metastasis and high expression correlates to a poor prognostic phenotype [302]. Importantly, other studies have shown lymph node metastasis to be one of the most reliable prognostic factors in this disease [303,304]. Furthermore, multivariate regression analysis indicated that high expression of ATDC mRNA was a statistically significant independent predicator for survival, lymph node metastasis, invasion and depth of invasion [302]. In 1995, a study of ATDC found it to interact and co-localise with vimentin protein. [305]. Unfortunately, the significance of these interactions was not clarified, as vimentin has been found to promote cancer metastasis in breast cancer and thus could contribute to ATDC's association with metastasis [306].

Pancreatic cancer is a highly lethal disease characterised by late diagnosis, and drug resistance [307]. Using Affymetrix gene expression profiling, Logsdon and colleagues, identified ATDC was 20-fold higher in pancreatitis-derived tissues compared with normal pancreas epithelial cells [308]. ATDC promotes cellular proliferation *in vitro* and pancreatic tumorigenesis *in vivo* via the beta-catenin signalling pathway. *In vitro,* enforced ATDC expression in pancreatic cancer cells increased beta-catenin, which exerts growth promoting effects by translocating from the cytoplasm to the nucleus and leads to transcription of Wnt target genes c-Myc and DKK1, whereas ATDC knockdown reduced these target genes [309]. The oncogenic effects of ATDC are partly mediated through its binding partner Dvl-2. In the context of pancreatic cancer, this interaction stabilises beta-catenin, which then translocates to the nucleus and promotes the TCF gene.

Recently, researchers have revisited early research involving the role of ATDC in radiosensitivity and exploring ATDC's possible involvement with p53 [310]. Yuan and colleagues demonstrated that acetylated ATDC promotes proliferation through inhibition of p53, via the binding and sequestering of p53 from the nucleus. ADTC also suppresses p53 mediated apoptosis following irradiation and reduces induction of p21 and NOXA (p53 target genes). In keratinocytes under UVB induced stress, ADTC is also involved as a pro-survival factor of these cells [311].

The majority of studies identify ATDC as oncogenic [302] [308], but another study has shown that ATDC expression is lower in breast and prostate cancers [312]. This indicates that ATDC has tissue specific functions yet to be differentiated.

1.5.4.4 EFP (Estrogen-responsive finger protein/TRIM 25)

EFP knockout mice are viable and fertile, even though uteri were underdeveloped [313]. Interestingly, EFP knockout mice had a lower than normal ratio of G1-S cell cycle phase during normal estrogen induced proliferation in uterine cells. EFP is widely expressed in the genital tract, thyroid gland, aorta, spleen, kidney and brain [314]. EFP is expressed in several tissues which are also responsive to estrogen. The EFP gene has an estrogen response element, further tying EFP and estrogen signalling together [315]. It is not surprising therefore that much of the research into EFP is in the context of breast cancer, also an estrogen responsive tissue [316].

A study into the expression of EFP in human breast tumours demonstrates high levels of EFP protein correlate with both estrogen receptor α status and overall survival [316,317]. However, RFP expression did not correlate with p53 status.

A recent paper highlights the clinical significance of EFP [317]. Ueyama and colleagues have shown that knockdown of EFP by DNA-modified small interfering RNA inhibits breast cancer cell proliferation *in vivo*. Importantly, using MCF-7 breast cancer cells, EFP was specifically knocked-down without inducing off target effects or an immune response. This strategy could be used for clinical trials for breast cancer in future where EFP is overexpressed or 14-3-3σ is downregulated by EFP or other factors.

EFP interactions with 14-3-3σ appear increasingly important, with EFP able to target the anti-proliferative protein 14-3-3σ for proteolysis via its E3 ligase activity [318,319]. EFP was not found to bind the cell cycle regulators p21, p27 and p57. EFP overexpression promoted cell cycle progression with increased proportions of breast cancer cells in S phase *in vitro,* which supports cell cycle studies in the EFP mouse knockout study, as discussed above. Like other TRIMs, EFP can be upregulated by interferons [320]. Importantly, this study confirms EFP can bind ubiquitin and that STAT-1 binds to the EFP DNA, demonstrating a role for EFP in more than hormone signalling.

1.5.5 Novel TRIMs involved in differentiation and cell cycle regulation

1.5.5.1 TRIM10 (HERF1)

TRIM10 has a Ring domain, 2 B-boxes, coiled-coil domain and RFP-like C-terminal domain and may have a role in erythropoiesis [321]. Significantly, inhibition of TRIM10 is able to block erythroid differentiation and TRIM10 levels increase by 30 fold during differentiation. Additionally, downregulation of the spi-PU.1 (a leukaemic oncogene) induces the expression of TRIM10 and overexpression of TRIM10 enhances Dimethyl sulfoxide-induced apoptosis [322]. This meagre evidence suggests TRIM10

may have an inhibitory association with some leukaemia although this association needs to be definitely investigated.

1.5.5.2 TRIM31

TRIM31 is another TRIM protein that has an interaction with nuclear receptor signalling. It has a putative retinoid response element and also is rapidly induced upon retinoid treatment in a retinoid sensitive breast cancer cell line [323]. It was identified as a candidate gene involved in stomach cancer via the Bioexpress database (Gene Logic Inc., Gaithersburg, MA) [324]. TRIM31 was also shown to exhibit ubiquitin ligase activity, which is not unexpected as it possesses a RING finger domain. Another study demonstrates TRIM31's interactions with $p52^{Shc}$ which is involved in the powerful Src signalling pathway, which has been linked to gastro-intestinal tract cancer, cell proliferation and movement. The involvement of TRIM31 in the Src or retinoid signalling pathways remains to be fully explored.

1.5.5.3 TRIM35 (haemopoietic lineage switch 5/Hls5)

TRIM35 was identified as a gene associated with the lineage shift from of the J2E erythroleukaemic cell line to monocytic cells. [325]. Expression was found during different stages of embryogenesis including limb buds, brachial arches, spinal cord, dorsal root ganglia and brain, and in several adult tissues. This gene is located on the 8p21.1 locus, a region involved with numerous cancers. TRIM35 protein is expressed as granules in the cytoplasm and in punctate nuclear bodies, which did not co-localise with PML bodies. Notably, TRIM35 overexpression in HeLa cells inhibited cell growth, clonogenicity and tumorigenicity, leading to the possibility that TRIM35 is a tumour suppressor. Cells overexpressing TRIM35 were found to accumulate in the G_2/M and to

then undergo apoptosis. At a molecular level TRIM35 did not change the expression level of p53, or various cyclins with the exception of CDK1.

Other studies have also demonstrated the involvement of TRIM35 with erythroid differentiation and inhibition of proliferation, partly by suppression of GATA-1 DNA binding and gene transactivation [326]. Interestingly, the B-boxes and coiled-coil domains of TRIM35 were required for binding to GATA-1.

These studies suggest a different anti-cancer mode of action for TRIM35, compared to well-studied TRIMs such as PML which interact with p53 and are heavily involved at G1 in cell cycle in PML bodies.

1.5.5.4 TRIM36

TRIM36 has a RING, 2 B-boxes, coiled-coil, B30.2/SPRY and COS-Fibronectin (III) domains. TRIM36 is on 5q22.3 a loci often mutated in urogenital tumours and has cytoplasmic, slightly filamentous localisation pattern in COS-7 prostate cancer cells [327]. Interestingly, mitotic cells are TRIM36 negative and high protein expression was associated with areas of cell-cell contact. Lack of TRIM36 mutations in tumour cells indicate it is not a classical tumour suppressor gene, however; TRIM36 overexpression was detected in the majority of prostate cancers by RT-PCR. Another study found TRIM36 is potentially associated with chromosome segregation in collaboration with CENP-H and that TRIM36 overexpression may influence chromosome stability [328]. In fact, TRIM36 overexpression decelerates cell cycle progression and attenuates cell growth which is in accordance with the hypothesis of it being a tumour suppressor.

1.5.5.5 TRIM16 (Estrogen-responsive B-box protein/EBBP)

Unlike the majority of TRIM proteins, TRIM16 lacks the RING domain, but has two B-boxes, coiled-coil and B30.1/SPRY domains. The crystal structure of TRIM16 has not been solved. It was first identified in a screen for estrogen responsive genes [329], hence its alias, Estrogen-responsive B-box protein (EBBP). Overexpression of TRIM16 has the ability to differentiate skin cells and TRIM16 also has a role in wound healing [330]. It is expressed in most tissues, especially in the foetal brain.

In a screen to identify proteins that regulate retinoid signalling, our group found that TRIM16 bound to the retinoic acid receptor element (RARE) DNA [8]. TRIM16 was validated as binding the RARE and was able to increase transcription of the nuclear receptor and tumour suppressor gene, retinoic acid receptor β gene (RARβ) in neuroblastoma cells. TRIM16 also co-localised with PML (TRIM19), in PML-like nuclear bodies after retinoid treatment. Furthermore, we also found that TRIM16 was able to restore retinoid response, as indicated by growth inhibition and RARβ induction in retinoid drug resistant breast and lung cancer cell lines [216]. Significantly, TRIM16 was found to interact with the important cell cycle regulator E2F1 [331]. TRIM16 was also shown to bind the intermediate filament, vimentin which is known to influence migration and aggression in some tumour types [306]. TRIM16 overexpression and downregulation was shown to influence cell migration *in vivo*, indicating TRIM16 to negatively affect cell movement.

TRIM16, like other TRIMs may have role in the innate immune system. TRIM16 was found to associate with the autoinflammatory mediators proIL-1β, NALP1 and procaspase-1, specifically binding at the B30.2 domain of TRIM16 in all cases [332]. These proteins were found to co-localise at the peri-nuclear region. Significantly,

TRIM16 expression is induced by overexpression of its inflammatory binding partners. How its innate immune function could impact on its role in cancer is unknown, but theoretically, this characteristic would inhibit carcinogenesis *in vivo*.

Surveying the various databases on cancer and gene expression we can glean further information on TRIM16. According to the Human Protein Altas [333], malignant tissues exhibited strong cytoplasmic immunoreactivity for their anti-TRIM16 antibody, which is not surprising as TRIM16 is also highly expressed in the normal counterparts of these cancers. Interestingly, most basal cell carcinomas in skin were weakly stained. Unfortunately, there was no information on TRIM16 protein expression in neuroblastoma tissues.

As previously discussed, the decision of cells to differentiate is commonly made in cell cycle G1 phase, and induction of differentiation in cells requires cell cycle arrest [2,334]. How the cell cycle machinery coordinates cell cycle arrest with differentiation activation is not fully elucidated in neuroblastoma. TRIM16 overexpression induces keratinocyte differentiation *in vitro* [330]. However, it is yet to be determined if TRIM16's role in differentiation involves elements of G1 phase in the cell cycle. Also the expression and localisation characteristics of TRIM16 through the phases of cell cycle has not been previously investigated and is a major step towards understanding TRIM16 function in cells. Importantly, TRIM16 also has putative functional domains which remain to be explored in relation to TRIM16's function in cancer.

1.5.6 The roles of TRIM proteins in cancer

It is clear from various sources that TRIM proteins are transcriptional regulators. These regulators have been shown to affect cell cycle, proliferation, apoptosis, migration, differentiation and self-renewal in many cancer cell types. Most TRIM proteins relevant

to cancer biology do interact with other TRIM proteins, Myc, Rb, p53, HDACs and nuclear receptor pathways. However, a consensus on the broad function of all cancer relevant TRIMs is a difficult one as the literature is sparse and occasionally conflicting. It would be reasonable to assume that in future, different gene isoforms or cell environment will explain most controversies. Recent papers into TRIM proteins' modulations of miRNA add another layer to TRIM proteins' function and possible role in the context of cancer [335-337]. Based on this review, I believe it is the involvement with nuclear receptors and transcription which holds the pivotal role of TRIM proteins in normal cell function and ultimately cancer.

Many cancer-associated TRIMs are implicated through tissue arrays or immunohistochemical studies and more work is required at the molecular level to understand the mechanism of these TRIMs. Knockout mouse models have proved useful for TRIM24 and PML studies and knockout models of genes such as ATDC and TRIM16 could lead to a more detailed knowledge of TRIM function in cancer. This is increasingly important as the role of TRIM proteins in the innate immune system becomes more apparent. Unfortunately most TRIM models look at one cell type and not the environment. More mouse models investigating TRIM protein function are required. The scores of significant immunohistochemistry clinical studies have to be supported with not only further overexpression and knock down *in vitro* studies, but also with *in vivo* work, which would allow for the interactions between innate immune function, stress response and cancer development to be analysed. Importantly, mechanistic studies into the various domains of TRIMs have proved useful in PML and other TRIMs, this type of research is lacking in the large proportion of TRIM research.

With at least 70 TRIM proteins in humans, it is likely that other TRIM proteins also have significant roles in cancer and potentially markers of specific cancer types. Also it is likely that TRIM proteins work in balance and in signalling networks involving transcription factors and extrinsic factors. Ultimately, there is also some redundancy required by evolution. As many TRIM proteins homodimerise and even heterodimerise with other TRIM proteins, research into how groups of TRIM proteins function could elucidate further biological significance of TRIM proteins.

1.6 Research Perspectives

Neuroblastoma is a disease with poor patient outcome and has had few improvements in its treatment, in the last 20 years. Neuroblastoma is one of the few human malignancies known to exhibit spontaneous regression from an undifferentiated state to a benign one. As outlined in the literature review, the understanding of the mechanisms governing neuroblastoma differentiation and proliferation are limited. Thus, an improved understanding of these processes is required and could lead to novel markers of disease and targets for neuroblastoma drug development. Retinoids are used as a differentiating agent in current neuroblastoma treatment regimes. Significantly, previous studies have shown TRIM16 promotes the retinoid anti-cancer signal in neuroblastoma. Hence, TRIM16's implications on tumorigenicity and the mechanisms behind its action require study. Such investigations would further the understanding of TRIM16 function in neuroblastoma and would also evaluate TRIM16's significance in neuroblastoma biology.

As TRIM16 can promote the retinoid anti-cancer signal, the first aim of my thesis is to investigate the role of TRIM16 in neuroblastoma cell growth and tumorigenicity. The hypothesis to be tested is that TRIM16 is a potential tumour suppressor in neuroblastoma and that TRIM16 overexpression will reduce neuroblastoma tumour growth.

If TRIM16 is involved in neuroblastoma tumour growth, then the mechanism of its influence needs to be elucidated and characterised. This leads to the second aim of this thesis, which is to examine the role of TRIM16 in differentiation and cell cycle progression. These areas of cell function are complex and three hypotheses will be tested to fulfil this aim. Firstly, that TRIM16 is differentially expressed during

neuroblastoma development *in vivo.* Secondly, that TRIM16 overexpression will increase neuroblastoma differentiation *in vitro,* and lastly that TRIM16 has a role in cell cycle progression.

TRIM16 is a protein that has not been well characterised. Studies of other TRIM proteins have shown their domains convey various attributes, and many key TRIM protein traits are yet to be studied in TRIM16. Exploration of these characterisations would gain a valuable insight into general aspects of TRIM16, which has significance beyond the field of neuroblastoma research. Therefore, the last aim of this thesis is to define the relationship between TRIM16 protein structure and function in neuroblastoma. To meet this aim, the first hypothesis to be tested is that TRIM16 harbours functional protein domains. The second hypothesis is more specific and poses that one region of the TRIM16 protein is required for its localisation and growth inhibitory effects.

In summary, the objective of this thesis is to research TRIM16's role in tumorigenicity, differentiation and proliferation, in neuroblastoma.

CHAPTER 2

MATERIALS AND METHODS

2.1 Cell biology techniques

2.1.1 Cell lines and culture conditions

The Neuroblastoma cell lines BE2C, SH-SY5Y, SHEP, IMR-32, NBLS cells lines were a gift from Dr. J. Biedler (Memorial Sloan-Kettering Cancer Center, New York). The human lung cancer cell lines (CALU-6 and SK-MES-1), breast cancer cells (MDA-MB-231 and MDA-MB-468), human embryonic kidney cells (HEK293), MRC-5 (lung fibroblasts), and MCF10A1 (breast fibroblasts) were obtained from the American Type Culture Collection. All cells were cultured at 37°C in 5% CO_2 as an adherent monolayer in Dulbecco's modified Eagle's medium (DMEM) supplemented with L-glutamine (Gibco/Invitrogen, USA) and 10% foetal calf serum (FCS) (Thermo Fisher Scientific), with the exception for MCF10A1 cells which had Growth Medium composed of DMEM/F12 (Invitrogen) supplemented with 10% FCS, 20 ng/mL epidermal growth factor (EGF)(Sigma, Germany), 10 μg/L insulin, 0.5 μg/mL hydrocortisone (Sigma).

2.1.2 Viability counts

The number of viable cells was determined by Trypan Blue exclusion. 30 μL of suspended cells was mixed with 30 μL of Trypan Blue solution (Gibco/Invitrogen). Using phase contrast microscopy, cells which stained blue were considered dead, whereas those that were exclusive to the stain were counted as viable. Calculation: dilution factor (2) x average of squares x 10^4 cells/ml.

2.1.3 Retinoid treatment

All-*trans*-retinoic acid (RA) (Sigma) was dissolved in 100% Ethanol to give a stock solution of 5 mM. This was made fresh weekly and stored in the dark at -70 ^{o}C. Cells treated with RA were wrapped in foil to protect from light during cell incubations and

cell culture was performed in low light conditions. Refer to Table 2.1 for further information on drugs used in tissue culture experiments.

2.1.4 Cell cycle phase synchronisation of cells

Cells were plated in 6 well plates for either flow cytometry or protein analysis, at 2 x 10^5 cells per well in 2 mL. For immunofluorescent studies this experiment was scaled down proportionally by 20 fold for cells and 5 fold for volumes, as these cells were treated in 8 well chamber slides (Lab-TekII, Thermo Fischer Scientific). The following day cells were subjected to synchronisation treatments. Cells were synchronised at the G1/S boundary using 0.7 μL of 3 μg/μL aphidicolin (AP) in 1 mL of media (Sigma) for 16 h incubation, and at the G2/M boundary using nocodazole (NZ) (Biomol, USA) 0.2 μL of 5 mg/mL in 2 mL media for 16 h following serum starvation. Synchronisation to G0 was achieved by serum starvation with 0.1% foetal bovine serum DMEM for 48 h and G1 cells were achieved by 3 h of feeding G0 cells with complete culture medium, after serum starvation. After removal of drugs, the cells were harvested at different time points 30 min, 45 min, 1 h, 2 h, 3 h, 4 h for optimisation. Cells were collected in parallel for analysis by immunofluorescence and protein extraction and for validation of cell cycle phase distribution by flow cytometry. For the cells studied, optimisation showed 3 h after feeding of AP treated cells resulted in S phase cells. 45-55 minutes of feeding of NZ treated cells produced mitotic cells.

2.1.5 Inhibition of protein synthesis and degradation

MG132 (Biomol, USA) was used to inhibit protein degradation via the proteasome. 80% confluent cells were treated with MG132 at 30 μM for 4 hours, directly before harvest. Cycloheximide (Biomol) was added to the cells at 0, 1, 2, 4, 6, 8 hours to reach

a final concentration of 0.1 mg/mL before harvest of cells. This study was used to determine the protein half-life.

Table 2.1 Summary of drugs used in tissue culture experiments

Name	**[Working]**	**[Stock]**	**Incu-bation**	**Catalogue number**	**Company**	**Stock Storage**
Retinoic Acid (RA)	10 μM	5 mM Ethanol	<7 days	R2625-50MG	Sigma	-70 ^{o}C
MG132	30 μM	10 mM DMSO	3-5 hours	PI102-0005	Biomol	-70 ^{o}C
Aphidicolin (AP)	1 μg/mL	3 μg/μL DMSO	12-18 hours	A0781-1mg	Sigma	-70 ^{o}C
Nocodazole (NZ)	0.5 μg/mL	5 mg/mL DMSO	12-18 hours	BML-T101-0010	Biomol	-70 ^{o}C
Cyclohexi mide (CHX)	0.1 mg/mL	25 mg/mL DMSO	<24 hours	GR310-1000	Biomol	-70 ^{o}C

2.2 Assays of cell phenotype

2.2.1 Measurement of DNA synthesis (proliferation) by BrdU ELISA

Incorporation of 5-bromo-2′-deoxyuridine (BrdU) was determined to evaluate DNA synthesis by a proliferation kit (Roche, Australia) according to the instructions provided by the manufacturer. Briefly, 10,000 cells were seeded in a 96 well plate, transiently transfected the following day (if transfection was required) and treated as described. The cells were incubated with BrdU (10 μM) solution for 2 hours (with the exception of MRC-5 and MCF10A1 cells, which required 5 hours), fixed with supplied solution followed by a 15 minute incubation with 5% FCS for blocking non-specific antibody binding before the addition of the primary antibody (Peroxidase-conjugated anti-BrdU). After washing in PBS the peroxidase substrate was added and the absorbance of the well contents was measured on a microplate reader at 370 nm test wavelength and 490 nm reference wavelength. Wells that were not plated with cells but subjected to treatment and ELISA steps were used as blank controls.

2.2.2 Measurement of cell viability by Alamar Blue

Alamar Blue (Molecular Diagnostics, USA) is a widely used non-toxic indicator of cell viability and metabolism, which penetrates quickly through the biological membranes and can be easily reduced by intracellular enzymes. Alamar Blue metabolism is associated with mitochondrial activity. Alamar Blue was diluted from a 10X solution (stored at -20^{o}C) in PBS and stored at 4^{o}C in the dark. It was added directly to the cell culture media of 96 well plates at a 1:9 dilution. The change of medium colour from blue to pink indicates the utilisation of Alamar Blue by actively metabolic cells. This change was quantified colourimetrically on a microplate reader at 570 nm absorbance

and 595 nm reference wavelengths. Absorbances of between 0.1 and 0.5 were used for accurate readings. Readings were performed 5 hours after the addition of Alamar Blue.

2.2.3 Cell doubling time assay

1×10^4 cells were plated in 96 well plates (day 0) and incubated overnight at 37 ^oC. On days 1,2,3,4 after plating cell viability was accessed via Alamar Blue metabolism via its absorbance. Doubling times were calculated with Prism 5 software (Graph Pad) and the initial variations in plating were adjusted for, using the day 1 absorbances in the calculations.

2.2.4 Colony assay for anchorage-dependant growth

TRIM16 overexpressing clones 4 and 5 and negative control clones 1 and 8 of the neuroblastoma BE2C cell line were mixed in 0.33% sea plaque ® Agarose (Lonza, Switzerland) in DMEM supplemented with 10% foetal bovine serum medium and plated at 1.78×10^3 cells/well on to 6 well plates containing a 0.5% agar solidified media layer. After 14 days, cells were stained with 200 µL of 5 mg/mL MTT (Sigma) per well for 3 hours, before storage at 4^oC. Cells were photographed before and after staining. Colony size and colony number were determined with Image J software (National Institute of Health, USA). At least 26 colonies were measured for each clone per experimental run. As it is not possible to determine the number of cells quantitatively for use as a threshold, the colony size which could be recognised by Image J above the background staining of the MTT was used.

2.2.5 Neurite counts

Cell neurite formation was used as an indicator of neuronal differentiation in neuroblastoma cell lines. 3×10^4 stable TRIM16 transfected clones cells were plated in 6 well plates and treated the following day, and then media was replaced every two days

with or without RA as required. Cells were analysed for neurites after 0, 2, 4 and 6 days of continuous exposure to 10 μM RA. Image J (National Institutes of Health) was used to count percentage of cells from 20X phase contrast microscopic photographs which were blinded by another researcher. Cells were scored (by eye) as positive for neurite outgrowth if they had at least one neuritic process which was approximately two times longer than the cell body width. At least three photographs were taken for each clone, time point and condition and the experiment was undertaken three times.

2.2.6 Flow cytometry

The cell cycle phase distribution of a cell population was determined by measuring cell DNA content by flow cytometry using propidium iodide (PI) (Sigma). To prepare cell samples for flow cytometry, cells were trypsinised and resuspended at a concentration of 1 x 10^6 in complete medium, then pelleted by cold centrifugation at 500 standard gravity/g-force (g_n), rinsed with PBS and recollected as a cell pellet. The cells were then resuspended in 1 mL cold PBS and were fixed in 75% cold ethanol, by adding 10 mL on top of the cell suspension and stored at 4°C, for at least overnight. Prior to flow cytometric analysis, cells were pelleted and the entire supernatant carefully discarded. Cells were resuspended in 100 μL MilliQ H_20, vortexed, and heated at 90°C for 5 minutes. The samples were treated with RNase A (Sigma) for 30 min at room temperature and then stained with propidium iodide (50 μg/mL, final concentration) for 1 hour at room temperature. The samples were analysed using a BD Caliber Flow cytometer (BD, Germany). In cell cycle analysis, cells were divided into three subsets of cells that represented the G_0+G_1 phase, S phase, and G_2+M (as determined from comparison with untreated cell control gating).

2.2.7 Immunofluorescence of endogenous proteins

Cells were grown in 8 well chamber slides (Lab-Tek II, Thermo Fischer Scientific). When cells were 50% confluent, cells were exposed to conditions required or transfected. At the time of harvest, cells were washed briefly with PBS then fixed in 4% paraformaldehyde for 15 minutes, followed by cold methanol for 10 minutes. 2% Bovine Serum Albumin (BSA) Tris-Buffered Saline with 0.5% Tween20 (TBST) was used to block non-specific antibody binding and dilute antibodies. For endogenous TRIM16 expression, cells were incubated with a 1/100 dilution of TRIM16 rabbit antibody (Rb Ab)(Sigma) in 2% BSA + TBST for 2 hours at RT followed by three washes in TBST. An Alexafluor 488 anti-Rb Ab (Invitrogen) was then added at 1/1000 dilution to detect TRIM16 protein. Appropriate isotype control antibodies were included as negative controls (DAKO, Denmark). Cells were mounted in Vector Shield media containing DAPI (Vector, USA), and confocal images were captured using an Olympus FV1000 confocal microscope, on a 100X objective.

2.3 Transfection of cells

2.3.1 Stable transfection of plasmid

Stable TRIM16 cells lines were created with TRIM16.pcDNA3.1(-).myc-His vector (modified from Invitrogen) or the empty vector. Cells were transfected with Lipofectamine 2000 (Invitrogen) as per transient transfection (below). Selection of clones occurred onwards from 48-72 h post transfection with 1 mg/ml G418. Visible colonies were expanded and screened for TRIM16 transgene protein expression. Cells were maintained in normal cell culture growth conditions during the experiment. Please note, that after thawing frozen cells, selection media was added after 48 h and reduced or ceased 24 h prior to experimentation.

2.3.2 Transient transfection of plasmid

Plasmids used for transfection are outlined in Table 2.2. Transient transfection conditions were the same for all plasmids. 50-70% confluent cells were transfected with Lipofectamine:DNA complexes in a 3:1 ratio for 6-12 hours with 1 μg DNA transfected per 1 x 10^5 cells. BE2C and SY5Y cells were transfected in serum free conditions, whereas other cells used complete culture media without the addition of antibiotics. After transfection, cells were fed with complete culture media. Cells were then maintained in normal cell culture growth conditions during the experiment unless specified otherwise. This protocol aimed for 50% or more transfected cells. Although, typically 40-70% of cells were transfected.

The pcDNA3.1-His-TRIM24 vector was gifted by Hong-Zhuang Peng of the Wistar Institute, USA. The pSG5-PML plasmid was gifted by Kun-Sang Chang of the University of Texas M.D. Anderson Cancer Centre, USA.

Table 2.2 Expression plasmids

Plasmid	Company	Tags	Resistance	Size (no insert)
pcDNA3.1(-) TRIM16-myc-His	Custom (Invitrogen)	myc His	Ampicillin Neomycin	5.5 Kb
pCMV6-TRIM16- GFP	OriGene	TurboGFP	Ampicillin Neomycin	6.6 Kb
pCMV6-MID1- GFP	OriGene	TurboGFP	Ampicillin Neomycin	6.6 Kb
HA-Ubiquitin	Custom	HA	Ampicillin	-
pcDNA3.1(-)Ub-HA	Custom (Invitrogen)	HA	Ampicillin Neomycin	5.5 Kb
pCMV6-ENTRY-p27	OriGene	myc DKK	Kanamycin Neomycin	4.9 Kb
pcDNA3.1.His-TRIM24	Custom	His	Ampicillin Neomycin	5.5 Kb
pSG5-PML	Custom	No tag	Ampicillin Neomycin	4.1 Kb

2.3.3 Transient transfection of siRNA

Knockdown of gene expression was achieved by RNA interference. Small interfering RNAs (siRNAs) were purchased commercially from Dharmacon (Thermo Fisher Scientific) and stored at -70^{o}C as aliquoted 20 μM stock (Table 2.3). Concentrations of Lipofectamine 2000, cell densities and volumes of media were all used according to manufacturer's instructions, with cells being 50-70% confluent or retro-transfected to result in this confluence. 10 nM of siRNA and 4 μL Lipofectamine2000/mL was used in the final transfection solution, which was placed onto cells. When making complexes, siRNA and Lipofectamine 2000 (Invitrogen) were diluted separately in OptiMEM (Gibco/Invitrogen) and incubated for 5 minutes at RT and then combined and incubated for 10 minutes at RT. The resulting complexes were then diluted 1:9 in OptiMEM). Media was substituted with complete culture media 8 hours after transfection (or as specified). Knockdown was assessed at the protein level at various time points after transfection.

Table 2.3 siRNA sequences used for TRIM16 knockdown

siRNA name	Target gene sequence 5'-3'	Size	Company
TRIM16_AM1	Sense: ACCUGCAUGGUGAAUUACUUU Anti-sense: PAGUAAUUCACCAUGCAGGUUU	21 mer	Dharmacon
TRIM16_AM2	Sense: CACAAAUGCAGGAGGGAGAUU Anti-sense: PUCUCCCUCCUGCAUUUGUGUU	21 mer	Dharmacon

2.4 Molecular biological techniques

2.4.1 RNA isolation and cDNA synthesis

RNA was isolated using the RNeasy mini extraction kits (Qiagen, Germany) according to manufacturer's instructions and stored at -70^{o}C. In brief, PBS washed cells were lysed directly from the culture plate either immediately or after storage at -70^{o}C. RNA was quantified using 2 µL elutate on the ND1000 Spectrophometer (Nanodrop). 1 µg of total RNA was incubated in a reaction mixture with 1 µL of 50 µM Oligo (dT) 20, 1 µL of 10 mM dNTPs, made up to 10 µL with RNase free water (Invitrogen) for 5 minutes at 65^{o}C. The solution was then placed on ice for 1 minute before the addition of 2 µL of 10X RT buffer, 4 µL of 25 mM $MgCl_2$, 2 µL of 0.1 M DTT, 1 µL of RNaseOUT, and Superscript III RT. This mixture was incubated for 50 minutes at 50^{o}C followed by a 5 minute incubation at 75^{o}C. The samples were diluted in 30 µL RNase free water and stored at -20^{o}C. All components (except the RNA) of the cDNA synthesis reaction were sourced from Invitrogen.

2.4.2 DNA isolation

Small scale DNA (both plasmid and genomic) was extracted using SV Miniprep DNA purification System Wizard (Promega) as per manufactures instructions with the exception of using half the recommended elution water volume. Large scale Plasmid DNA amounts were isolated using HiPure Plasmid Filter Maxiprep (Invitrogen) following the manufactures instructions for high-copy plasmids. DNA was quantified using 2 µL elutate on the ND1000 Spectrophometer (Nanodrop) and stored at -20^{o}C.

2.4.3 Agarose gel for DNA electrophoresis

Agarose solution (2%) was made up with Tris-Acetate-EDTA (TAE) buffer and heated in the microwave until dissolved. When cooled, SybrSafe stain (Invitrogen) was diluted

1/10,000 in sufficient volume of agarose solution for the required gel and left to set covered in foil. The gel was placed in TAE buffer in an electrophoresis tank (Bio-Rad). DNA samples were mixed in in loading buffer (Biolab, Australia) and loaded into wells. The 1 kb plus (Invitrogen) loading marker was used for quantification and size calculation of product size. Electrophoresis was at 80 V for 60 minutes, covered with foil. The gel was then visualised under UV light and specific SybrSafe filter using the Geldoc (Bio-Rad).

2.4.4 RT-PCR

1 μL of purified cDNA (0.1-1 μg) was added to a reaction mix containing, 2.5 μL 10X PCR buffer, 1.5 μL 25 mM MgCl, 2.5 μL of 10 mM dNTPs, 0.5 μL Gold taq (Invitrogen) and 1 μL of each of forward and reverse primers (10nM) (Table 2.4). The PCR starts with a denaturing step of 95^{o}C for 5 minutes then there are 30 cycles consisting of 55^{o}C annealing, 72^{o}C extension and 95^{o}C denaturation, each step running for 30 seconds. 5 μL of PCR product was then run on 12% polyacrylamide gel and checked for product size and purity.

Table 2.4 TRIM16 RT-PCR primers

Name	Sequence	Length of primer (bp)	Product size (bp)
EBBP F1	CAGGCTCCAGGCTAACCAAAAG	20	130
EBBP R1	TCCTCTAAGAAGGGCATCACATTG	24	
β2M F1	ACCCCCACTGAAAAAGATGA	20	114
β2M R1	ATCTTCAAACCTCCATGATG	22	

2.4.5 DNA Sequencing

When there was one dominant DNA band of the correct size, 5 μL of the PCR product was incubated at 37^{o}C for 30 minutes with 2 μL Exo/SAP-IT (USB, Affymetrix, USA) enzyme mix to cleave primers from the PCR product. 10 μL of purified DNA (500 μg) was sent at ambient temperature with 100 ng of a single primer in 1.5 mL eppendorf tubes. The sequencing reaction was carried out by Australian Genomic Research Facility, Sydney node, using capillary separation on AB3730xI sequencer. Sequences were analysed on Mutational Surveyor 3.97V-Demo (Soft Genetics, USA).

2.4.6 Extraction of protein whole cell lysates

Cells were washed twice with cold PBS, and either lysed immediately wherever possible or stored at -70^{o}C. Lysis was performed with ice cold lysis buffer containing a protease inhibitor cocktail (Complete tablets, Roche). Cells were incubated in buffer for 10-20 minutes on ice and then scraped with a cell scraper and pipetted into 1.5 mL eppendorf tubes, followed by a 5 second vortex. Tubes were then placed in a wet ice water bath sonicator for 10 minutes, then votexed again briefly. Cell lysates were then centrifuged at 14,000 g_n for 20 minutes and the supernatant transferred to new tubes for storage.

Either RIPA buffer or NP-40 buffer was used to obtain whole cell protein lysates. RIPA buffer was comprised of 150 mM NaCl (Ajax Finechem), 0.5% Sodium deoxycholate (Sigma), 10 mM Tris-Cl (Ajax Finechem), 0.125% SDS (MP Biochemicals), 0.01% Nonidet-40 (NP-40) (Fluka). NP-40 buffer was used specifically for immunoprecipitation experiments. The NP-40 buffer used consisted of 50 mM Tris-HCl pH8 (Ajax Finechem), 5 mM EDTA pH8 (Ajax Finechem), 0.5% NP40 (Fluka)

and 50-150 mM NaCl (Ajax Finechem) as specified. Both buffers were stored at 4^{o}C or frozen in aliquots at -20^{o}C after the addition of protease inhibitors.

2.4.7 NE-PER nuclear and cytoplasm protein extraction

The Pierce NE-PER® Nuclear and Cytoplasmic Extraction Kit (Thermo Scientific) was used according to manufactures instructions, with the exception that cells were lysed fresh from the culture plate. All incubations and centrifugations were on ice or at 4^{o}C. In brief, cells were lysed fresh from 6 well plates with 100 µL CERI solution with protease inhibitors (Roche) and incubated until cells detached from the culture plates, as determined by phase contrast microscopic evaluation. Cells and buffer were transferred to 1.5 mL eppendorf tubes and briefly vortexed and incubated with CERII solution for 1 minute and centrifuged for 10 minutes at 14,000 g_n. The supernatant (cytoplasmic protein fraction) were transferred into new tubes. The remaining cell nuclei were lysed with NER solution with protease inhibitors and incubated for 40 minutes with votexing every 10 minutes. Finally the solution was centrifuged for 10 minutes at 14,000 g_n. The supernatant (nuclear protein fraction) was transferred into a new tube and stored at -70^{o}C.

2.4.8 Protein quantification

Quantification of proteins was conducted using the Pierce BCA protein Assay Kit (Thermo) as per manufacturer's instructions.

2.4.9 Immunoprecipitation

During all steps lysates were kept at 4^{o}C. Cells were lysed fresh on ice in NP-40 buffer. 1 mg of protein was diluted to reach a volume of 500 µL in NP-40 buffer, this was incubated on a rocker with 50 µL of sepharose for 30 minutes to pre-clear the lysate. Sepharose A (ZYMED) was used for conjugation with rabbit antibodies and Sepharose

G for mouse antibodies (GE bioscience). Beads were centrifuged at 10,000 g_n for 2 minutes and the supernatant kept and transferred to a new 1.5 mL tube. 25 μL of lysate was put aside for later use in Western blotting to ensure adequate expression of the proteins of interest in the input solutions of the experiment. 0.5 μg of antibody was added to the remaining lysate and incubated for 2 hours with gentle rocking. 50 μL of sepharose beads were then added for 1 hour with rocking. Beads were spun down, the supernatant was disposed and the beads were washed three times with 500 μL of NP-40 buffer. 50 μL of 2X XT (previously diluted with NP-40 buffer to 2X) loading buffer (Bio-Rad) containing 100 mM DTT was vortexed with the beads and boiled at 95^{o}C for 5 minutes. The samples were vortexed again, followed by mini-centrifugation and placed on ice before loading on a Western blot gel.

2.4.10 Ubiquitination assay

Cells were transfected with GFP/myc tagged TRIM16/mutant and HA-Ub expression plasmid for 24 hours before 4 hours incubation with the proteasome inhibitor MG132 (Biomol) to preserve the polyubiquitin chain and then lysed under denaturing conditions. 2 mg of protein was immunoprecipitated as above with 1 μL of specified antibodies, before denaturation.

2.4.11 Western blotting

Samples containing 20 μg of protein (or otherwise specified) were mixed with 4X XT protein loading buffer (Bio-Rad) containing 200 mM DTT (Sigma) and boiled at 95^{o}C for 5 minutes. Samples were quick spun and placed on ice before loading. The samples were loaded on to 10% polyacrylamide criterion gels manufactured by Bio-Rad. Gels were run for 10 minutes at 80 V and then increased to 120 V for 10 minutes, before being run at 150 V until the dye front reached the bottom of the gel in Tris-Glycine-

SDS solution. The proteins on the gel were transferred onto Hybond-C nitrocellulose membrane (Amersham, UK) at 4^{o}C, at 20 V overnight or 30 V for 2 hours in 20% methanol Tris-Glycine solution. Membranes were then stained with Ponceau-S stain (Sigma) and trimmed for particular protein sizes.

Membranes were blocked in 10% skim milk in TBST for 1 hour. Membranes were washed briefly in TBST for 2 minutes, before incubation with primary antibody for 2 hours at RT or overnight at 4^{o}C, at concentrations and conditions as specified in Table 2.5. Generally dilution of antibodies was in 0.5% milk TBST, unless otherwise stated. Membranes were washed in TBST for 3 x 5 minute incubations. After washing membranes were incubated with 0.5% milk TBST containing 1:2000 dilution of HRP-conjugated anti-mouse antibody (Pierce/GE, USA) (if primary Ab was raised in mouse), or 1:10,000 dilution of HRP-conjugated anti-rabbit (Pierce) (if primary Ab was raised in rabbit). Membranes were then washed in TBST three times for 5 minute incubations.

Chemiluminescence detection was performed using SuperSignal reagents (Pierce). Solutions were mixed at a 1:1 ratio and poured over membranes and incubated in the dark for 5 minutes, before excess solution was removed and plastic film was used to encase the membrane. X-ray films were exposed to the membrane in the dark and placed in X-Ray film developer for a range of exposures times. QuantityOne software (Bio-Rad) was used to quantify the resulting protein bands.

If re-probing of another antibody was required, membranes were striped with Restore Striping Reagent (Pierce) for 20 minutes at RT, and then washed twice with TBST for 2 minutes.

Table 2.5 Primary antibodies used for Western blots and their conditions

Primary Antibody	Manufacturer	Catalogue number	Source	Dilution	Size
TRIM16	Bethyl	A-301-160A	Rabbit	1:3000	68
TurboGFP	Evrogen	AB514	Rabbit	1:10,000 (10% milk TBST)	-
Myc tag	Cell signalling	2276	Mouse	1:2000	-
His tag	Cell signalling	2366	Mouse	1:500	-
HA tag	Santa Cruz	Sc-805	Rabbit	1:250	-
Cyclin E1	Cell signalling	4129	Mouse	1:500	42+50
Cyclin D	Calbiochem	DCS-6	Mouse	1:300	35
Cyclin A	Cell signalling	4656	Mouse	1:500	55
Cyclin B	Cell signalling	4138S	Rabbit	1:500	59
CDK4	Cell signalling	2906	Mouse	1:500	30
CDK6	Santa Cruz	Sc-177	Rabbit	1:500	35
pRb Ser780	Cell signalling	9307	Rabbit	1:500	110
p27	BD	610241	Mouse	1:5000	27
Topoisomerase	Santa Cruz	Sc-10783	Mouse	1:5000	100
αTubulin	Sigma	T9026	Mouse	1:5000	50
Actin	Sigma	A2066	Rabbit	1:10, 000	42
PML	Abcam	Ab53773-100	Rabbit	1:400	80
Ubiquitin	Santa Cruz	Sc-8017	Mouse	1:500	-

2.5 TRIM16 domain deletion and localisation mutants

2.5.1 GFP construct design

The domain mutants were created by cloning TRIM16 (NM_006470.3) into the pCMV6-AC-GFP vector (OriGene, USA) (Figure 2.1).

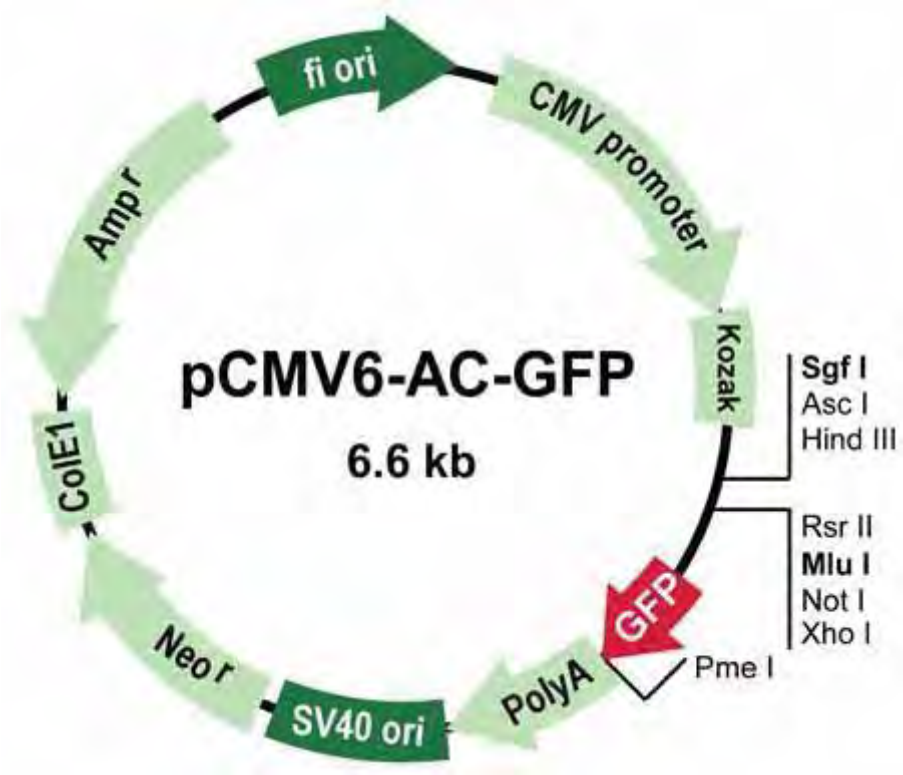

Figure 2.1 Structure of the GFP empty vector (EV) from OriGene

2.5.2 Synthesis of TRIM16-GFP domain deletion mutants

The TRIM16-GFP domain deletion mutants were produced by OriGene (Rockville, MD, USA) (Figure 2.2). Deletion mutants were produced by PCR of full length TRIM16 cDNA (NM_006470.3) using the primers in Table 2.6. The PCR product was purified, phosphorylated with T4 DNA kinase, then recirculised by ligation, and used for transformation. Bacteria were selected with ampicillin plates and single colonies expanded for plasmid DNA purification (Mini Wizard Kit, Promega, USA) and validation by sequencing (performed by OriGene), restriction digest and Western blot. Predicted kDa sizes were calculated on The Sequence Manipulation Suite (Bioinformatics Organization, USA) http://www.bioinformatics.org/sms/prot_mw.html .

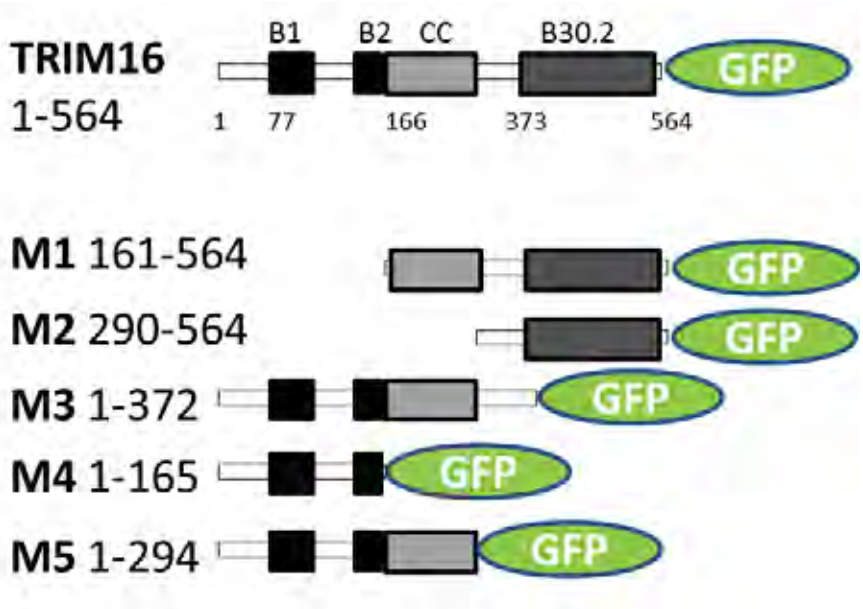

Figure 2.2 TRIM16 domain deletion mutants

B = B-box, CC = coiled coil, B30.2 = B30.2/SPRY/RFP-like

2.5.3 Synthesis of TRIM16-GFP localisation point mutants

Wildtype TRIM16 expression vector pCMV-AC-TRIM16-GFP was used as the template to produce the protein localisation mutants (in house). The Quick Change Site Directed Mutagenesis Kit (Stratagene, USA) was used as per manufactures instructions. Primers were designed with mismatched pairing to create a PCR produced vector with the desired base changes (refer to Table 2.6 for primers). Two evolutionarily conserved amino acids were mutated in TRIM16 for each site of interest (Figure 2.3). The PCR products were cleaved with DpnI restriction enzyme to remove non-mutated plasmid and this product was used to transform competent bacteria provided by the Quick Change Kit. Bacteria were selected with ampicillin plates and single colonies expanded for plasmid DNA purification (Mini Wizard Kit, Promega) and DNA sequencing validation. EBBP primers for RT-PCR were used to sequence TRIM16 DNA inserts. GFP fluorescence and protein expression further confirmed sequence maintained wildtype TRIM16 size and correct in-frame translation.

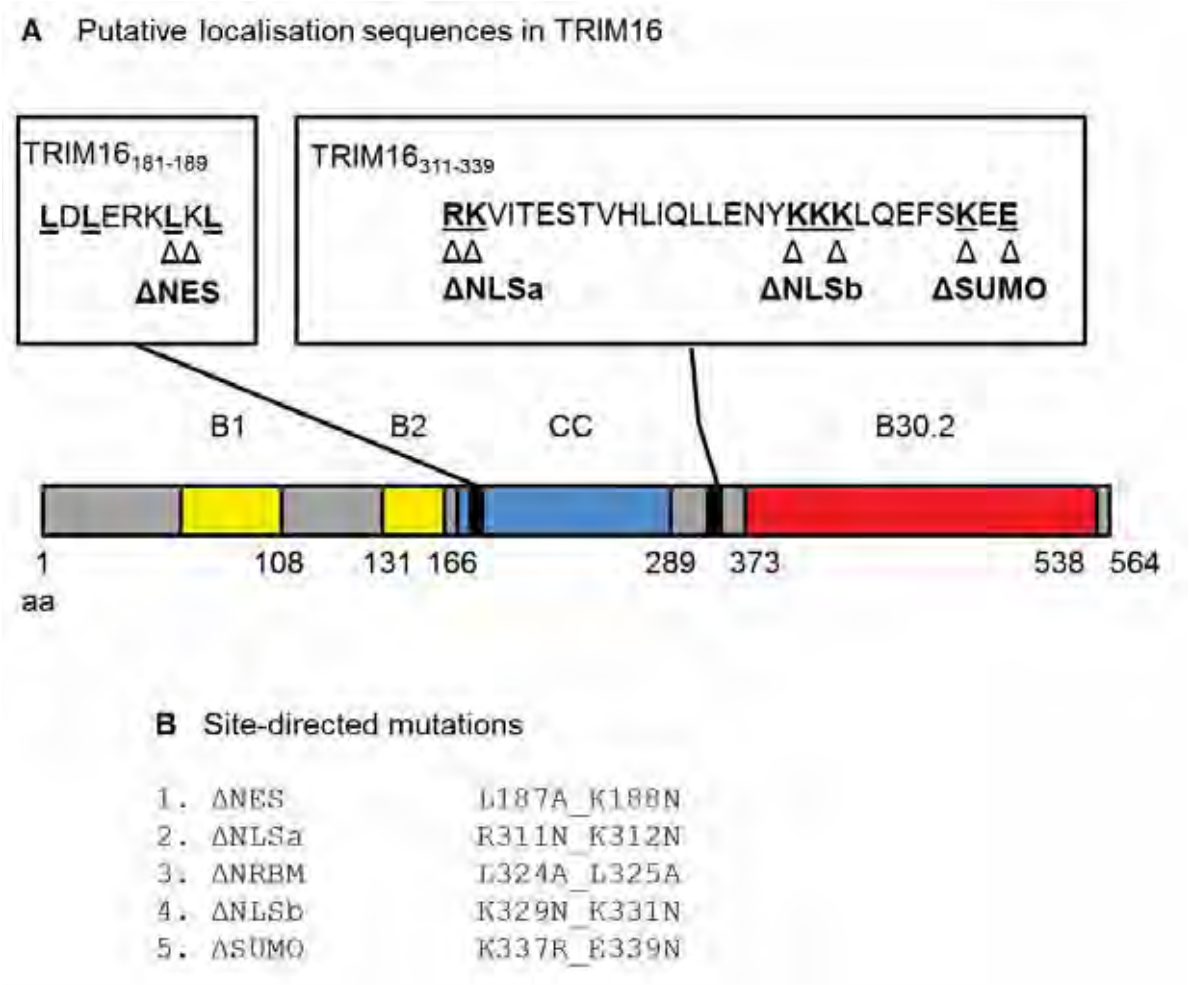

Figure 2.3 Putative protein localisation sites for TRIM16 and corresponding mutants

A) Putative localisation sequences within wildtype. Amino acid underlined and in bold show putative sequences, delta signs show the amino acids mutated. TRIM16. B) Site directed mutations.

Table 2.6 Primers used to generate and sequence TRIM16-GFP mutants

Primer name	Primer sequence 5'-3'	Mutant
Fm1	ATGACCATAGTCTCCCTGGATGCAG	M1
pEntry_Rm	GGCGATCGCGGCGGCAGATCTCCTC	
Fm2	ATGAACACTGAAGACATCACCTTCCC	M2
pEntry_Rm	GGCGATCGCGGCGGCAGATCTCCTC	
Rm3	CGCATATTGGAGGAACTGTTCCCTG	M3
pEntry_Fm	ACGCGTACGCGGCCGCTCGAGATG	
Rm4	CAGGGAGACTATGGTGTGGCCACTG	M4
pEntry_Fm	ACGCGTACGCGGCCGCTCGAGATG	
M5 F	CTCTGGCGATCGCCATGGCTGAGTTGGATCTAATGGCTCCAGG	M5
M5 R	GGTGTACGCGTGATGTCTTCAGTGTTCTTAAACTTGCAG	
L187A_K188N	CAGTTAGACTTGGAGCGGAAAGCCAATTTGAATGAAAATGCC ATCTC	ΔNES
L187A_K188N _as	GGAGATGGCATTTTCATTCAAATTGGCTTTCCGCTCCAAGTCT AACT	
R311N_K312N	AGGATAAACTCTCGGGCATCAACAATGTTATCACGGAATCCA CTGT	ΔNLSa
R311N_K312N_as	ACAGTGGATTCCGTGATAACATTGTTGATGCCCGAGAGTTTAT CCT	
L324A_L325A	GGAATCCACTGTACACTTAATCCAGGCGGCGGAGAACTATAA GAAAAAGCTCCAG	ΔNRBM
L324A_as	CTGGAGCTTTTTCTTATAGTTCTCCGCCGCCTGGATTAAGTGTA CAGTGGATTCC	
K329N_K331N	CTTAATCCAGTTGCTGGAGAACTATAATAAAAATCTCCAGGAG TTTT	ΔNLSb
K329N_K331N_as	TGGAAAACTCCTGGAGATTTTTATTATAGTTCTCCAGCAACTG GATTAAG	
K337R_E339N	GAAAAAGCTCCAGGAGTTTTCCAGGGAAAATGAGTATGACAT CAGAACTCAAGT	ΔSUMO
K337R_E339N_as	ACTTGAGTTCTGATGTCATACTCATTTTCCCTGGAAAACTCCTG GAGCTTTTTC	
EBBP F1	CAGGCTCCAGGCTAACCAAAAG	Used for sequencing
EBBP R1	TCCTCTAAGAAGGGCATCACATTG	

2.5.4 Transformation of bacteria with plasmid DNA

Competent bacteria (either XL10-Gold (Stratagene) or DH5α (Biolab) were thawed on ice and aliquoted at 25 μL into 5 ml (BD) round bottomed tubes. For StXL10-Gold cells 4 μL of β-mercaptoethanol was added for 5 minutes. 1 μg Plasmid DNA was added to the bacteria for 10 minutes on ice. Cells were then subjected to 45 seconds at 42^{o}C in a water bath, before being placed immediately on ice for 2 minutes. 300 μL SOC buffer (Bioline, Australia) was added to each tube and the cells were incubated in a shaking incubator at 37^{o}C for 30 minutes. The transformed cells were plated at 1:100 and 1:2 dilutions on antibiotic containing plates with a sterile plastic hockey stick. Non-transformed cells were used as a negative control to ensure adequate selection.

2.5.5 Restriction enzyme digest for confirmation of plasmid quality and insert size

For OriGene vectors CMV6-AC-GFP and pCMV6-ENTRY, a total volume of 25 μL reaction mix was used. 1 μg of vector was incubated with 1 μL MluI and 1 μL SgfI enzymes with 2.5 μL 10X buffer C (Promega) for 2 h at 37 ^{o}C. Digested fragments were loaded on a 2% Agarose gel, and electrophoresed for 1 hour at 80 V.

2.5.6 Detection of mutant protein expression

Cells were plated to reach a confluence of 60% 24 h prior to transfection. Cells were transfected with Lipofectamine:DNA complexes in a 3:1 ratio for 36 hours and whole cell lysates were analysed for the presence of the transgene by Western blot using TurboGFP antibody (Evrogen, Russia) according to manufactures instructions. Mutant expression was also visualised by fluorescent microscopy via the GFP tag on the transgene proteins. Cells were transfected in 8 well chamber slides and fixed at 36 hours post-transfection. Fixing involved a quick PBS wash followed by 15 minute incubation

with 4% paraformaldehyde in PBS. Cells were then given a quick wash in PBS before a five minute incubation with 0.1% Triton X-PBS solution and two subsequent PBS washes. Cells were mounted with DAPI stain Vector Shield Media (Vector) and a glass coverslip anchored in place with nail polish and stored in the dark at 4^{o}C. Confocal images were captured on an Olympus FV1000 confocal microscope, using a100X objective (Olympus, Japan). Quantification of exogenous localisation was performed by eye with counts of at least 30 cells from multiple runs. For mutants ΔNES and ΔNLSb less than 30 cells in some runs were counted due to low levels of expression. Transfected cells were recorded as either 'cytoplasmic and nuclear' or 'predominately cytoplasmic'. The results were expressed as a percentage rounded to the nearest 5%. Predominantly nuclear localisations were not observed for exogenous expressions studies.

2.6 Mouse models of neuroblastoma

2.6.1 BE2C Xenografts

2.6.1.1 Engraftment and monitoring

To produce neuroblastoma xenografts in mice, $5x10^6$ stably transfected BE2C cells were injected into BALB/c nu/nu mice (Sourced from the Australian BioResources, Sydney). Tumours were measured at least twice weekly and mice were culled when tumour mass equalled or exceeded 1000 mg, as determined by calculation of tumour volume ([length x width x depth]/2). Tumour mass was calculated as previously described [338,339]. The size of tumours was calculated from measurements on live animals. Tumours were portioned and either frozen for molecular analysis or fixed in 10% buffered formalin, followed by 70% ethanol before paraffin embedding and histological sectioning.

2.6.2 TH-MYCN animal Model

2.6.2.1 Genotyping TH-MYCN mice

TH-MYCN mice were housed at CCIA and maintained according to ACEC UNSW Ethical Approval 03/89. After birth mice were genotyped by DNA extracted by Chelex (Bio-Rad, Australia) from tail tipped samples and analysed by real time as PCR described in Burkhart *et al.* [340].

2.6.2.2 Tissue preparation of TH-MYCN animal tissues

Mice were culled via CO2 asphyxiation and an incision at the base of the skull and across the abdomen allowed infusion of 4% formalin in PBS, for at least 24 hours. Later mice were fixed in 70% ethanol (v/v) for at least 24 hours. Mice were dissected into ventral halves and placed in histology cassettes. Larger animals were also divided into

smaller segments at the base of the skull and at the diaphragm as required. The tissues were decalcified by fresh 4% HCl and 4% formic acid solution overnight. Tissues were incubated in 5% ammonia solution for 30 minutes before rinsing in water than stored for up to a week in 70% ethanol before paraffin embedding.

2.6.2.3 Immunohistochemistry

The Histology and Microscopy Unit at the University of New South Wales or The Veterinary Histology Unit at The University of Sydney, performed all sectioning and paraffin embedding of tissues onto glass histology slides.

Slides were de-parafinised and rehydrated through a series of washes including 3 x 5 minute incubations in Xylene and then 2 x 5 minutes incubations in 100% (v/v) Ethanol, followed by 2 minute washes in 95%, 90%, 70% ethanol baths, and a 2 minute wash in milli-Q water.

Samples were then subjected to antigen retrieval by placing slides in boiling hot 10 mM sodium citrate antigen retrieval buffer (9 mL of 0.1 M citric acid solution and 41 mL of 0.1 M sodium citrate solution pH6 in 450 mL of water) for 20 minutes in a dry oven set at 104 ^{o}C. Slides were left to cool on the bench for a further 20 minutes. The tissues were then blocked against endogenous peroxidise activity with 3% peroxide in water for 10 minutes, followed by 2 x 2 minute washes in PBS. A hydrophobic marker was used to draw a barrier around the tissue.

Slides were then blocked in 2% goat serum (Invitrogen), or 2% BSA (Sigma) in PBS-0.5% Tween 20 (Tween20 is sourced from Sigma) (PBST) for 30 minutes or MOM immunodetection kit (Vector) diluted blocking reagent (if the primary antibody was raised in mouse). If using the MOM reagents, tissues were then washed briefly in

PBST and incubated in the MOM diluent for five minutes. This same diluent was then used to dilute the antibodies. Otherwise antibodies were diluted in 2% goat serum or 2% BSA in PBST. The primary antibodies were diluted (as shown in Table 2.7) and incubated on sections overnight at 4^{o}C. The following morning, slides were left at room temperature for 30 mins. Tissues were washed 3 x 2 minutes in PBST. Biotinylated secondary antibodies (DAKO/Vector) were diluted (1/500) and added to sections for a 1 hour incubation at RT. Tissues were then washed 3 x 2 minutes in PBST.

Two drops of streptavidin/HRP (DAKO) or sufficient volume to just cover the tissues was added to the sections and allowed to incubate for 45 minutes. The tissues were then washed three times briefly in PBST. Staining was visualised by adding DAB (3-3' diaminodenzidine tetrachloride) (DAKO) for up to 10 minutes or as soon as staining appeared. Tissues were washed in water for 5 minutes and then immersed in haematoxylin (Fluka) for 5 minutes for counterstaining of the cell nuclei. Slides were than immersed in gently running hot tap water for 5 minutes to activate the haematoxylin staining.

The tissues were dehydrated by 2 minute washes in 70%, 80%, 95% ethanol baths, followed by 3 x5 minute washes in 100% ethanol, with the last wash using fresh Ethanol. This was followed by 3 x 10 minute washes in xylene (the first being fresh). Mounting media (EUKITT) was then placed in the middle of the specimens, before covering with a glass coverslip (Menzel-Glaser GmbH). Slides were left in the fume cabinet for 2 days to ensure adequate hardening of the mounting media.

Whole slides were digitally scanned with Aperio ScanScope XT (San Diego, USA), at The Histology and Microscopy Unit at the University of New South Wales.

Table 2.7 Antibodies used for immunohistochemistry staining of TH-MYCN mouse tissues

Name	Manufacturer	Catalogue Number	Animal	Dilution	Secondary Antibody
TRIM16	Bethyl	A301-160A	Rabbit	1/200	Anti-Rabbit (DAKO) 1/500
βIII-Tubulin	Covance	PRB-435P	Rabbit	1/2000	Anti-Rabbit (DAKO) 1/500
p27	BD	610241	Mouse	1/100	MOM (Vector)
Cyclin E	Cell Signalling	4129	Mouse	1/100	MOM (Vector)

2.7 Statistical analysis

Averaged replicates of three independent experiments were used in molecular and tissue culture studies. This data was statistically analysed using the two-tailed, unpaired Student t-test. Results were expressed as mean values with 95% confidence intervals. Error bars displayed represent the standard error of the mean. Differences were analysed among groups using ANOVA. Values with a p value less that 0.05 were considered statically significant. The statistics software GraphPad Prism 5 was used for statistical calculations and to produce graphs.

CHAPTER 3

RESULTS I: THE ROLE OF TRIM16 IN PROLIFERATION AND TUMORIGENICITY

3.1 Introduction

The retinoid anti-cancer pathway is an important growth and differentiation regulatory pathway in neuronal tissue and neuroblastoma [54]. RARβ is a key factor in the signalling of this pathway and a tumour suppressor gene in neuroblastoma and other cancer types (discussed in 1.4.5, 1.4.6). Human neuroblastoma cells undergo growth inhibition and differentiation after treatment with retinoid *in vitro* [4]. In 2006, TRIM16 was identified as a novel positive regulator of RARβ transcription [8]. TRIM16 binds the βRARE element in the promoter region of the RARβ gene and promotes the retinoid anti-cancer signal in neuroblastoma. TRIM16 was also able to restore sensitivity to retinoid treatment by induced RARβ expression and growth inhibition, in retinoid resistant lung and breast cancer cell lines [216]. Additionally, in skin wound models, TRIM16 endogenous expression was reduced in highly proliferative regions of healing skin. [330]. Thus, it was predicted that TRIM16 would have a negative effect on neuroblastoma cell proliferation and tumour growth.

Other TRIM proteins, PML and TRIM24, have been recognised as classical tumour suppressors [9]. PML was first described in 1991 [237], due to its association with the chromosomal translocations that cause the majority of acute promyelocytic leukaemia (APL) cases. Also, the deletion or aberrant expression of PML is involved in several human cancers [239]. Furthermore PML has been shown to have a tumour suppressor-like role in neuroblastoma [264,265]. Interestingly, the treatment of neuroblastoma with retinoic acid promotes the formation of PML bodies. PML bodies are large protein complexes in the nuclei of cells, which are associated with stress responses, differentiation and transcriptional control, among several published functions [236,238,241,246,261,264,265,341,342]. Research has also shown that TRIM16 co-

localises with PML in retinoid stimulated PML bodies in neuroblastoma [8]. TRIM16 and PML both possess the putative B-box and coiled-coil domains of TRIM proteins and both also have a functional role in retinoid treatment response, adding strength to the hypothesis that like PML, TRIM16 can also inhibit tumour growth.

The focus of this study was to examine the role of TRIM16 in cell proliferation and tumorigenicity in neuroblastoma. The hypothesis to be tested was that TRIM16 is a potential tumour suppressor in neuroblastoma and TRIM16 overexpression will reduce neuroblastoma (tumour) growth. In order to get a robust answer, the best approach was to use both *in vivo* and *in vitro* studies. Thus, one critical goal of this study was to establish stable TRIM16 overexpressing neuroblastoma cells, which were suitable for *in vitro* experiments and also mouse xenograft studies.

To address my aims, I used an approach as follows; firstly, a study for determining endogenous TRIM16 protein expression was performed on various cancer and normal cell types. This was in order to understand the range of protein levels of TRIM16 in cells. Then, TRIM16 was transiently transfected into neuroblastoma and normal cell lines, and the proliferation of these cell lines was accessed. Then a stable cell model of TRIM16 overexpression was developed and validated. The initial validation involved transgene expression studies and an assessment of cell growth, to ascertain if a similar model to that achieved with transient transfection experiments had been produced. Furthermore, these clones were used to determine whether TRIM16 stable overexpression conveyed increased sensitivity to retinoid. Anchorage-independent growth, in soft agar was used to determine if these cells had a high probability of growth in the Balb/c nu/nu nude mouse model. Finally, the stable transfected cells were used in xenograft studies in Balb/c nu/nu nude mice.

3.2 Results

3.2.1 Endogenous TRIM16 expression in various cancer and non-cancer cells

In order to understand the basal levels of TRIM16 in neuroblastoma cell lines as well as other cancer and non-cancer cell lines, the protein expression levels in a variety of cell lines were determined by Western blot (Figure 3.1A). This shows that TRIM16 is highly expressed in the majority of cell lines tested. For each neuroblastoma cell line there are different banding patterns, each having multiple bands of protein detected by the anti-TRIM16 antibody. Of the other cells types, the MDA-MB-231, MDA-MB-468 breast cancer cells and SKMES-1 lung cancer cells had distinctly high expression of TRIM16 protein.

The localisation properties of TRIM16 have not been studied in depth. Others have shown that COS-1 (immortalised kidney) cells, HaCaT (immortalised keratinocytes) cells and BE2C neuroblastoma cells have predominately cytoplasmic, expression of TRIM16 [8,330]. To confirm this finding, we investigated the cellular location of endogenous TRIM16 in four cell lines with high TRIM16 protein expression. These immunofluorescence studies demonstrate that TRIM16 is expressed predominately in the cytoplasm of the cell lines tested (Figure 3.1B). RA has been shown to affect the endogenous localisation of TRIM16 in BE2C neuroblastoma cells [8], a trend which was confirmed in this study. BE2C cells had increased levels of nuclear TRIM16 after retinoid treatment. However, only neuroblastoma cells showed an increase in TRIM16 in the nucleus when compared to other cell lines. Interestingly, the breast (MDA-MB-231) and lung cancer (SKMES-1) cell lines which are known to be retinoid resistant, have peri-nuclear accumulations of TRIM16 after RA treatment.

TRIM16 is therefore expressed in a wide variety of tissues at the protein level and its expression is predominately cytoplasmic.

A

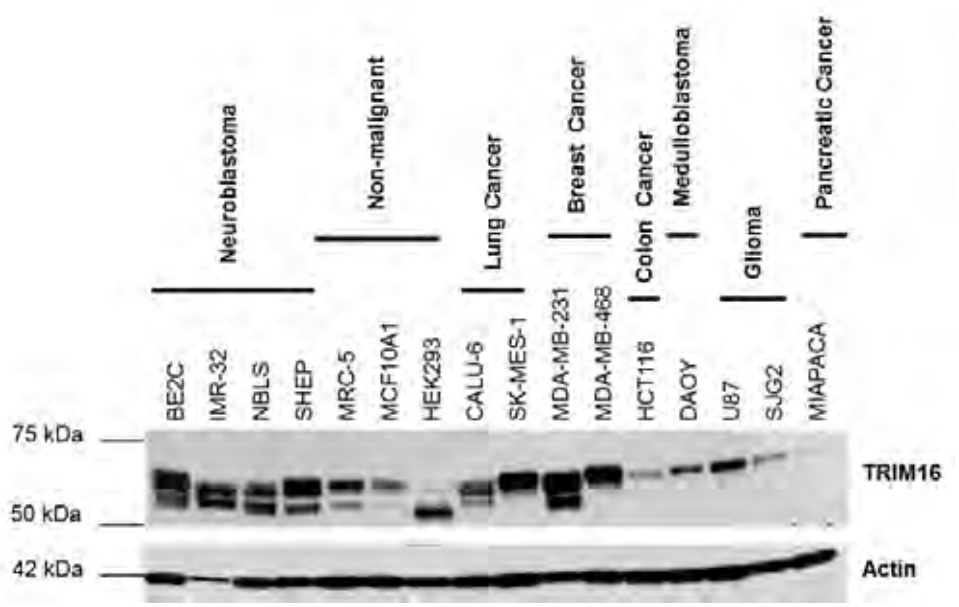

B

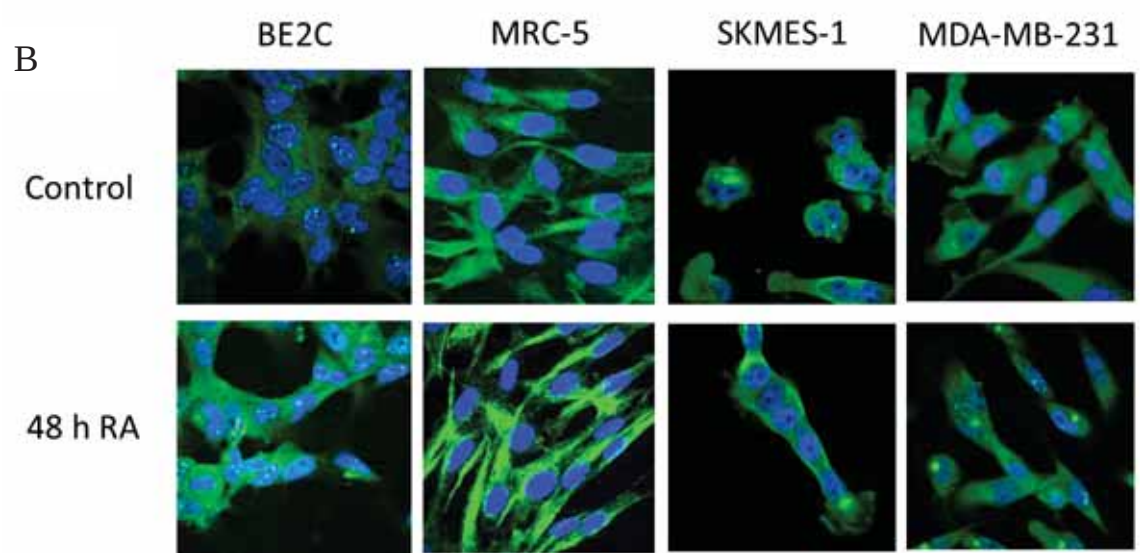

Figure 3.1 Endogenous TRIM16 protein expression in cancer and non-cancer cells

A) Western blot of endogenous TRIM16 (Bethyl Ab) from whole cell lysates. B) Endogenous TRIM16 (Custom Ab B4001) conjugated with alexafluor488 (green fluorescence). Cells were counterstained with DAPI (blue nuclear marker). Images were captured with confocal objectives at 100x (FV1000, Olympus).

3.2.2 TRIM16 overexpression causes decreased proliferation in neuroblastoma cell lines

To determine if TRIM16 overexpression could cause growth inhibition in neuroblastoma, TRIM16 was overexpressed in two neuroblastoma cell lines and BrdU incorporation was used to access the number of cells in the S phase of the cell cycle, 72 hours after transfection. The transfection was also combined with retinoid treatment to determine if both TRIM16 overexpression and retinoid treatment produced an additive inhibitory effect on cell proliferation.

In both neuroblastoma cell lines, there was a significant decrease in the number of proliferating cells when TRIM16 was overexpressed compared to those cells transfected with the empty vector (EV) (Figure 3.2). Interestingly, there was also an enhanced effect upon the combination of retinoid treatment and TRIM16 overexpression in the BE2C cells (compared with either condition alone).

3.2.3 TRIM16 overexpression does not cause decreased proliferation in non-malignant cells

In order to investigate if growth inhibition after TRIM16 overexpression was specific to neuroblastoma cells, non-malignant cells were transfected with TRIM16. As there are no non-malignant tissue equivalent cell lines for neuroblastoma commercially available, two non-malignant and well characterised cell lines, which could be easily transfected were used from different tissue origins. As shown in Figure 3.3, TRIM16 overexpression did not decrease the proliferation of the lung cell line MRC-5 and the breast cell line MCF10A1. Even in the MCF10A1 line which is retinoid responsive, TRIM16 overexpression failed to slow cell proliferation.

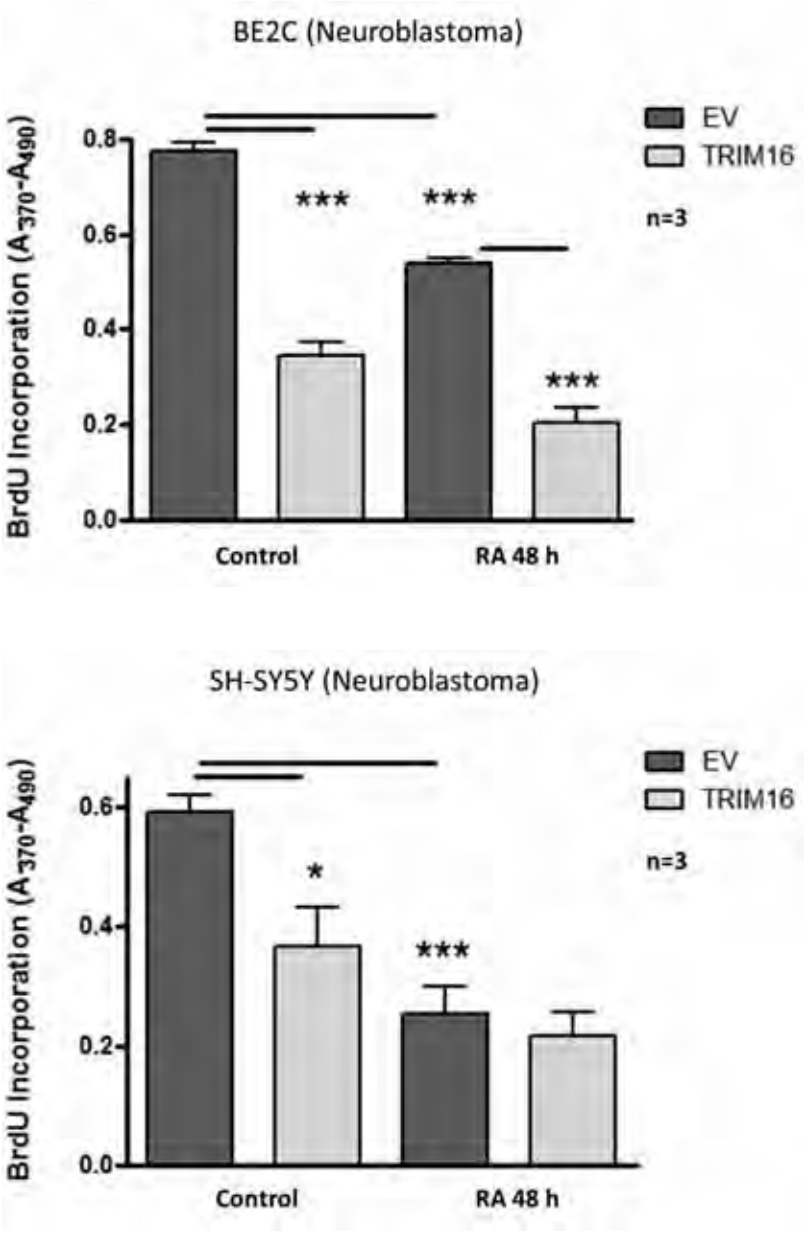

Figure 3.2 TRIM16 overexpression causes decreased cell proliferation in neuroblastoma cell lines

Cells were transfected with empty vector (EV) or TRIM16-myc-His plasmids. 24 h post transfection, cells were treated with 10 μM RA. At 72 h post transfection cells were accessed by proliferation BrdU ELISA (Roche). *p<0.05, ***p<0.001

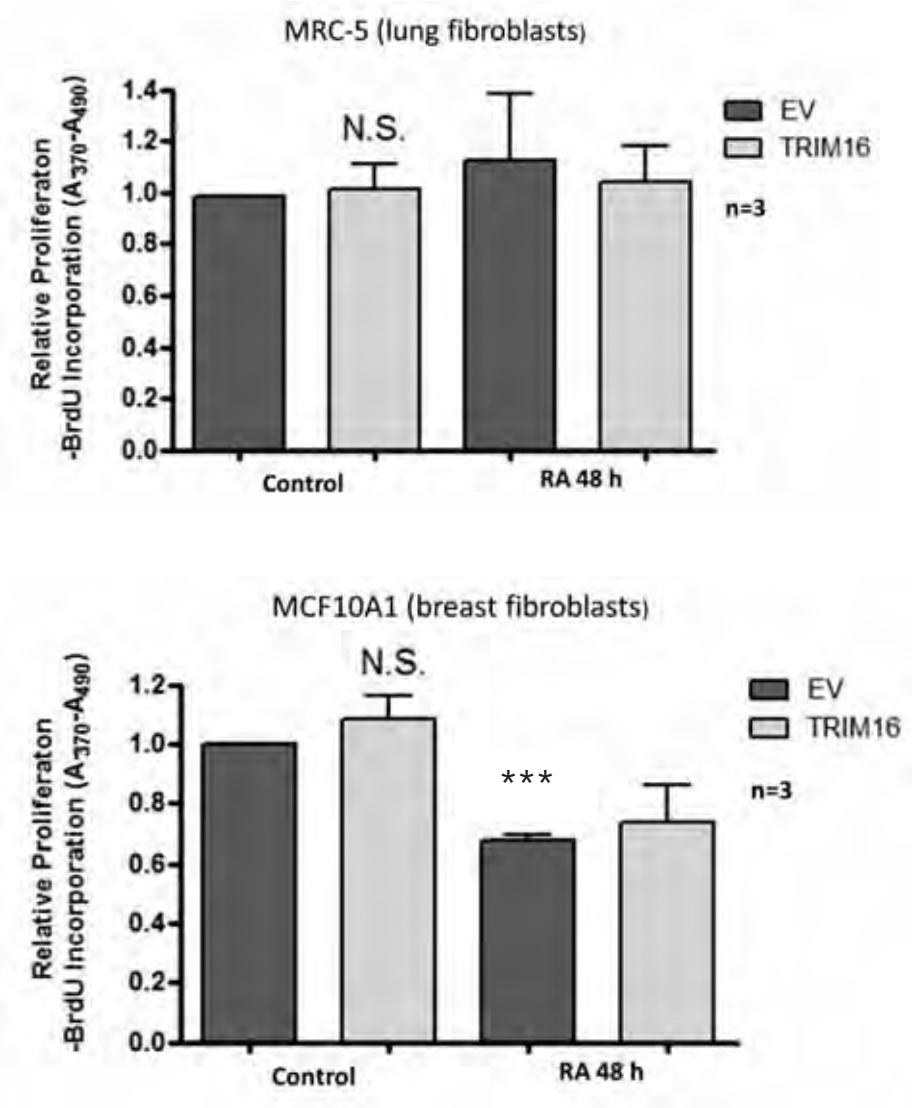

Figure 3.3 TRIM16 overexpression does not cause growth inhibition in non-malignant cell lines

Cells were transiently transfected with empty vector (EV) or TRIM16-myc-His plasmids. 24 h post transfection cells were treated with 10 μM RA. At 72 h post transfection cells were accessed by proliferation BrdU ELISA (Roche). ***p<0.001 . N.S. = Not significant

3.2.4 Screening and identification of TRIM16 overexpressing stable cells

As TRIM16 overexpression produced growth inhibition, I wanted to determine if this effect would also result in decreased tumour growth *in vivo*. For this research, stably transfected cells were required. BE2C cells were transfected with a TRIM16-myc-His tag plasmid. Clones which survived G418 selection were expanded and screened for protein expression of the transgene (2.3.1).

Of the 60 clones originally isolated and expanded, 12 clones could be established, and of these, 4 clones expressed exogenous TRIM16 at the protein level. Two empty vector clones (EV-1 and EV-8) and 2 TRIM16-myc-His clones (TRIM16-4 and TRIM16-5) were chosen for characterisation and use in future experiments. To confirm TRIM16-myc-His expression, protein expression was determined by Western blot and immunofluorescence (Figure 3.4).

TRIM16-myc-His was expressed at the protein level in TRIM16-4 and TRIM16-5 clones, as determined by the anti-myc antibody, corresponding to the expected 70 KDa size. For immunofluorescence, anti-myc tag antibody was conjugated to Alexafluor555 secondary antibody, and DAPI was used to stain the cell nuclei. The localisation of the TRIM16 transgene was predominantly cytoplasmic, similar to that seen previously (Figure 3.1) with endogenous TRIM16 in BE2C parental cells. Fluorescence intensities varied from cell to cell, however, 100% of cells had specific magenta fluorescence, above any background red fluorescence detected in the empty vector (EV) control clones (EV transfected cells had negligible magenta fluorescence), conferring transgene expression in all cells. Therefore, TRIM16-4 and TRIM16-5 could be used for further research.

A

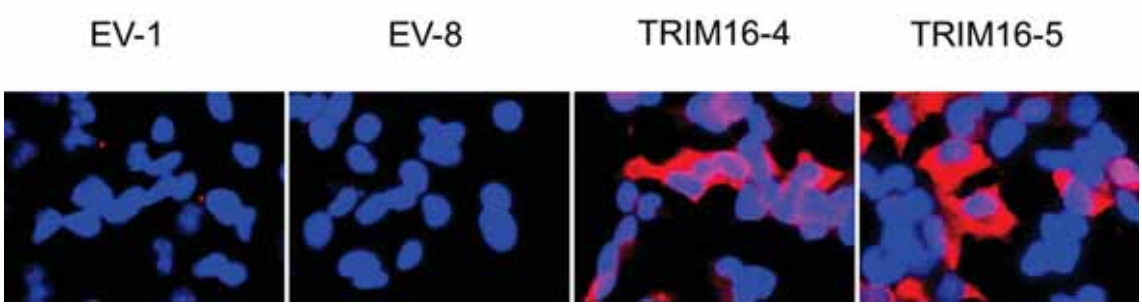

B

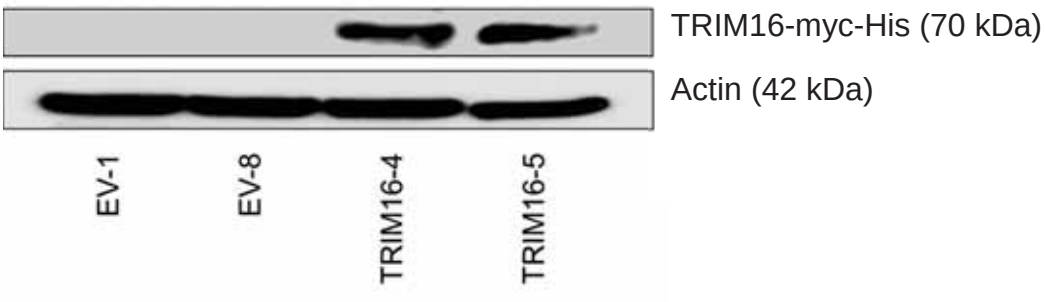

Figure 3.4 Stable TRIM16-myc-His protein expression in BE2C neuroblastoma cells

A) Cells were stained for myc-tagged transgene protein, via anti-myc and anti-mouse-Alexafluor 555 (magenta) and counter stained with DAPI DNA stain. Images were captured with Zeiss Fluorescent microscope with the 63X objective. B) Whole cell lysates were obtained from sub-confluent clones and subjected to Western blot with antibodies against myc tag (for detection of TRIM16-myc-His) and actin Ab was used as a loading control.

3.2.5 TRIM16 overexpression decreases cell doubling time and proliferation

As part of the characterisation of the TRIM16-myc-His clones, a cell doubling time study was performed (Figure 3.5). Due to the growth inhibition produced during transient transfections, it was hypothesised that TRIM16 overexpression would negatively affect cell doubling time. Cells were plated, and the amount of viable cells was accessed and analysed for the 4 following days by Alamar blue assay (2.2.3). Both TRIM16 overexpressing cell clones grouped together, with days 3 and 4 having significantly lower levels of cells compared with the faster growing empty vector clones. Using the absorbance values from days 1-4, the doubling time for each cell line was calculated as shown in Figure 3.5. TRIM16 overexpressing lines had lower doubling times than the control lines.

To confirm a decrease in doubling time of clones, the proliferation of these clones was quantified by a BrdU ELISA. TRIM16 is known to enhance retinoid growth inhibition in neuroblastoma cells, thus it was important to determine the influence of RA treatment on proliferation in the stable clones. TRIM16 overexpression decreased proliferation and this overexpression also markedly increased the response of cells to RA treatment (Figure 3.6). There was a greater than 80% decrease in the number of proliferating cells, with both RA treatment and the transgene transfection, whereas the empty vector clones had less than a 40% decrease in proliferation after RA treatment.

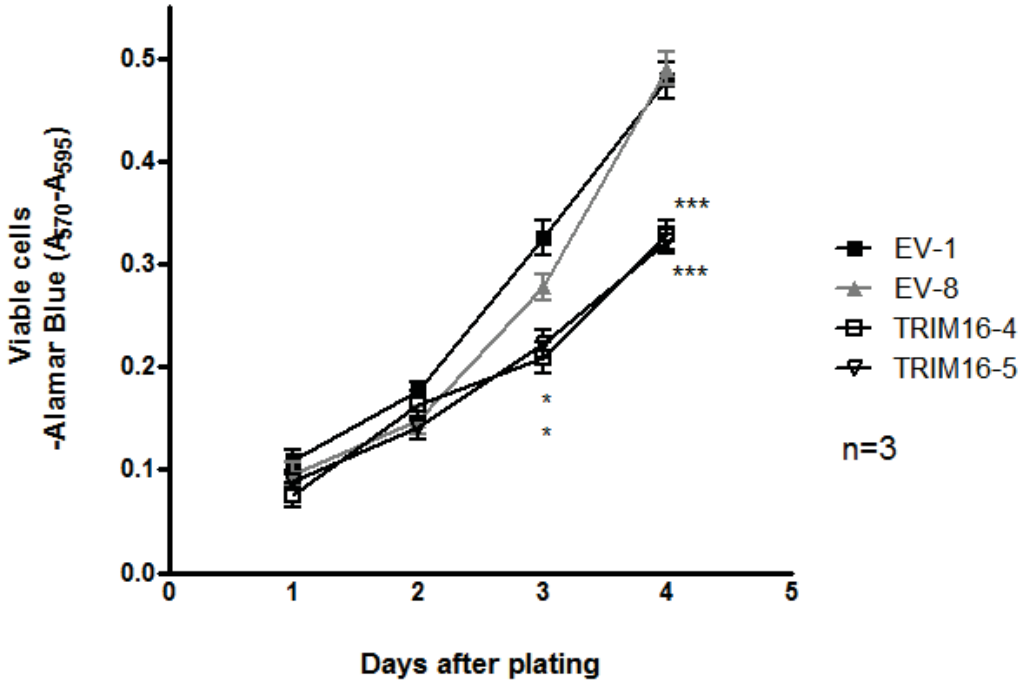

Doubling Times:	EV-1 = 35.1 h	TRIM16-4 = 39.3 h
	EV-8 = 29.1 h	TRIM16-5 = 40.2 h

Figure 3.5 TRIM16 overexpression reduces cell doubling time

BE2C TRIM16-myc-His stable cell clones had their viability measured every day, for 4 days. Prism software was used to calculate doubling time as shown in lower panel. P values were calculated against EV8, *p<0.05, ***p<0.001

A

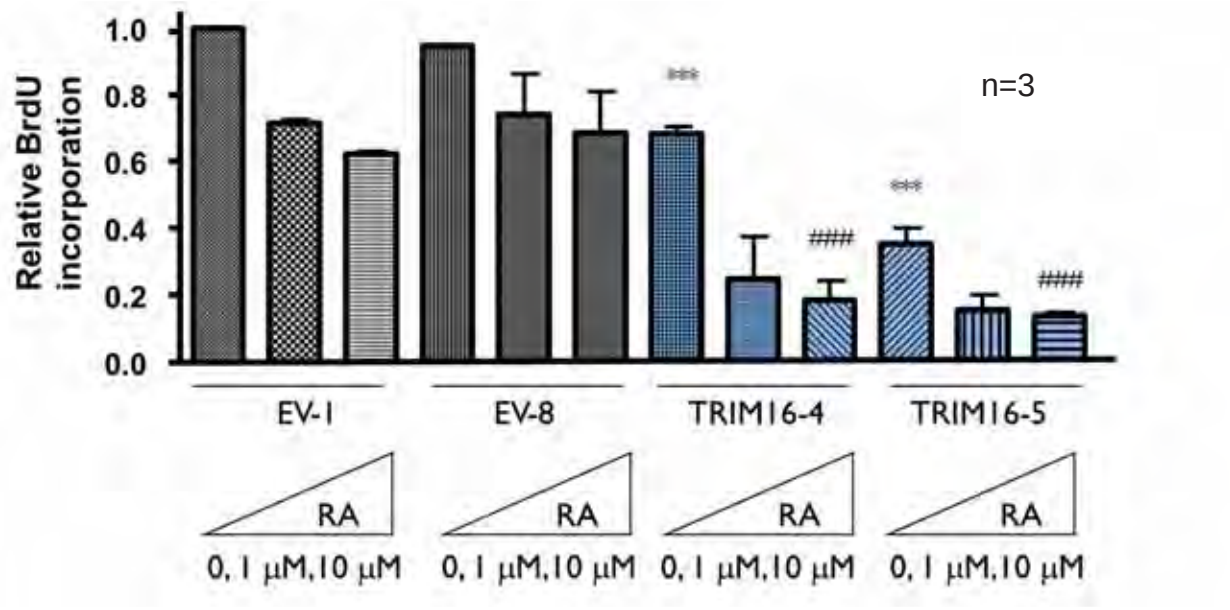

B

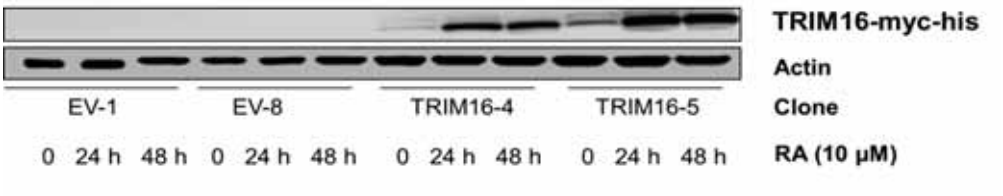

Figure 3.6 TRIM16 stable overexpression decreases proliferation and increases retinoid sensitivity

A) 5 x 10^3 TRIM16-myc-His stable clone cells per well were treated with or without RA (1 μM/10 μM) for 5 days. Absorbance was used as a measure of cell proliferation. ***p<0.001 shows comparison to the EV-1 untreated samples, ### p<0.001 shows comparisons to the untreated control of the same clone. B) Western blot showing TRIM16-myc-His protein (as detected by the anti-myc Ab).

Due to the marked increase in RA response in TRIM16 overexpressing clones, an investigation into the effect of TRIM16 overexpression on the activity of other drugs used in neuroblastoma treatment regimens including doxorubicin, vincristine and cisplatin was undertaken (Figure 3.7). Doxorubicin works by intercalating DNA of cells [343]. Vincristine is a vinca alkaloid and inhibits mitosis through interaction with microtubules [344]. Cisplatin cross-links DNA leading to cell apoptosis [345].

Doxorubicin concentrations between 3.3 nM and 810 nM were used to treat the BE2C stable clones. Surprisingly, at the 30 nM treatment, cells overexpressing TRIM16 had a slight increase in viability compared to the empty vector controls. However, this difference was not statistically significant.

Vincristine concentrations between 1.1 nM and 270 nM were used to treat the BE2C cells. Clones with TRIM16 overexpression did have a slight increase in drug sensitivity compared to EV controls. This trend achieved statistically significance in sensitivity to the drug in the exponential part of the death curve at 10 nM.

Cisplatin concentrations between 0.37 μM and 90 μM were used to treat the BE2C cells, 50% of all clone cells died at the 10 μM point. There was no increase or decrease in viability of TRIM16 overexpressing cells with cisplatin treatment compared with the empty vector clones.

Generally, there is no marked significant trend towards increased drug sensitivity when TRIM16 is overexpressed and any differences are not maintained over more than one concentration in both sets of clones.

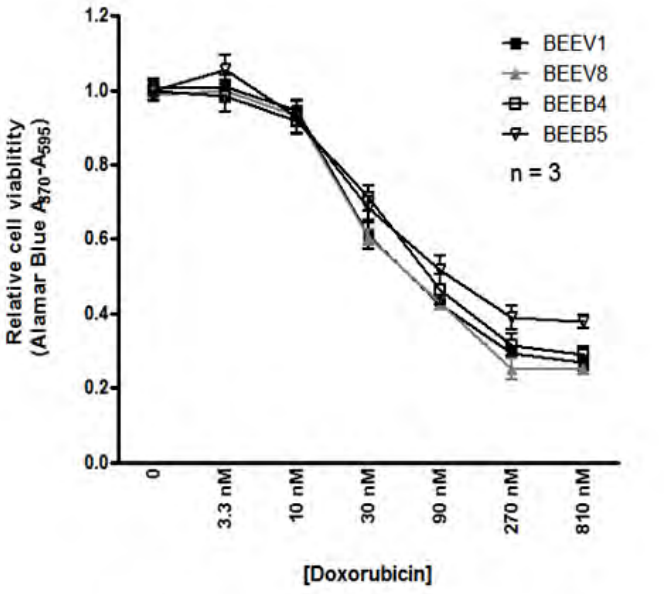

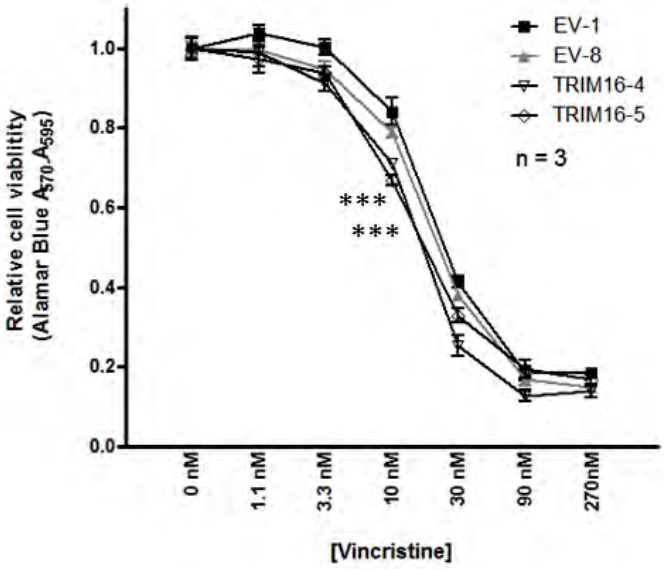

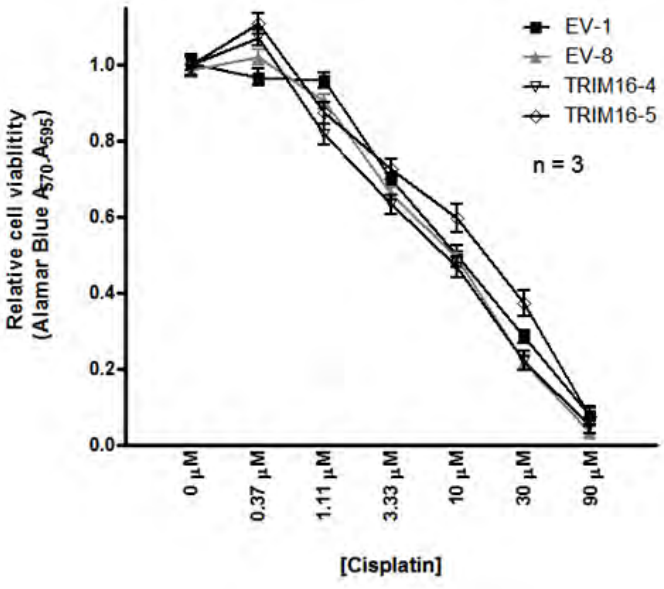

Figure 3.7 TRIM16 does not significantly enhance potencies of three drugs used in neuroblastoma therapy

TRIM16 clones were plated at 1 x 10^4 cells per well of a 96 well plate and exposed for 72 hours to drug concentrations as shown on the x-axis for each drug. Absorbance was used as a measure of cell proliferation. ***p<0.001

3.2.6 TRIM16 overexpression decreases clonogenicity in semi-solid agar

As the stable clones had been characterised, a study was performed to confirm that the clones maintained the ability to grow in soft agar (in an anchorage independent environment) as this is an indicator of the ability to develop tumours in mice. The hypothesis tested here, was that TRIM16 overexpression would decrease the anchorage independent growth of BE2C cells. Clones were grown in 0.33% agarose in complete culture media. After 14 days each well was photographed before and after MTT staining (MTT staining is only incorporated into live cells). Images were taken of the whole wells and also of individual colonies for later quantifications.

TRIM16 overexpression resulted in a dramatic decrease ($P<0.001$) in the number of colonies which were able to form in the agar (Figure 3.8). Although less in number, some colonies did form when TRIM16 was overexpressed, which indicates that tumours would also grow from these clones in nude mice, although the overexpressing cells may grow at a slower rate or have reduced survival compared to the empty vector controls. The TRIM16-4 clone showed the greatest decrease in clone number (>90%), with TRIM16-5 showing more than a 60% decrease in clone number compared to the empty vector clones. There were no significant differences between the two EV clones.

It appeared that in general the TRIM16 overexpressing colonies were smaller in size compared to the empty vector controls (Figure 3.9). This led to the hypothesis that the effect of TRIM16 overexpression on cell proliferation caused decreased proliferation in the semi-solid agar environment. To quantify the size of the colonies, images of the colonies were analysed using Image J (2.2.4). When TRIM16 was overexpressed, colonies were ¼ the size of those observed in the control clones. Thus,

TRIM16 overexpression reduces the size and number of neuroblastoma colonies grown in semi-solid media.

A

B

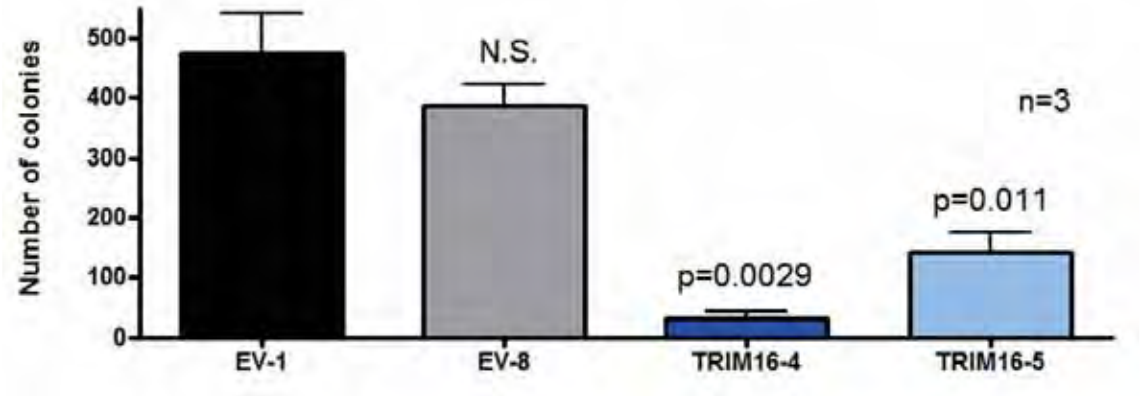

Figure 3.8 TRIM16 overexpression causes reduced clonogenicity in semi-solid medium

BE2C neuroblastoma (TRIM16-myc-His clones: TRIM16-4 and TRIM16-5) cells were used for this assay. A) Representative images of MTT stained colonies, 14 d after plating in semi-solid agar. B) Quantification of colony number for each stable clone. TRIM16 overexpression clones were statistically compared with EV-8. N.S. = Not significant.

A

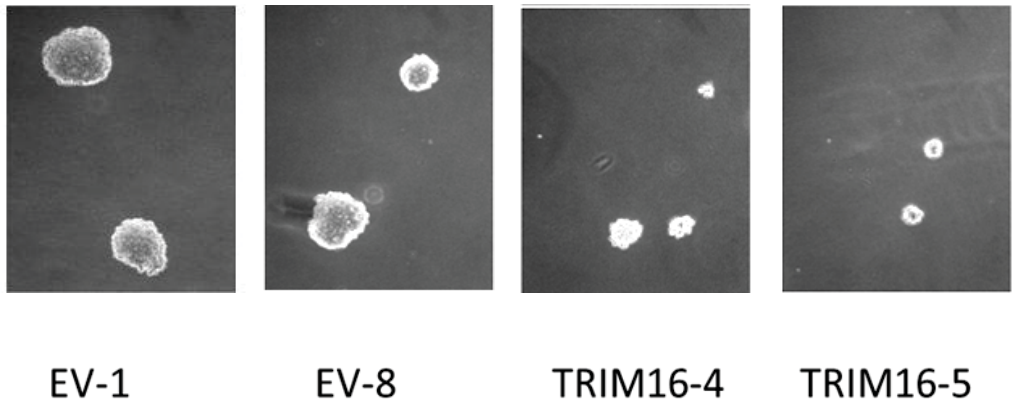

B

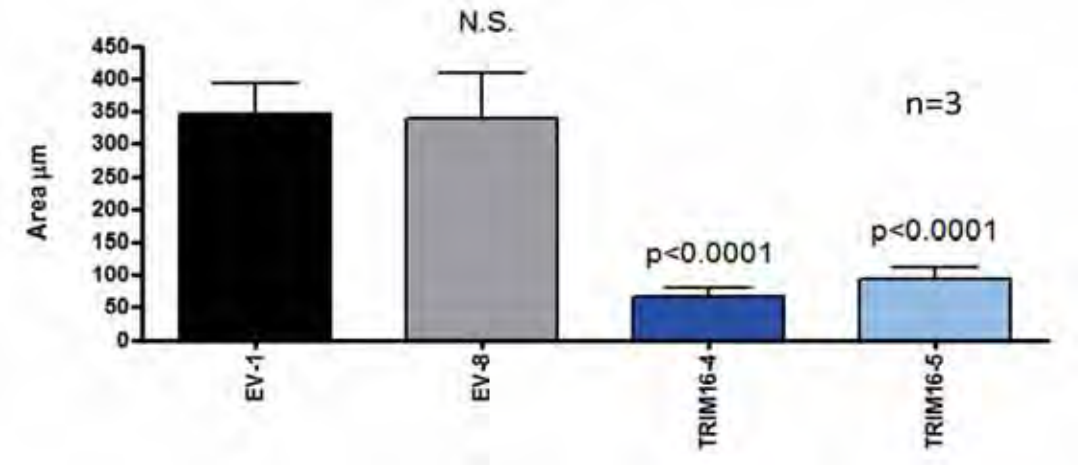

Figure 3.9 TRIM16 overexpression decreases colony size

BE2C neuroblastoma cell clones were used for this assay. A) Representative images of colonies of each clone. B) These images were used to quantify the average size of the colonies from each clone. Image J was used to measure the area of each clone. TRIM16 overexpressing clones were compared to EV-8. N.S. = Not significant.

3.2.7 TRIM16 overexpression reduces tumorigenicity

The effect of TRIM16 overexpression on *in vivo* neuroblastoma growth was tested in a xenograft BALB/c nu/nu nude mouse model (outlined in 2.6.1.1). It was hypothesised that TRIM16 overexpression would reduce tumour growth. Three events were recorded for statistical evaluation; detection of the tumour (when the tumour grew above 50 mg in weight), death (when the tumour grew above 1000 mg in weight) and the tumour mass at 4 weeks after cell engraftment. The 4 week time point showed the most significant difference, with both TRIM16 overexpressing clones having an average size of less than 50 mg (Figure 3.10A). In contrast, the empty vector clones had average sizes ranging from approximately 300 mg to above 400 mg.

The development of an observable tumour was defined as a tumour of more than 50 mg in weight. The use of this first event in the protocol gives information on tumour latency. The TRIM16-4 overexpressing cell line was statistically different from both empty vector clones (Figure 3.10B). However, the TRIM16-5 clone failed to reach significance from one of the empty vectors (EV-8). There is an apparent trend though, with TRIM16-5 having a slower tumour appearance in the mice compared with the empty vector controls. Due to ethical regulations mice were culled when tumours reached or exceeded 1000 mg. When TRIM16 was overexpressed the mice had an increased life span when compared with the empty vector control mice (Figure 3.10C). Again only TRIM16-4 was significantly different from both control cell lines. However, there was a trend showing TRIM16 overexpression, delayed the development of large tumours.

In this study, the empty vector control cell lines both had a 15/16 tumour frequency (proportion of successful tumour engraftment). The frequency rate was

slightly lower in the TRIM overexpression clones compared to the EV control clones, with a frequency of 11/16 for TRIM16-4 and 14/16 for TRIM16-5. Analysis of the above events in the neuroblastoma xenograft model showed that TRIM16 has a significant negative impact on neuroblastoma tumour growth.

A

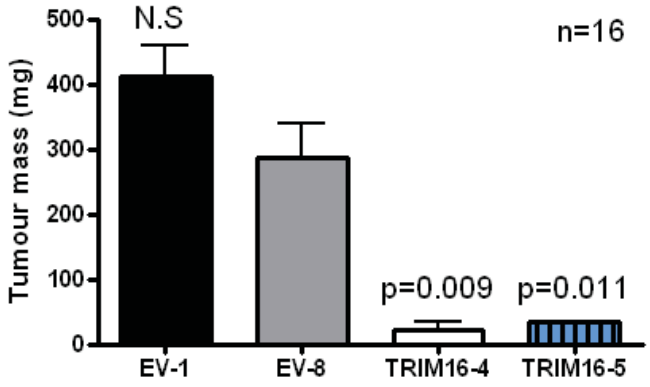

B

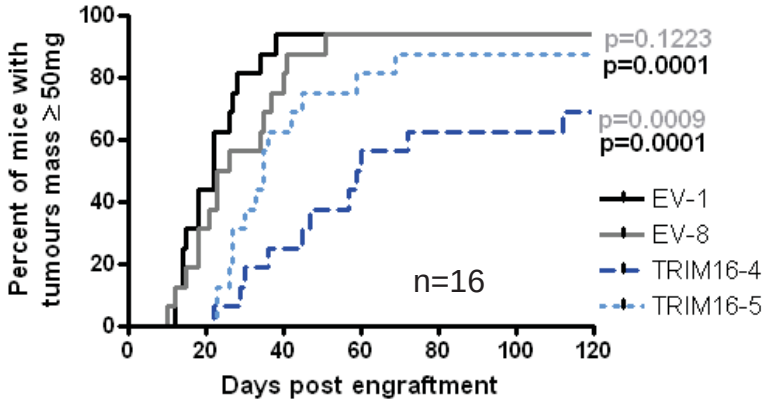

Means:
EV-1 = 21.5 d
EV-8 = 28.1 d
TRIM16-4 = 51.7 d
TRIM16-5 = 34.0 d

C

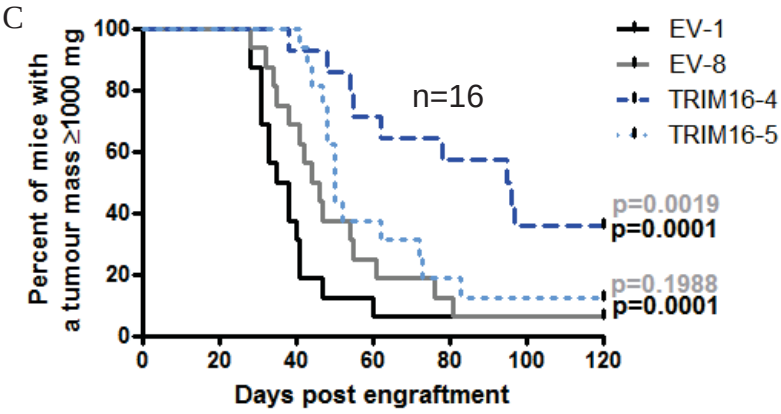

Means:
EV-1 = 37.0 d
EV-8 = 47.6 d
TRIM16-4 = 76.0 d
TRIM16-5 = 51.1 d

Figure 3.10 TRIM16 reduces tumorigenicity *in vivo*

BE2C neuroblastoma cells stably transfected with TRIM16 or EV were subcutaneously injected into the flank of balb/c nu/nu nude mice and tumour size was measured at least three times a week. A) Tumour size 4 weeks post engraftment. B) Percentage of mice with observable tumours over 50 mg. C) Percentage of mice with large tumours (1000 mg), survival over time. For B) & C) Grey p values are compared to EV-8, black to EV-1. The mean event days are on the right hand side of the graphs.

3.3 Discussion

TRIM16 is known to have a role in the retinoid anti-cancer signalling pathway in neuroblastoma [8,216]. However, to my knowledge, the effects of TRIM16 overexpression on neuroblastoma proliferation and tumour growth have yet to be investigated. The results of this study demonstrate that overexpression of TRIM16 has a significant negative impact on the growth of neuroblastoma cells both *in vitro* and *in vivo* and confirms the hypothesis that TRIM16 is a potential tumour suppressor in neuroblastoma.

This work has shown that TRIM16 is expressed in a wide variety of cell lines, including neuroblastoma, lung cancer, breast cancer, colon cancer, medulloblastoma, glioma and pancreatic cancer cell lines, as well as breast, lung, kidney and non-malignant cell lines. This suggests that the levels of TRIM16 are still high in normal cells. The banding varied with single and multiple bands expressed at the basal levels of cells, indicating the possibility of different isoforms of the TRIM16 protein, and/or post-transcriptional modifications. Non-specific bands could also be a possibility, however (in the experience of our laboratory) with different antibodies multiple weaker bands are still observed, which suggests the multiple bands represent variants of TRIM16. Immunofluorescence staining demonstrated that the majority of TRIM16 is expressed in the cytoplasm. The above data are in accord with published Northern blot results of TRIM16, which show mRNA expression in all tissues studied, with the exception of lymphocytes [329]. Both Liu and colleagues [329] and Beer and colleagues [330] have also reported that the expression of TRIM16 is predominately cytoplasmic. A database search of the ‘human protein atlas’ site (which is an immunohistochemical atlas of human tissues and cells lines, http://www.proteinatlas.org) also demonstrates

TRIM16 as a highly ubiquitously expressed protein, predominately expressed in the cytoplasm [333].

TRIM16 overexpression has a negative effect on proliferation in both BE2C and SH-SY5Y cells. In the breast and lung non-malignant cell lines, TRIM16 overexpression had no effect on proliferation. These normal cell lines were used 'in lieu' of neuronal normal cells as non-malignant neuroblasts cell lines could not be obtained. Also, as these studies used transiently transfected cells, the cells are a population of both transfected and untransfected cells and therefore the results obtained here are likely an underestimation of TRIM16's effect on proliferation. As TRIM16 overexpression causes growth inhibition in neuroblastoma and not in non-malignant cells, this result presents the possibility that TRIM16 has a therapeutic potential in selective growth inhibition of neuroblastoma. Our research group has previously shown that TRIM16 overexpression is able to act on the RARβ promoter and reverse retinoid resistance in retinoid resistant breast and lung cancer cell lines [216]. As the retinoid pathway has a negative effect on proliferation in neuroblastoma, I also tested if TRIM16 overexpression in combination with RA treatment had an additive growth inhibition in both neuroblastoma and non-malignant cell lines. Even though other TRIM proteins such as PML are tumour suppressors, to date, no other TRIM has been used in therapeutic drug design or as a specific drug target in government approved therapies.

Stable neuroblastoma cells overexpressing TRIM16 were developed and validated. These clones exhibited a phenotype similar to transiently transfected cells. Transgene protein was predominately cytoplasmic. Furthermore, overexpression of TRIM16 produced decreased proliferation as demonstrated by Alamar blue and BrdU assays. Overexpressing cells also had increased sensitivity to retinoid treatment, with a

more than an 80% decrease in proliferation in cells with both RA treatment and the transgene expression, whereas the empty vector clones had less than a 40% decrease in proliferation. Interestingly, the protein levels of TRIM16 increased with RA treatment, demonstrating the transgene TRIM16 (like endogenous TRIM16 [8]) increases upon RA treatment.

TRIM16 is not a general enhancer of neuroblastoma standard chemotherapies. Doxorubicin and cisplatin showed no increase in sensitivity to the drug in combination with TRIM16 stable overexpression. In contrast, vincristine did achieve a statistically significant result at the 10 nM point in the cytotoxicity curve. Both empty vector clones and overexpression clones were grouped separately. However, this difference represents only a 10% reduction, which although statistically significant, is unlikely to represent a biological significance which could be exploited.

TRIM16 overexpression reduces clonogenicity and colony size in semi-solid media. The TRIM16 overexpressing clones both showed a significant decrease in the number and size of colonies, 14 days post cell seeding. The TRIM16-4 clone had a lower clonogenicity compared with TRIM16-5, and possibly reflects a slight difference between the two clones, resulting from different integration of the TRIM16 expression vector and clonal expansion. Interestingly, the size of the colonies was significantly reduced to just 1/3 of that seen in the empty vector controls. This decrease in size indicates a decrease in cell proliferation, and correlates with the *in vitro* growth curves and BrdU incorporation experiments reported in this chapter (3.2.5). This data is consistent with that of Mu *et al*., (1997) who demonstrated that overexpression of another TRIM protein, PML also results in reduced colony formation in anchorage-independent medium, and causes reduced tumorigenicity in nude mice [346].

Significantly, *in vivo* work demonstrated that TRIM16 overexpression decreases tumorigenicity. Stable TRIM16 overexpressing clones were engrafted in nude mice. At the 4 week time point, TRIM16 overexpressing neuroblastoma xenografts had a significantly reduced growth compared to the empty vector clones. Furthermore, the TRIM16-4 overexpressing cell line was statistically different from both empty vector clones, in both tumour appearance and mouse survival. However, the TRIM16-5 clone failed to reach significance from EV-8. The failure of TRIM16-5 to reach significance at some points of the xenograft study may be linked to its higher clonogenicity compared with TRIM16-4. This issue may have been rectified with an increase in mouse number. There is an apparent trend though, with TRIM16-5 having a slower tumour appearance and slower time to produce large tumours. Here, the tumour frequency rates of TRIM16-4 and TRIM16-5 were slightly lower than the empty vectors, which could indicate a more differentiated cell phenotype in the TRIM16 overexpressing clones, according to the xenograft study by Walton *et al*. (2004) [347]. This could also partly explain the decreased proliferation in TRIM16 overexpressing cells.

In conclusion, this body of work shows for the first time that TRIM16 has an impact on tumour formation. This supports the hypothesis that TRIM16 acts as a tumour suppressor in neuroblastoma and possibly other cancer cell types. Due to TRIM16's influence on the retinoid pathway, it is likely that the enhancement of RARβ function by TRIM16 (independent of RA treatment) is a major mechanism in the TRIM16 anti-cancer function. However, the mechanism of TRIM16 action in proliferation is largely unknown and needs to be further elucidated. Such significant biological effects on tumour formation must involve regulation of the cell cycle and related pathways within the cell. The increased retinoid sensitivity of stable TRIM16

overexpressing clones and their less aggressive tumour formation may also indicate TRIM16 has a role in neuronal cell differentiation. This research gives grounds to study endogenous TRIM16 in neuroblastoma tumour formation and cell differentiation, which is the topic of the next thesis chapter.

CHAPTER 4

RESULTS II: A STUDY OF TRIM16 FUNCTION IN BOTH NEUROBLASTOMA DIFFERENTIATION AND CELL CYCLE PROGRESSION

4.1 Introduction

Neuroblastoma is a solid tumour of embryonal neural crest origin. Although the causes of neuroblastoma are largely unknown, the cancer is believed to arise from the failure of embryonal neuroblasts to undergo growth arrest, differentiation and/or apoptosis [348]. Chapter 3 demonstrated that TRIM16 overexpression decreased neuroblastoma proliferation and tumorigenicity. Consequently, this chapter explores the possibility that in neuroblastoma, endogenous TRIM16 has a growth inhibitory role via the processes of neuroblastoma differentiation and cell cycle progression.

As TRIM16 overexpression had a significant impact on tumorigeniciy in a xenograft neuroblastoma model, I therefore exploited a unique and valuable opportunity to investigate endogenous TRIM16 in another model of neuroblastoma, the TH-MYCN mouse model (1.2.4.2). I aimed to characterise endogenous TRIM16 expression during neuroblast differentiation and development. In addition, this model allows important observation of TRIM16 protein expression during the initiation and progression of neuroblastoma tumours. The TH-MYCN neuroblastoma model is also more closely related to that of the human disease compared to the xenograft model, as it arises in the para-sympathetic ganglia, among other attributes [33,34,92]. Notably, all TH-MYCN homozygous mice develop tumours by 6.5 weeks of age.

Another aim of this chapter was to determine if TRIM16 could influence retinoid-induced differentiation. Rationale for this research avenue is quite strong because TRIM16 was identified by our laboratory group as a retinoid signalling enhancer in neuroblastoma [8], and the retinoid signalling pathway has a major positive role in neuronal cell differentiation [349](1.4). This pathway also has clinical significance in neuroblastoma and is exploited in the use of retinoids in minimal

residual disease treatments [7]. Neuroblastoma cell differentiation *in vitro* is typically analysed by the presence and length of neurites, which are long projections from the cell body of neuronal cells.

Evidence for a role of TRIM16 in differentiation exists in the context of skin. TRIM16 overexpression has been shown to induce keratinocyte differentiation [330]. In this study, the highly proliferative layer of healing skin had low levels of endogenous TRIM16 protein expression, indicating that TRIM16 protein levels are dynamic throughout the skin healing process. Although distinct tissue types, keratinocytes and neuroblasts both arise from the ectoderm germ cells in the developing embryo [350]. However, it is unknown whether the overexpression of TRIM16 would also cause differentiation in neuroblastoma cells. Furthermore, the functional links between differentiation and proliferation arrest add to the possibility that TRIM16 proliferation inhibition is linked with a role in differentiation.

A possible mechanism of TRIM16 growth inhibition is through involvement with the cell cycle components. Many TRIM proteins, including PML, are highly expressed during G1 [140,249]. TRIM16 is also known to co-localise with PML within the nucleus, in structures called PML-bodies [8]. Importantly, these nuclear structures are critically involved in growth inhibition and retinoid signalling [9,140,249,351].

In Figure 4.1, I have outlined the principle machinery involved in the cell cycle, with a particular focus on the G1 cell cycle phase, which is involved in retinoid treatment response and also neuroblastoma differentiation.

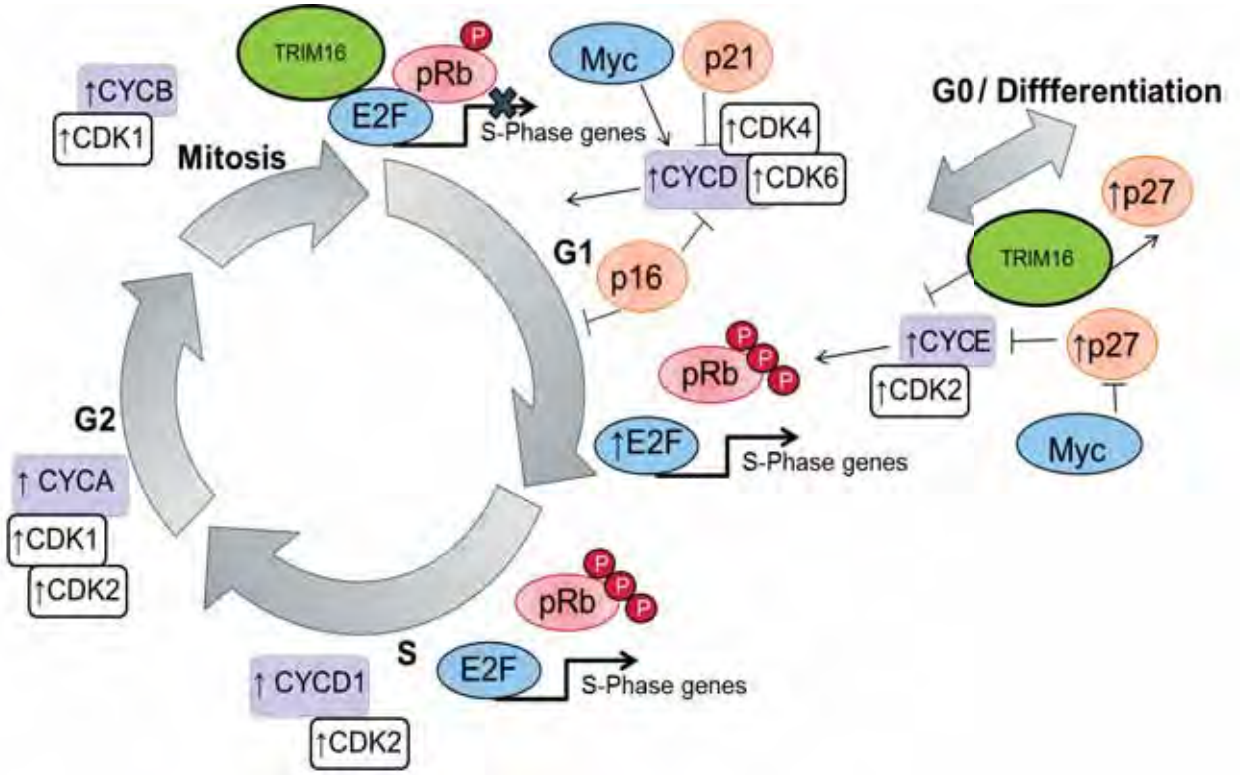

Figure 4.1 A model of possible TRIM16 interaction with cell cycle phase components

Further reading [2,5,8,128,216,238,249,331,352-355] .

Retinoids produce cell differentiation through G1 arrest (1.4) [5,352], and the decision of neuronal cells to differentiate requires a pause in cell cycle progression, which is generally made during the G1 cell cycle phase (1.3.1)[2,334]. The G1/S transition is mediated by cyclin Ds and CDK4/CDK6 complexes which operate at mid-G1 and then cyclin E/CDK2 which operate late in G1 [124-127]. Both the Ink4 family and the Cip/Kip family including p21, p27 and p57 can inhibit the progression to S phase via inhibition of mainly CDK kinase activity. In both neuronal progenitor cells and neuroblastoma cells, p27 has a critical role in cell cycle signalling and in differentiation [5,334,352,356]. Therefore, p27 is clearly a prime candidate protein for a role in TRIM16's anti-proliferative function.

Recently, our research group reported that TRIM16 binds and downregulates E2F1 [331]. Significantly, E2F1 is a transcription factor, essential for promoting progression through the G1/S checkpoint [357], and can also suppress neuronal differentiation [351]. Furthermore, TRIM16 overexpression downregulates the E2F1 binding partner pRB in the hyper-phosphorylated form [216]. This further implicates a role for TRIM16 in neuronal differentiation and cell cycle.

Therefore, to further investigate the biological function of TRIM16 and its role in neuroblastoma cell growth control, I investigated the expression of TRIM16 during early neuroblastoma cancer initiation and differentiation *in vivo* and *in vitro*. This was followed by a thorough investigation of endogenous TRIM16 protein expression throughout the cell cycle. Finally, the role of TRIM16 in the context of the cell cycle was elucidated through overexpression and knockdown studies of TRIM16.

4.2 Results

4.2.1 TRIM16 protein is highly expressed in the nucleus of differentiating ganglia cells, but decreased in neuroblastoma tumours *in vivo*.

It was hypothesised that TRIM16 expression would be decreased in tumours, compared to their normal controls. To address this hypothesis, tissues from the histologically well characterised TH-MYCN mouse model were examined for both wildtype and homozygous transgenic mice at birth, 7, 14 and 42 days of age.

Firstly, tumour tissues from 6 week old mice were studied. In these mice, specific TRIM16 staining was evident in all tumours ranging from weak to moderate intensity (Figure 4.2). In the tumour cells, the staining was diffuse (without areas of strong staining) and often localised to the cytoplasm. Non-malignant, neuroblastoma related tissues were also analysed. In the TH-MYCN mice, the cervical ganglia contain the cells from which the neuroblastoma tumours generally arise. Compared with the tumour tissues, these ganglia cells had slightly more intense TRIM16 staining, with moderate expression throughout both the nucleus and cytoplasm. A similar staining pattern was observed in the dorsal root ganglia. The adrenal gland, which is commonly the site of origin in human neuroblastoma, had weak to moderate TRIM16 staining. The differences were small between these tissues indicating TRIM16 is not an important discriminating factor after 6 weeks of age when comparing neuroblastoma and normal tissue equivalents.

In order to determine if TRIM16 is expressed dynamically during normal paravertebral ganglia development and neuroblastoma tumour formation, mice were culled at birth, 7, 14 and 42 days, and processed for immunohistochemistry to expose the paravertebral ganglia regions for both wildtype and homozygous TH-NMYC

transgenic mice. These time points sample a critical period of growth and differentiation in normal ganglia and also span tumour initiation and development of mature tumours. In the wildtype animals, the newly differentiated ganglia cells at day 0-14 had strong, predominately nuclear TRIM16 expression (Figure 4.3). In contrast, the mature and terminally differentiated ganglia cells at day 42 had low levels of diffuse TRIM16 staining. In the presence of two copies of transgenic MYCN, neuroblast cells in the hyperplastic regions of the ganglia go on to form mature tumours. These neuroblast cells of the ganglia were mostly negative for TRIM16 staining. In contrast, the ganglia cells adjacent to the hyperplastic regions possessed strong nuclear TRIM16 staining.

βIII-Tubulin staining was used in this study as a marker of both ganglia and neuroblastoma tissue and confirmed that the tissues studied were paravertebral ganglia or neuroblastoma.

To gain greater insight into the cell cycle status of the cells involved in the neuroblastoma development, tissues were stained with antibodies directed against components of G1 cell cycle phase. Both ganglia and hyperplastic cells (neuroblasts) were negative for cyclin E, showing that the ganglia cells were not in the late stages of G1. Cyclin E expression was observed in a minority of tumour cells, confirming that the antibody was working. Intense p27 staining was observed in the nucleus of the large ganglia cells. Strong p27 staining was not observed in the nucleus of the neuroblasts in the hyperplastic regions of the ganglia. This indicates the ganglia cells (and not the neuroblasts) were in G0/G1 or differentiating. Interestingly, strong ubiquitous p27 staining was observed in the neuroblastoma tumours, an unexplained finding which is in accordance with immunohistochemical studies of human neuroblastomas [137,358], and will be discussed later (in 4.3).

During neuroblastoma development, the expression pattern of p27 and cyclin E indicated that the cells which expressed TRIM16 in the nucleus were arrested in early to mid-G1, which is consistent with early differentiation.

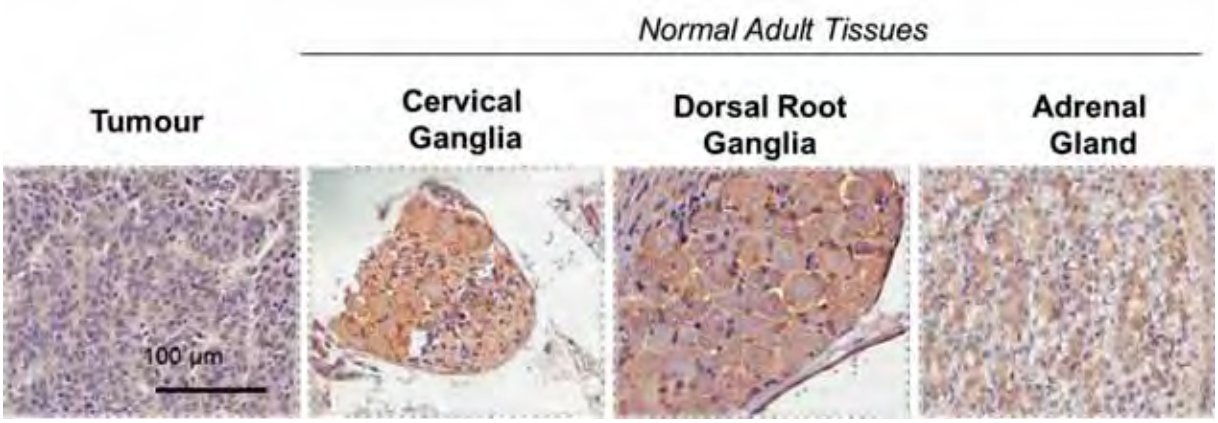

Figure 4.2 TRIM16 protein expression is diffuse in neuroblastoma mouse tumours

40X representative images (Aperio ScanScope XT). DAB (Brown) is conjugated to anti-TRIM16 (Bethyl Ab). Hematoxylin (Blue) is used as a nuclear stain.

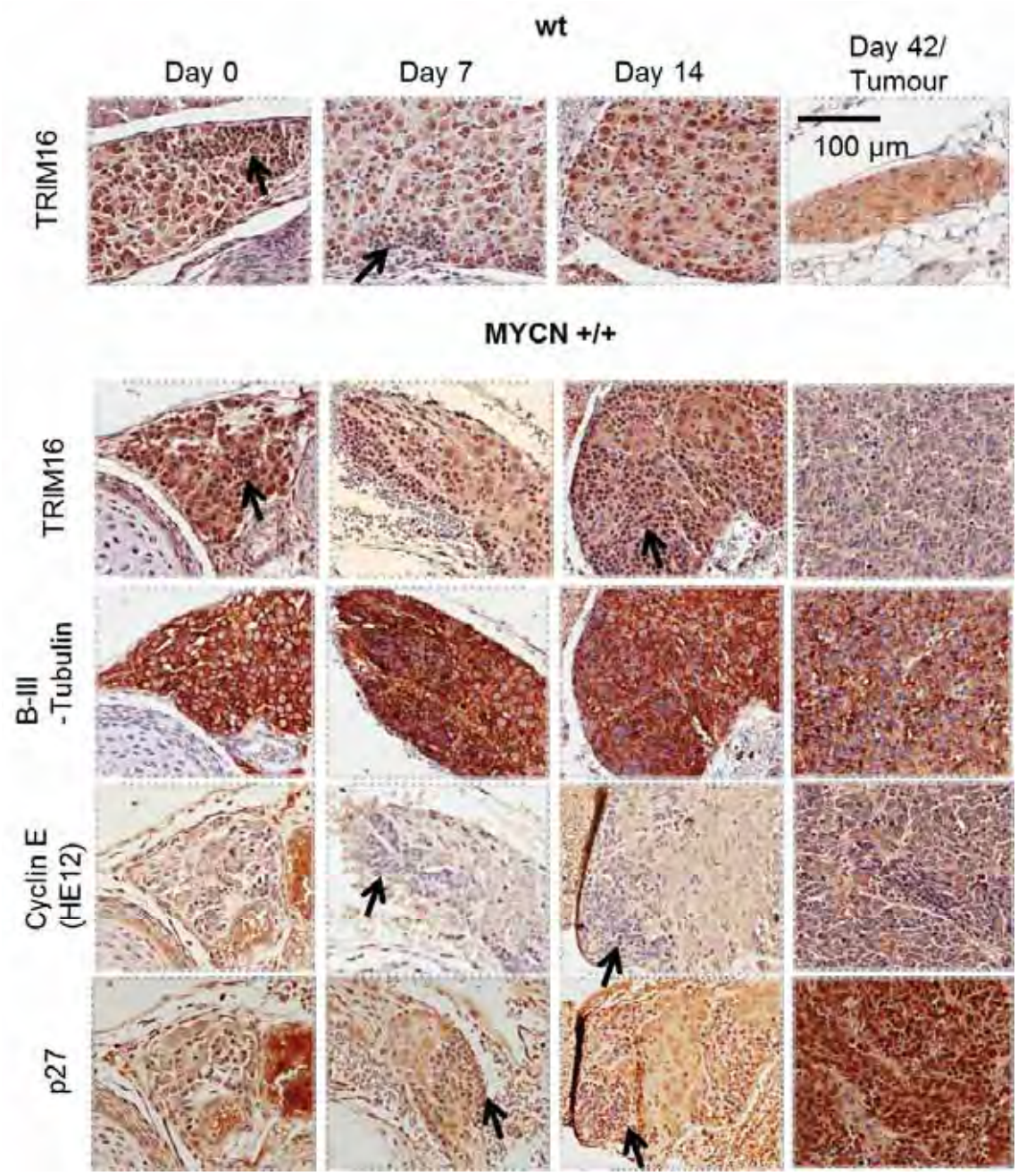

Figure 4.3 TRIM16 protein is expressed in the nucleus of differentiating ganglia cells

40X representative images (Aperio ScanScope XT). DAB (Brown) is conjugated to anti-TRIM16 (Bethyl Ab) or other primary antibody as indicated. Hematoxylin (Blue) is used as a nuclear stain. Arrows indicate areas of hyperplasia/neuroblast cells. Wildtype (wt).

4.2.2 TRIM16 overexpression increases retinoid-induced neuroblastoma differentiation.

In TH-MYCN mice, high TRIM16 expression was associated with newly differentiated or differentiating cells. This result suggests that TRIM16 has a role in differentiation, leading to the hypothesis that TRIM16 overexpressing clones would have a higher percentage of retinoid-induced differentiated cells compared with the empty vector controls. Differentiated cells were defined as cells bearing neurites (2.2.5).

Neurite formation through RA treatment requires a long time frame. Here TRIM16 overexpressing lines were exposed to 10 μM RA for 0, 2, 4 and 6 days. Images of cells treated for 6 days with RA demonstrate that, as expected, all cell lines have evidence of induced differentiation. However, TRIM16-4/5 clones both show an enriched differentiated cell population (Figure 4.4). Quantitative analysis from reproducible phenotypic studies revealed a pronounced significant doubling of differentiation at both the 4 and 6 day time points in the TRIM16 overexpressing cell lines compared with the empty vector controls (Figure 4.5). Thus, TRIM16 enhances neuronal differentiation in neuroblastoma.

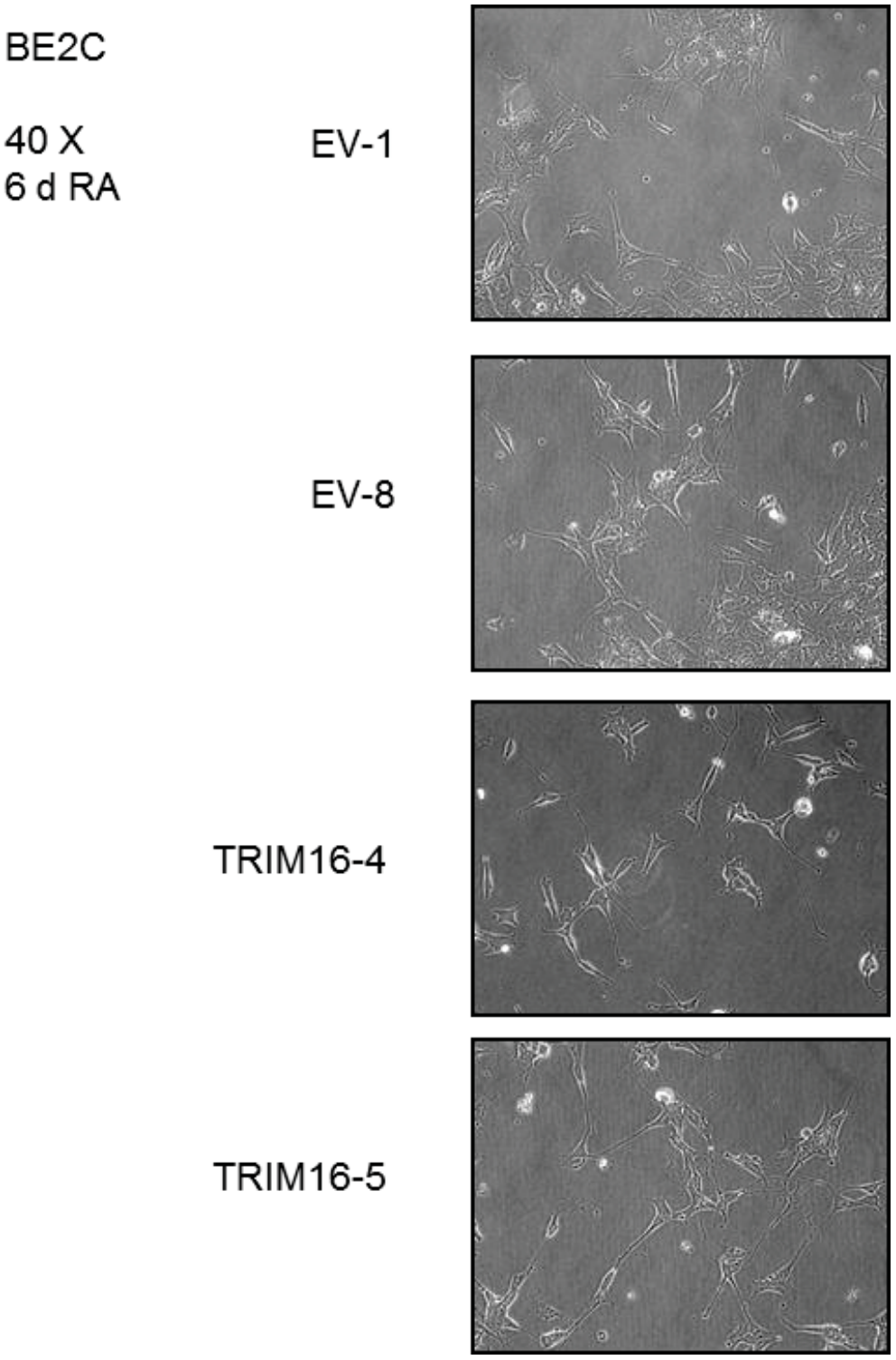

Figure 4.4 TRIM16 overexpression combined with retinoid treatment influences neuroblastoma cell morphology

Phase contrast images show more differentiated cells in the TRIM16 clones after 6 d RA treatment. BE2C neuroblastoma stable TRIM16-myc-His cell clones were used. TRIM16-4 and TRIM16-5 cells appear to have a more differentiated phenotype compared to the EV control lines, when treated with RA. Differentiated cells have at least one neurite per cell (a long, thin extension of a neuronal cell body).

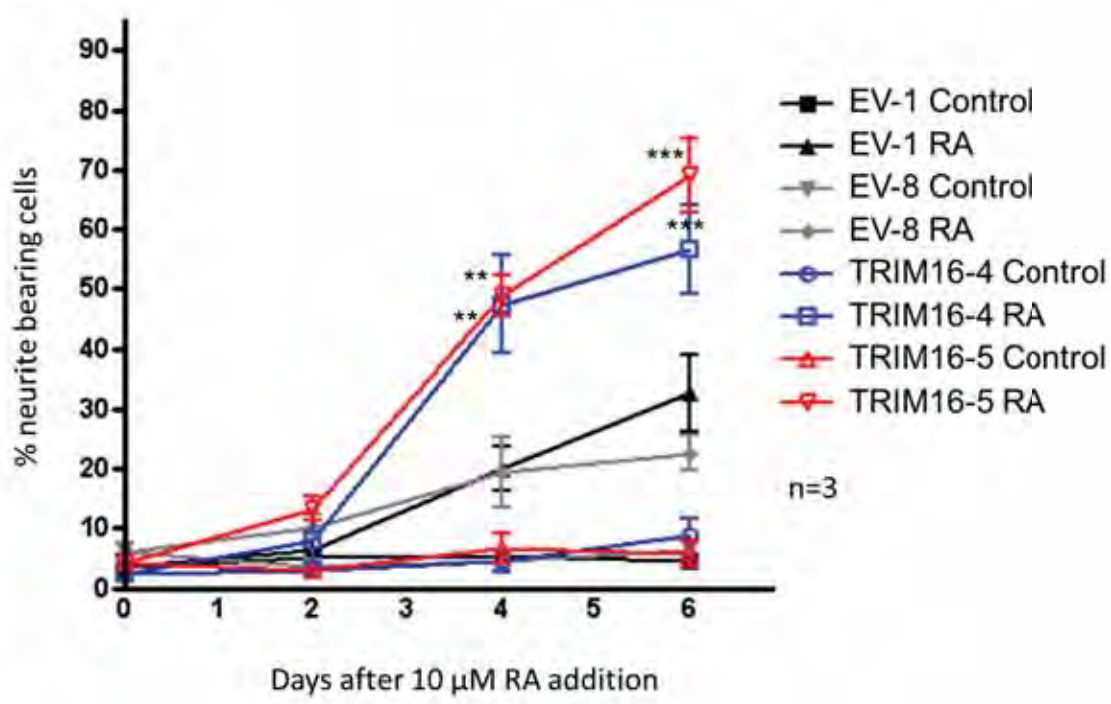

Figure 4.5 TRIM16 overexpression enhances retinoid-induced differentiation

Neurite bearing cells are an indicator of differentiated neurons. ** $p<0.01$, *** $p<0.001$. BE2C neuroblastoma TRIM16-myc-His cell clones were used.

4.2.3 TRIM16 protein expression is cell cycle dependent

It was clear from the above studies that TRIM16 has a promoting role in neuroblast differentiation. Differentiation requires the arrest of proliferation. Therefore, the hypothesis driving the next section of experimentation was that TRIM16 is highly expressed during G0 and/or G1 cell cycle phases. This is because these phases of the cell cycle are required for differentiation.

To determine whether TRIM16 has a differential pattern of expression during the cell cycle, BE2C and SHEP cells were synchronised and analysed by immunofluorescence and Western blots (2.1.4). Firstly, cells were fixed and their DNA content assessed by Propidium iodine staining and flow cytometry. Conditions were evaluated and chosen to be the most enriched for each cell cycle phase and asynchronised cells were used as a control. Western blot analysis revealed that after synchronisation to G0, the level of TRIM16 protein was decreased, when compared to asynchronous cells (Figure 4.6). In contrast, cells synchronised to the G1 phase had a marked increase in protein expression. Cells arrested at the G1/S boundary were also found to have induced TRIM16 protein expression. Early S phase cells maintained high expression of TRIM16. However, cells synchronised to G2/M or mitosis had much reduced levels of TRIM16. As in the differentiating ganglia (4.2.1), high TRIM16 protein expression was strongly associated with the G1 cell cycle phase in the above *in vitro* studies.

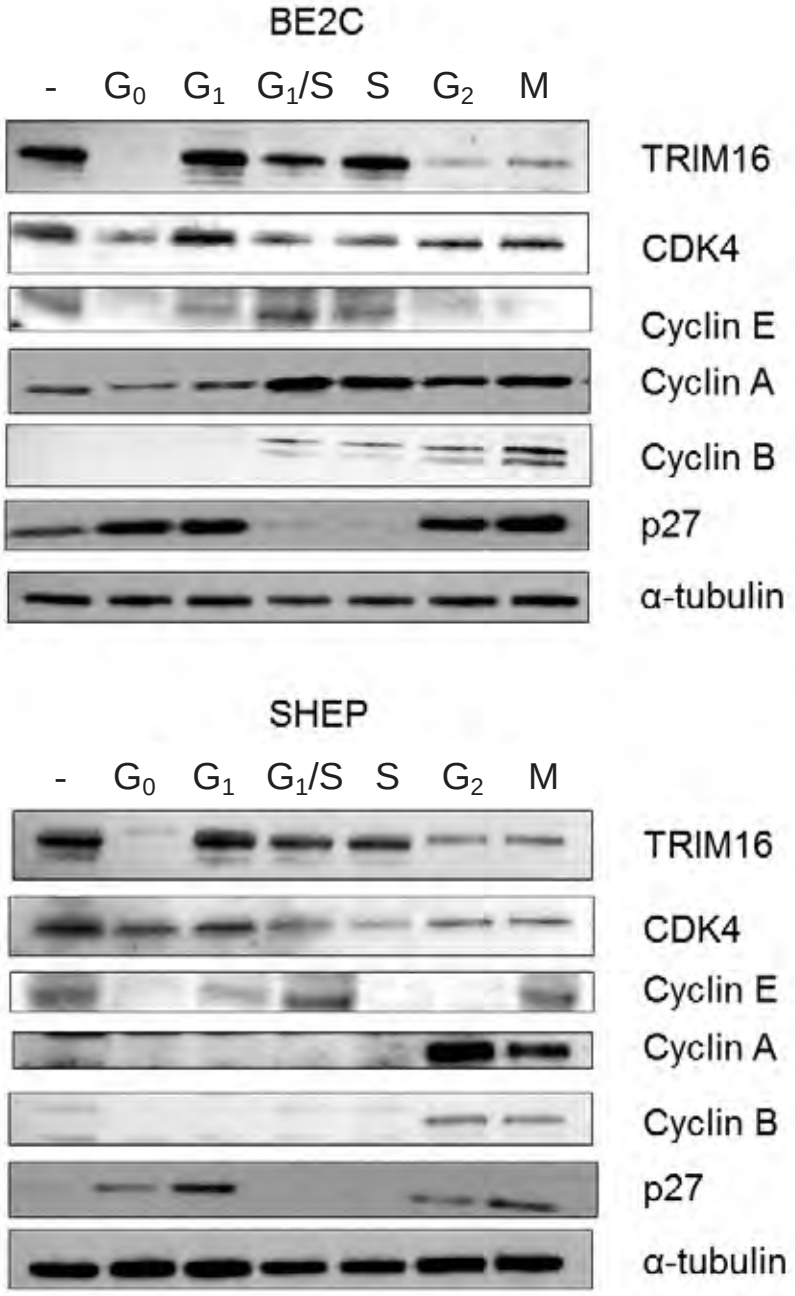

Figure 4.6 TRIM16 is induced in G1 cell cycle phase at the protein level

Western blots showing TRIM16 expression at various phases of the cell cycle in two neuroblastoma cell lines (BE2C and SHEP). Markers of the cell cycle phases: CDK4 (G1), cyclin E (G1/S), cyclin A (G2/M) cyclin B (mitosis/M). α-tubulin was used as a loading control. (-) denotes asynchronous cells.

In the newly differentiated ganglia cells, TRIM16 protein expression was predominately in the nucleus. Therefore, nuclear and cytoplasmic protein extracts were processed for Western blots from synchronised neuroblastoma cells. G2/M and mitotic cells were not used as there are no nuclear/cytoplasmic compartments in these phases, by their definition. Nuclear protein lysates from both BE2C and SHEP cells indicated that the TRIM16 protein induction observed in G1 occurred in the nuclei of cells (Figure 4.7). The banding of TRIM16 protein appeared to change depending on the protein compartment or synchronisation status, indicating potential differential TRIM16 protein modifications.

The cell synchronisation experiments revealed TRIM16 was dynamic in localisation and expression, but it was uncertain if this was through changes to TRIM16 protein stability, or increased TRIM16 mRNA expression. RT-PCR results show that the induction of TRIM16 protein from G0 to G1 in the cell cycle was not due to the upregulation of TRIM16 transcription (Figure 4.8).

To further determine whether TRIM16's dynamic expression during cell cycle was unique to neuroblastoma, the human embryonic fibroblast cell line HEK293, MDA-MB-231 (breast cancer cells) and CALU-6 (lung cancer cells) were utilised and subjected to synchronisation and analysis as with the neuroblastoma cell lines. The non-neuroblastoma cells all yielded similar results to the neuroblastoma cells studied (Figure 4.9).

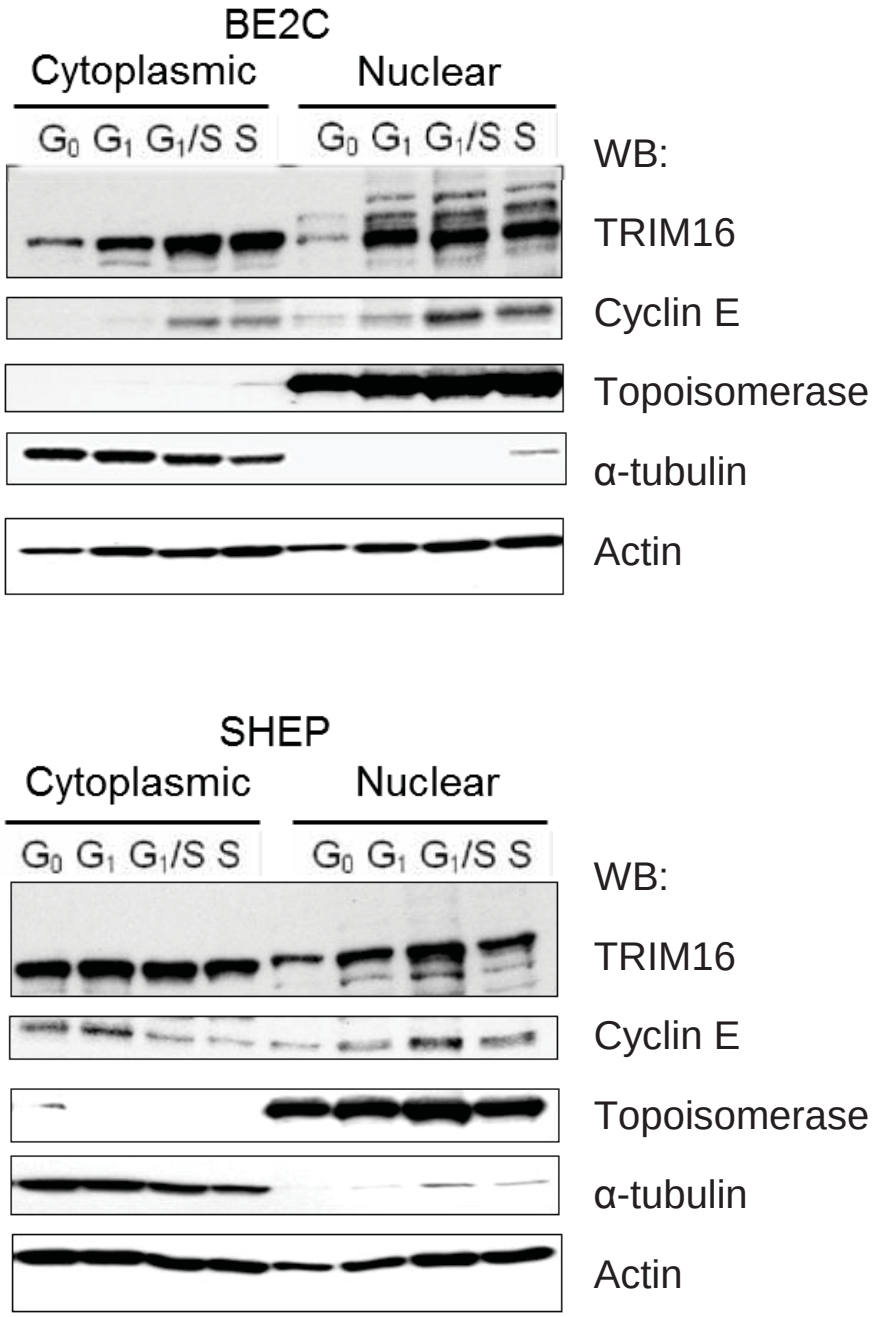

Figure 4.7 TRIM16 protein shifts to the nucleus in the transition between G0 to G1 cell cycle phases

Western blot analysis of cytoplasmic and nuclear lysates. Topoisomerase was used as a nuclear marker and α-tubulin as a cytoplasmic marker. Cyclin E was used as a marker for G1/S checkpoint. Two neuroblastoma cell lines (BE2C and SHEP) were used.

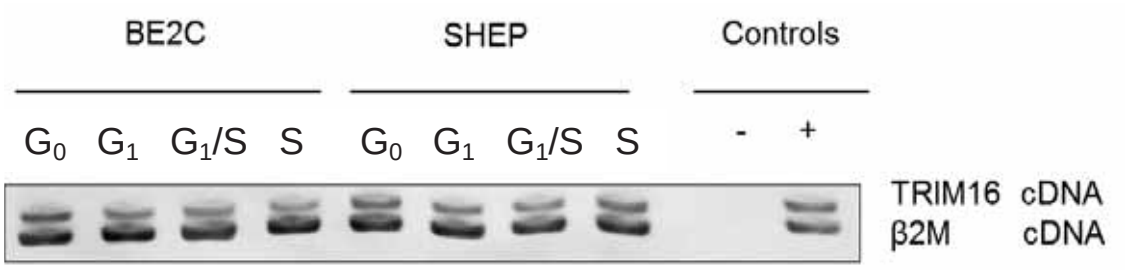

Figure 4.8 TRIM16 mRNA is not induced with the G1 cell cycle phase

RT-PCR with TRIM16 primers and β2M primers (as a template and loading control). Two neuroblastoma cell lines (BE2C and SHEP) were used. Representative gel image displayed.

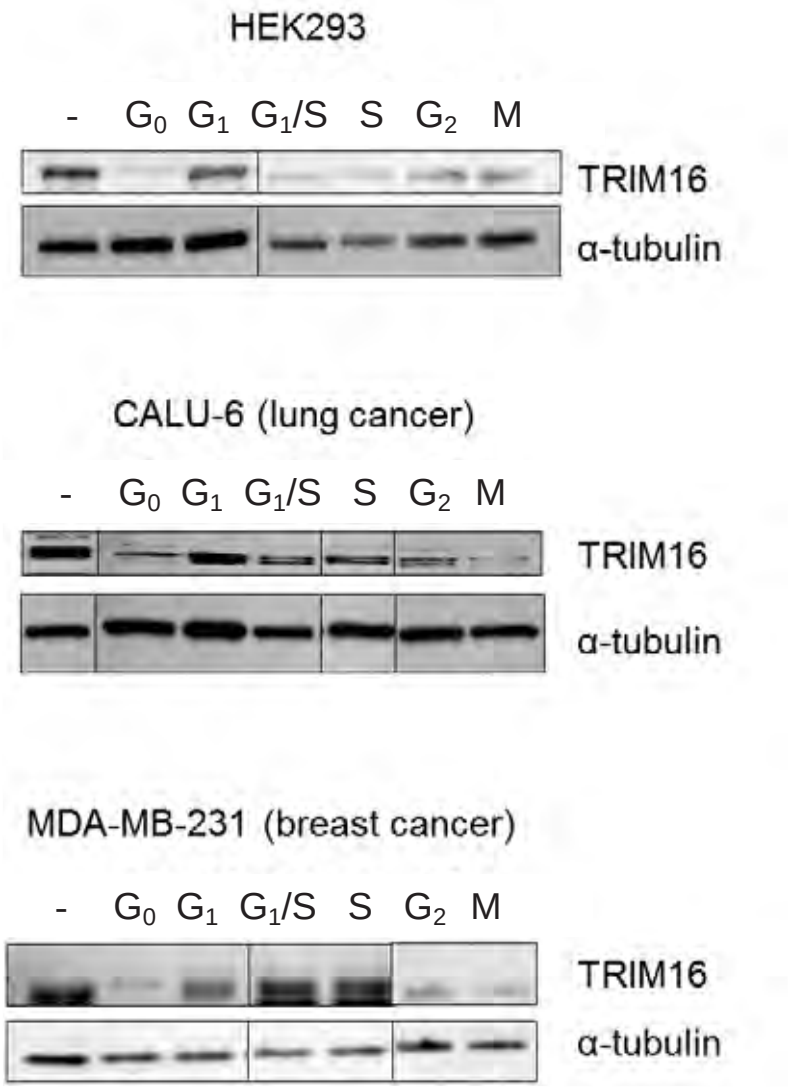

Figure 4.9 TRIM16 protein is induced during the G1 cell cycle phase in various tissue types

Western blots of cells: HEK293, CALU-6 and MDA-MB-231. α-tubulin was used as a loading control. (-) denotes asynchronous cells. Panels are representative from three replicates. Panels shown are from a single blot cropped after confirmation of cell cycle status of samples from different conditions.

4.2.4 TRIM16 localisation shifts to the nucleus during G1 of the cell cycle

As TRIM16 nuclear protein increased during G1 of the cell cycle it was important to verify if this was consistent with immunofluorescent studies. The localisation of endogenous TRIM16 was assessed via immunofluorescent staining of TRIM16 and co-staining with DAPI (Figure 4.10). In both BE2C and SHEP neuroblastoma cell lines, TRIM16 was expressed predominately in the cytoplasm of asynchronous cells. At G0, TRIM16 expression decreased and was cytoplasmic. In contrast, after entrance into the G1 phase, TRIM16 expression was markedly more intense and TRIM16 increased in the nucleus, although the majority of TRIM16 remained cytoplasmic. At the G1/S boundary, there was a higher expression of TRIM16 in the nucleus compared with asynchronous cells. Strikingly, in SHEP cells, G1/S arrested cells achieved predominately nuclear TRIM16. S phase cells maintained high expression of TRIM16, however, there was a loss of nuclear TRIM16. In contrast, cells synchronised to G2/M or mitosis did not display any observable involvement of TRIM16 with the DNA and had relatively weak expression. Therefore, during the G1 cell cycle phase, TRIM16 protein is increased and its localisation shifts from the cytoplasm into the nuclear compartment. CALU-6 and HEK293 had a similar staining pattern to the neuroblastoma cells, but in addition had induction of large nuclear bodies in the nucleus of G1 and G1/S synchronised cells (Figure 4.11). Therefore, the TRIM16 nuclear protein increase in the G1 cell cycle phase is likely a common yet compelling event in many cells, where TRIM16 is expressed.

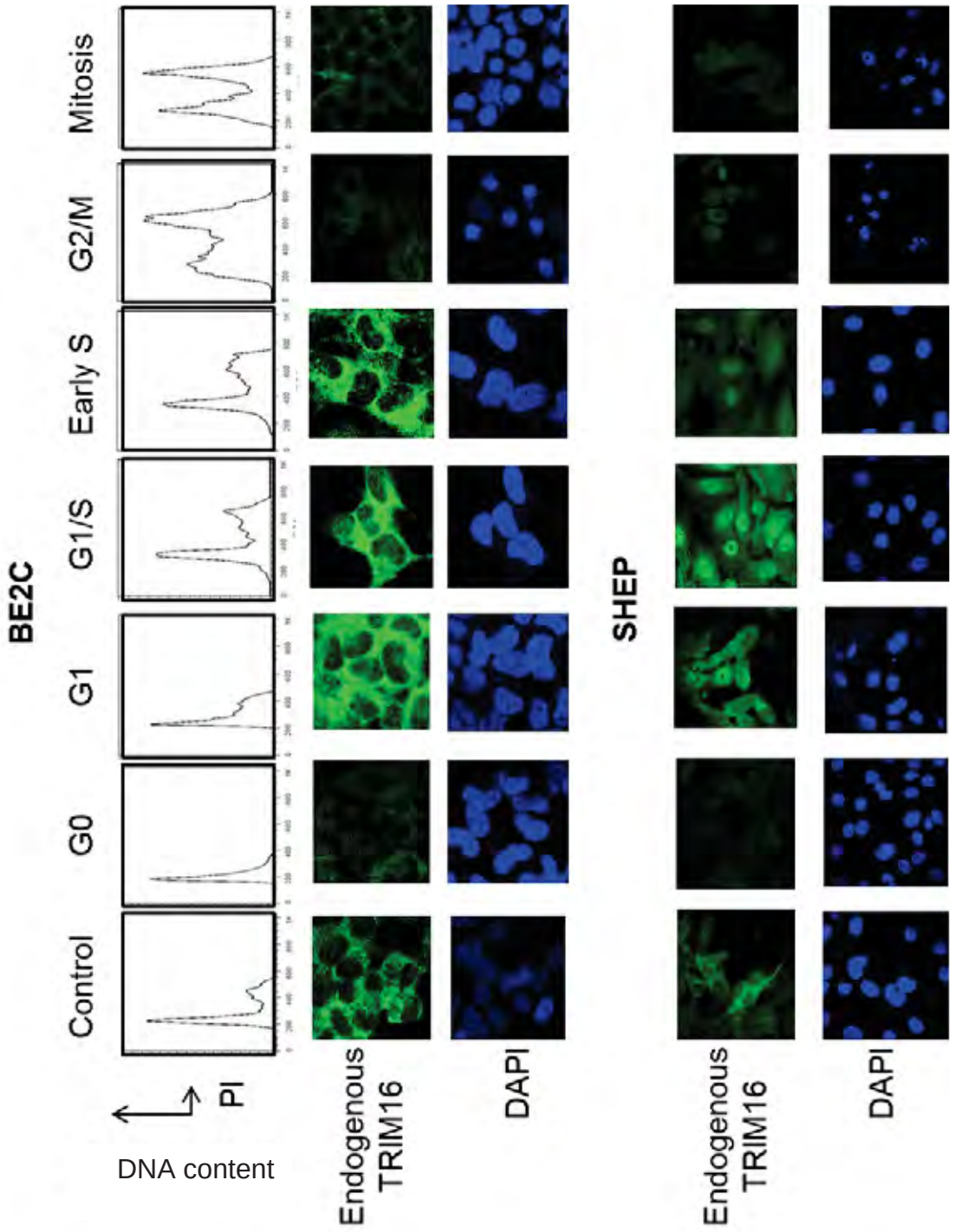

Figure 4.10 TRIM16 has increased nuclear localisation at G1 cell cycle phase in neuroblastoma cell lines

Propidium iodide was used to optimise the synchronisation of cells by DNA content analysis. Immunofluorescent studies used confocal microscopy at the 100X objective on the Olympus FV1000. BE2C cells images have an additional 2X zoom. Endogenous TRIM16 is stained with 488 (green) channels. DAPI (a nuclear/DNA stain) has blue staining.

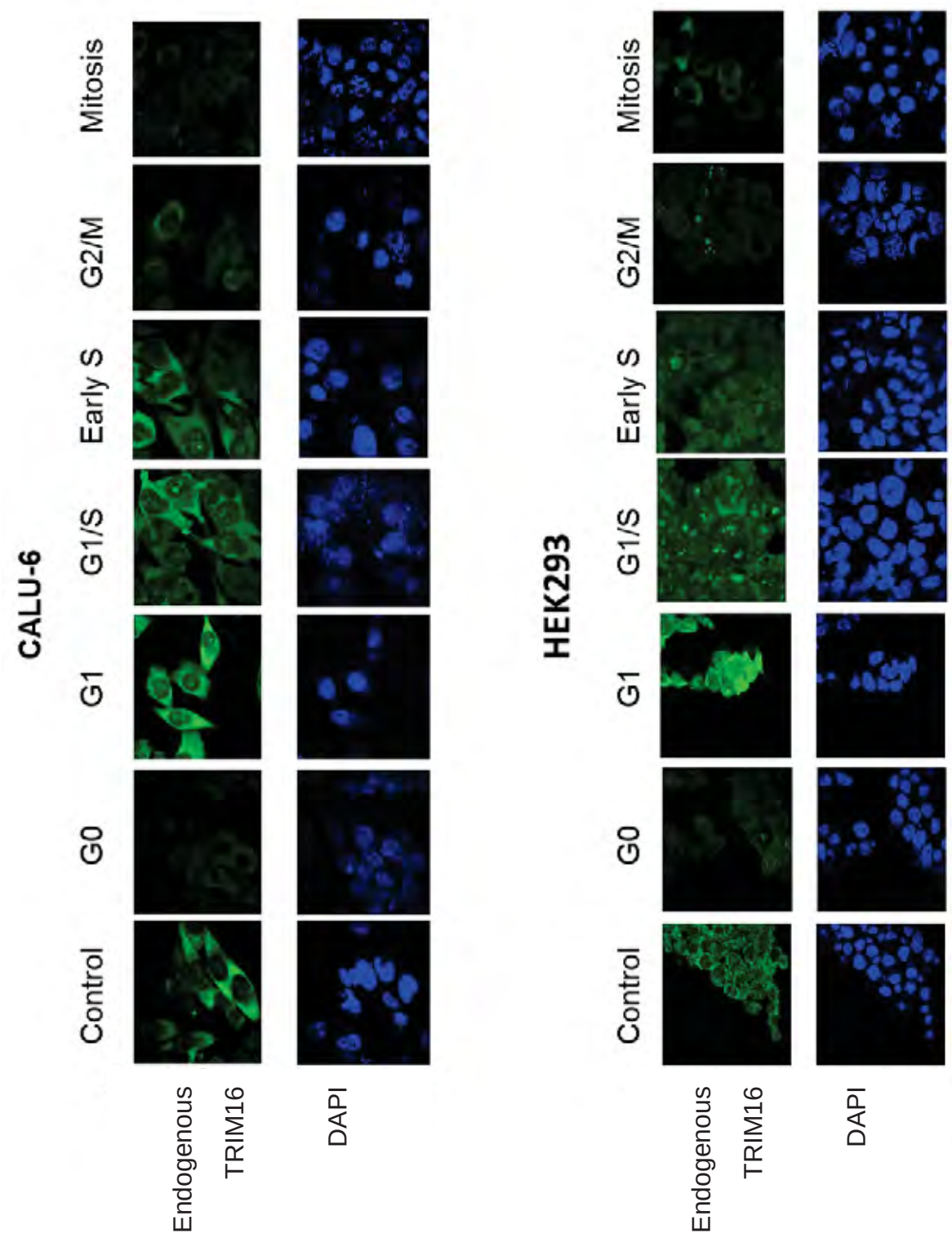

Figure 4.11 TRIM16 has increased nuclear localisation at G1 cell cycle phase in non-neuroblastoma cell lines

Immunofluorescent confocal studies, 100X objective, Olympus FV1000. Endogenous TRIM16 is stained with Alexafluor 488 (green). Staining of the nucleus is shown in blue (DAPI). CALU-6 (Lung Cancer), HEK293 (Human Embryonic Kidney Cells).

4.2.5 TRIM16 has a role in cell cycle progression

TRIM16 overexpression reduced proliferation and doubling time in neuroblastoma cells (3.2.2, 3.2.5), however, further characterisation of the mechanism underlying this effect required more extensive study. TRIM16 overexpression and knockdown studies were performed to determine if TRIM16 is associated with cell cycle progression or has an active role in cell cycle progression.

TRIM16 was overexpressed in BE2C cells for 48 hours and DNA content was then accessed by flow cytometry to determine the distribution of cells at different phases of the cell cycle. TRIM16 had a small, but nonetheless significant influence on the cell cycle status of cells, with replicate experiments showing at least a 5% increase in the G0/G1 cell cycle distribution (Figure 4.12). However, there was no evidence of an increase in the sub-G1 peak (indicative of apoptosis). Additionally, our own studies have also shown that TRIM16 knockdown increases the number of S-phase cells, as shown by BrdU incorporation in asynchronous cells [331].

As synchronisation dramatically affected TRIM16 cell phenotype and there was a marked induction at G1, it was likely that TRIM16 was required in synchronised cells for progression to G1. This prompted investigation into whether TRIM16 was required for the proper transition from G0 to G1 in the cell cycle. BE2C cells were synchronised by serum starvation and simultaneously transfected with TRIM16 specific siRNAs. At the protein level, many markers of the G1 cycle phase were analysed after cells were fed serum.

Both specific siRNA sequences knocked-down TRIM16 protein levels by 36 hours post transfection and this knockdown was maintained during the subsequent time points (Figure 4.13). The tumour suppressor p27 and cyclin D1 were both

downregulated by the specific TRIM16 siRNAs. Critical mid-G1 factors, CDK4 and CDK6 were upregulated by TRIM16 knockdown. pRb and cyclin E showed no significant trends across the time points studied.

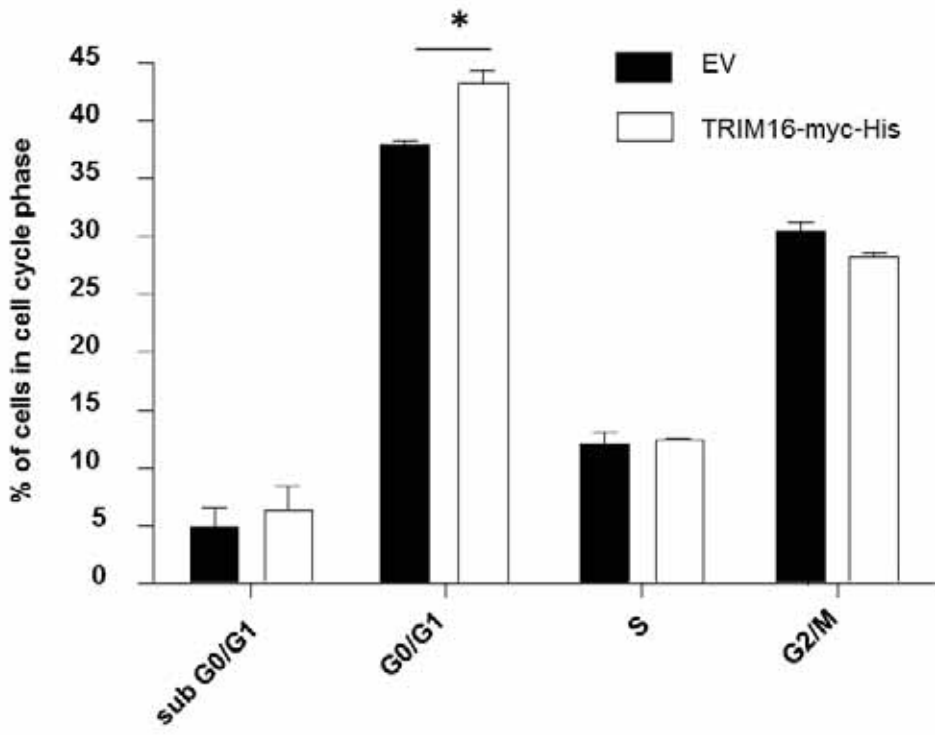

Figure 4.12 Overexpression of TRIM16 produces a small significant accumulation of cells in the G0/G1 DNA content via flow cytometry

BE2C cells were transiently transfected with the TRIM16-myc-His plasmid or EV control, for 48 h before harvest. Propidium iodide was used to determine DNA content. *$p<0.05$.

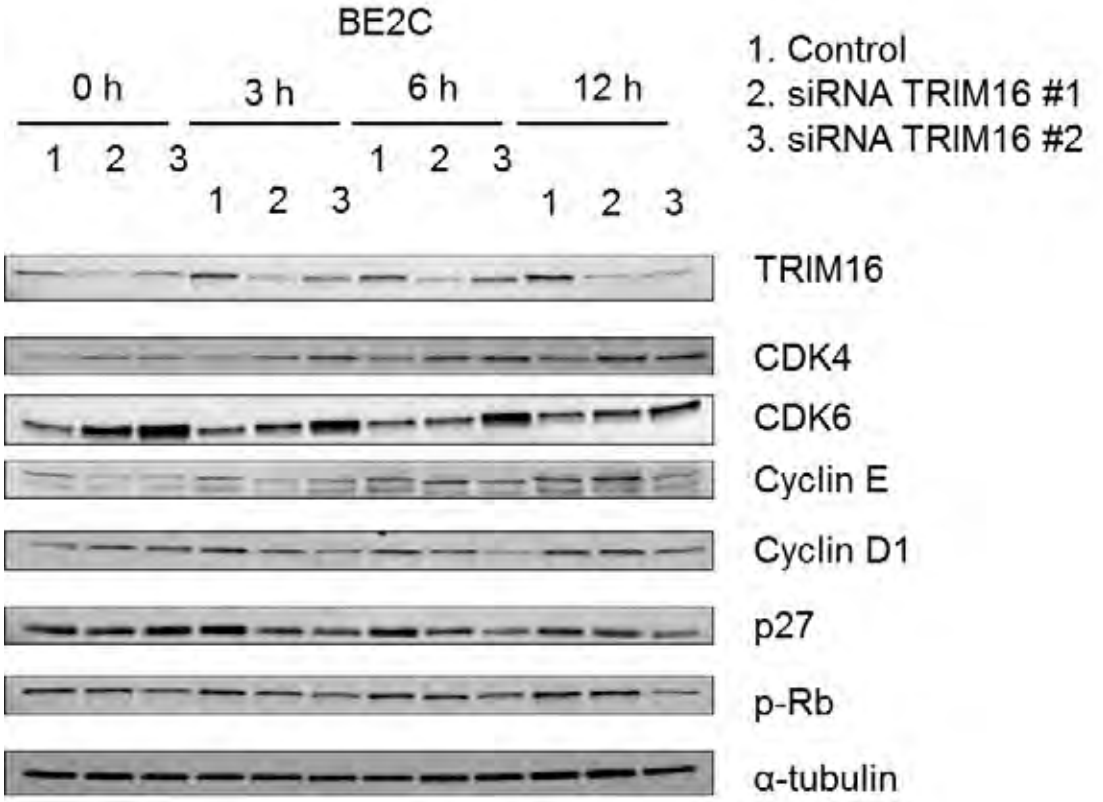

Figure 4.13 TRIM16 knockdown modulates G1 components; CDK4/6, CyclinD1 and p27

Western blot of TRIM16 siRNA transfected cells synchronised in G0 and released for time points to 12 h. BE2C, neuroblastoma cells were used.

4.3 Discussion

Differentiation and cell cycle progression are processes strongly linked in all cells. For the first time, TRIM16's influence and expression in both differentiation and cell cycle control were evaluated. This chapter demonstrated that TRIM16 has dynamic expression at the protein level in both differentiating cells and during the cell cycle. Furthermore, TRIM16 is highly expressed in the nucleus during the G1 cell cycle phase and differentiating cells. Lastly, TRIM16 has a role in the cell cycle and modulates several cell cycle proteins required in the G1 cell cycle phase.

TRIM16 is dynamically expressed during normal parasympathetic ganglia development and suppressed in neuroblastoma cells. Evidence of this was gained by using the TH-MYCN mouse model of neuroblastoma [33,34,92]. Notably, TRIM16 was highly expressed in the nuclei of the large differentiating ganglia cells of both wildtype and transgenic mice. This was in contrast to the tumour initiating cells in the hyperplastic regions, where the majority of cells had lost TRIM16 expression. Interestingly, in the highly proliferative neuroblastoma tumours, TRIM16 was expressed weakly in the cytoplasm. In the mature ganglia of the wildtype mice TRIM16 was ubiquitously and moderately stained throughout the nucleus and cytoplasm of the ganglia cells and was greatly reduced compared with the high expression observed for TRIM16 at day 0. This decrease in TRIM16 expression in mature, non-dividing cells was reminiscent of TRIM16's decrease in expression in G0 cell cycle phase *in vitro*.

As TRIM16 is downregulated at G0 *in vitro*, it probable that the nuclear TRIM16 stained ganglia cells were in the G1 cell cycle phase or in the early stages of differentiation, due to their high TRIM16 expression and comparisons with cell cycle phase markers. Importantly, nuclear TRIM16 is therefore, a marker of early

differentiation or early G1 cell cycle phase, in the neuronal cells studied. As the mature ganglia cells of the 6 week old mice did not have predominately nuclear TRIM16, nuclear TRIM16 is not associated with terminally differentiated cells. This indicates that TRIM16 localisation and expression is also cell cycle dependant *in vivo*. In the literature, TRIM16 is shown to display a similar expression phenomenon in differentiating skin as observed in the differentiating neuroblasts [330]. TRIM16 was highly expressed during the early differentiation process of the skin, but not in the highly proliferative epithelium of wounded skin. Importantly, TRIM16 knockdown has previously been shown to increase cell proliferation and the proportion of cells in the S phase of the cell cycle in neuroblastoma cells [359]

A surprising result of the immunohistochemistry studies was the massive induction of predominately nuclear p27 throughout the entire cohort of mouse tumour tissues. In human neuroblastoma, high p27 protein expression was a favourable prognostic factor and independent of MYCN amplification [137,358]. However, surprisingly homogenous induction of p27 was observed in the majority of neuroblastoma tissues, suggesting a common deregulation of p27 in human neuroblastoma tissue *in vivo*. p27 deregulation and induction in mature tumours is an interesting phenomenon that is perplexingly, as it is in contrast to the classic function of the tumour suppressor p27, and requires further study.

My data suggests that endogenous TRIM16 expression is not merely associated with differentiating neuroblast cells, but that TRIM16 is also a promoter of neuroblast differentiation. Furthermore, the nuclear localisation of TRIM16 has a function in differentiating, rather than in terminally differentiated cells. Evidence of the ability of TRIM16 to enhance differentiation was gained by forced TRIM16 expression studies

and it was demonstrated that RA-induced differentiation is markedly increased by TRIM16. Unfortunately, the basal levels of neurite bearing cells were not at a rate high enough (around 5%) to allow statistical separation of clones. Therefore it could not be definitively determined through this experimental system if TRIM16 was able to induce differentiation independent of RA. Furthermore, in the TH-MYCN mice, nuclear TRIM16 was specifically associated with differentiating ganglia cells, which suggests the localisation of TRIM16 may also play a part in its role in differentiation. My colleagues and I have recently published that in human neuroblastoma tissue, within heterogeneous tumours, TRIM16 is highly expressed in the differentiated regions and lowly expressed in the less differentiated cell regions [331]. Additionally, it is important to appreciate that neuronal differentiation (including via retinoid) is known to be via G1 cell cycle arrest (1.3, 1.4). Importantly, Beer *et al*. have shown TRIM16 overexpression induces skin differentiation [330]. Their *in vitro* studies also show that overexpression of TRIM16 enhanced early differentiation. This further confirms the conclusion that TRIM16 is an enhancer of differentiation.

Induced TRIM16 expression is associated with the G1 cell cycle phase in various cell types, including neuroblastoma (Figure 4.14). TRIM16, although being weakly expressed in G0 and mitosis was highly expressed during the G1 cell cycle phase. Furthermore, TRIM16's localisation became more nuclear during G1 and shifted back towards the cytoplasm during S phase, as evidenced by Western blot and immunofluorescent studies. It was surprising that TRIM16 was not more highly expressed in G0 cells, but this indicates that TRIM16 is more important in an actively differentiating or G1 cell, rather than a cell at rest. Taken together, these data suggest that involvement of TRIM16 in differentiation occurs via interactions with G1 cell cycle phase machinery. My research has shown, TRIM16's role in G1 cell cycle phase is

partly through increased protein levels, probably via decreased protein degradation of TRIM16 and that TRIM16 transcription was not increased during the G0 to G1 phases. Retinoid treatment which is known to arrest neuroblastoma cell lines in G1 before differentiation has also been shown in earlier research on TRIM16 to increase TRIM16 protein half-life [8]. This indicates TRIM16 levels are post-transcriptionally regulated. Further research using cycloheximide treatments of synchronised cells would confirm the protein half-life of TRIM16 is altered at different stages of the cell cycle.

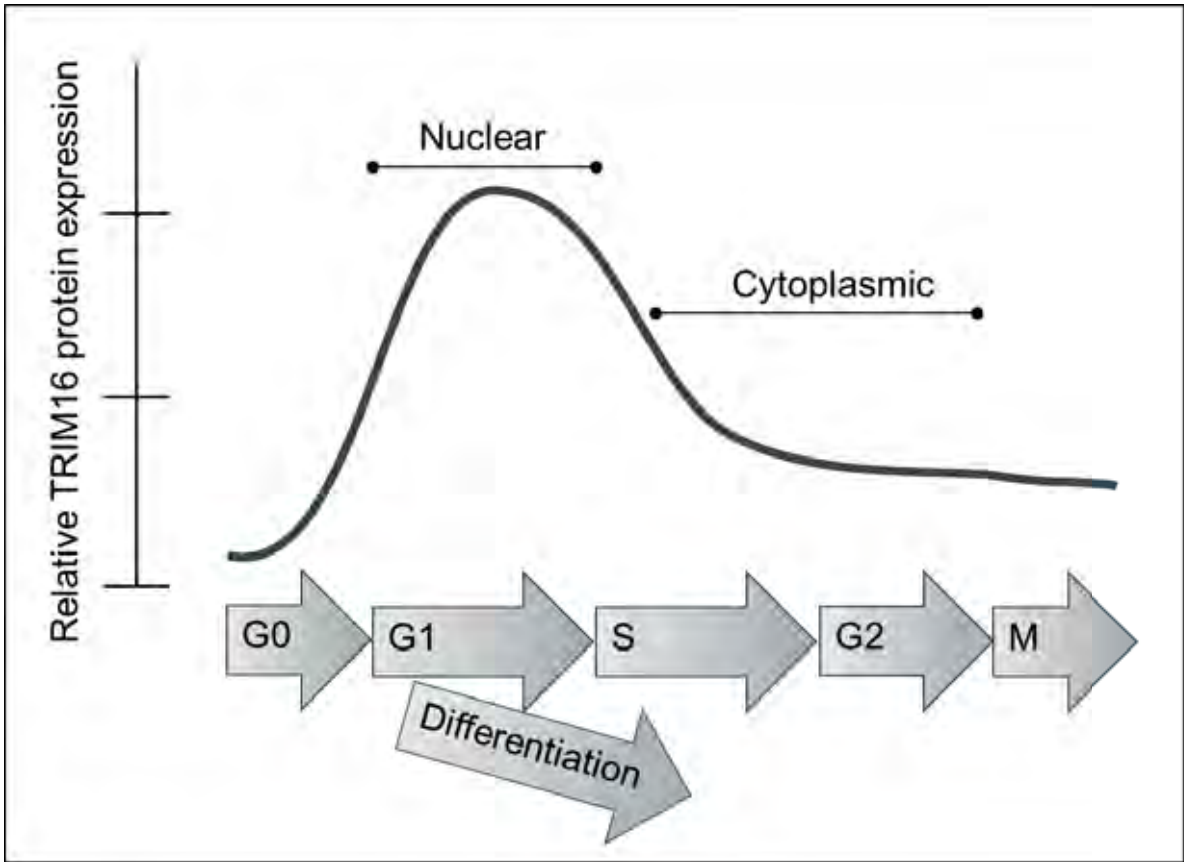

Figure 4.14 TRIM16 protein expression increases and shifts to the nucleus during both G1 and in early differentiation.

My research into the induction of TRIM16 during the cell cycle, sheds new light on results published by Beer *et al*. [330]. They showed a marked induction of TRIM16 protein (but not mRNA) in skin cells after serum starvation and release at two time points. My work demonstrates that Beer *et al.*'s results were likely due to the cell cycle status of the cells and that the biphasic induction of TRIM16 observed by Beer *et al*. after release from serum starvation, was likely due to the cells re-entering the G1 cell cycle phase and not from a pre-determined bi-phasic induction of protein as hypothesised by Beer and colleagues.

TRIM16 expression significantly modulates the G1 cell cycle phase. During cell cycle progression TRIM16's role is not merely an associative role, but an active one. TRIM16 overexpression resulted in a small, yet significant accumulation of cells in the G1 cell cycle phase. This small change may have been due to use of asynchronous cells or a mixed population of transfected and untransfected cells, which may have obscured a more measurable effect. Interestingly, knockdown studies have shown an increase in BrdU incorporation (increase in S-phase cells) and increased proliferation [331] These cells were also unsynchronised.

One strength of my research over previous studies is that I have chosen to synchronise cells. My own TRIM16 knockdown data was performed on synchronised cells, and Western blotting analysis of components of the G1 cell cycle phase demonstrated that TRIM16 has significant involvement with the mid-G1 machinery. p27, which is highly involved with retinoid differentiation and cell cycle control, was significantly affected by the knockdown of TRIM16. CDK4 and CDK6 were both induced by TRIM16 knockdown.

As TRIM16 overexpression promotes differentiation and decreased proliferation, in which TRIM16 had been knocked-down would be expected to progress through G1 faster. However, the data presented does not indicate a faster progression through G1, at least when cells are synchronised. Instead the data suggests a deregulation of G1 following knockdown of TRIM16. Cyclin D1 was downregulated by the TRIM16 knockdown. The time points used indicated a delay in this cell cycle factor's induction by at least 9 hours, upon TRIM16 depletion. Cyclin D1 protein has been shown to enhance retinoid treatment response in breast cancer cells [360]. Cyclin D1 is also deregulated in many cancers, including breast cancer, but is usually overexpressed, rather than repressed [361]. However, the downregulation of cyclin D1 by TRIM16 could have been through a feedback loop, in which TRIM16 knockdown increased E2F1 activity and thereby repressed cyclin D1 transcription. [331,362]. One interesting study demonstrated that c-Myc has a similar effect on the cell cycle to that observed for TRIM16 knockdown [363]. When c-Myc was overexpressed from G0-S phases, p27 and cyclin D1 were reduced with CDK4 and CDK6 being induced. C-Myc is an oncogene and the effect observed for TRIM16 knockdown may explain how TRIM16 acts as a tumour suppressor through changes in the cell cycle.

As already discussed p27 is integral to promote differentiation, retinoid signalling and in cell cycle control. Interestingly, p27 regulation has also been shown to be controlled by another TRIM protein, TRIM21 [354]. In this study, a mutant of TRIM21, which has a structure similar to TRIM16, was able to protect p27 from degradation through the proteasome. Thus, it could be speculated that TRIM16 may also protect p27 in the same way.

In conclusion, TRIM16's inhibition of tumorigenicity and proliferation observed in Chapter 3 are likely due to TRIM16's involvement in differentiation and the G1 cell cycle phase. Importantly, TRIM16 nuclear protein increases in the nucleus during G1. With presumably rare changes at the transcription level TRIM16's nuclear localisation is probably an important factor in its growth inhibitory function and indicative of post-translational modification changes or effects of an unknown protein binding partner. Furthermore, TRIM16 is an enhancer of retinoid-induced differentiation, and is expressed in the nucleus of differentiated ganglia cells. TRIM16 is a dynamically expressed protein, and has a role in proliferation through influencing G1 cell cycle factors in the nucleus. The next step to understanding the role of TRIM16 in neuroblastoma is through a thorough examination of the function of the TRIM16 domains.

CHAPTER 5

RESULTS III: PUTATIVE TRIM16 PROTEIN DOMAINS CONVEY TRIM16 FUNCTIONS

5.1 Introduction

This final chapter aimed to investigate the function of the putative domains of TRIM16 and their role in TRIM16 function in neuroblastoma. TRIM16 possesses a B-box1, B-box2, coiled-coil domains and B30.2 domain but does not have a RING domain (Figure 5.1). Furthermore, it remains to be tested whether the putative domains of TRIM16 can convey functions similar to other TRIM proteins. Therefore, key functional traits of TRIM proteins such as the ability for homodimerisation and ubiquitin binding were explored. Additionally, domain deletion mutants were employed to gain a greater insight into the known traits of TRIM16, including its ability to inhibit growth and clarify its protein localisation.

The first aim of this chapter was to determine if the B-boxes of TRIM16 could bind ubiquitin and enable a role for TRIM16 in protein degradation. TRIM protein B-boxes have not been shown to have ubiquitin activity, independent of an autologous RING domain. However, B-boxes, like those of the TRIM protein MID1, have strong potential ubiquitin activity according to research by Massiah and colleagues [364,365]. They speculated that B-boxes can interact with UbcH7 and have ubiquitin ligase activity. This activity would be through an evolutionary conserved consensus sequence, which is potentially present across different species, and also amongst several TRIM proteins including TRIM16. Therefore, for my research, the sequences of the B-boxes of TRIM16 and MID1 should be compared, and if TRIM16 has the zinc-binding consensus region which allows ubiquitin binding then it is possible that TRIM16 can have ubiquitin activity, and also play a role in proteasome degradation.

It is unknown if TRIM16 has a role in the proteasome pathway like other TRIM proteins (eg. TRIM24 and TRIM25) [9,268,319]. Several TRIM proteins with RING domains have a role in proteolysis, acting as E3 ubiquitin ligases. B-boxes are required

for the E3 ligase ability of PML and its ability to transfer the small ubiquitin-like modifier (SUMO) from Ubc9 to p53 [366]. Similarly, MID1's B-boxes enhance the E3 activity of its RING domain [367]. Common features of E3 ligases are their ability to auto-ubiquitinate and self-degrade. TRIM16 expression has already been shown to be highly regulated at the protein level, without any change to mRNA levels [8], (4.2.3). However, this aspect of TRIM16 would have to be formally addressed experimentally in order to further characterise TRIM16's role in proteasome degradation.

The second aim of this chapter was to address whether TRIM16 can homodimerise, or if it can heterodimerise with other TRIM proteins. Such an ability would have a significant influence on TRIM16 function and present the possibility that TRIM16 is involved in important large protein complexes with other TRIM proteins. Higher order complexes of TRIM proteins are known to be essential transcription regulators in cell processes such as differentiation involving TRIM homo- and heterodimerisation [9,341]. Interestingly, several of the TRIM proteins are known to homodimerise, with the coiled-coil domain generally required for the homodimerisation [9,224-226,368].

From research performed in Chapters 3 and 4 of this thesis, it is known that TRIM16 has a role in proliferation and that neuroblastoma proliferation arrest is potentially dependent on the expression of nuclear TRIM16 (3.2.2, 3.2.5, 4.2.1, 4.2.4), and these significant attributes of TRIM16 required further characterisation. Because localisation of TRIM16 is important for its function, domain deletion mutants need to be used to determine if particular domains of TRIM16 are related to localisation of the protein. Given that several TRIM proteins have validated localisation sequences [224,235,369], it is therefore possible that TRIM16 harbours localisation signals of its

own, within its protein domains. Domain deletion mutants of TRIM16 would also be essential to assess which domains of TRIM16 are required for its growth inhibition.

Thus, based on these rationales, TRIM16 deletion mutants were used to study TRIM16's ability to act in protein degradation, homodimerisation, affect localisation and induce growth inhibition.

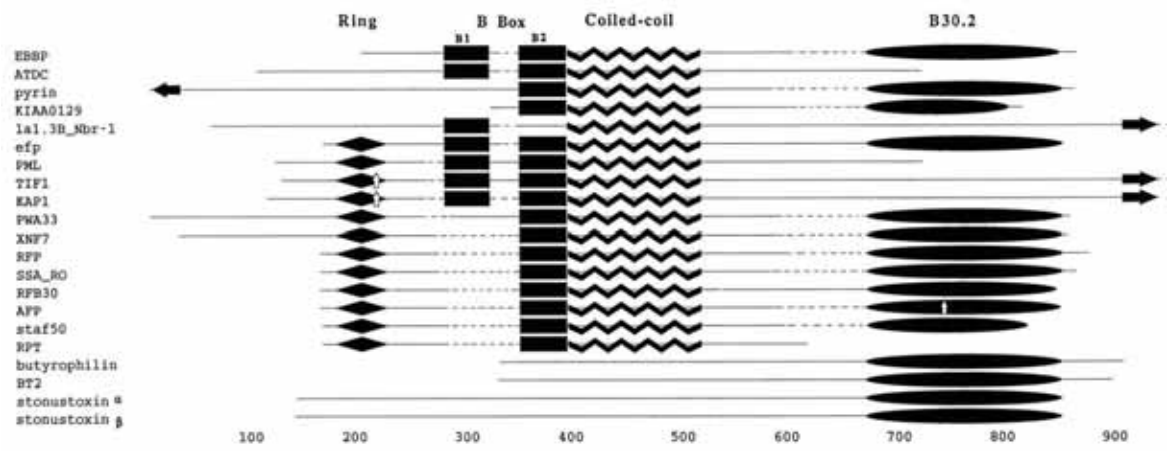

Figure 5.1 Schematic representation of TRIM16 (EBBP) and other TRIM proteins

The numbers listed at the bottom represent the TRIM16 (EBBP) amino acid positions. The schematic of TRIM16 is the upper most protein. The contiguous protein sequence is shown by solid lines, and gaps are indicated by dashed lines. Vertical arrows represent insertions. Horizontal arrows represent additional sequences in the direction indicated. This figure was sourced from a Liu and colleagues research paper [329].

5.2 Results

5.2.1 Validation of the TRIM16-GFP construct

To study a wide range of TRIM16 attributes, green fluorescence protein (GFP) vectors were used to create a panel of constructs (2.5). Firstly, the full length TRIM16 expression vector was validated and optimised. In brief, BE2C cells were transfected as per the myc-His tag vector protocol (2.3.1), and protein was freshly extracted from cells at a range of time points to determine when the TRIM16-GFP protein is expressed. Western blot analysis of whole cell lysates showed that the highest expression occurred at the 24 hour time point (Figure 5.2A). Protein expression was observed at all the time points studied. 10 μM RA treatments increased the amount of TRIM16-GFP protein.

A live cell imaging fluorescent microscope (Olympus FV1000) was used to determine if the GFP fused to TRIM16 could be visualised. In contrast to the Western blot results, TRIM16-GFP could only be observed after 24 hours, and the 48 and 72 hour time points displayed the most cells expressing the GFP construct (Figure 5.2B).

As cells could be easily transfected and monitored using transfection of the TRIM16-GFP, proliferation studies were performed with the GFP plasmids. Both the 48 hour and 72 hour time points showed significant growth inhibition with overexpression of the full length TRIM16-GFP, with the largest effect demonstrated at 72 hours (Figure 5.3). The effect was not as large as reported with equivalent myc-His tag experiments (Figure 3.2), but was nonetheless within the range of experimental experience with the myc-His vector.

A

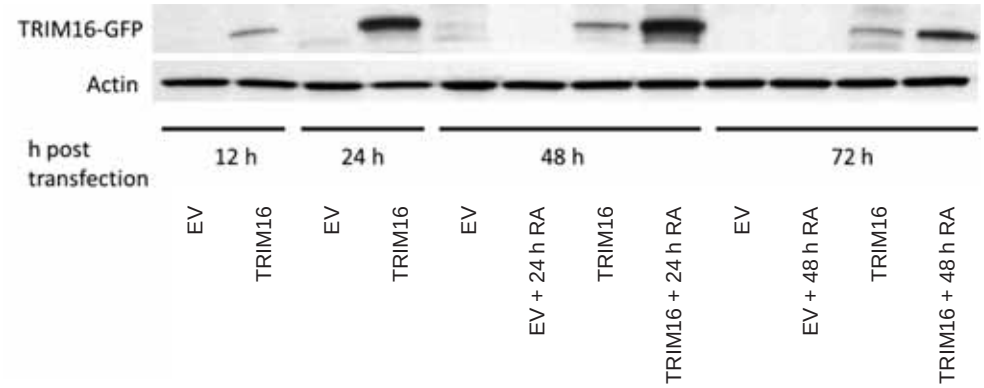

B

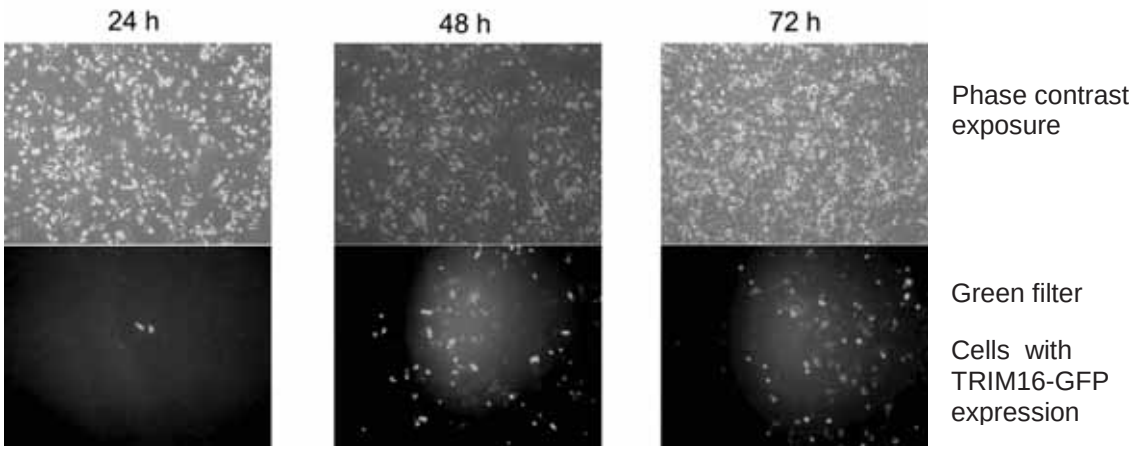

Figure 5.2 TRIM16-GFP expression in BE2C

A) Western blot of transgene protein expression over time course with 10 μM RA (24 or 48 h, as indicated). B) Live cell imaging with the 40X objective of phase contrast images (top panel) and with the green filter channel (lower panel).

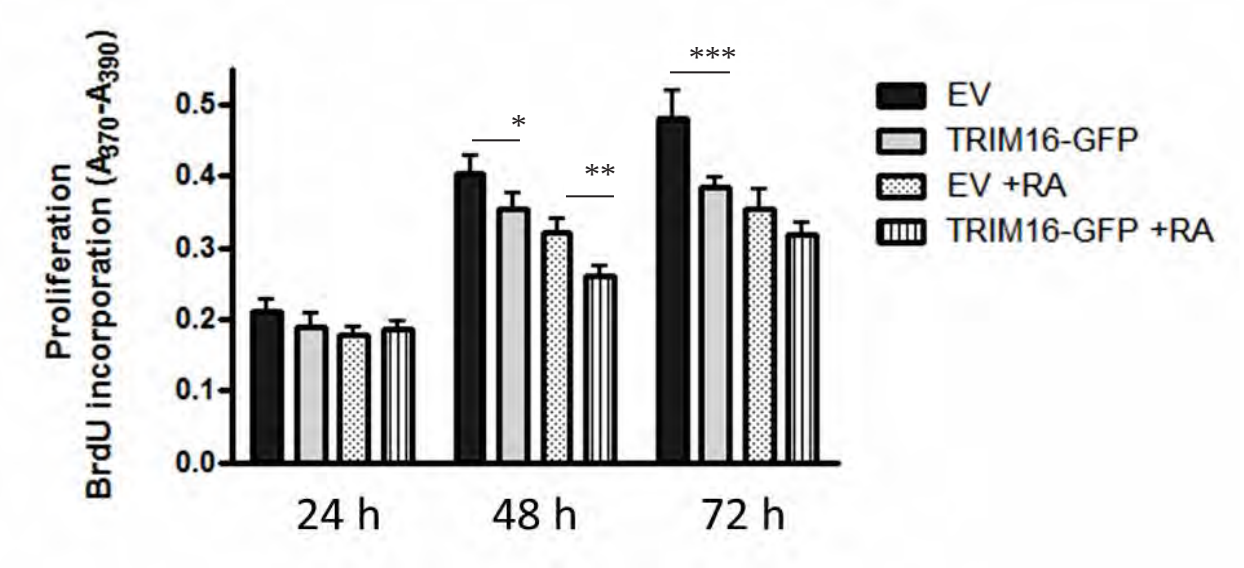

Figure 5.3 TRIM16-GFP causes growth inhibition in BE2C

10 μM of RA was used to treat BE2C cells. Treatment commenced 24 h post transfection (12h for 24 h time point) and maintained until the BrdU assay was performed. * $p<0.05$, **$p<0.01$, ***$p<0.001$

5.2.2 TRIM16 domain deletion mutants

TRIM16 domain deletion mutants were produced as outlined in the materials and methods section of this thesis (2.5.2). TurboGFP (GFP) was fused to the C-terminus of TRIM16 mutant proteins. The presence of inserts of correct size and quality was confirmed by restriction digest and agarose gel electrophoresis (Figure 5.4).

Western blots were performed to confirm transgene protein expression. All vectors were able to be expressed in several cell lines (e.g. BE2C, SHEP, CALU-6 and HEK293 cell lines) and showed banding at the expected kDa weight. HEK293 had the highest transfection rate and showed the clearest expression of the mutants by Western blot (Figure 5.5). All mutants were expressed at similar levels, except M1. M1 which is without B-box domains, resulted in about half the expressed protein compared with the other mutants.

The antibody used to detect turboGFP had low specificity. At the time of undertaking these experiments, only an Evrogen antibody was available for the turboGFP tag. While this rabbit antibody had an extremely high affinity for the tag, it also had an affinity to non-specific bands around the 60 and 45 kDa ranges, and additional bands were also observed in cases where the transfection efficiency was not high. High concentrations of blocking peptides were therefore essential for assays using this antibody. Three other GFP (normal) antibodies were trialled but did not show affinity for the turboGFP tag (data not shown).

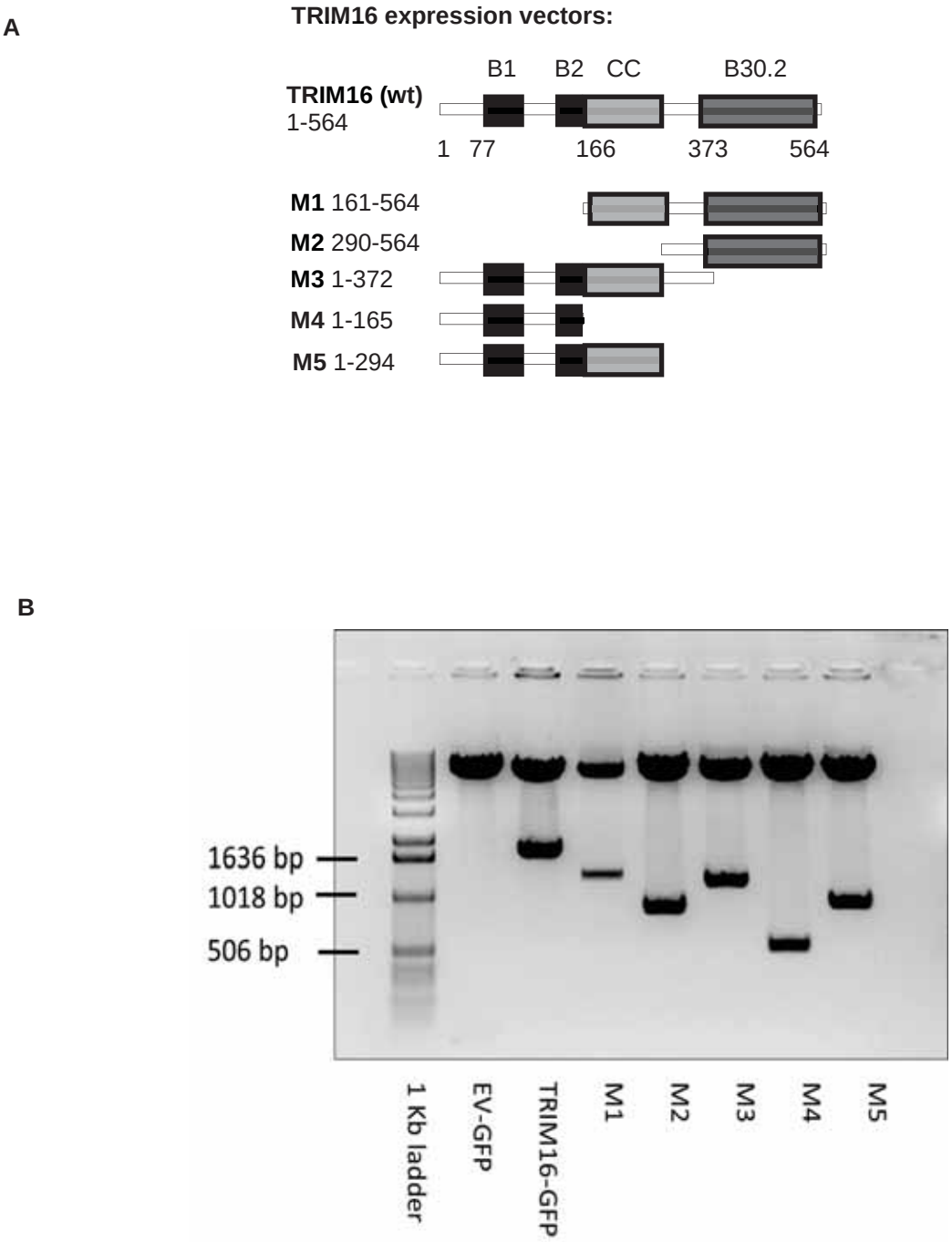

Figure 5.4 TRIM16 domain deletion mutants restriction digests

A) TRIM16 domain deletion mutants. B1 (B-box1). B2 (B-box2). CC (coiled-coil).

B) TRIM16 constructs were digested for 2 hours with MluI and SgfI enzymes and separated by electrophoresis on a 1% Agarose gel. bp sizes of mutants exclusive of GFP: wt (1692), M1 (1209), M2 (822), M3 (1116), M4 (495), M5 (882).

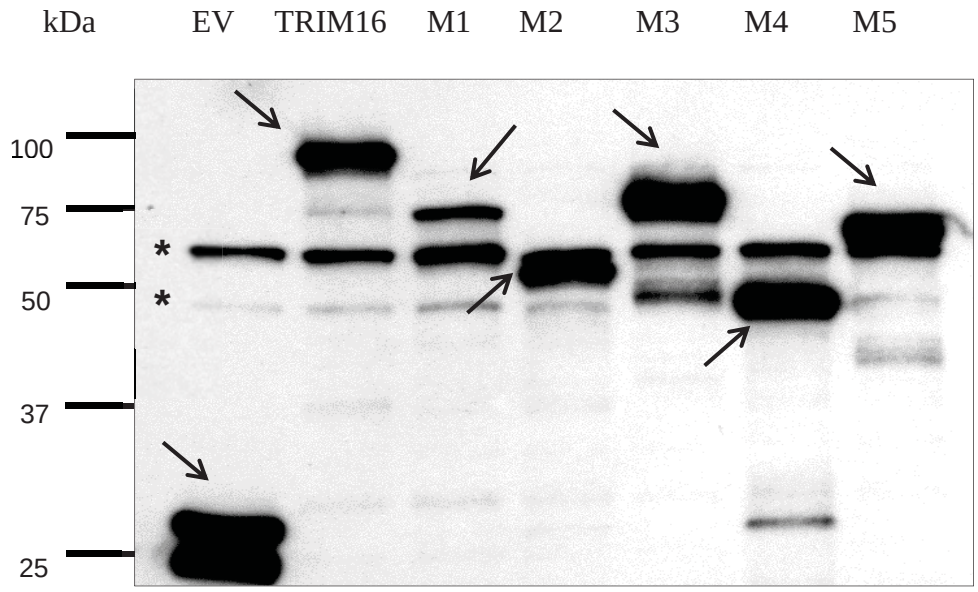

Figure 5.5 Western blot of TRIM16-GFP domain deletion mutants

HEK293 cell lysates shown. Arrows denote the presence of transgene protein. Expected kDa sizes (inclusive of the 27 kDa GFP) are: TRIM16 (92), M1 (74), M2 (59), M3 (69), M4 (45), M5 (60).

* denotes non-specific band.

5.2.3 Amino acid sequence comparison of TRIM16 and MID1 B-boxes suggest zinc binding capacity in TRIM16

Two papers describing the structure of MID1, by Massiah and colleagues [364,365], demonstrate that B-boxes, like those of TRIM16, can adopt a structure similar to the RING domain in MID1 (TRIM18). This led to the hypothesis that like MID1, TRIM16 also possesses a zinc-binding consensus sequence. To test this, an amino acid sequence alignment study with the human MID1 sequence and TRIM16 from various species was performed (Figure 5.6A). The results revealed a 46% identity between the human B-box1 sequences of the two proteins (Sim, ExPASy, CA). TRIM16 did in fact share a similar consensus sequence as MID1, with one exception, in that the 6th cysteine residue in MID1's B-box1 (in the consensus sequence) was substituted with a histidine residue in TRIM16. Other TRIMs; TRIM29 (ATDC) and TRIM25 (EFP) also share this particular substitution [365]. Spacing of the predicted zinc-binding residues is remarkably similar between TRIM16 and MID1. An unbiased blast search (NCBI) of TRIM16's B-box1 sequence displayed significant identities with human TRIM16, TRIM29, TRIM25, MID1, RFP and MID2 (in order of significance all with E-values <0.009, and scores above 37.7). Apart from the TRIM family members, no other characterised protein families were represented. There was also a relatively high 58% identity between human and zebrafish TRIM16 for B-box1.

Analysis of TRIM16's B-box2 yielded similar results as found in B-box1 (Figure 5.6B). However, there was lower identity between the human sequences of MID1 and TRIM16, in the B-box2 region, of only 28% (Sim, ExPASy, CA). Interestingly, when compared with human MID1 and human TRIM16, the rodent sequences of TRIM16 had an interchange between the aspartic acid and histidine residues binding to the second zinc atom. The zebrafish did not retain the aspartic acid residue at all, which was

substituted with a cystidine, in that case. For B-box2, there was also only 34% identity between human and zebrafish TRIM16.

Taken together, TRIM16 is not similar to any other TRIM proteins apart from the TRIM16-like protein (with which TRIM16 shares the coiled-coil and B30.2 domains). However, the notable exception to this trend is in TRIM16's B-box1 region, where significant similarities exist with several other TRIM proteins.

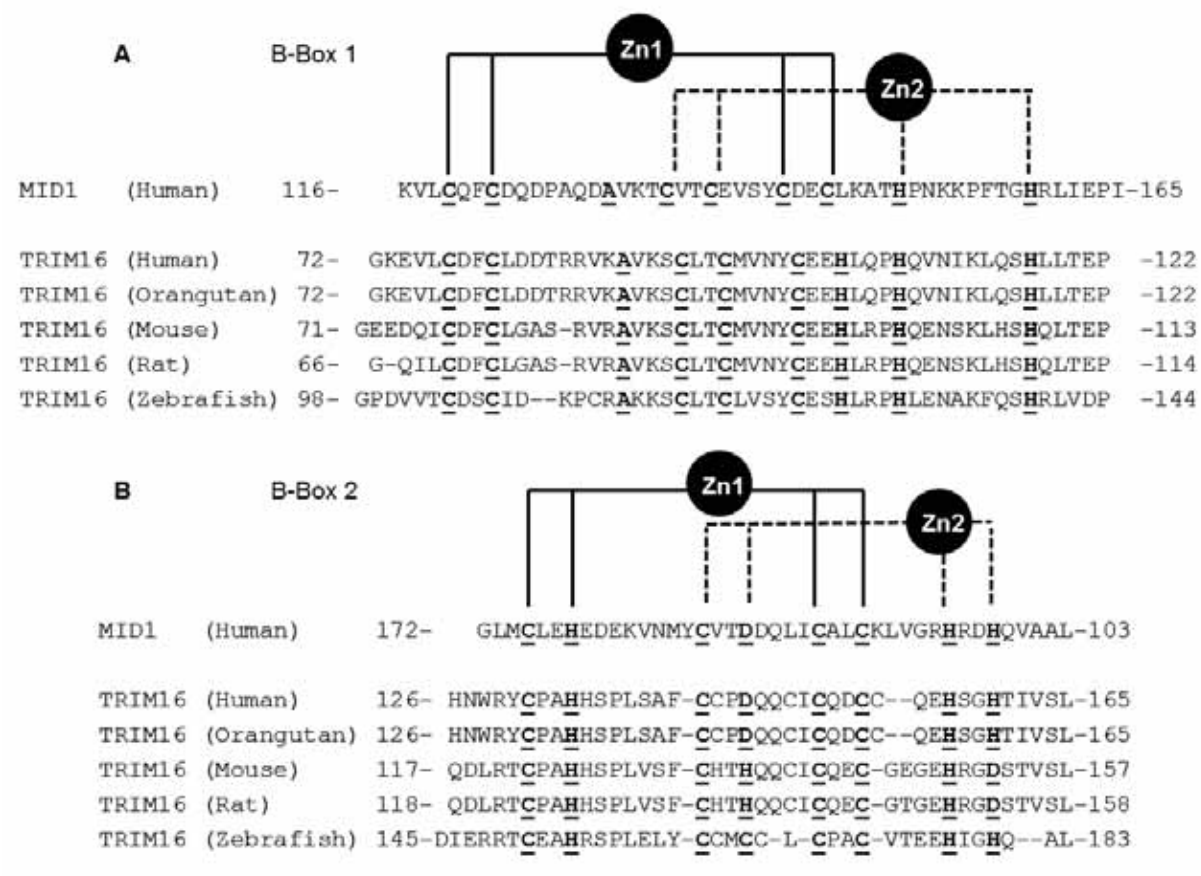

Figure 5.6 Amino acid sequence comparison of TRIM16 and MID1 reveals zinc binding potential of TRIM16

The conserved residues in the zinc binding regions are in bold underlined type and are; cysteine (C), histidine (H), alanine, (A) aspartic acid (D). **(A) B-Box1. (B) B-Box2**

5.2.4 B-Boxes are required for *in vivo* auto-ubiquitination of TRIM16

A common characteristic of E3 ligases is their ability to auto-ubiquitinate and self-degrade. TRIM16 is an unstable protein, which is likely degraded by proteasome mediated degradation. This was confirmed in various cells types, where treatment with the proteasome inhibitor MG132, led to an increase in the TRIM16 protein compared to untreated samples (Figure 5.7). Furthermore, TRIM16 has a short protein half-life of around 4 hours measured by cycloheximide-based protein chase experiments in both SH-SY5Y and HEK293 cells.

As proteasome degradation activity is an indicator of ubiquitin binding and E3 ligase function, it was investigated whether TRIM16 can be auto-polyubiquitinated in HEK293 cells. TRIM16 ubiquitin binding activity was examined by *in vivo* ubiquitination assay (2.4.10). TRIM16-GFP and HA-tagged ubiquitin (Ub) were expressed in cells. GFP-tagged proteins were immunoprecipitated and the presence of polyubiquitinated TRIM16 was detected by Western blot. Only full length TRIM16 had a high-molecular-weight smear, representing heavily polyubiquitinated TRIM16, in contrast to TRIM16, the domain deletion mutants had smears similar to the EV control (Figure 5.8A). In the BE2C neuroblastoma cell line, M1 also failed to polyubiquitinate, whereas the full TRIM16 protein did polyubiquitinate (Figure 5.8B). This demonstrates that auto-ubiquitination is dependent on B-boxes in more than one tissue type.

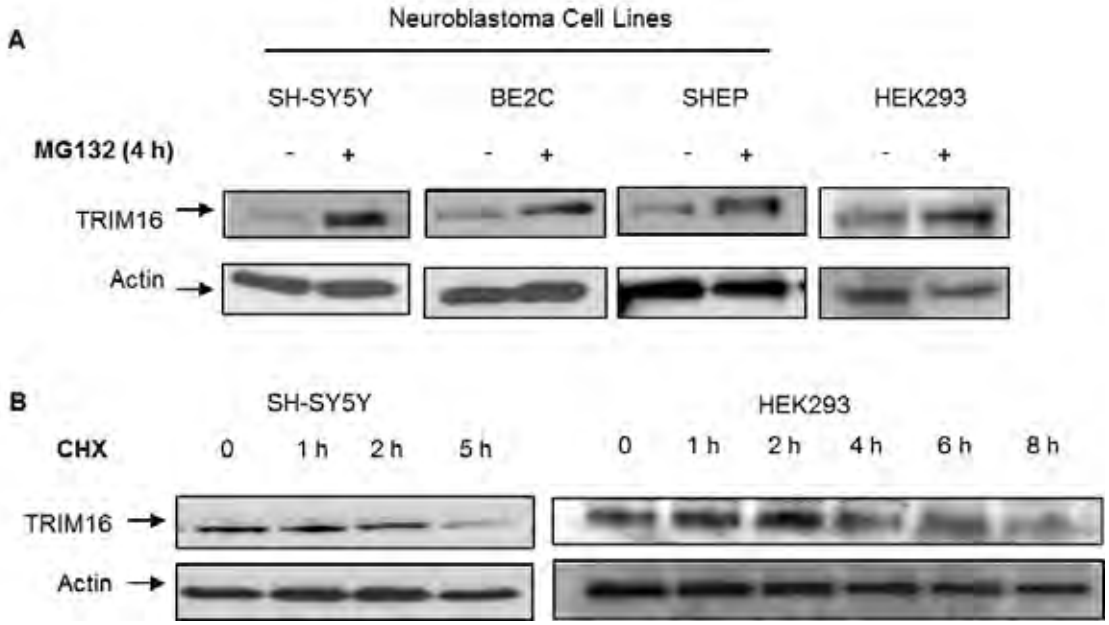

Figure 5.7 TRIM16 is an unstable protein regulated by the ubiquitin-proteasome system

(A) *In vivo* degradation assay was performed with cells being incubated with and without 30 μM MG132. Lysates were subjected to Western blot analysis of endogenous TRIM16 antibody. Actin was used as a loading control (B) The liable nature of TRIM16 was further evaluated by inhibition of translation by 100 μg/ml cycloheximide. At the indicated time points the cells were harvested and the protein extracted for analysis by Western blots. SH-SY5Y and BE2C panels of this figure were kindly produced by colleague, Alena Malyukova

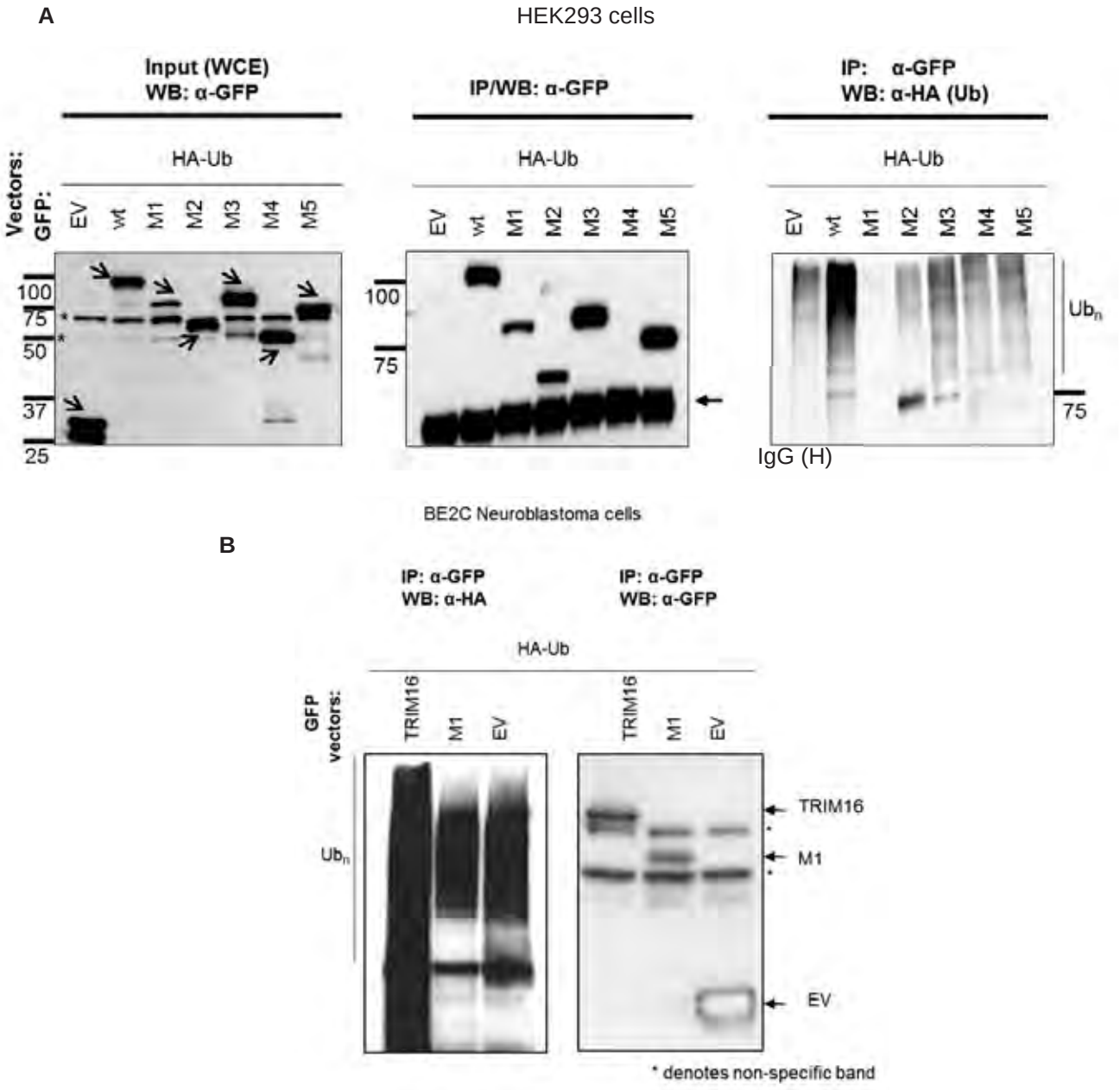

Figure 5.8 TRIM16 *in vivo* auto-polyubiquitination assay

(**A**) In HEK293 cells, HA-Ub was co-transfected with various TRIM16-GFP domain deletion expression plasmids. The protein lysate was subjected to immunoprecipitation by GFP Ab, and subjected to Western blot and probed with anti-HA Ab for Ub. 5% of the resulting denatured proteins were also analysed by Western blot with anti-GFP to confirm immunoprecipitation of all the GFP plasmids (middle gel). IP Input showing transfection of all the GFP plasmids (gel on the left), arrows denote transgene proteins. * non-specific bands.

(**B**) B-boxes are required for *in vivo* auto-ubiquitination of TRIM16 in BE2C neuroblastoma cell line. In a similar protocol to HEK293 cells (Fig 2A), an auto-ubiquitin assay was performed on the neuroblastoma cell line, BE2C. The B-Box deleted TRIM16 mutant (M1) fails to form auto-ubiquitination high molecular weight smear at observed in wt TRIM16. The assay in BE2C cells was performed by Alena Malyukova.

5.2.5 TRIM16 can homodimerise through its coiled-coil domain

Many TRIM proteins homodimerise via their coiled-coil domains [9,224,225]. Therefore it was tested if TRIM16 was also able to homodimerise. HEK293 cells were co-transfected with TRIM16-GFP and either empty vector (EV)-myc-His or TRIM16-myc-His. Immunoprecipitation of the myc-tag strongly indicated that TRIM16-GFP and TRIM16-myc-His were able to homodimerise (Figure 5.9A). These results were confirmed by using the anti-GFP antibody (Ab) for immunoprecipitation, and investigating whether GFP-tagged deletion mutants of TRIM16 were able to retain homodimerisation with the TRIM16-myc-His. GFP fusion mutants bearing coiled-coil domains (mutant 1, 3 and 5) were able to homodimerise with the TRIM16-myc-His protein, indicating this region is required for TRIM16 homodimerisation (Figure 5.9B). However, a weak band (# in Figure 5.9C) indicates that B-boxes are able to form homodimers to a much reduced extent.

TRIM16 has been shown to co-localise with PML bodies (high-molecular-weight structures) after retinoid treatment [8]. Thus, retinoid treatment and another G1 cell cycle phase arrester (Aphidicolin) were used to ascertain if homodimerisation could be enhanced by cell cycle arrest. TRIM16 was found to homodimerise in two neuroblastoma cell lines (BE2C and SHEP), which was not affected by both the G1 cell cycle arresting agents (Figure 5.10). However, in the case of BE2C cells treated with RA, the level of homodimerised TRIM16 did increase.

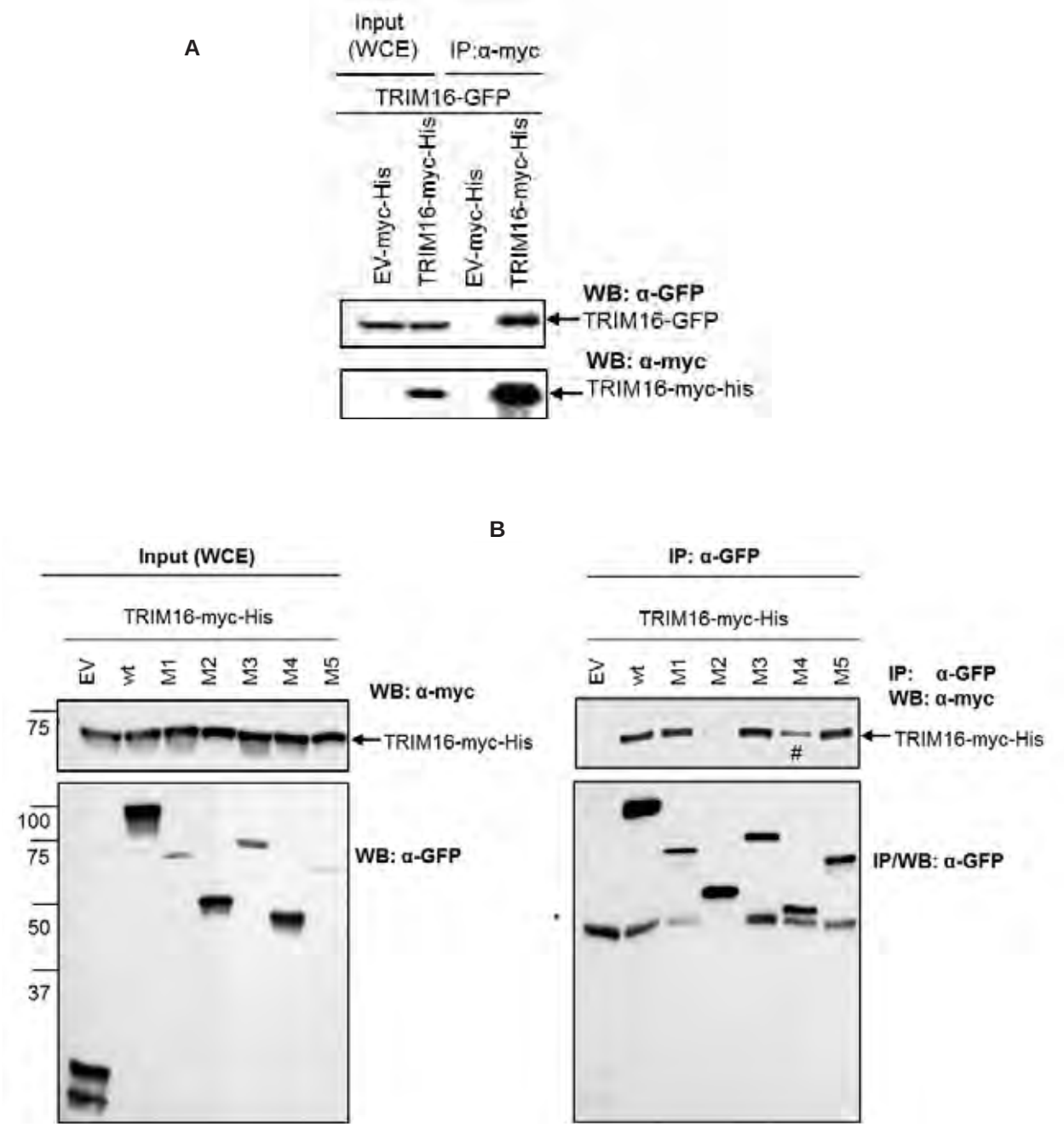

Figure 5.9 TRIM16 homodimerises through its coiled-coil domain

(**A**) Co-transfection of TRIM16-GFP and TRIM16-myc-His in HEK293 cells and subsequent immunoprecipitation by anti-myc antibody (Ab) and Western blot with anti-GFP Ab. (**B**) TRIM16 homodimerises through its coiled-coil domain. GFP deletion mutants were co-transfected with the TRIM16-myc-His vector. Anti-GFP Ab was used to pull down proteins binding the GFP tagged proteins and the TRIM16-myc-His was used to detect self-association via its different tag (top-right). Transfection efficiency was confirmed (left gels). Whole cell extract (WCE). TRIM16-GFP mutants were efficiently pulled down (bottom-right). * non-specific bands, # refer to text.

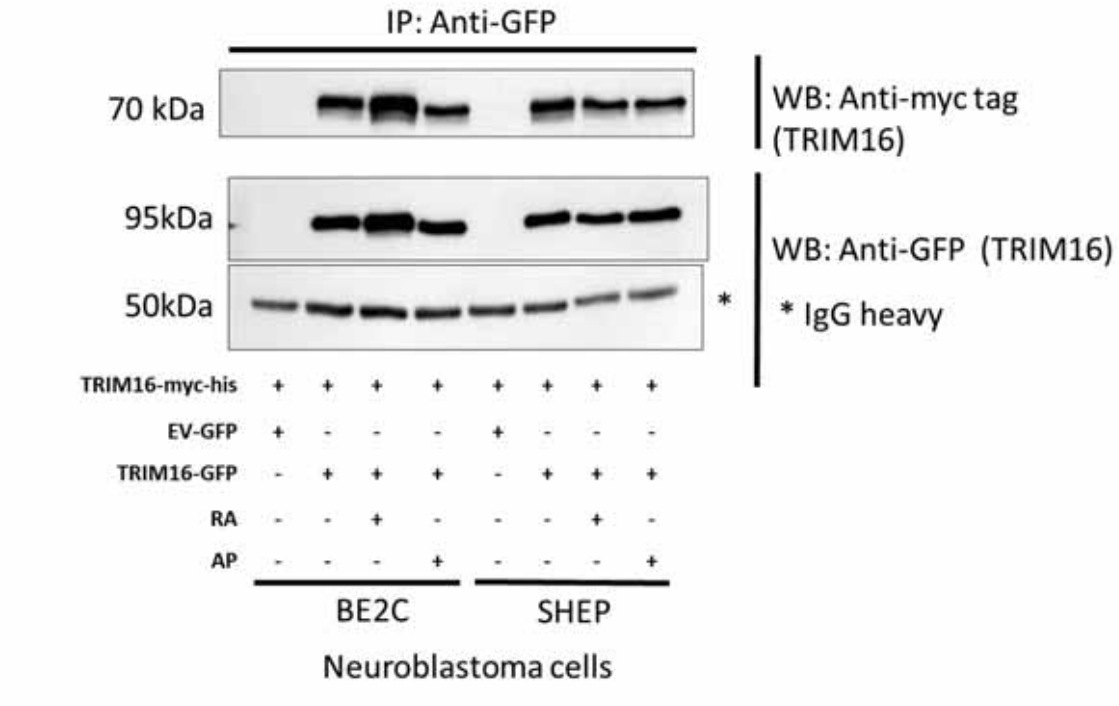

Figure 5.10 TRIM16 homodimerises in neuroblastoma cell lines

TRIM16-myc-His and TRIM16-GFP were immunoprecipitated together under stringent conditions via anti-GFP tag Ab and subjected to Western blot. Cells were also treated with cell cycle arresting agents RA and AP (Aphidicolin) for 24 h where indicated.

5.2.6 TRIM16 can heterodimerise with other TRIM proteins

Another common feature of TRIM proteins is their ability to heterodimerise, often in large protein complexes involved in transcription [9,224,225]. The ability to homodimerise through the coiled-coil domain also increased the possibility that TRIM16 could bind to other TRIM proteins, a significant factor which needed to be studied. PML, TRIM24 and MID1 (Figure 5.11A) have E3-ligase ability through their RING domain and generally homo/heterodimerise through their coiled-coil domains [9,224,225].

Indeed, MID1 can interact strongly with TRIM16 (Figure 5.11B). This was determined by vector co-expression and immunoprecipitation with myc-tag antibody (for TRIM16-myc-His) and probing for the presence of the MID1-GFP. The specificity of this interaction was validated by MID1 immunoprecipitation with an anti-GFP tag antibody and Western blot analysed by myc-tag antibody, probing for TRIM16-myc-His (Figure 5.11C). Furthermore, TRIM proteins; PML (Figure 5.11D) and TRIM24 (Figure 5.11E) were also able to bind TRIM16.

This research into TRIM16's interactions with MID1, PML and TRIM24, clearly demonstrates that TRIM16 can heterodimerise with at least three classes of TRIM proteins.

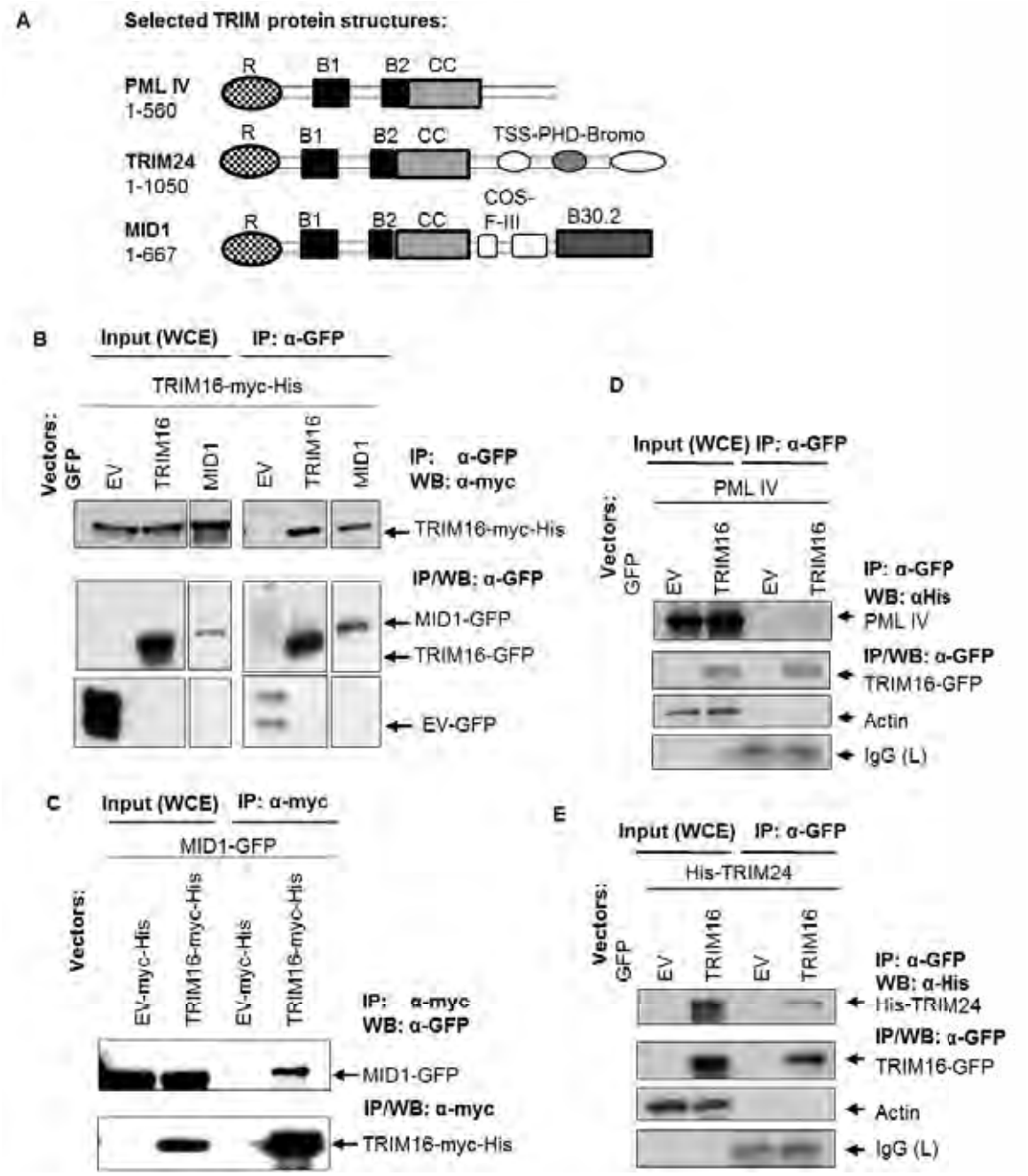

Figure 5.11 TRIM16 can heterodimerise with MID1, TRIM24 and PML

(**A**) Schematic structures of TRIM proteins used in heterodimerisation studies. (**B**) TRIM16 interacts with MID1. Co-transfection of MID1-GFP and TRIM16-myc-His in HEK293 cells and subsequent immunoprecipitation by anti-myc Ab and Western blot with anti-GFP Ab. (**C**) MID1 was immunoprecipitated via its GFP Ab and a Western blot was performed to detect TRIM16-myc-His in the immunoprecipitated protein complex (**D**) TRIM16 binds TRIM24. Lysates containing both TRIM16-GFP and His-TRIM24 exogenous proteins were pulled down by anti-GFP (**E**) TRIM16 binds PML. Lysates containing both TRIM16-GFP and PML proteins were immunoprecipitated via anti-GFP, an anti-PML Ab was used to determine PML as a binding partner of TRIM16. Jessica Koach provided assistance with the PML and TRIM24 experiments.

5.2.7 TRIM16 protein localisation is domain dependent

As nuclear TRIM16 localisation was likely to be important in the involvement of TRIM16 in cell cycle progression and differentiation, GFP fused domain deletion mutants of TRIM16 were used to determine if specific domains of TRIM16 were responsible for its cellular localisation. Confocal images were taken 36 hours post transfection of SHEP neuroblastoma cells (Figure 5.12), BE2C and HEK293 cells (Appendix I). For the neuroblastoma cell lines, EV and M4 constructs displayed similar ubiquitous expression. M1 and M2 both had cytoplasmic bodies and also displayed some diffuse expression throughout the nucleus and cytoplasm. TRIM16 (wt) and M3 had a similar fluorescent pattern, both having cells of either cytoplasmic, or both cytoplasmic and nuclear expression, whilst M5 was cytoplasmic. HEK293 cells displayed an extreme preference for cytoplasmic expression, for all vectors and thus it was determined that it was not an ideal cell line for understanding TRIM16 nuclear localisation with the GFP vectors.

As M3 could maintain a wildtype localisation pattern whereas M5 was cytoplasmic, the difference between their cDNA should harbour a region responsible for TRIM16's ability to be nuclear. These results suggest that a region between AA294 and AA373 (termed the 'linker' domain in this thesis) is involved in nuclear localisation of TRIM16. Moreover, the region of AA165-294 (putative coiled-coil domain) is potentially responsible for nuclear exclusion/export of the TRIM16 protein.

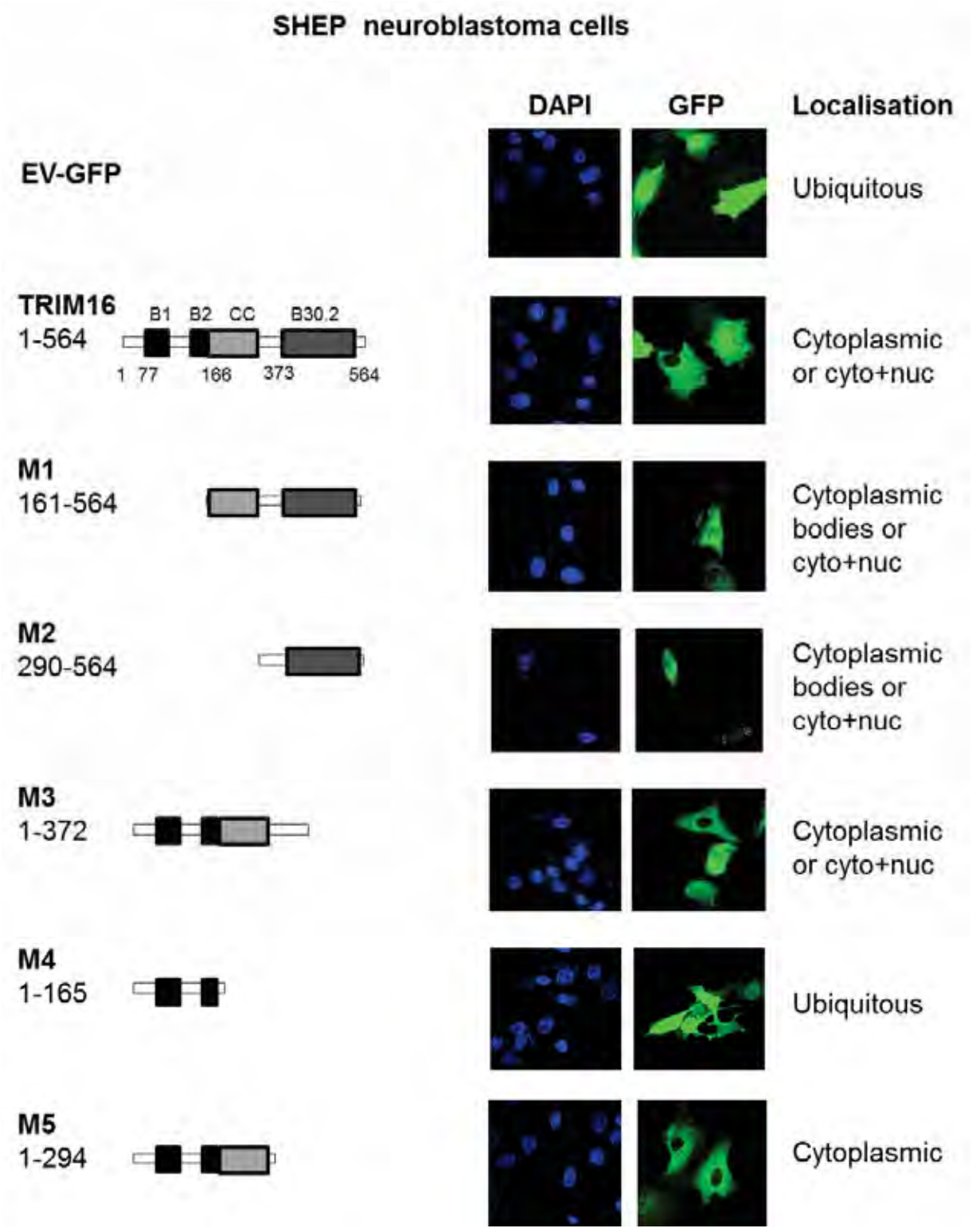

Figure 5.12 The region linking the coiled-coil and B30.2 domain is required for the nuclear localisation of TRIM16

Confocal images with 100X objective (FV1000 Olympus). Cytoplasmic and nuclear (cyto+nuc).

5.2.8 TRIM16 has both a putative nuclear export signal (NES) and putative nuclear localisation signal (NLS)

To further understand the amino acid requirements for TRIM16 localisation, analysis of amino acid sequences of the coiled-coil and 'linker' domains was performed through comparison with the literature. From this research, five sites of interest were elucidated (Figure 5.13).

A putative NES was found in a leucine-rich sequence within the coiled-coil domain. TRIM16 had a putative NES similar to RFP (TRIM27) (which is also in RFP's coiled-coil domain) and cell cycle regulating proteins such as p53 and cyclin B [224,369] (Figure 5.13C). TRIM16's putative NES, being leucine-rich, adheres well to published motifs [370].

Analysis of the 'linker' domain revealed a putative bi-partite nuclear localisation sequence (NLS) similar to PML, nucleoplasmin and p53 (Figure 5.13D) [141,235,371]. Furthermore, TRIM16's putative NLS also had a potential sumoylation site similar to a NLS sumoylation site on PML [235]. Interestingly, the two basic regions of the putative TRIM16 NLS, flank a putative nuclear receptor binding motif (NRBM), as identified (but not validated) by Liu and colleagues [329], which could also explain a nuclear localisation of TRIM16. This motif is LxxLL, which appears in many retinoid receptors [189].

To examine whether these sites were functional in TRIM16 localisation, evolutionarily conserved amino acids (as determined by the clustalw2 website) were chosen in pairs for site-directed mutagenesis (point mutation) of the full length TRIM16-GFP plasmid (Figure 5.13B). DNA sequencing was used to select and validate clones (Appendix II). Vectors were first expressed in HEK293 cells to validate expression of the transgene construct by Western blot (Figure 5.14). The Western blot

was slightly overexposed in order to view all mutants. Disappointingly, only point mutants, ΔNLSa, ΔNRBM and ΔSUMO had proteins levels similar to the wildtype control protein. ΔNES had much reduced levels of protein and strikingly, ΔNLSb had no visible banding at the same magnitude as the other transgene proteins. Flow cytometric analysis showed that less than 0.5% of BE2C cells were expressing transfected ΔNLSb, compared with more than 50% observed with the wildtype control runs (data not shown). The variability between expression of the vectors limited research to localisation studies.

Validated constructs were expressed in SHEP cells. The putative NES sequence did increase the levels of TRIM16 in the nucleus, however, transgene protein remained predominately in the cytoplasm in over 30% the cells compared with 60% in the wildtype control (Figure 5.15). The ΔSUMO mutant displayed an increase in cytoplasmic expression of the transgene with over 95% of cells having predominately cytoplasmic protein. The ΔNRBM had no change in localisation compared to the wildtype protein. The ΔNLSa mutant displayed a more than 80% cytoplasmic expression. Although the ΔNLSb mutant had very low protein expression, in those cells that displayed expression, the localisation was cytoplasmic. Both ΔNRBM and ΔNES had a proportion of transfected cells (above 25%) showing blebbing, a phenomenon rarely seen with the wildtype vector, indicating that these amino acid changes may have also affected TRIM16's function separate from localisation, which is outside the scope of this study.

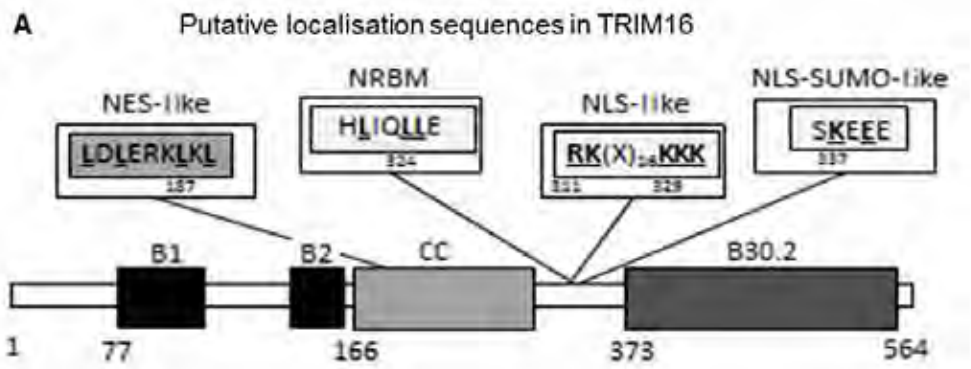

B Site-directed mutations:

1. **ΔNES**	L187A_K188N
2. **ΔNLSa**	R311N_K312N
3. **ΔNRBM**	L324A_L325A
4. **ΔNLSb**	K329N_K331N
5. **ΔSUMO**	K337R_E339N

C Selected human sequences with TRIM16 NES-like motif:

TRIM16	**Q**L**D**L**E**R**K**L**K**L**N**
TRIM27(RFP)	R**L**LAR**L**E**E**L**D**L**A**
MAPKK	**Q**L**Q**K**K**L**E**E**L**E**L**D**
MDM2	L**S**F**D**E**S**L**A**L**C**
CyclinB1	D**L**CQA**F**SD**V**I**L**A**
p53	**MF**RE**L**NEA**L**E**L**K**

D Selected human sequences with TRIM16 NLS-like motif

TRIM16	**RK**(X)16	**KKK**LQEFS**K**E**E**
TRIM19(PML)	**KRK**(X)7	**RK**VI**K**M**E**SEE
TRIM24	**KKK**(X)12	**KRK**CE**R**
p53	**KR**(X)12	**KKK**
Estrogen	**RK**(X)11	**RK**D**R**
mDia2	**RRK**(X)15	**KR**P**K**

Figure 5.13 Putative localisation sequences of TRIM16 and comparison studies

Undefined Amino acid (X). Consensus sequence amino acids in bold and underlined type.

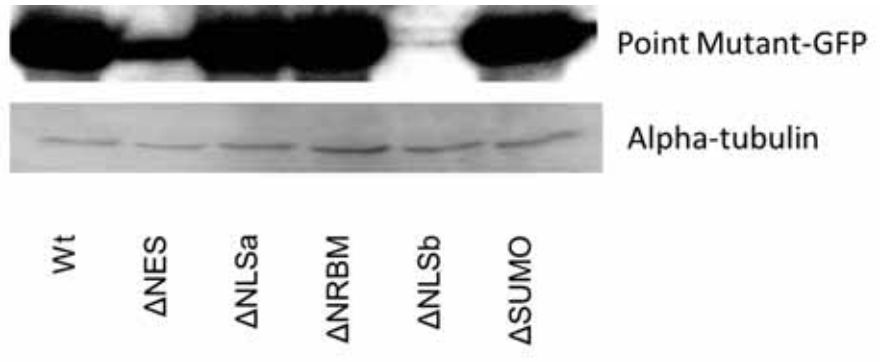

Figure 5.14 Western blot of TRIM16 localisation (point) mutants

Anti-GFP Ab was used to detect the localisation mutants (with point mutations) in HEK293 cells. wt (wildtype/TRIM16-GFP).

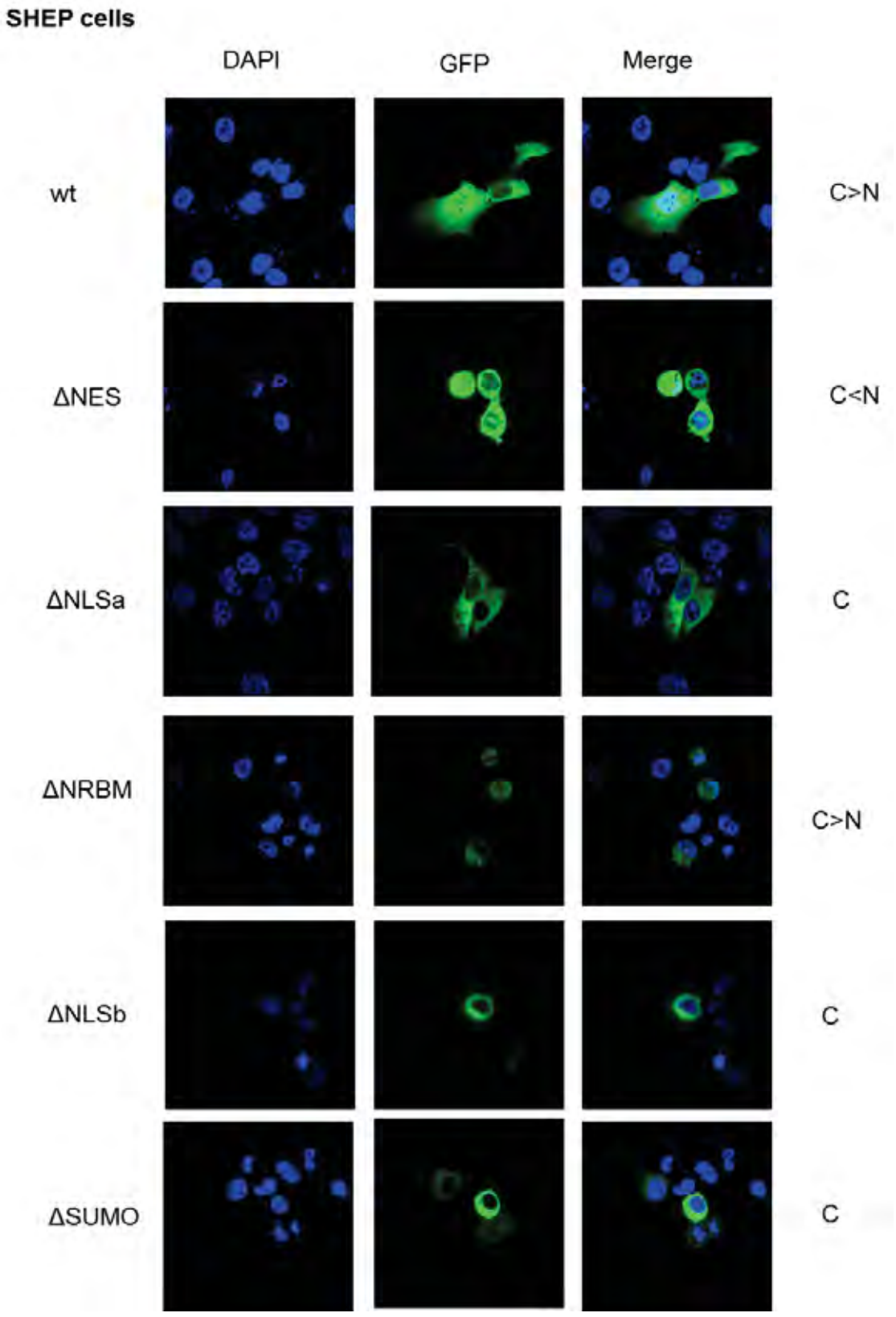

Figure 5.15 Confocal Images of SHEP cells transfected with localisation mutants

N = Nuclear, C = Cytoplasmic, > = is greater than, < = is less than. 100X objective FV1000 Olympus. . wt (wildtype/TRIM16-GFP).

5.2.9 The ‘linker region of TRIM16 is required for TRIM16’s inhibition of proliferation

As the ‘linker’ region of TRIM16 was required for nuclear localisation, it was hypothesised that this same domain would also be required for TRIM16’s effects on proliferation. Experimental results obtained during this thesis suggested that the nuclear localisation of TRIM16 was functionally linked with its inhibition of proliferation (including: 4.2.1, 4.2.4). Demonstrating the same domain was responsible for both traits of TRIM16 would substantially support this hypothesis.

The domain deletion mutants of TRIM16 were used to determine which domain causes the growth inhibition associated with the overexpressed full length TRIM16. TRIM16 (wt), M1, M2 and M3 constructs caused a significant decrease in proliferation in BE2C and SHEP cells, with M4 and M5 being comparable to the EV control (Figure 5.16). Interestingly, there was a trend where M1 had a slightly greater decrease in proliferation compared with the wildtype vector. However, this only reached significance in the BE2C cell line. These results imply that the region between the TRIM16 amino acid (AA) 294 and AA373 (‘linker’ domain) is required for proliferation inhibition.

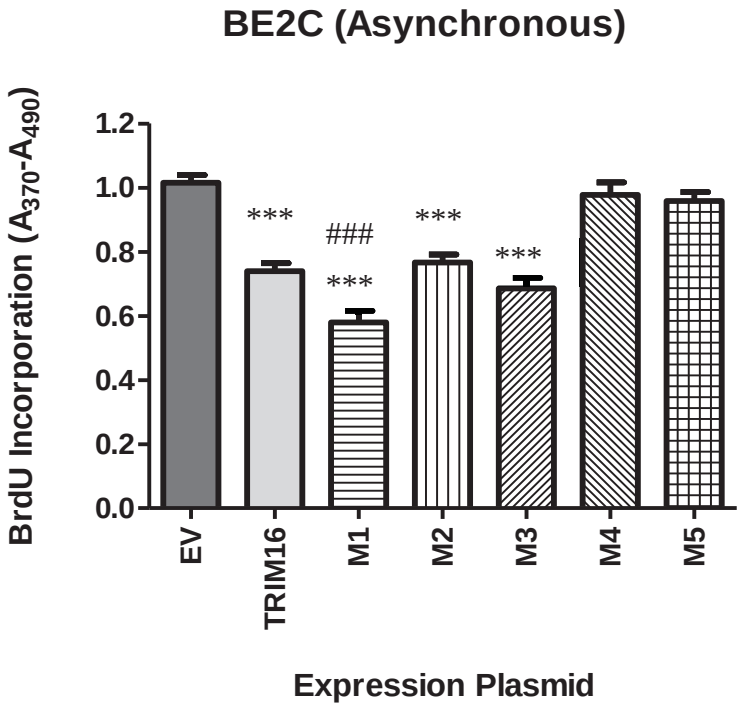

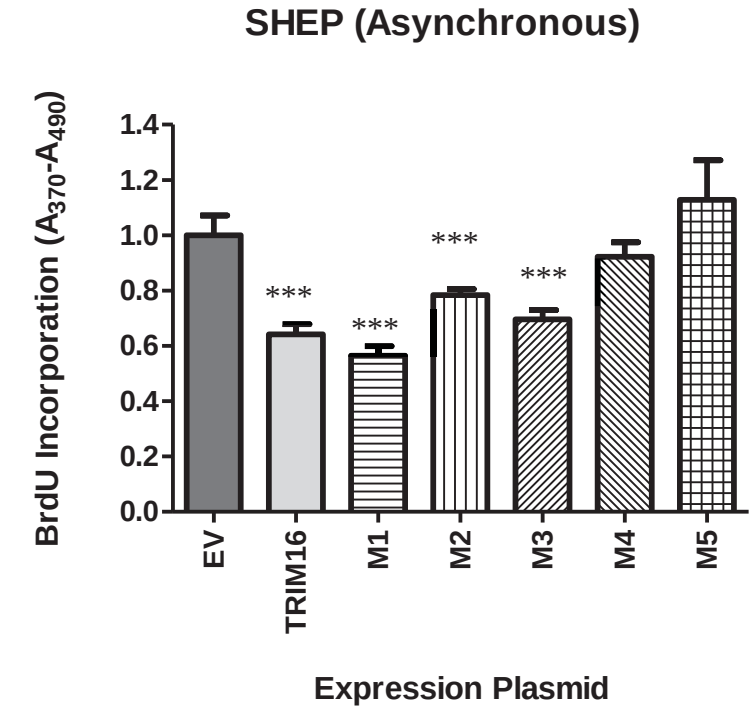

Figure 5.16 The 'linker' domain is required for TRIM16 inhibition of neuroblastoma cell proliferation

Proliferation was assessed via BrdU incorporation ELISA. *** p>0.001 compared to EV. ### p>0.001 compared to TRIM16 full length (wt).

5.3 Discussion

This chapter sought to define the relationship between TRIM16 protein structure, localisation and functions in neuroblastoma. Previous investigations into TRIM16 generally used full length TRIM16 and did not demonstrate and characterise TRIM16 function in ubiquitin activity, homodimerisation, localisation and proliferation. In the large and evolutionarily conserved TRIM family, protein domains often operate as functional units. For the first time it has been demonstrated here, that TRIM16 also harbours a structure with diverse functions. Importantly, the 'linker' domain was shown to be required for both nuclear localisation and inhibition of cell proliferation.

TRIM16's B-boxes have a zinc binding amino acid consensus sequence and can bind ubiquitin. Overall, TRIM16 shared low sequence identity with other TRIMs such as TRIM29, TRIM25, RFP, MID1 and MID2, except in the B-box1 region where the high homology amongst these TRIM proteins suggests a subgroup of TRIMs having a specific zinc-binding role in homeostasis. TRIM16 is one of the oldest TRIM proteins [219], yet it is the only functionally studied TRIM with a B1-B2-CC-B30.2 motif. This indicates the evolution of a RING-less TRIM is an ancient and biologically required phenomenon. Ubiquitin binding domains are often built around zinc binding sites of a protein [372], and TRIM16 was also shown to require B-boxes to bind ubiquitin and auto-polyubiquitinate *in vivo*. This suggests that TRIM16 is an E3 ligase. Significantly, further studies in our group by a colleague have demonstrated that TRIM16 has E3 ligase activity, *in vitro* (Bell *et al.,* 2012, in press).

TRIM16 can to hetereodimerise with other TRIM proteins, and homodimerise via its coiled-coil domains. As MID1 associates with microtubules and the cytoskeleton [373], TRIM16's interaction with MID1 suggests that TRIM16 may have a functional role in the cytoskeleton. Interestingly, TRIM16 has also been shown to bind the

cytoskeletal protein, vimentin [331], which further indicates a role of TRIM16 in the cytoskeleton.

Both TRIM24 and PML proteins interact with TRIM16. TRIM16 is known to bind the promoter region of the RARβ gene [8]. Interestingly, TRIM24, also a transcription factor, has been shown to act in a complex with PML and the RARα and RXR receptors, which are known to bind to the same sequence of the RARE promoter region sequence of RARβ as TRIM16 [183,368]. PML is a tumour suppressor which has a significant role in the cell cycle, differentiation and apoptosis (1.5.3.1). TRIM16's heterodimerisation ability with these TRIM proteins suggests that TRIM16 may influence the ubiquitination function of these RING-bearing TRIMs; acting in complexes, influencing transcription and protein degradation.

The 'linker' domain of TRIM16 is required both for TRIM16 nuclear localisation and its growth inhibitory effects in neuroblastoma. Confocal localisation showed the 'linker' region was required for TRIM16 protein to persist in the nucleus. Furthermore, the BrdU incorporation assay also demonstrated that overexpression of plasmids containing the 'linker' region of TRIM16 produced a significant decrease in proliferating cells. As the transient transfection led to a mixed population of transfected and untransfected cells, it is likely that the trends observed here are an underestimation of the effect which would have been observed if all cells were transfected.

It remains controversial if the 'linker' domain is actually part of an undefined domain as presented in the Liu *et al.* paper [329], or part of the coiled-coil domain (being a small third coiled-coil) as illustrated by Beer and colleagues [330]. A crystal structure of TRIM16 is required to resolve this controversy, and would also give insight into the surface amino acids of TRIM16. It would be important to determine if the

putative localisation sequences are located on the surface of the TRIM16 molecule, in particular the ΔNES and ΔSUMO which had clear activity.

This Chapter also demonstrated that TRIM16 possesses putative localisation sites. ΔNES mutant protein increased TRIM16 in the nucleus, but this did not result in a total shift to the nucleus. This indicates the ΔNES site has an influence on nuclear localisation, but is not sufficient to drive TRIM16 nuclear export. Nuclear export therefore may involve other sites and binding proteins, or is partially suppressed by the transgenic protein homodimerising to the endogenous TRIM16. The ΔSUMO site gave the most striking result with the vast majority of cells being cytoplasmic, which was reminiscent of the trend seen with M5 domain mutant (without both the 'linker' and B30.2 domains). The activity of NES and NLS-associated sequences supports the localisation findings produced by the localisation of domain deletion mutants of TRIM16. Thus, TRIM16 is potentially under the influence of exportin and importin proteins which are responsible for NLS and NES localisation activity [370,374].

Interestingly, the B-boxes and their ubiquitination activity were not required for TRIM16 nuclear localisation and induced growth inhibition. In fact, the loss of the B-boxes with overexpression of TRIM16 M1, resulted in an even further decrease in proliferation in BE2C. It is hard to explain how this B-box deficient TRIM16 has potentially greater growth inhibition activity. One could speculate that TRIM16 is an antagonist of TRIM E3-ligsae-initiated degradation. That although TRIM16 has ubiquitination activity, it acts less efficiently compared with other TRIMs that have RING domains, and that whilst full length TRIM16 has some ubiquitination activity, M1 has no activity, and yet M1 is still able to bind substrates through its coiled-coil domain. Thus, in this scenario, M1 may better sequester substrates from RING bearing TRIMs and ubiquitination, compared to full length TRIM16. Interestingly, a putative

"beta" isoform of TRIM16 and a TRIM16-like protein (TRIM70) are described on the Uniprot website, though not functionally validated. Both of these proteins are almost identical to M1, and are therefore likely to have an activity similar to M1.

This research did not show a role for the B30.2 domain of TRIM16. Hypotheses were function driven and hypotheses concerning the role of the B30.2 domain were not directly tested. Research on the B30.2 domain in other TRIM proteins has shown it to be important in immune response and inflammation [332].

Although TRIM16 is devoid of a RING domain, TRIM16's B-Boxes can bind ubiquitin and its coiled-coil domain facilitates homodimerisation. Furthermore, the domain linking the coiled-coil domain and the B30.2 domain is required for both TRIM16 nuclear localisation and proliferation inhibition. Thus, TRIM16 has powerful attributes found in other TRIM proteins.

CHAPTER 6

CONCLUSIONS AND FUTURE PERSPECTIVES

6.1 Conclusions

This thesis demonstrates, for the first time, that TRIM16 is a potential tumour suppressor in neuroblastoma. Neuronal differentiation requires G1 cell cycle arrest and TRIM16 has been shown to be a significant factor involved in this critical part of cell fate decision making. TRIM16, through its unique TRIM protein structure, harbours the ability to inhibit proliferation, promote differentiation, and reduce tumorigenicity. TRIM16 also retains characteristics that are common to other TRIM proteins such as homo- and hetero-dimerisation and ubiquitin binding. Furthermore, the trait of nuclear localisation and growth inhibition are associated with overexpression of the 'linker' region of TRIM16. Improved understanding of the role of TRIM16 could lead to the identification of drug targets, which are capable of initiating regression of neuroblastoma. Results from this thesis have significantly contributed to the understanding and knowledge of TRIM16 and thus a new model of TRIM16 activity is proposed Figure 6.1). The model shows the localisation of TRIM16 in different cell types. Localisation of TRIM16 is important for its function and this can be influenced by cell differentiation, cell cycle phase and the activity of TRIM16 protein domains.

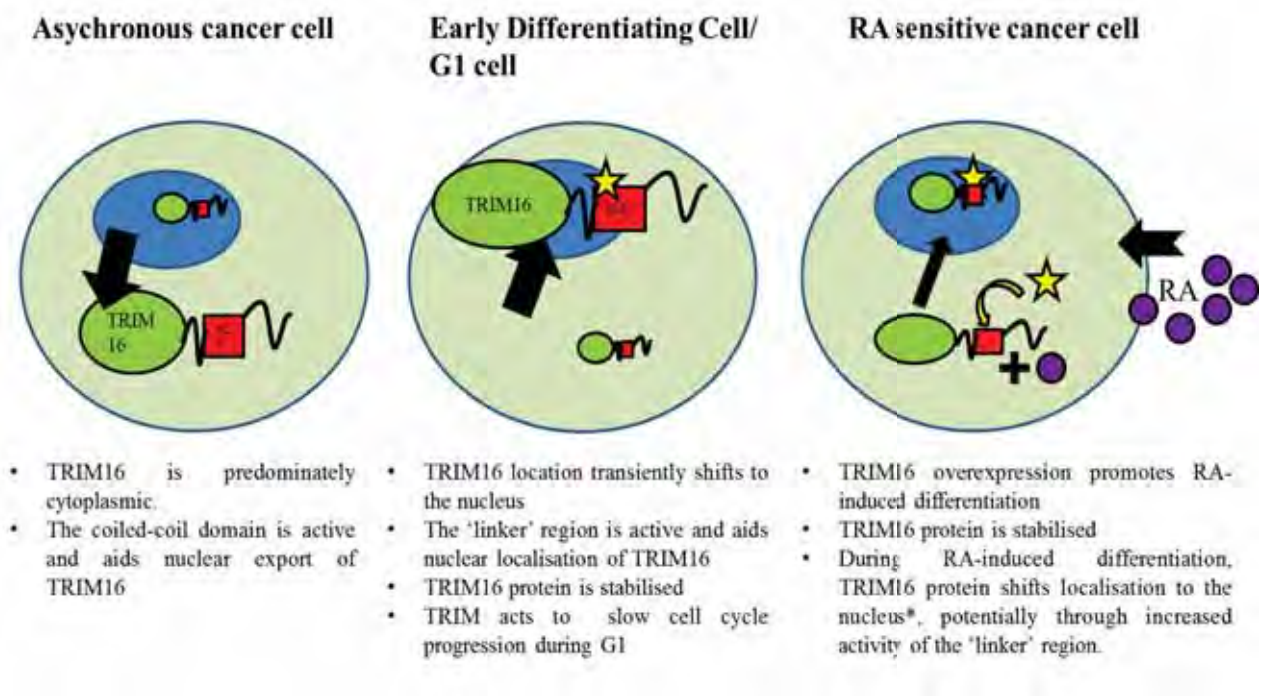

* evidenced in previous research [8,331]

Figure 6.1 TRIM16 localisation is dependent on the neuroblastoma cell's differentiation state and cell cycle phase

This new model of TRIM16 activity shows TRIM16 localisation shifts via the activity of TRIM16 domains in different cell conditions. The blue oval represents the cell nucleus and the cytoplasm is light green in colour. The yellow star represents active nuclear localisation sites/domains.

Although neuroblastoma is the most common solid childhood cancer, it remains a disease with poor patient outcome compared to other common childhood malignancies [10]. One phenomenon of neuroblastoma is that in some cases it can spontaneously regress through terminal differentiation of the cancer cells [14,96]. Whilst presently the details of this phenomenon remain unknown, it has been shown that the retinoid anti-cancer pathway is able to differentiate neuroblastoma cells [122,161]. Thus, improving the understanding of this pathway is a novel and rational research avenue.

TRIM16 has a role in the disease context of neuroblastoma and is a potential tumour suppressor in neuroblastoma. In this thesis, TRIM16 overexpression causes reduced tumorigenicity in a neuroblastoma xenograft model. Additionally, TRIM16 displays a reduced endogenous expression in neuroblastoma mouse tumours compared with the ganglia from which neuroblastoma arise. Taken together, these data demonstrate a clear *in vivo* role for TRIM16 in neuroblastoma, and also the potential significance of TRIM16 in neuroblastoma development and progression in humans.

TRIM16 is likely to be promoting differentiation through changes in the G1 cell cycle phase machinery. Findings from this thesis implicate TRIM16 as having a role that is not limited to retinoid response. Significantly, in the absence of retinoid treatment, TRIM16 still exerts a growth inhibitory effect on neuroblastoma cells and tumours. The research presented in this thesis clearly shows a role of TRIM16 in decision making during the G1 cell cycle phase, and that under differentiating conditions its role is also to promote differentiation. TRIM16's known binding to E2F1 [331], as well as TRIM16's modification of several key G1 cell cycle components including p27, shows that TRIM16 functions directly within the cell cycle. This considered with the fact that TRIM16 protein is also induced during both G1 and

retinoid-differentiation, locates TRIM16's range of activity more precisely at early-G1 to the mid-G1 part of the cell cycle. Furthermore, the *in vivo* expression of TRIM16 in the nucleus of newly differentiating ganglia and its ability to enhance differentiation also indicates that TRIM16 is predominately active in both the G1 cell cycle and early differentiation.

TRIM16 expression and localisation activity in the cell cycle is 'all about the timing'. An important concept is that TRIM16 is a negative regulator ('break') on cell cycle progression and that TRIM16 does not stop proliferation exclusively. This thesis shows that overexpression of TRIM16 causes decreased proliferation and an accumulation of cells in G1. Consistent with this, is that the siRNA knockdown of TRIM16 increases proliferation in asynchronous cells [331]. Moreover, this thesis also shows that TRIM16 knockdown significantly retards induction of key G1 components when released from G0. Thus TRIM16 is required during the G0/G1checkpoint to progress through the cell cycle but also acts as a 'break' around mid-G1. This fine balance in TRIM16 activity is a probable explanation as to why TRIM16 protein expression is induced during G1, and also why TRIM16 is a predominately cytoplasmic protein in asynchronous cells.

TRIM16's transient peak in nuclear expression highlights that its localisation is highly regulated in the neuroblastoma cell and represents a crucial aspect of its function. These data show that regulation of TRIM16 function is, at least, partly through the nuclear localisation potential of the 'linker domain' and the export potential of the coiled-coil domain of TRIM16, as well as through protein stabilisation. This was evidenced by the use of the expression vectors (domain deletion and localisation point mutants). But also via total cell extracts, which show that the endogenous level of

TRIM16 protein (not mRNA) is increased during RA differentiation treatment [8], and in the G1 cell cycle phase (Figure 4.8). Therefore, during G1/differentiation, in addition to nuclear localisation facilitated by TRIM16's 'linker' region, a decrease of TRIM16's proteasome degradation is also occurring.

PML and p27 potentially play the most important role in TRIM16's tumour suppressor-like functions. This is due to their involvement in both the G1 cell cycle phase and retinoid-induced differentiation, in neuroblastoma. This also suggests a greater scope of functional potential for TRIM16 in nuclear receptor signalling than allowed by previous investigations.

6.2 Future perspectives

To date, no regulating proteins of TRIM16 have been identified and this is an aspect of TRIM16 function that requires more extensive investigation. TRIM16 is an important regulator of neuroblastoma differentiation and proliferation, which provides rationale to establishing the mechanism of how this significant protein is controlled. Regulation of its movement can be explained through the function and presence of its protein domains, and thus, the next step is to identify the proteins which bind to specific TRIM16 domains and then validate that these elucidated proteins are required for the activity of these domains.

Proteins involved in the stabilisation and degradation of TRIM16 also need to be elucidated. From a drug discovery viewpoint, the most significant proteins would be those which degrade TRIM16. If such a reaction could be inhibited pharmacologically, the amount of TRIM16 would increase and produce neuroblastoma cell growth inhibition comparable to that caused by full length TRIM16 overexpression. Furthermore, this inhibitor could be theoretically combined with retinoid treatment to enhance neuroblastoma differentiation. Prime candidates for regulators of TRIM16 are TRIM protein family members, which are heavily involved in proteasomal degradation. Proteins binding to TRIM16 specifically during S phase may also be responsible for TRIM16 downregulation.

It would be a valuable asset for further TRIM16 research to have both C- and N-terminally tagged TRIM16 expression vectors. Here, overexpression studies of TRIM16 used a C-terminal tagged protein. The position of the tag could affect the function of the TRIM16 protein and would be relevant for specific functional studies of the B30.2 domain, which is located at the N-terminus of the TRIM16 protein.

A detailed study of TRIM16 isoforms and their function remains a novel and significant research avenue. At present, the isoforms of TRIM16 remain experimentally unproven. When reviewing the literature of TRIM proteins, the abundance of isoforms and their various functions are clearly apparent [9,375]. Furthermore, due to my work on the requirement of specific domains in TRIM16 function, isoform elucidation could therefore prove an important field of study. This thesis comprehensively addressed my hypotheses using an array of well described techniques directed to the full length 65-70 kDa TRIM16 protein. Yet it remains to be ascertained if the functions of TRIM16 defined in this thesis are influenced by the expression of TRIM16 isoforms.

A major scientific concern for research on TRIM16 is the possible presence of TRIM16-like (TRIM70), a putative duplicated genomic copy of TRIM16 that is devoid of B-boxes. The TRIM16 domain mutant (M1) which is similar to TRIM16-like possesses some TRIM16 functions, highlighting a need to elucidate potential TRIM16-like expression and function. Moreover, there is great need to develop methods to differentiate mRNA and protein expressed from the TRIM16 and TRIM16-like genomic sources.

Further *in vivo* work is essential to prove that TRIM16 is a classical tumour suppressor. A classic tumour suppressor is proved through overexpression and endogenous research (as completed in this thesis), but also through knockout mouse studies and human expression/mutation studies. Following this, it is therefore necessary to prove TRIM16 is a gene which, when expressed appropriately, protects the cell from progression to a cancer cell. Principally, a knockout mouse study of TRIM16 and/or TRIM16-like is required to prove TRIM16 as a tumour suppressor. For neuroblastoma, this would be ideally proved through the conditional knockout of TRIM16 under the TH

promoter and crossing these mice with the well-studied TH-MYCN hemizygous mice, for the purpose of quantifying neuroblastoma incidence.

Further evidence demonstrating that TRIM16 acts as a tumour suppressor in neuroblastoma could be gained by showing aberrant expression of TRIM16, in a cohort of human neuroblastoma protein samples. As TRIM16 protein levels are controlled post-translationally, protein samples should be analysed for both quantity and modifications. It's important to consider that total protein levels of TRIM16 are relatively similar in normal and cancer cells, and thus post-translational modifications of the protein itself could be the device for a significant change in TRIM16 function. If TRIM16 is deregulated through the mutation of a protein modification site, DNA sequencing analysis could be a fruitful tool to understand TRIM16's action in cancer. For example, a mutated phosphorylation site on TRIM16 could be responsible for reduced or increased TRIM16 activity in cancer cells.

In conclusion, TRIM16 is a highly expressed protein in humans, which has a tumour suppressor-like role in neuroblastoma. Its putative protein domains not only act to influence TRIM16 dynamic localisation, but also influence its inhibitory activity during proliferation. The 'linker' domain of TRIM16 is required for both nuclear localisation potential and proliferation inhibition. TRIM16 is devoid of a RING domain, nonetheless this 'handicapped' TRIM family member is one of the oldest evolved TRIM proteins and is a protein highly relevant to cancer biology and drug discovery. Future studies into TRIM16's mechanisms as a tumour suppressor may potentially prove crucial to the understanding of tumour differentiation and progression, in cancers such as neuroblastoma.

CHAPTER 7

REFERENCES

1. Brodeur GM, Sawada T, Tsuchida Y, Voute PA, editors (2000) Neuroblastoma. New York: Elsevier.
2. Galderisi U, Jori FP, Giordano A (2003) Cell cycle regulation and neural differentiation. Oncogene 22: 5208-5219.
3. Tang X-H, Gudas LJ (2011) Retinoids, Retinoic Acid Receptors, and Cancer. Annual Review of Pathology: Mechanisms of Disease 6: 345-364.
4. Sidell N (1982) Retinoid acid-induced growth-inhibition and morphologic differentiation of human neuro-blasoma cells in vitro. Journal of the National Cancer Institute 68: 589-596.
5. Matsuo T, Thiele CJ (1998) p27(Kip1): a key mediator of retinoic acid induced growth arrest in the SMS-KCNR human neuroblastoma cell line. Oncogene 16: 3337-3343.
6. Matthay KK, Reynolds CP (2000) Is there a role for retinoids to treat minimal residual disease in neuroblastoma? British Journal of Cancer 83: 1121-1123.
7. Matthay KK, Villablanca JG, Seeger RC, Stram DO, Harris RE, et al. (1999) Treatment of high-risk neuroblastoma with intensive chemotherapy, radiotherapy, autologous bone marrow transplantation, and 13-cis-retinoic acid. New England Journal of Medicine 341: 1165-1173.
8. Cheung BB, Bell J, Raif A, Bohlken A, Yan J, et al. (2006) The estrogen-responsive B box protein is a novel regulator of the retinoid signal. Journal of Biological Chemistry 281: 18246-18256.
9. Meroni G, Diez-Roux G (2005) TRIM/RBCC, a novel class of 'single protein RING finger' E3 ubiquitin ligases. Bioessays 27: 1147-1157.
10. Brodeur GM (2003) Neuroblastoma: Biological insights into a clinical enigma. Nature Reviews Cancer 3: 203-216.
11. Julie RP, Angelika E, Huib C (2008) Neuroblastoma: Biology, Prognosis, and Treatment. Pediatric clinics of North America 55: 97-120.
12. Maris JM, Hogarty MD, Bagatell R, Cohn SL (2007) Neuroblastoma. The Lancet 369: 2106-2120.
13. Nakagawara A, Luigi A, Laura C (2004) Neural crest development and neuroblastoma: the genetic and biological link. Progress in Brain Research: Elsevier. pp. 231-242.
14. Carvalho L (1974) Spontaneous regression of untreated neuroblastoma British Journal of Ophthalmology 57: 832-835.
15. Tracey E, Baker D, Chen W, Stavrou E, Bishop J (2007) Cancer in New South Wales: Incidence, mortality and prevalence report 2005. Sydney: Cancer Institute NSW.
16. Yamamoto K, Hanada R, Kikuchi A, Ichikawa M, Aihara T, et al. (1998) Spontaneous regression of localized neuroblastoma detected by mass screening. Journal of Clinical Oncology 16: 1265-1269.
17. Yamamoto K, Hayashi Y, Hanada R, Kikuchi A, Ichikawa M, et al. (1995) Mass-screening and age-specific incidence of neuroblastoma in Saitama prefecture, Japan. Journal of Clinical Oncology 13: 2033-2038.
18. Beckwith JB, Perrin EV (1963) In situ neuroblastomas: a contribution to the natural history of neural crest tumors. American Journal of Pathology 43: 5.
19. Maris JM, Weiss MJ, Mosse Y, Hii G, Guo C, et al. (2002) Evidence for a hereditary neuroblastoma predisposition locus at chromosome 16p12-13. Cancer Research 62: 6651-6658.
20. Maris JM, Brodeur GM (1997) Are certain children more likely to develop neuroblastoma? Journal of Pediatrics 131: 656-657.

21. Schwab M (1999) Oncogene amplification in solid tumors. Seminars in Cancer Biology 9: 319-325.
22. Nuchtern JG (2006) Perinatal neuroblastoma. Seminars in Pediatric Surgery 15: 10-16.
23. DuBois SG, Kalika Y, Lukens JN, Brodeur GM, Seeger RC, et al. (1999) Metastatic Sites in Stage IV and IVS Neuroblastoma Correlate With Age, Tumor Biology, and Survival. Journal of Pediatric Hematology/Oncology 21: 181-189.
24. Pfluger T, Schmid I, Coppenrath E, Weiss M (2010) Modern nuclear medicine evaluation of neuroblastoma. Quarterly Journal of Nuclear Medicine and Molecular Imaging 54: 389-400.
25. Shimada H, Ambros IM, Dehner LP, Hata J, Joshi VV, et al. (1999) The International Neuroblastoma Pathology classification (the Shimada system). Cancer 86: 364-372.
26. Evans AE, Dangio GJ, Randolph J (1971) Proposed staging for children with neuroblastoma – Childrens cancer study group-A. Cancer 27: 374-&.
27. Brodeur GM, Seeger RC, Barrett A, Berthold F, Castleberry RP, et al. (1988) International criteria for neuroblastoma diagnosis, staging, and response to treatment in patients with neuro-blastoma. Journal of Clinical Oncology 6: 1874-1881.
28. Hayes FA, Green A, Hustu HO, Kumar M (1983) Surgicopathologic staging of neuro-blastoma – prognostic significance of regional lymph-node metastases. Journal of Pediatrics 102: 59-62.
29. Brodeur GM, Pritchard J, Berthold F, Carlsen NLT, Castel V, et al. (1993) Revisions of the international criteria for neuroblastoma diagnosis, staging, and response to treatment Journal of Clinical Oncology 11: 1466-1477.
30. Monclair T, Brodeur GM, Ambros PF, Brisse HJ, Cecchetto G, et al. (2009) The International Neuroblastoma Risk Group (INRG) Staging System: An INRG Task Force Report. Journal of Clinical Oncology 27: 298-303.
31. Seeger RC, Brodeur GM, Sather H, Dalton A, Siegel SE, et al. (1985) Association of multiple copies of the N-Myc oncogene with rapid progression of neuroblastomas. New England Journal of Medicine 313: 1111-1116.
32. Schwab M, Varmus HE, Bishop JM (1985) Human N-myc gene contributes to neoplastic transformation of mammalian cells in culture. Nature 316: 160-162.
33. Weiss WA, Aldape K, Mohapatra G, Feuerstein BG, Bishop JM (1997) Targeted expression of MYCN causes neuroblastoma in transgenic mice. EMBO J 16: 2985-2995.
34. Weiss WA, Godfrey T, Francisco C, Bishop JM (2000) Genome-wide screen for allelic imbalance in a mouse model for neuroblastoma. Cancer Research 60: 2483-2487.
35. Hackett CS, Hodgson JG, Law ME, Fridlyand J, Osoegawa K, et al. (2003) Genome-wide array CGH analysis of murine neuroblastoma reveals distinct genomic aberrations which parallel those in human tumors. Cancer Research 63: 5266-5273.
36. Nesbit CE, Tersak JM, Prochownik EV (1999) MYC oncogenes and human neoplastic disease. Oncogene 18: 3004-3016.
37. Lee WH, Murphree AL, Benedict WF (1984) Expression and amplification of the N-Myc gene in primary retinoblastoma. Nature 309: 458-460.
38. Reiter JL, Brodeur GM (1996) High-resolution mapping of a 130-kb core region of the MYCN amplicon in neuroblastomas. Genomics 32: 97-103.

39. Shaw APW, Poirier V, Tyler S, Mott M, Berry J, et al. (1988) Expression of the N-Myc oncogene in Wilms tumor and related-tissues Oncogene 3: 143-149.
40. Eilers M, Schirm S, Bishop JM (1991) The Myc protein activates transcription of the alpha-prothymosin gene. Embo Journal 10: 133-141.
41. Iritani BM, Eisenman RN (1999) c-Myc enhances protein synthesis and cell size during B lymphocyte development. Proceedings of the National Academy of Sciences of the United States of America 96: 13180-13185.
42. Freytag SO, Geddes TJ (1992) RECIPROCAL REGULATION OF ADIPOGENESIS BY MYC AND C/EBP-ALPHA. Science 256: 379-382.
43. de Alboran IM, O'Hagan RC, Gartner F, Malynn B, Davidson L, et al. (2001) Analysis of C-MYC function in normal cells via conditional gene-targeted mutation. Immunity 14: 45-55.
44. Mateyak MK, Obaya AJ, Adachi S, Sedivy JM (1997) Phenotypes of c-myc-deficient rat fibroblasts isolated by targeted homologous recombination. Cell Growth & Differentiation 8: 1039-1048.
45. Mateyak MK, Obaya AJ, Sedivy JM (1999) c-Myc regulates cyclin D-Cdk4 and-Cdk6 activity but affects cell cycle progression at multiple independent points. Molecular and Cellular Biology 19: 4672-4683.
46. Knoepfler PS, Cheng PF, Eisenman RN (2002) N-myc is essential during neurogenesis for the rapid expansion of progenitor cell populations and the inhibition of neuronal differentiation. Genes & Development 16: 2699-2712.
47. Slack A, Chen ZW, Tonelli R, Pule M, Hunt L, et al. (2005) The p53 regulatory gene MDM2 is a direct transcriptional target of MYCN in neuroblastoma. Proceedings of the National Academy of Sciences of the United States of America 102: 731-736.
48. Beierle EA, Trujillo A, Nagaram A, Kurenova EV, Finch R, et al. (2007) N-MYC regulates focal adhesion kinase expression in human neuroblastoma. Journal of Biological Chemistry 282: 12503-12516.
49. Gupta A, Williams BRG, Hanash SM, Rawwas J (2006) Cellular retinoic acid-binding protein II is a direct transcriptional target of MycN in neuroblastoma. Cancer Research 66: 8100-8108.
50. Nakagawara A (2001) Trk receptor tyrosine kinases: A bridge between cancer and neural development. Cancer Letters 169: 107-114.
51. Nakagawara A (1998) Topical topic - The NGF story and neuroblastoma. Medical and Pediatric Oncology 31: 113-115.
52. Chao MV (2003) Neurotrophins and their receptors: A convergence point for many signalling pathways. Nature Reviews Neuroscience 4: 299-309.
53. Eggert A, Ikegaki N, Kwiatkowski J, Zhao HQ, Brodeur GM, et al. (2000) High-level expression of angiogenic factors is associated with advanced tumor stage in human neuroblastomas. Clinical Cancer Research 6: 1900-1908.
54. Vuillaume I, Schraen-Maschke S, Formstecher P, Sablonniere B (2001) Real time RT-PCR shows correlation between retinoid-induced apoptosis and NGF-R mRNA levels. Biochemical and Biophysical Research Communications 289: 647-652.
55. Tanaka T, Hiyama E, Sugimoto T, Sawada T, Tanabe M, et al. (1995) TRK-A gene-expression in neuroblastoma – the clinical-significance of an immunohistochemical study Cancer 76: 1086-1095.
56. Nakagawara A, Arimanakagawara M, Scavarda NJ, Azar CG, Cantor AB, et al. (1993) Association between high-levels of expression of the TRK gene and

favourable outcome in human neuroblastoma. New England Journal of Medicine 328: 847-854.
57. Nakagawara A, Azar CG, Scavarda NJ, Brodeur GM (1994) Expression and function of TRK-B and BDNF in human neuroblastomas. Molecular and Cellular Biology 14: 759-767.
58. Westermann F, Schwab M (2002) Genetic parameters of neuroblastomas. Cancer Letters 184: 127-147.
59. Attiyeh EF, London WB, Mosse YP, Wang Q, Winter C, et al. (2005) Chromosome 1p and 11q deletions and outcome in neuroblastoma. New England Journal of Medicine 353: 2243-2253.
60. Fong CT, Dracopoli NC, White PS, Merrill PT, Griffith RC, et al. (1989) Loss of heterozygosity for the short arm of chromosome-1 in human neuroblastomas – correlation with N-Myc amplification. Proceedings of the National Academy of Sciences of the United States of America 86: 3753-3757.
61. Bown N (2001) Neuroblastoma tumour genetics: clinical and biological aspects. Journal of Clinical Pathology 54: 897-910.
62. White PS, Thompson PM, Gotoh T, Okawa ER, Igarashi J, et al. (2004) Definition and characterization of a region of 1p36.3 consistently deleted in neuroblastoma. 24: 2684-2694.
63. Maris JM, Weiss MJ, Guo C, Gerbing RB, Stram DO, et al. (2000) Loss of heterozygosity at 1p36 independently predicts for disease progression but not decreased overall survival probability in neuroblastoma patients: A Children's Cancer Group study. Journal of Clinical Oncology 18: 1888-1899.
64. Caren H, Fransson S, Ejeskar K, Kogner P, Martinsson T (2007) Genetic and epigenetic changes in the common Ip36 deletion in neuroblastoma tumours. British Journal of Cancer 97: 1416-1424.
65. Fransson S, Martinsson T, Ejeskar K (2007) Neuroblastoma tumors with favorable and unfavorable outcomes: Significant differences in mRNA expression of genes mapped at Ip36.2. Genes Chromosomes & Cancer 46: 45-52.
66. Wang Q, Diskin S, Rappaport E, Attiyeh E, Mosse Y, et al. (2006) Integrative Genomics Identifies Distinct Molecular Classes of Neuroblastoma and Shows That Multiple Genes Are Targeted by Regional Alterations in DNA Copy Number. Cancer Research 66: 6050-6062.
67. Tomioka N, Kobayashi H, Kageyama H, Ohira M, Nakamura Y, et al. (2003) Chromosomes that show partial loss or gain in near-diploid tumors coincide with chromosomes that show whole loss or gain in near-triploid tumors: Evidence suggesting the involvement of the same genes in the tumorigenesis of high- and low-risk neuroblastomas. Genes Chromosomes & Cancer 36: 139-150.
68. Islam A, Kageyama H, Takada N, Kawamato T, Takayasu H, et al. (2000) High expression of Survivin, mapped to 17q25, is significantly associated with poor prognostic factors and promotes cell survival in human neuroblastoma. Oncogene 19: 617-623.
69. Yoon KJ, Danks MK, Ragsdale ST, Valentine MB, Valentine VA (2006) Translocations of 17q21 similar to qter in neuroblastoma cell lines infrequently include the topoisomerase II alpha gene. Cancer Genetics and Cytogenetics 167: 92-94.
70. Hailat N, Keim DR, Melhem RF, Zhu XX, Eckerskorn C, et al. (1991) High-levels of P19/NM23 protein in neuroblastoma are associated with advanced stage and with N-Myc gene amplification Journal of Clinical Investigation 88: 341-345.

71. Chang CL, Zhu XX, Thoraval DH, Ungar D, Rawwas J, et al. (1994) NM23-H1 mutation in neuroblastoma. Nature 370: 335-336.
72. Leone A, Seeger RC, Hong CM, Hu YY, Arboleda MJ, et al. (1993) Evidence for NM23 RNA overexpression, DNA amplification and mutation in aggressive childhood neuroblastomas Oncogene 8: 855-865.
73. Yu M, Ohira M, Li YY, Niizuma H, Oo ML, et al. (2009) High expression of ncRAN, a novel non-coding RNA mapped to chromosome 17q25.1, is associated with poor prognosis in neuroblastoma. International Journal of Oncology 34: 931-938.
74. Guo YJ, Harris RB, Rosson D, Boorman D, O'Brien TG (2000) Functional analysis of human ornithine decarboxylase alleles. Cancer Research 60: 6314-6317.
75. Vandesompele J, Speleman F, Van Roy N, Laureys C, Brinkschmidt C, et al. (2001) Multicentre analysis of patterns of DNA gains and losses in 204 neuroblastoma tumors: How many genetic subgroups are there? Medical and Pediatric Oncology 36: 5-10.
76. Janoueix-Lerosey I, Schleiermacher G, Michels E, Mosseri V, Ribeiro A, et al. (2009) Overall Genomic Pattern Is a Predictor of Outcome in Neuroblastoma. Journal of Clinical Oncology 27: 1026-1033.
77. Schramm A, Vandesompele J, Schulte JH, Dreesmann S, Kaderali L, et al. (2007) Translating expression profiling into a clinically feasible test to predict neuroblastoma outcome. Clinical Cancer Research 13: 1459-1465.
78. De Preter K, Vermeulen J, Brors B, Delattre O, Eggert A, et al. (2010) Accurate Outcome Prediction in Neuroblastoma across Independent Data Sets Using a Multigene Signature. Clinical Cancer Research 16: 1532-1541.
79. Lin RJ, Lin YC, Chen J, Kuo HH, Chen YY, et al. (2010) microRNA Signature and Expression of Dicer and Drosha Can Predict Prognosis and Delineate Risk Groups in Neuroblastoma. Cancer Research 70: 7841-7850.
80. Schulte JH, Schowe B, Mestdagh P, Kaderali L, Kalaghatgi P, et al. (2010) Accurate prediction of neuroblastoma outcome based on miRNA expression profiles. International Journal of Cancer 127: 2374-2385.
81. Schlesinger HR, Gerson JM, Moorhead PS, Maguire H, Hummeler K (1976) Establishment and Characterization of Human Neuroblastoma Cell Lines. Cancer Research 36: 3094-3100.
82. Biedler JL, Roffler-Tarlov S, Schachner M, Freedman LS (1978) Multiple Neurotransmitter Synthesis by Human Neuroblastoma Cell Lines and Clones. Cancer Research 38: 3751-3757.
83. Ciccarone V, Spengler BA, Meyers MB, Biedler JL, Ross RA (1989) Phenotypic Diversification in Human Neuroblastoma Cells: Expression of Distinct Neural Crest Lineages. Cancer Research 49: 219-225.
84. Ross RA, Biedler JL, Spengler BA, Reis DJ (1981) Neurotransmitter-synthesizing enzymes in 14 human neuroblastoma cell lines. Cellular and Molecular Neurobiology 1: 301-312.
85. Vogan K, Bernstein M, Leclerc J-M, Brisson L, Brossard J, et al. (1993) Absence of p53 Gene Mutations in Primary Neuroblastomas. Cancer Research 53: 5269-5273.
86. Keshelava N, Zuo JJ, Chen P, Waidyaratne SN, Luna MC, et al. (2001) Loss of p53 Function Confers High-Level Multidrug Resistance in Neuroblastoma Cell Lines. Cancer Research 61: 6185-6193.
87. Bi X, Zhang JZ (2003) Experimental study of thymidine kinase gene therapy of neuroblastoma in vitro and in vivo. Pediatric Surgery International 19: 400-405.

88. Streck CJ, Zhang Y, Miyamoto R, Zhou J, Ng CYC, et al. (2004) Restriction of neuroblastoma angiogenesis and growth by interferon-alpha/beta. Surgery 136: 183-189.
89. Patterson DM, Shohet JM, Kim ES (2001) Preclinical Models of Pediatric Solid Tumors (Neuroblastoma) and Their Use in Drug Discovery. Current Protocols in Pharmacology: John Wiley & Sons, Inc.
90. Khanna C, Jaboin JJ, Drakos E, Tsokos M, Thiele CJ (2002) Biologically relevant orthotopic neuroblastoma xenograft models: Primary adrenal tumor growth and spontaneous distant metastasis. In Vivo 16: 77-85.
91. Banerjee AK, Sharma BS, Vashista RK, Kak VK (1992) Intracranial olfactory neuroblastoma – evidence for olfactory epithelial origin. Journal of Clinical Pathology 45: 299-302.
92. Hansford LM, Thomas WD, Keating JM, Burkhart CA, Peaston AE, et al. (2004) Mechanisms of embryonal tumor initiation: Distinct roles for MycN expression and MYCN amplification. Proceedings of the National Academy of Sciences of the United States of America 101: 12664-12669.
93. Dyer MA (2004) Mouse models of childhood cancer of the nervous system. Journal of Clinical Pathology 57: 561-576.
94. George RE, Diller L, Bernstein ML (2010) Pharmacotherapy of neuroblastoma. Expert Opinion on Pharmacotherapy 11: 1467-1478.
95. Wagner LM, Danks MK (2009) New Therapeutic Targets for the Treatment of High-Risk Neuroblastoma. Journal of Cellular Biochemistry 107: 46-57.
96. Hero B, Simon T, Spitz R, Ernestus K, Gnekow AK, et al. (2008) Localized infant neuroblastomas often show spontaneous regression: Results of the prospective trials NB95-S and NB97. Journal of Clinical Oncology 26: 1504-1510.
97. Kushner BH, Kramer K, LaQuaglia MP, Modak S, Yataghene K, et al. (2004) Reduction from seven to five cycles of intensive induction chemotherapy in children with high-risk neuroblastoma. Journal of Clinical Oncology 22: 4888-4892.
98. Donfrancesco A, Jenkner A, Castellano A, Ilari I, Milano GM, et al. (2004) Ifosfamide/carboplatin/etoposide (ICE) as front-line, topotecan/cyclophosphamide as second-line and oral temozolomide as third-line treatment for advanced neuroblastoma over one year of age. Acta Paediatrica 93: 6-11.
99. Saylors RL, Stine KC, Sullivan J, Kepner JL, Wall DA, et al. (2001) Cyclophosphamide plus topotecan in children with recurrent or refractory solid tumors: A pediatric oncology group phase II study. Journal of Clinical Oncology 19: 3463-3469.
100. Finklestein JZ, Krailo MD, Lenarsky C, Ladisch S, Blair GK, et al. (1992) 13-cis-retinoic acid (NSC-122758) in the treatment of children with metastatic neuroblastoma unresponsive to conventional chemotherapy – report from the childrens-cancer-study-group. Medical and Pediatric Oncology 20: 307-311.
101. Kohler JA, Imeson J, Ellershaw C, Lie SO (2000) A randomized trial of 13-Cis retinoic acid in children with advanced neuroblastoma after high-dose therapy. British Journal of Cancer 83: 1124-1127.
102. Baker DL, Schmidt ML, Cohn SL, Maris JM, London WB, et al. (2010) Outcome after Reduced Chemotherapy for Intermediate-Risk Neuroblastoma. New England Journal of Medicine 363: 1313-1323.

103. Schulz G, Cheresh DA, Varki NM, Yu A, Staffileno LK, et al. (1984) Detection of Ganglioside GD2 in Tumor Tissues and Sera of Neuroblastoma Patients. Cancer Research 44: 5914-5920.
104. Modak S, Cheung NKV (2007) Disialoganglioside directed immunotherapy of neuroblastoma. Cancer Investigation 25: 67-77.
105. Shusterman SS, London WB, Gillies SD, Hank JA, Voss SD, et al. (2010) Antitumor Activity of Hu14.18-IL2 in Patients With Relapsed/Refractory Neuroblastoma: A Children's Oncology Group (COG) Phase II Study. Journal of Clinical Oncology.
106. DuBois SG, Matthay KK (2008) Radiolabeled metaiodobenzylguanidine for the treatment of neuroblastoma. Nuclear Medicine and Biology 35: S35-S48.
107. de Kraker J, Hoefnagel KA, Verschuur AC, van Eck B, van Santen HM, et al. (2008) Iodine-131-metaiodobenzylguanidine as initial induction therapy in stage 4 neuroblastoma patients over 1 year of age. European Journal of Cancer 44: 551-556.
108. Kushner BH, Kramer K, Modak S, Cheung N-KV (2011) Successful Multifold Dose Escalation of Anti-GD2 Monoclonal Antibody 3F8 in Patients With Neuroblastoma: A Phase I Study. Journal of Clinical Oncology 29: 1168-1174.
109. Cheung NKV, Kushner BH, Yeh SDJ, Larson SM (1998) 3F8 monoclonal antibody treatment of patients with stage 4 neuroblastoma: a phase II study. International Journal of Oncology 12: 1299-1306.
110. Maris JM, Morton CL, Gorlick R, Kolb EA, Lock R, et al. (2010) Initial Testing of the Aurora Kinase A Inhibitor MLN8237 by the Pediatric Preclinical Testing Program (PPTP). Pediatric Blood & Cancer 55: 26-34.
111. Lovat PE, Di Sano F, Corazzari M, Fazi B, Donnorso RP, et al. (2004) Gangliosides Link the Acidic Sphingomyelinase-Mediated Induction of Ceramide to 12-Lipoxygenase-Dependent Apoptosis of Neuroblastoma in Response to Fenretinide. Journal of the National Cancer Institute 96: 1288-1299.
112. Maurer BJ, Metelitsa LS, Seeger RC, Cabot MC, Reynolds CP (1999) Increase of Ceramide and Induction of Mixed Apoptosis/Necrosis by N-(4-Hydroxyphenyl)-retinamide in Neuroblastoma Cell Lines. Journal of the National Cancer Institute 91: 1138-1146.
113. Hansen LA, Sigman CC, Andreola F, Ross SA, Kelloff GJ, et al. (2000) Retinoids in chemoprevention and differentiation therapy. Carcinogenesis 21: 1271-1279.
114. Sell S (2004) Stem cell origin of cancer and differentiation therapy. Critical Reviews in Oncology/Hematology 51: 1-28.
115. Huang M, Ye Y, Chen S, Chai J, Lu J, et al. (1988) Use of all-trans retinoic acid in the treatment of acute promyelocytic leukemia. Blood 72: 567-572.
116. Chen Z, Xue Y, Zhang R, Tao R, Xia X, et al. (1991) A clinical and experimental study on all-trans retinoic acid-treated acute promyelocytic leukemia patients. Blood 78: 1413-1419.
117. Tallman MS, Andersen JW, Schiffer CA, Appelbaum FR, Feusner JH, et al. (2002) All-trans retinoic acid in acute promyelocytic leukemia: long-term outcome and prognostic factor analysis from the North American Intergroup protocol. Blood 100: 4298-4302.
118. Carrera P, Johnstone O, Nakamura A, Casanova J, Jackle H, et al. (2000) VASA mediates translation through interaction with a Drosophila yIF2 homolog. Mol Cell 5: 181-187.
119. Look AT, Hayes FA, Shuster JJ, Douglas EC, Castleberry RP, et al. (1991) Clinical relevance of tumor-cell ploidy and N-Myc gene amplification in

childhood neuroblastoma – a pediatric oncology group-study Journal of Clinical Oncology 9: 581-591.
120. Seeger R, Brodeur G, Sather H, Dalton A, Siegel S, et al. (1985) Genomic amplification of N-Myc in untreated primary neuroblastomas correlates with advanced disease stage at diagnosis and rapid tumor progression. Proceedings of the American Association for Cancer Research 26: 64-64.
121. Janardhanan R, Banik NL, Ray SK (2009) N-Myc down regulation induced differentiation, early cell cycle exit, and apoptosis in human malignant neuroblastoma cells having wild type or mutant p53. Biochemical Pharmacology In Press, Corrected Proof.
122. Reynolds CP, Matthay KK, Villablanca JG, Maurer BJ (2003) Retinoid therapy of high-risk neuroblastoma. Cancer Letters 197: 185-192.
123. Edlund T, Jessell TM (1999) Progression from Extrinsic to Intrinsic Signaling in Cell Fate Specification: A View from the Nervous System. Cell 96: 211-224.
124. Galderisi U, Jori FP, Giordano A Cell cycle regulation and neural differentiation. Oncogene 22: 5208-5219.
125. Watanabe Y, Watanabe T, Kitagawa M, Taya Y, Nakayama K-i, et al. (1999) pRb phosphorylation is regulated differentially by cyclin-dependent kinase (Cdk) 2 and Cdk4 in retinoic acid-induced neuronal differentiation of P19 cells. Brain Research 842: 342-350.
126. Harbour JW, Luo RX, Santi AD, Postigo AA, Dean DC (1999) Cdk Phosphorylation Triggers Sequential Intramolecular Interactions that Progressively Block Rb Functions as Cells Move through G1. Cell 98: 859-869.
127. Sherr CJ (1994) G1 phase progression: Cycling on cue. Cell 79: 551-555.
128. Ferguson KL, Callaghan SM, O'Hare MJ, Park DS, Slack RS (2000) The Rb-CDK4/6 Signaling Pathway Is Critical in Neural Precursor Cell Cycle Regulation. Journal of Biological Chemistry 275: 33593-33600.
129. Macleod KF, Hu YW, Jacks T (1996) Loss of Rb activates both p53-dependent and independent cell death pathways in the developing mouse nervous system. Embo Journal 15: 6178-6188.
130. Slack RS, El-Bizri H, Wong J, Belliveau DJ, Miller FD (1998) A critical temporal requirement for the retinoblastoma protein family during neuronal determination. Journal of Cell Biology 140: 1497-1509.
131. Rustgi AK, Dyson N, Bernards R (1991) Amino-terminal domains of C-Myc and N-Myc proteins mediate binding to the retinoblastoma gene-product. Nature 352: 541-544.
132. Wakamatsu Y, Watanabe Y, Nakamura H, Kondoh H (1997) Regulation of the neural crest cell fate by N-myc: promotion of ventral migration and neuronal differentiation. Development 124: 1953-1962.
133. ElShamy WM, Fridvall LK, Ernfors P (1998) Growth Arrest Failure, G1 Restriction Point Override, and S Phase Death of Sensory Precursor Cells in the Absence of Neurotrophin-3. Neuron 21: 1003-1015.
134. Wartiovaara K, Barnabe-Heider F, Miller FD, Kaplan DR (2002) N-myc promotes survival and induces S-phase entry of postmitotic sympathetic neurons. Journal of Neuroscience 22: 815-824.
135. Lee MH, Nikolic M, Baptista CA, Lai E, Tsai LH, et al. (1996) The brain-specific activator p35 allows Cdk5 to escape inhibition by p27Kip1 in neurons. Proceedings of the National Academy of Sciences 93: 3259-3263.
136. Baldassarre G, Boccia A, Bruni P, Sandomenico C, Barone MV, et al. (2000) Retinoic acid induces neuronal differentiation of embryonal carcinoma cells by

reducing proteasome-dependent proteolysis of the cyclin-dependent inhibitor p27. Cell Growth & Differentiation 11: 517-526.
137. Bergmann E, Wanzel M, Weber A, Shin I, Christiansen H, et al. (2001) Expression of p27(kip1) is prognostic and independent in MYCN amplification in human neuroblastoma. International Journal of Cancer 95: 176-183.
138. Blain SW, Massague J (2002) Breast cancer banishes p27 from nucleus. Nature Medicine 8: 1076-1078.
139. Bellodi C, Kindle K, Bernassola F (2006) A cytoplasmic PML mutant inhibits p53 function. Cell Cycle 5: 2688-2692.
140. Chan JY, Li L, Fan YH (1997) Cell-cycle regulation of DNA damage-induced expression of the suppressor gene PML. Biochem Biophys Res Commun 240: 640-646.
141. Shaulsky G, Goldfinger N, Tosky MS, Levine AJ, Rotter V (1991) Nuclear-localization is essential for the activity of the p53 protein Oncogene 6: 2055-2065.
142. Alcalay M, Tomassoni L, Colombo E (1998) The promyelocytic leukemia gene product (PML) forms stable complexes with the retinoblastoma protein. Mol Cell Biol 18: 1084-1093.
143. Bernardi R (2004) PML regulates p53 stability by sequestering Mdm2 to the nucleolus. Nature Cell Biol 6: 665-672.
144. Bain DL, Heneghan AF, Connaghan-Jones KD, Miura MT (2007) Nuclear Receptor Structure: Implications for Function. Annual Review of Physiology 69: 201-220.
145. Ponthan F, Johnsen JI, Klevenvall L, Castro J, Kogner P (2003) The synthetic retinoid RO 13-6307 induces neuroblastoma differentiation in vitro and inhibits neuroblastoma tumour growth in vivo. International Journal of Cancer 104: 418-424.
146. Brabender J, Metzger R, Salonga D, Danenberg KD, Danenberg PV, et al. (2005) Comprehensive expression analysis of retinoic acid receptors and retinoid X receptors in non-small cell lung cancer: implications for tumor development and prognosis. Carcinogenesis 26: 525-530.
147. Schmutzler C, Cuong HV, Ruger B, Kohrle J (2004) Human thyroid carcinoma cell lines show different retinoic acid receptor repertoires and retinoid responses. European Journal of Endocrinology 150: 547-556.
148. Narayan G, Arias-Pulido H, Koul S, Vargas H, Zhang F, et al. (2003) Frequent Promoter Methylation of CDH1, DAPK, RARB, and HIC1 Genes in Carcinoma of Cervix Uteri: Its Relationship to Clinical Outcome. Molecular Cancer 2: 24.
149. Cheung B, Hocker JE, Smith SA, Norris MD, Haber M, et al. (1998) Favorable prognostic significance of high-level retinoic acid receptor beta expression in neuroblastoma mediated by effects on cell cycle regulation. Oncogene 17: 751-759.
150. Wolf G (1996) A history of vitamin A and retinoids. Faseb Journal 10: 1102-1107.
151. Karrer P, Helfenstein A, Wehrli H, Wettstein A (1930) Pflanzenfarbstoffe XXV. Über die Konstitution des Lycopins und Carotins. Helvetica Chimica Acta 13: 1084-1099.
152. Clagett-Dame M, DeLuca HF (2002) The role of vitamin A in mammalian reproduction and embryonic development. Annual Review of Nutrition 22: 347-381.
153. Heine UI, Roberts AB, Munoz EF, Roche NS, Sporn MB (1985) Effects of retinoid deficiency on the development of the heart and vascular system of the quail

embryo. Virchows Archiv B-Cell Pathology Including Molecular Pathology 50: 135-152.
154. Dersch H, Zile MH (1993) Induction of Normal Cardiovascular Development in the Vitamin A-Deprived Quail Embryo by Natural Retinoids. Developmental Biology 160: 424-433.
155. Zile MH (1998) Vitamin A and embryonic development: An overview. Journal of Nutrition 128: 455S-458S.
156. Niederreither K, Subbarayan V, Dolle P, Chambon P (1999) Embryonic retinoic acid synthesis is essential for early mouse post-implantation development. Nat Genet 21: 444-448.
157. White JC, Highland M, Kaiser M, Clagett-Dame M (2000) Vitamin A Deficiency Results in the Dose-Dependent Acquisition of Anterior Character and Shortening of the Caudal Hindbrain of the Rat Embryo. Developmental Biology 220: 263-284.
158. Deleenheer AP, Lambert WE, Claeys I (1982) All-trans-retinoic acid – measurement of reference values in human-serum by high-performance liquid-chromatography. Journal of Lipid Research 23: 1362-1367.
159. Tang GW, Russell RM (1990) 13-cis-retinoic acid is an endogenous compound in human serum. Journal of Lipid Research 31: 175-182.
160. Eckhoff C, Nau H (1990) Vitamin A supplementation increases levels of retinoic acid compounds in human plasma: possible implications for teratogenesis. Archives of Toxicology 64: 502-503.
161. Lovat PE, Irving H, Annicchiarico-Petruzzelli M, Bernassola F, Malcolm AJ, et al. (1997) Retinoids in neuroblastoma therapy: distinct biological properties of 9-cis- and all-trans-retinoic acid. European journal of cancer (Oxford, England : 1990) 33: 2075-2080.
162. Creech Kraft J, Shepard T, Juchau MR (1993) Tissue levels of retinoids in human embryos/fetuses. Reproductive Toxicology 7: 11-15.
163. Nagpal S (2004) Retinoids: Inducers of Tumor//Growth Suppressors. J Investig Dermatol 123: xx-xxi.
164. Nagpal S, Chandraratna RAS (1998) Vitamin A and regulation of gene expression. Current Opinion in Clinical Nutrition & Metabolic Care 1: 341-346.
165. Martine C (2005) Retinoid Therapy for Acne: A Comparative Review. American Journal of Clinical Dermatology 6: 13-19.
166. Pang M-L, E Murase J, Koo J (2008) An updated review of acitretin - a systemic retinoid for the treatment of psoriasis. Expert Opinion on Drug Metabolism 26; Toxicology 4: 953-964.
167. Langton AK, Sherratt MJ, Griffiths CEM, Watson REB (2010) Review Article: A new wrinkle on old skin: the role of elastic fibres in skin ageing. International Journal of Cosmetic Science 32: 330-339.
168. Farol LT, Hymes KB (2004) Bexarotene: a clinical review. Expert Review of Anticancer Therapy 4: 180-188.
169. Gniadecki R, Assaf C, Bagot M, Dummer R, Duvic M, et al. (2007) The optimal use of bexarotene in cutaneous T-cell lymphoma. British Journal of Dermatology 157: 433-440.
170. Dragnev KH, Petty WJ, Shah SJ, Lewis LD, Black CC, et al. (2007) A Proof-of-Principle Clinical Trial of Bexarotene in Patients with Non-Small Cell Lung Cancer. Clinical Cancer Research 13: 1794-1800.

171. Saffiotti U, Montesano R, Sellakumar AR, Borg SA (1967) Experimental cancer of the lung. Inhibition by vitamin A of the induction of tracheobronchial squamous metaplasia and squamous cell tumors. Cancer 20: 857-864.
172. Altucci L, Gronemeyer H (2001) The promise of retinoids to fight against cancer. Nature Rev Cancer 1: 181-193.
173. Benner SE, Pajak TF, Lippman SM, Earley C, Hong WK (1994) Prevention of Second Primary Tumors With Isotretinoin in Patients With Squamous Cell Carcinoma of the Head and Neck: Long-term Follow-up. Journal of the National Cancer Institute 86: 140-141.
174. Lee JJ, Wu X, Hildebrandt MAT, Yang H, Khuri FR, et al. (2011) Global Assessment of Genetic Variation Influencing Response to Retinoid Chemoprevention in Head and Neck Cancer Patients. Cancer Prevention Research 4: 185-193.
175. Pendino F, Hillion J, Dudognon C, Delaunay J, Mourah S, et al. (2006) Telomerase targeting by retinoids in cells from patients with myeloid leukemias of various subtypes, not only APL. Leukemia 20: 599-603.
176. Thiele CJ, Reynolds CP, Israel MA (1985) Decreased expression of N-myc precedes retinoic acid-induced morphological differentiation of human neuroblastoma. Nature 313: 404-406.
177. Petkovich M, Brand NJ, Krust A, Chambon P (1987) A human retinoic acid receptor which belongs to the family of nuclear receptors. Nature 330: 444-450.
178. Giguere V, Ong ES, Segui P, Evans RM (1987) Identification of a receptor for the morphogen retinoic acid. Nature 330: 624-629.
179. Mangelsdorf DJ, Thummel C, Beato M, Herrlich P, SchÃ¼tz Gn, et al. (1995) The nuclear receptor superfamily: The second decade. Cell 83: 835-839.
180. Bertrand S (2004) Evolutionary genomics of nuclear receptors: from 25 ancestral genes to derived endocrine systems. Molecular Biology and Evolution 21: 1923-1937.
181. Edwards DP (2000) The role of coactivators and corepressors in the biology and mechanism of action of steroid hormone receptors. Journal of Mammary Gland Biology and Neoplasia 5: 307-324.
182. Escriva H, Bertrand S, Laudet V (2004) The evolution of the nuclear receptor superfamily. Essays Biochem 40: 11-26.
183. Gronemeyer H, Gustafsson J-A, Laudet V (2004) Principles for modulation of the nuclear receptor superfamily. Nat Rev Drug Discov 3: 950-964.
184. Robinson-Rechavi M, Escriva-Garcia H, Laudet V (2003) The nuclear receptor superfamily. J Cell Sci 116: 585-586.
185. Rochette-Egly C (2003) Nuclear receptors: integration of multiple signalling pathways through phosphorylation. Cell Signal 15: 355-366.
186. Osborne CK (1998) Tamoxifen in the Treatment of Breast Cancer. New England Journal of Medicine 339: 1609-1618.
187. Shiau AK, Barstad D, Loria PM, Cheng L, Kushner PJ, et al. (1998) The Structural Basis of Estrogen Receptor/Coactivator Recognition and the Antagonism of This Interaction by Tamoxifen. Cell 95: 927-937.
188. Crabtree GR, Smith KA, Munck A (1978) Glucocorticoid Receptors and Sensitivity of Isolated Human Leukemia and Lymphoma Cells. Cancer Research 38: 4268-4272.
189. Loinder K, Soderstrom M (2004) Functional analyses of an LXXLL motif in nuclear receptor corepressor (N-CoR). Journal of Steroid Biochemistry and Molecular Biology 91: 191-196.

190. Laudet V, Hanni C, Coll J, Catzeflis F, Stehelin D (1992) Evolution of the nuclear receptor gene superfamily. Embo Journal 11: 1003-1013.
191. Gustafsson JA (2003) What pharmacologists can learn from recent advances in oestrogen signaling. Trends Pharmacol Sci 24: 479-485.
192. Helguero LA, Faulds MH, Gustafsson J-A, Haldosen L-A (2005) Estrogen receptors alfa (ER[alpha]) and beta (ER[beta]) differentially regulate proliferation and apoptosis of the normal murine mammary epithelial cell line HC11. Oncogene 24: 6605-6616.
193. Matthews J, Gustafsson J-A (2003) Estrogen signaling: a subtle balance between ER alpha and ER beta. Molecular interventions 3: 281-292.
194. Germain P, Chambon P, Eichele G, Evans RM, Lazar MA, et al. (2006) International Union of Pharmacology. LX. Retinoic Acid Receptors. Pharmacological Reviews 58: 712-725.
195. Bourguet W, Germain P, Gronemeyer H (2000) Nuclear receptor ligand-binding domains: 3D structures, molecular interactions and pharmacological implications. Trends Pharmacol Sci 21: 381-388.
196. Xu L, Glass CK, Rosenfeld MG (1999) Coactivator and corepressor complexes in nuclear receptor function. Current Opinion in Genetics & Development 9: 140-147.
197. Wei L-N (2003) Retinoid receptors and their coregulators Annual Review of Pharmacology and Toxicology 43: 47-72.
198. Toulouse A, Morin J, Pelletier M, Bradley WEC (1996) Structure of the human retinoic acid receptor [beta] 1 gene. Biochimica et Biophysica Acta (BBA) - Gene Structure and Expression 1309: 1-4.
199. Chambon P (1996) A decade of molecular biology of retinoic acid receptors. The FASEB Journal 10: 940-954.
200. de The H, del Mar Vivanco-Ruiz M, Tiollais P, Stunnenberg H, Dejean A (1990) Identification of a retinoic acid responsive element in the retinoic acid receptor & beta;gene. Nature 343: 177-180.
201. Gillespie RF, Gudas LJ (2007) Retinoic Acid Receptor Isotype Specificity in F9 Teratocarcinoma Stem Cells Results from the Differential Recruitment of Coregulators to Retinoic Acid Response Elements. Journal of Biological Chemistry 282: 33421-33434.
202. Cheung B, Hocker JE, Smith SA, Reichert U, Norris MD, et al. (1996) Retinoic Acid Receptors [beta] and [gamma] Distinguish Retinoid Signals for Growth Inhibition and Neuritogenesis in Human Neuroblastoma Cells. Biochemical and Biophysical Research Communications 229: 349-354.
203. Cheung B, Yan J, Smith SA, Nguyen T, Lee M, et al. (2003) Growth inhibitory retinoid effects after recruitment of retinoid X receptor β to the retinoic acid receptor β promoter. International Journal of Cancer 105: 856-867.
204. Sun SY, Lotan R (2002) Retinoids and their receptors in cancer development and chemoprevention. Crit Rev Oncol Hematol 41: 41-55.
205. Si SP, Lee X, Tsou HC, Buchsbaum R, Tibaduiza E, et al. (1996) RAR[beta]2-Mediated Growth Inhibition in HeLa Cells. Experimental Cell Research 223: 102-111.
206. Houle B, Rochette-Egly C, Bradley WEC (1993) Tumor-Suppressive Effect of the Retinoic Acid Receptor [beta] in Human Epidermoid Lung Cancer Cells. Proceedings of the National Academy of Sciences of the United States of America 90: 985-989.

207. Jones LC, Tefferi A, Idos GE, Kumagai T, Hofmann W-K, et al. (2004) RAR[beta]2 is a candidate tumor suppressor gene in myelofibrosis with myeloid metaplasia. Oncogene 23: 7846-7853.
208. Ushijima T (2005) Detection and interpretation of altered methylation patterns in cancer cells. Nat Rev Cancer 5: 223-231.
209. Miladi-Abdennadher I, Abdelmaksoud-Damak R, Ayadi L, Khabir A, Frikha F, et al. (2010) Hypermethylation of RAR[beta]2 correlates with high COX-2 expression and poor prognosis in patients with colorectal carcinoma. Tumor Biology 31: 503-511.
210. Zeschnigk M, Tschentscher F, Lich C, Brandt B, Horsthemke B, et al. (2003) Methylation analysis of several tumour suppressor genes shows a low frequency of methylation of CDKN2A and RARB in uveal melanomas. Comparative and Functional Genomics 4: 329-336.
211. Kuroki T, Trapasso F, Yendamuri S, Matsuyama A, Alder H, et al. (2003) Allele Loss and Promoter Hypermethylation of VHL, RAR-[beta], RASSF1A, and FHIT Tumor Suppressor Genes on Chromosome 3p in Esophageal Squamous Cell Carcinoma. Cancer Research 63: 3724-3728.
212. Castro M, Grau L, Puerta P, Gimenez L, Venditti J, et al. (2010) Multiplexed methylation profiles of tumor suppressor genes and clinical outcome in lung cancer. Journal of Translational Medicine 8.
213. Vasilatos SN, Broadwater G, Barry WT, Baker JC, Lem S, et al. (2009) CpG Island Tumor Suppressor Promoter Methylation in Non-BRCA-Associated Early Mammary Carcinogenesis. Cancer Epidemiology Biomarkers & Prevention 18: 901-914.
214. Feng WW, Orlandi R, Zhao NQ, Carcangiu ML, Tagliabue E, et al. (2010) Tumor suppressor genes are frequently methylated in lymph node metastases of breast cancers. Bmc Cancer 10.
215. Nguyen T, Hocker JE, Thomas W, Smith SA, Norris MD, et al. (2003) Combined RAR alpha- and RXR-specific ligands overcome N-myc-associated retinoid resistance in neuroblastoma cells. Biochemical and Biophysical Research Communications 302: 462-468.
216. Raif A, Marshall GM, Bell JL, Koach J, Tan O, et al. (2009) The estrogen-responsive B box protein (EBBP) restores retinoid sensitivity in retinoid-resistant cancer cells via effects on histone acetylation. Cancer Letters 277: 82-90.
217. Rhodes DA, de Bono B, Trowsdale J (2005) Relationship between SPRY and B30.2 protein domains. Evolution of a component of immune defence? Immunology 116: 411-417.
218. Sardiello M, Cairo S, Fontanella B, Ballabio A, Meroni G (2008) Genomic analysis of the TRIM family reveals two groups of genes with distinct evolutionary properties. Bmc Evolutionary Biology 8.
219. van der Aa LM, Levraud JP, Yahmi M, Lauret E, Briolat V, et al. (2009) A large new subset of TRIM genes highly diversified by duplication and positive selection in teleost fish. Bmc Biology 7.
220. Joazeiro CAP, Weissman AM (2000) RING Finger Proteins: Mediators of Ubiquitin Ligase Activity. Cell 102: 549-552.
221. Diaz-Griffero F, Qin XR, Hayashi F, Kigawa T, Finzi A, et al. (2009) A B-Box 2 Surface Patch Important for TRIM5 alpha Self-Association, Capsid Binding Avidity, and Retrovirus Restriction. Journal of Virology 83: 10737-10751.

222. Li X, Li Y, Stremlau M, Yuan W, Song B, et al. (2006) Functional replacement of the RING, B-Box 2, and coiled-coil domains of tripartite motif 5 alpha (TRIM5 alpha) by heterologous TRIM domains. Journal of Virology 80: 6198-6206.
223. Li X, Sodroski J (2008) The TRIM5 alpha B-Box 2 Domain Promotes Cooperative Binding to the Retroviral Capsid by Mediating Higher-Order Self-Association. Journal of Virology 82: 11495-11502.
224. Cao T, Borden KL, Freemont PS, Etkin LD (1997) Involvement of the rfp tripartite motif in protein-protein interactions and subcellular distribution. J Cell Sci 110: 1563-1571.
225. Reymond A, Meroni G, Fantozzi A, Merla G, Cairo S, et al. (2001) The tripartite motif family identifies cell compartments. EMBO J 20: 2140-2151.
226. Cao TY, Duprez E, Borden KLB, Freemont PS, Etkin LD (1998) Ret finger protein is a normal component of PML nuclear bodies and interacts directly with PML. Journal of Cell Science 111: 1319-1329.
227. Woo J-S, Imm J-H, Min C-K, Kim K-J, Cha S-S, et al. (2006) Structural and functional insights into the B30.2/SPRY domain. EMBO J 25: 1353-1363.
228. Vernet C, Boretto J, Mattei MG, Takahashi M, Jack LJ, et al. (1993) Evolutionary study of multigenic families mapping close to the human MHC class I region. J Mol Evol 37: 600-612.
229. Sawyer SL, Wu LI, Emerman M, Malik HS (2005) Positive selection of primate TRIM5alpha identifies a critical species-specific retroviral restriction domain. Proc Natl Acad Sci USA 102: 2832-2837.
230. Yap MW, Nisole S, Stoye JP (2005) A single amino acid change in the SPRY domain of human Trim5alpha leads to HIV-1 restriction. Curr Biol 15: 73-78.
231. De Falco F, Cainarca S, Andolfi G, Ferrentino R, Berti C, et al. (2003) X-linked Opitz syndrome: novel mutations in the MID1 gene and redefinition of the clinical spectrum. Am J Med Genet A 120: 222-228.
232. Schweiger S, Schneider R (2003) The MID1/PP2A complex: a key to the pathogenesis of Opitz BBB/G syndrome. Bioessays 25: 356-366.
233. The-International-FMF-Consortium (1997) Ancient missense mutations in a new member of the RoRet gene family are likely to cause familial Mediterranean fever. Cell 90: 797-807.
234. Ishii T, Aoki N, Noda A, Adachi T, Nakamura R, et al. (1995) Carboxy-terminal cytoplasmic domain of mouse butyrophilin specifically associates with a 150-kDa protein of mammary epithelial cells and milk fat globule membrane. Biochim Biophys Acta 1245: 285-292.
235. Duprez E (1999) SUMO-1 modification of the acute promyelocytic leukaemia protein PML: implications for nuclear localisation. J Cell Sci 112: 381-393.
236. Salomoni P (2009) Stemming out of a new PML era? Cell Death and Differentiation 16: 1083-1092.
237. Dethe H, Lavau C, Marchio A, Chomienne C, Degos L, et al. (1991) The PML-RAR-alpha fusion messenger-RNA generated by the T(15-17) translocation in acute promyelocytic leukemia encodes a functionally altered RAR Cell 66: 675-684.
238. Bernardi R, Papa A, Pandolfi PP (2008) Regulation of apoptosis by PML and the PML-NBs. Oncogene 27: 6299-6312.
239. Gurrieri C, Capodieci P, Bernardi R, Scaglioni PP, Nafa K, et al. (2004) Loss of the Tumor Suppressor PML in Human Cancers of Multiple Histologic Origins. J Natl Cancer Inst 96: 269-279.

240. Bernardi R, Pandolfi PP (2003) Role of PML and the PML-nuclear body in the control of programmed cell death. Oncogene 22: 9048-9057.
241. Guo A, Salomoni P, Luo JY, Shih A, Zhong S, et al. (2000) The function of PML in p53-dependent apoptosis. Nature Cell Biology 2: 730-736.
242. Lallemand-Breitenbach V, Zhu J, Puvion F, Koken M, Honore N, et al. (2001) Role of Promyelocytic Leukemia (Pml) Sumolation in Nuclear Body Formation, 11s Proteasome Recruitment, and as2O3-Induced Pml or Pml/Retinoic Acid Receptor [alpha] Degradation. The Journal of Experimental Medicine 193: 1361-1372.
243. Zhong S (1999) A role for PML and the nuclear body in genomic stability. Oncogene 18: 7941-7947.
244. Zhu J, Zhou J, Peres L (2005) A sumoylation site in PML/RARA is essential for leukemic transformation. Cancer Cell 7: 143-153.
245. Alsheich-Bartok O, Haupt S, Alkalay-Snir I, Saito S, Appella E, et al. (2008) PML enhances the regulation of p53 by CK1 in response to DNA damage. Oncogene 27: 3653-3661.
246. Kurki S, Latonen L, Laiho M (2003) Cellular stress and DNA damage invoke temporally distinct Mdm2, p53 and PML complexes and damage-specific nuclear relocalization. Journal of Cell Science 116: 3917-3925.
247. Rego EM, He LZ, Warrell RP, Wang ZG, Pandolfi PP (2000) Retinoic acid (RA) and As2O3 treatment in transgenic models of acute promyelocytic leukemia (APL) unravel the distinct nature of the leukemogenic process induced by the PML-RAR alpha and PLZF-RAR alpha oncoproteins. Proceedings of the National Academy of Sciences of the United States of America 97: 10173-10178.
248. Seker H, Rubbi C, Linke SP, Bowman ED, Garfield S, et al. (2003) UV-C-induced DNA damage leads to p53-dependent nuclear trafficking of PML. Oncogene 22: 1620-1628.
249. Everett R, Lomonte P, Sternsdorf T, van Driel R, Orr A (1999) Cell cycle regulation of PML modification and ND10 composition. J Cell Sci 112: 4581-4588.
250. Wang ZG, Ruggero D, Ronchetti S (1998) PML is essential for multiple apoptotic pathways. Nat Genet 20: 266-272.
251. Scaglioni PP, Yung TM, Cai LF (2006) A CK2-dependent mechanism for degradation of the PML tumor suppressor. Cell 126: 269-283.
252. Gao C, Ho C-C, Reineke E, Lam M, Cheng X, et al. (2008) Histone Deacetylase 7 Promotes PML Sumoylation and Is Essential for PML Nuclear Body Formation. Mol Cell Biol 28: 5658-5667.
253. Fanelli M, Fantozzi A, De Luca P, Caprodossi S, Matsuzawa S, et al. (2004) The coiled-coil domain is the structural determinant for mammalian homologues of Drosophila sina-mediated degradation of promyelocytic leukemia protein and other tripartite motif proteins by the proteasome. Journal of Biological Chemistry 279: 5374-5379.
254. Hollstein M, Sidransky D, Vogelstein B, Harris CC (1991) P53 mutations in human cancers. Science 253: 49-53.
255. de Stanchina E (2004) PML is a direct p53 target that modulates p53 effector functions. Mol Cell 13: 523-535.
256. Buschbeck M, Uribesalgo I, Ledl A, Gutierrez A, Minucci S, et al. (2007) PML4 induces differentiation by Myc destabilization. Oncogene 26: 3415-3422.

257. Cairo S, De Falco F, Pizzo M, Salomoni P, Pandolfi PP, et al. (2005) PML interacts with Myc, and Myc target gene expression is altered in PML-null fibroblasts. Oncogene 24: 2195-2203.
258. Smith KP, Byron M, O'Connell BC, Tam R, Schorl C, et al. (2004) c-Myc localization within the nucleus: Evidence for association with the PML nuclear body. Journal of Cellular Biochemistry 93: 1282-1296.
259. Lin HK, Bergmann S, Pandolfi PP (2004) Cytoplasmic PML function in TGF-beta signalling. Nature 431: 205-211.
260. Gurrieri C (2004) Mutations of the PML tumor suppressor gene in acute promyelocytic leukemia. Blood 103: 2358-2362.
261. Fang WZ, Mori T, Cobrinik D (2002) Regulation of PML-dependent transcriptional repression by pRB and low penetrance pRB mutants. Oncogene 21: 5557-5565.
262. Khan MM, Nomura T, Kim H (2001) PML-RARalpha alleviates the transcriptional repression mediated by tumor suppressor Rb. J Biol Chem 276: 43491-43494.
263. Labbaye C, Valtieri M, Grignani F (1999) Expression and role of PML gene in normal adult hematopoiesis: functional interaction between PML and Rb proteins in erythropoiesis. Oncogene 18: 3529-3540.
264. Delaune A, Corbiere C, Benjelloun FD, Legrand E, Vannier JP, et al. (2008) Promyelocytic leukemia-nuclear body formation is an early event leading to retinoic acid-induced differentiation of neuroblastoma cells. Journal of Neurochemistry 104: 89-99.
265. Yu JH, Nakajima A, Nakajima H, Diller LR, Bloch KD, et al. (2004) Restoration of promyelocytic leukemia protein-nuclear bodies in neuroblastoma cells enhances retinoic acid responsiveness. Cancer Research 64: 928-933.
266. Khetchoumian K, Teletin M, Tisserand J, Herquel B, Ouararhni K, et al. (2008) Trim24 (Tif1 alpha) An essential 'brake' for retinoic acid-induced transcription to prevent liver cancer. Cell Cycle 7: 3647-3652.
267. Khetchoumian K, Teletin M, Tisserand J, Mark M, Herquel B, et al. (2007) Loss of Trim24 (Tif1 alpha) gene function confers oncogenic activity to retinoic acid receptor alpha. Nature Genetics 39: 1500-1506.
268. Allton K, Jain AK, Herz HM, Tsai WW, Jung SY, et al. (2009) Trim24 targets endogenous p53 for degradation. Proceedings of the National Academy of Sciences of the United States of America 106: 11612-11616.
269. Fraser RA, Heard DJ, Adam S, Lavigne AC, Le Douarin B, et al. (1998) The putative cofactor TIF1 alpha is a protein kinase that is hyperphosphorylated upon interaction with liganded nuclear receptors. Journal of Biological Chemistry 273: 16199-16204.
270. Yondola MA, Hearing P (2007) The adenovirus E4 ORF3 protein binds and reorganizes the TRIM family member transcriptional intermediary factor 1 alpha. Journal of Virology 81: 4264-4271.
271. Takahashi M, Ritz J, Cooper GM (1985) Activation of a novel human transforming gene, ret, by DNA rearrangement. Cell 42: 581-588.
272. Kato M, Takahashi M, Akhand AA, Liu W, Dai Y, et al. (1998) Transgenic mouse model for skin malignant melanoma. Oncogene 17: 1885-1888.
273. Kato T, Shimono Y, Hasegawa M, Jijiwa M, Enomoto A, et al. (2009) Characterization of the HDAC1 Complex That Regulates the Sensitivity of Cancer Cells to Oxidative Stress. Cancer Research 69: 3597-3604.

274. Tsukamoto H, Kato T, Enomoto A, Nakamura N, Shimono Y, et al. (2009) Expression of Ret finger protein correlates with outcomes in endometrial cancer. Cancer Science 100: 1895-1901.
275. Tezel G, Nagasaka T, Iwahashi N, Asai N, Iwashita T, et al. (1999) Different nuclear/cytoplasmic distributions of RET finger protein in different cell types. Pathology International 49: 881-886.
276. Townson SM, Kang KY, Lee AV, Oesterreich S (2006) Novel role of the RET finger protein in estrogen receptor-mediated transcription in MCF-7 cells. Biochemical and Biophysical Research Communications 349: 540-548.
277. Jacobs JJL, van Lohuizen M (2002) Polycomb repression: from cellular memory to cellular proliferation and cancer. Biochimica Et Biophysica Acta-Reviews on Cancer 1602: 151-161.
278. Henry J, Mather IH, McDermott MF, Pontarotti P (1998) B30.2-like domain proteins: update and new insights into a rapidly expanding family of proteins. Mol Biol Evol 15: 1696-1705.
279. Krutzfeldt M, Ellis M, Weekes DB, Bull JJ, Eilers M, et al. (2005) Selective ablation of retinoblastoma protein function by the RET finger protein. Molecular Cell 18: 213-224.
280. Friedman JR, Fredericks WJ, Jensen DE, Speicher DW, Huang XP, et al. (1996) KAP-1, a novel corepressor for the highly conserved KRAB repression domain. Genes & Development 10: 2067-2078.
281. Kim S-S, Chen Y-M, Oâ€™Leary E, Witzgall R, Vidal M, et al. (1996) A novel member of the RING finger family, KRIP-1, associates with the KRAB-A transcriptional repressor domain of zinc fingerâ€‰proteins. Proceedings of the National Academy of Sciences 93: 15299-15304.
282. Cammas F, Mark M, Dolle P, Dierich A, Chambon P, et al. (2000) Mice lacking the transcriptional corepressor TIF1 beta are defective in early postimplantation development. Development 127: 2955-2963.
283. Yokoe T (2010) KAP1 is associated with peritoneal carcinomatosis in gastric cancer. Ann Surg Oncol 17: 821-828.
284. Kijanka G, Hector S, Kay EW, Murray F, Cummins R, et al. (2010) Human IgG antibody profiles differentiate between symptomatic patients with and without colorectal cancer. Gut 59: 69-78.
285. Ho J, Kong J-W-F, Choong L-Y, Loh M-C-S, Toy W, et al. (2009) Novel Breast Cancer Metastasis-Associated Proteins. Journal of Proteome Research 8: 583-594.
286. Underhill C, Qutob MS, Yee S-P, Torchia J (2000) A Novel Nuclear Receptor Corepressor Complex, N-CoR, Contains Components of the Mammalian SWI/SNF Complex and the Corepressor KAP-1. Journal of Biological Chemistry 275: 40463-40470.
287. Schultz DC, Friedman JR, Rauscher FJ (2001) Targeting histone deacetylase complexes via KRAB-zinc finger proteins: the PHD and bromodomains of KAP-1 form a cooperative unit that recruits a novel isoform of the Mi-2 alpha subunit of NuRD. Genes & Development 15: 428-443.
288. Schultz DC, Ayyanathan K, Negorev D, Maul GG, Rauscher FJ (2002) SETDB1: a novel KAP-1-associated histone H3, lysine 9-specific methyltransferase that contributes to HP1-mediated silencing of euchromatic genes by KRAB zinc-finger proteins. Genes & Development 16: 919-932.

289. Le Douarin B (1996) A possible involvement of TIF1 [alpha] and TIF1 [beta] in the epigenetic control of transcription by nuclear receptors. EMBO J 15: 6701-6715.
290. Wang C, Rauscher FJ, Cress WD, Chen J (2007) Regulation of E2F1 Function by the Nuclear Corepressor KAP1. Journal of Biological Chemistry 282: 29902-29909.
291. Okamoto K, Kitabayashi I, Taya Y (2006) KAP1 dictates p53 response induced by chemotherapeutic agents via Mdm2 interaction. Biochemical and Biophysical Research Communications 351: 216-222.
292. Satou A, Taira T, Iguchi-Ariga SMM, Ariga H (2001) A novel transrepression pathway of c-Myc. Recruitment of a transcriptional corepressor complex to c-Myc by MM-1, a c-Myc-binding protein. Journal of Biological Chemistry 276: 46562-46567.
293. Tsuruma R, Ohbayashi N, Kamitani S, Ikeda O, Sato N, et al. (2007) Physical and functional interactions between STAT3 and KAP1. Oncogene 27: 3054-3059.
294. Kamitani S, Ohbayashi N, Ikeda O, Togi S, Muromoto R, et al. (2008) KAP1 regulates type I interferon/STAT1-mediated IRF-1 gene expression. Biochemical and Biophysical Research Communications 370: 366-370.
295. Levy DE, Lee C-k (2002) What does Stat3 do? The Journal of Clinical Investigation 109: 1143-1148.
296. White DE, Negorev D, Peng H, Ivanov AV, Maul GG, et al. (2006) KAP1, a Novel Substrate for PIKK Family Members, Colocalizes with Numerous Damage Response Factors at DNA Lesions. Cancer Research 66: 11594-11599.
297. Noon AT, Shibata A, Rief N, Lobrich M, Stewart GS, et al. (2010) 53BP1-dependent robust localized KAP-1 phosphorylation is essential for heterochromatic DNA double-strand break repair. Nat Cell Biol 12: 177-184.
298. Hu G, Kim J, Xu QK, Leng YM, Orkin SH, et al. (2009) A genome-wide RNAi screen identifies a new transcriptional module required for self-renewal. Genes & Development 23: 837-848.
299. Seki Y, Kurisaki A, Watanabe-Susaki K, Nakajima Y, Nakanishi M, et al. (2010) TIF1 beta regulates the pluripotency of embryonic stem cells in a phosphorylation-dependent manner. Proceedings of the National Academy of Sciences of the United States of America 107: 10926-10931.
300. Kapp LN, Painter RB, Yu LC, Vanloon N, Richard CW, et al. (1992) CLONING OF A CANDIDATE GENE FOR ATAXIA-TELANGIECTASIA GROUP-D. American Journal of Human Genetics 51: 45-54.
301. Hosoi Y, Kapp LN (1994) Expression of a candidate ataxia-telangiectasia group-D gene in cultured fibroblast cell-lines and human tissues. International Journal of Radiation Biology 66: S71-S76.
302. Kosaka Y, Inoue H, Ohmachi T, Yokoe T, Matsumoto T, et al. (2007) Tripartite motif-containing 29 (TRIM29) is a novel marker for lymph node metastasis in gastric cancer. Annals of Surgical Oncology 14: 2543-2549.
303. Siewert JR, Bottcher K, Stein HJ, Roder JD, German Gastric Carcinoma Study G (1998) Relevant prognostic factors in gastric cancer - Ten-year results of the German Gastric Cancer Study. Annals of Surgery 228: 449-459.
304. Utsunomiya T, Inoue H, Taguchi KI, Shimada M, Sugimachi K, et al. (2002) G protein gamma 7 expression as a new clinicopathological marker in patients with intrahepatic cholangiocarcinoma. Archives of Surgery 137: 181-185.
305. Brzoska PM, Chen H, Zhu Y, Levin NA, Disatnik MH, et al. (1995) The product of the ataxia-telangiectasia group D complementing gene, ATDC, interacts with

a protein kinase C substrate and inhibitor. Proceedings of the National Academy of Sciences 92: 7824-7828.
306. Domagala W, Striker G, Szadowska A, Dukowicz A, Harezga B, et al. (1994) p53 protein and vimentin m invasive ductal NOS breast carcinoma-relationship with survival and sites of metastases. European Journal of Cancer 30: 1527-1534.
307. Li D, Xie K, Wolff R, Abbruzzese JL (2004) Pancreatic cancer. The Lancet 363: 1049-1057.
308. Logsdon CD, Simeone DM, Binkley C, Arumugam T, Greenson JK, et al. (2003) Molecular profiling of pancreatic adenocarcinoma and chronic pancreatitis identifies multiple genes differentially regulated in pancreatic cancer (vol 63, pg 2649, 2003). Cancer Research 63: 3445-3445.
309. Wang L, Heidt DG, Lee CJ, Yang H, Logsdon CD, et al. (2009) Oncogenic Function of ATDC in Pancreatic Cancer through Wnt Pathway Activation and [beta]-Catenin Stabilization. Cancer Cell 15: 207-219.
310. Yuan ZG, Villagra A, Peng LR, Coppola D, Glozak M, et al. (2010) The ATDC (TRIM29) Protein Binds p53 and Antagonizes p53-Mediated Functions. Molecular and Cellular Biology 30: 3004-3015.
311. Bertrand-Vallery V, Belot N, Dieu M, Delaive E, Ninane N, et al. (2010) Proteomic Profiling of Human Keratinocytes Undergoing UVB-Induced Alternative Differentiation Reveals TRIpartite Motif Protein 29 as a Survival Factor. PLoS ONE 5: e10462.
312. Hosoi Y, Kapp LN, Murnane JP, Matsumoto Y, Enomoto A, et al. (2006) Suppression of anchorage-independent growth by expression of the ataxia-telangiectasia group D complementing gene, ATDC. Biochemical and Biophysical Research Communications 348: 728-734.
313. Orimo A, Inoue S, Minowa O, Tominaga N, Tomioka Y, et al. (1999) Underdeveloped uterus and reduced estrogen responsiveness in mice with disruption of the estrogen-responsive finger protein gene, which is a direct target of estrogen receptor Î±. Proceedings of the National Academy of Sciences 96: 12027-12032.
314. Orimo A, Inoue S, Ikeda K, Noji S, Muramatsu M (1995) Molecular Cloning, Structure, and Expression of Mouse Estrogen-responsive Finger Protein Efp. Journal of Biological Chemistry 270: 24406-24413.
315. Ikeda K, Orimo A, Higashi Y, Muramatsu M, Inoue S (2000) Efp as a primary estrogen-responsive gene in human breast cancer. FEBS Letters 472: 9-13.
316. Suzuki T, Urano T, Tsukui T, Horie-Inoue K, Moriya T, et al. (2005) Estrogen-Responsive Finger Protein as a New Potential Biomarker for Breast Cancer. Clinical Cancer Research 11: 6148-6154.
317. Ueyama K, Ikeda K, Sato W, Nakasato N, Horie-Inoue K, et al. (2010) Knockdown of Efp by DNA-modified small interfering RNA inhibits breast cancer cell proliferation and in vivo tumor growth. Cancer Gene Ther 17: 624-632.
318. Horie K, Urano T, Ikeda K, Inoue S (2003) Estrogen-responsive RING finger protein controls breast cancer growth. The Journal of Steroid Biochemistry and Molecular Biology 85: 101-104.
319. Urano T, Saito T, Tsukui T, Fujita M, Hosoi T, et al. (2002) Efp targets 14-3-3[sigma] for proteolysis and promotes breast tumour growth. Nature 417: 871-875.

320. Nakasato N, Ikeda K, Urano T, Horie-Inoue K, Takeda S, et al. (2006) A ubiquitin E3 ligase Efp is up-regulated by interferons and conjugated with ISG15. Biochemical and Biophysical Research Communications 351: 540-546.
321. Harada H, Harada Y, O'Brien DP, Rice DS, Naeve CW, et al. (1999) HERF1, a novel hematopoiesis-specific RING finger protein, is required for terminal differentiation of erythroid cells. Molecular and Cellular Biology 19: 3808-3815.
322. Blaybel R, Tholeyre O, Douablin A, Baklouti F (2008) Downregulation of the Spi-1/PU.1 oncogene induces the expression of TRIM10/HERF1, a key factor required for terminal erythroid cell differentiation and survival. Cell Research 18: 834-845.
323. Dokmanovic M, Chang BD, Fang J, Roninson IB (2002) Retinoid-induced growth arrest of breast carcinoma cells involves co-activation of multiple growth-inhibitory genes. Cancer Biology & Therapy 1: 24-27.
324. Sugiura T, Miyamoto K (2008) Characterization of TRIM31, Upregulated in Gastric Adenocarcinoma, as a Novel RBCC Protein. Journal of Cellular Biochemistry 105: 1081-1091.
325. Lalonde JP, Lim R, Ingley E, Tilbrook PA, Thompson MJ, et al. (2004) HLS5, a novel RBCC (ring finger, B box, coiled-coil) family member isolated from a hemopoietic lineage switch, is a candidate tumor suppressor. Journal of Biological Chemistry 279: 8181-8189.
326. Endersby R, Majewski IJ, Winteringham L, Beaumont JG, Samuels A, et al. (2008) Hls5 regulated erythroid differentiation by modulating GATA-1 activity. Blood 111: 1946-1950.
327. Balint I, Müller A, Nagy A, Kovacs G (2004) Cloning and characterisation of the RBCC728/TRIM36 zinc-binding protein from the tumor suppressor gene region at chromosome 5q22.3. Gene 332: 45-50.
328. Miyajima N, Maruyama S, Nonomura K, Hatakeyama S (2009) TRIM36 interacts with the kinetochore protein CENP-H and delays cell cycle progression. Biochemical and Biophysical Research Communications 381: 383-387.
329. Liu H-LC, Golder-Novoselsky E, Seto MH, Webster L, McClary J, et al. (1998) The Novel Estrogen-Responsive B Box Protein (EBBP) Gene Is Tamoxifen Regulated in Cells Expressing an Estrogen Receptor DNA-Binding Domain Mutant. Mol Endocrinol 12: 1733-1748.
330. Beer HD, Munding C, Dubois N, Mamie C, Hohl D, et al. (2002) The estrogen-responsive B box protein - A novel regulator of keratinocyte differentiation. Journal of Biological Chemistry 277: 20740-20749.
331. Marshall GM, Bell JL, Koach J, Tan O, Kim P, et al. (2010) TRIM16 acts as a tumour suppressor by inhibitory effects on cytoplasmic vimentin and nuclear E2F1 in neuroblastoma cells. Oncogene 29: 6172-6183.
332. Munding C, Keller M, Niklaus G, Papin S, Tschopp J, et al. (2006) The estrogen-responsive B box protein: a novel enhancer of interleukin-1 beta secretion. Cell Death and Differentiation 13: 1938-1949.
333. Uhlén M, Björling E, Agaton C, Szigyarto CA-K, Amini B, et al. (2005) A Human Protein Atlas for Normal and Cancer Tissues Based on Antibody Proteomics. Molecular & Cellular Proteomics 4: 1920-1932.
334. Borriello A, Della Pietra V, Criscuolo M, Oliva A, Tonini GP, et al. (2000) p27(Kip1) accumulation is associated with retinoic-induced neuroblastoma differentiation: evidence of a decreased proteasome-dependent degradation. Oncogene 19: 51-60.

335. Loedige I, Filipowicz W (2009) TRIM-NHL Proteins Take on miRNA Regulation. Cell 136: 818-820.
336. Hammell CM, Lubin I, Boag PR, Blackwell TK, Ambros V (2009) nhl-2 Modulates MicroRNA Activity in Caenorhabditis elegans. Cell 136: 926-938.
337. Schwamborn JC, Berezikov E, Knoblich JA (2009) The TRIM-NHL Protein TRIM32 Activates MicroRNAs and Prevents Self-Renewal in Mouse Neural Progenitors. Cell 136: 913-925.
338. Geran R, Greenberg N, Macdonald M, Schumacher A, Abbott B (1972) Protocols for screening chemical agents and natural products against tumors and other biological systems. Cancer Chemotherapy Reports 3: 47-57.
339. Nelson JSR, Carpenter RE, Parker RG (1975) Response of mouse skin and C3HBA mammary-carcinoma of C3H mouse to X-rays and cyclotron neutrons – effect of mixed neutron-photon fractionation schemes. European Journal of Cancer 11: 891-901.
340. Burkhart CA, Cheng AJ, Madafiglio J, Kavallaris M, Mili M, et al. (2003) Effects of MYCN Antisense Oligonucleotide Administration on Tumorigenesis in a Murine Model of Neuroblastoma. Journal of the National Cancer Institute 95: 1394-1403.
341. Dellaire G, Bazett-Jones DP (2004) PML nuclear bodies: dynamic sensors of DNA damage and cellular stress. Bioessays 26: 963-977.
342. Khan MM, Nomura T, Kim H, Kaul SC, Wadhwa R, et al. (2001) PML-RAR alpha alleviates the transcriptional repression mediated by tumor suppressor Rb. Journal of Biological Chemistry 276: 43491-43494.
343. Cutts SM, Nudelman A, Rephaeli A, Phillips DR (2005) The power and potential of doxorubicin-DNA adducts. Iubmb Life 57: 73-81.
344. Lobert S, Vulevic B, Correia JJ (1996) Interaction of vinca alkaloids with tubulin: A comparison of vinblastine, vincristine, and vinorelbine. Biochemistry 35: 6806-6814.
345. Chu G (1994) Cellular-responses to cisplatin – the roles of DNA-binding proteins and DNA-repair. Journal of Biological Chemistry 269: 787-790.
346. Mu ZM, Chin KV, Liu JH, Lozano G, Chang KS (1994) PML, a growth suppressor disrupted in acute Promyelocytic leukemia. Molecular and Cellular Biology 14: 6858-6867.
347. Walton JD, Kattan DR, Thomas SK, Spengler BA, Guo HF, et al. (2004) Characteristics of stem cells from human neuroblastoma cell lines and in tumors. Neoplasia 6: 838-845.
348. Rettig WJ, Spengler BA, Chesa PG, Old LJ, Biedler JL (1987) Coordinate changes in neuronal phenotype and surface-antigen expression in human neuroblastoma cell variants. Cancer Research 47: 1383-1389.
349. Marshall GM, Cheung B, Stacey KP, Camacho ML, Simpson AM, et al. (1995) Increased retinoic acid receptor-gamma expression supresses the malignant phenotype and alters the differentiation potential of human neuroblastoma-cells. Oncogene 11: 485-491.
350. Gilbert SF (2000) Developmental biology: Sinauer Associates.
351. Kobayashi M, Taniura H, Yoshikawa K (2002) Ectopic Expression of Necdin Induces Differentiation of Mouse Neuroblastoma Cells. Journal of Biological Chemistry 277: 42128-42135.
352. Hsu SL, Hsu JW, Liu MC, Chen LY, Chang CD (2000) Retinoic acid-mediated G1 arrest is associated with induction of p27(Kip1) and inhibition of cyclin-

dependent kinase 3 in human lung squamous carcinoma CH27 cells. Experimental Cell Research 258: 322-331.
353. Mu ZM, Le XF, Vallian S, Glassman AB, Chang KS (1997) Stable overexpression of PML alters regulation of cell cycle progression in HeLa cells. Carcinogenesis 18: 2063-2069.
354. Sabile A, Meyer AM, Wirbelauer C, Hess D, Kogel U, et al. (2006) Regulation of p27 Degradation and S-Phase Progression by Ro52 RING Finger Protein. Molecular and Cellular Biology 26: 5994-6004.
355. Watanabe G, Albanese C, Lee RJ, Reutens A, Vairo G, et al. (1998) Inhibition of Cyclin D1 Kinase Activity Is Associated with E2F-Mediated Inhibition of Cyclin D1 Promoter Activity through E2F and Sp1. Mol Cell Biol 18: 3212-3222.
356. Goto T, Mitsuhashi T, Takahashi T (2004) Altered patterns of neuron production in the p27 knockout mouse. Developmental neuroscience 26: 208-217.
357. Qin XQ, Barsoum J (1997) Differential cell cycle effects induced by E2F1 mutants. Oncogene 14: 53-62.
358. Gebauer S, Lu AL, Omura-Minamisawa M, Batova A, Diccianni MB (2004) Expression profiles and clinical relationships of ID2, CDKNIB, and CDKN2A in primary neuroblastoma. Genes Chromosomes & Cancer 41: 297-308.
359. Cheung BB, Koach J, Tan O, Kim P, Bell JL, et al. (2011) The retinoid signalling molecule, TRIM16, is repressed during squamous cell carcinoma skin carcinogenesis in vivo and reduces skin cancer cell migration in vitro. Journal of Pathology 226: 451-462.
360. Niu MY, Menard M, Reed JC, Krajewski S, Pratt MAC (2001) Ectopic expression of cyclin D1 amplifies a retinoic acid-induced mitochondrial death pathway in breast cancer cells. Oncogene 20: 3506-3518.
361. Gillett C, Fantl V, Smith R, Fisher C, Bartek J, et al. (1994) Amplification and Overexpression of Cyclin D1 in Breast Cancer Detected by Immunohistochemical Staining. Cancer Research 54: 1812-1817.
362. Watanabe G, Albanese C, Lee RJ, Reutens A, Vairo G, et al. (1998) Inhibition of cyclin D1 kinase activity is associated with E2F-mediated inhibition of cyclin D1 promoter activity through E2F and Sp1. Molecular and Cellular Biology 18: 3212-3222.
363. Mateyak MK, Obaya AJ, Sedivy JM (1999) c-Myc Regulates Cyclin D-Cdk4 and -Cdk6 Activity but Affects Cell Cycle Progression at Multiple Independent Points. Molecular and Cellular Biology 19: 4672-4683.
364. Massiah MA, Matts JAB, Short KM, Simmons BN, Singireddy S, et al. (2007) Solution Structure of the MID1 B-box2 CHC(D/C)C2H2 Zinc-binding Domain: Insights into an Evolutionarily Conserved RING Fold. Journal of Molecular Biology 369: 1-10.
365. Massiah MA, Simmons BN, Short KM, Cox TC (2006) Solution Structure of the RBCC/TRIM B-box1 Domain of Human MID1: B-box with a RING. Journal of Molecular Biology 358: 532-545.
366. Chu Y, Yang X (*2011*) SUMO E3 ligase activity of TRIM proteins

Oncogene 30: 1108-1116.
367. Han XF, Du HJ, Massiah MA (2011) Detection and Characterization of the In Vitro E3 Ligase Activity of the Human MID1 Protein. Journal of Molecular Biology 407: 505-520.

368. Zhong S (1999) A RA-dependent, tumour-growth suppressive transcription complex is the target of the PML-RAR[alpha] and T18 oncoproteins. Nature Genet 23: 287-295.
369. Stommel JM, Marchenko ND, Jimenez GS, Moll UM, Hope TJ, et al. (1999) A leucine-rich nuclear export signal in the p53 tetramerization domain: regulation of subcellular localization and p53 activity by NES masking. Embo Journal 18: 1660-1672.
370. la Cour T, Gupta R, Rapacki K, Skriver K, Poulsen FM, et al. (2003) NESbase version 1.0: a database of nuclear export signals. Nucleic Acids Research 31: 393-396.
371. Robbins J, Dilworth SM, Laskey RA, Dingwall C (1991) 2 interdependent basic domain in nucleoplasmin nuclear targeting sequence – identification of a class of bipartite nuclear targeting sequence. Cell 64: 615-623.
372. Hurley JH, Lee S, Prag G (2006) Ubiquitin-binding domains. Biochemical Journal 399: 361-372.
373. Aranda-Orgilles B, Aigner J, Kunath M, Lurz R, Schneider R, et al. (2008) Active Transport of the Ubiquitin Ligase MID1 along the Microtubules Is Regulated by Protein Phosphatase 2A. PLoS ONE 3.
374. Hill CS (2009) Nucleocytoplasmic shuttling of Smad proteins. Cell Res 19: 36-46.
375. Jensen K, Shiels C, Freemont PS (2001) PML protein isoforms and the RBCC/TRIM motif. Oncogene 20: 7223-7233.

APPENDICES

Appendix I: Domain mutant localisation

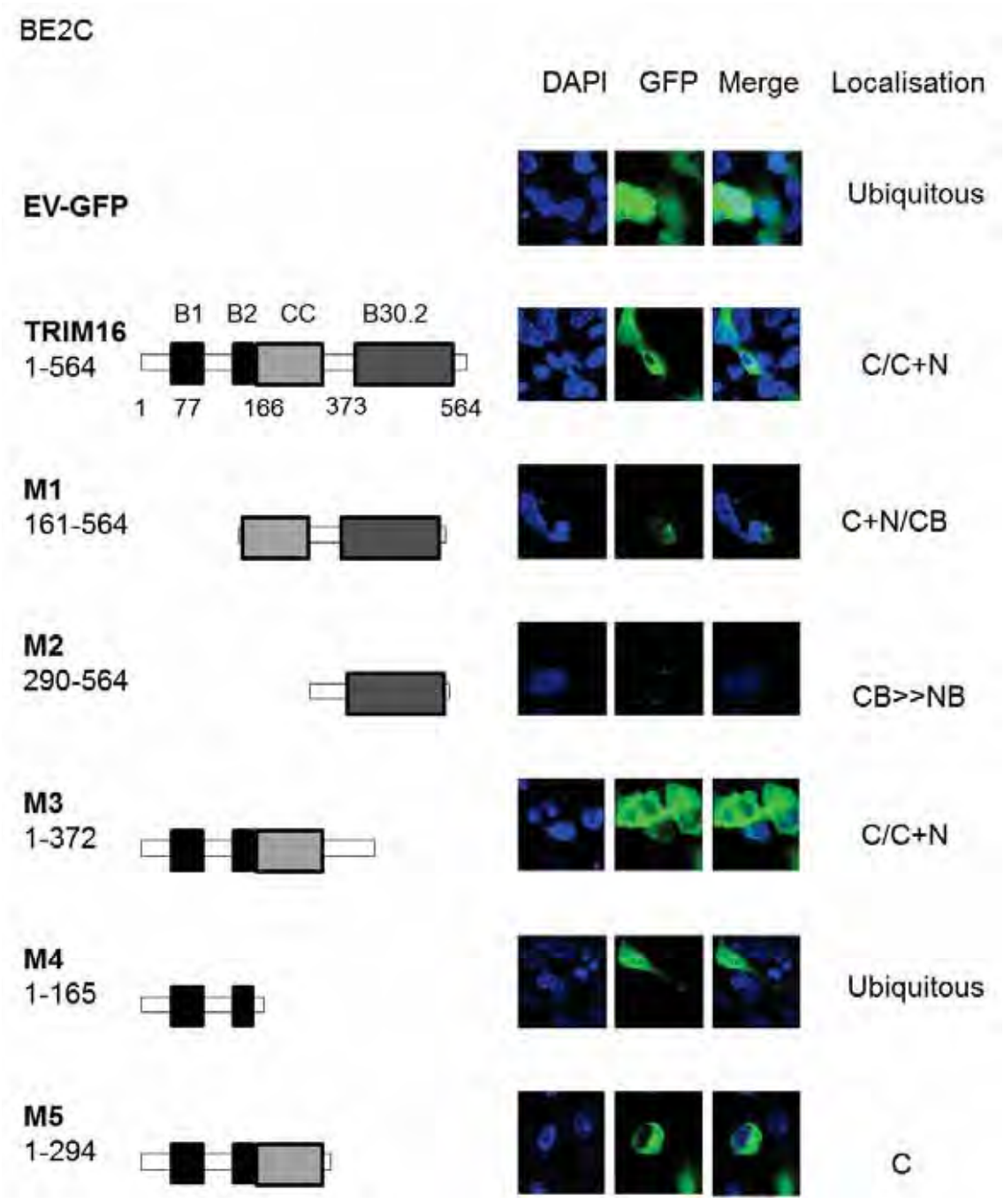

TRIM16-GFP deletion domain mutants expressed in BE2C cells, 200X confocal images. C=Cytoplasmic, N=Nuclear, B=Body, > = more than

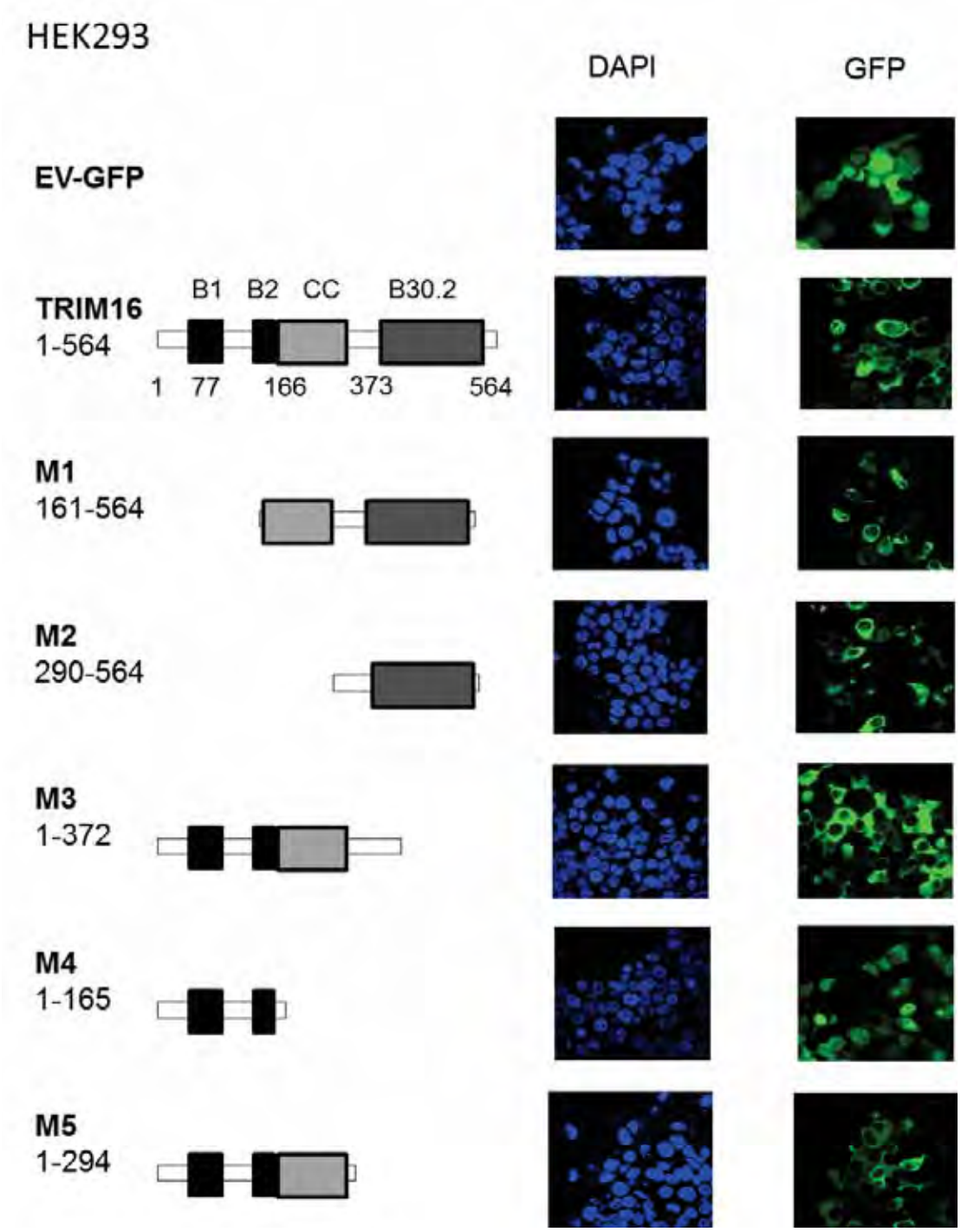

TRIM16-GFP deletion domain mutants expressed in HEK293 cells, 100X confocal images. Localisation is mostly cytoplasmic for all mutants, except M4 and EV are ubiquitous.

Appendix II: Localisation mutant validation by sequencing

Images shown are screen captures from the freeware version of Mutational Surveyor 3.97V-Demo (Soft Genetics, USA). Arrows highlight the successful amino acid sequence mutation compared to wildtype plasmid DNA. The clone is the bacterial clone chosen for sequencing and subsequent DNA production for transfection into mammalian cells.

ΔNES-Clone 1.2

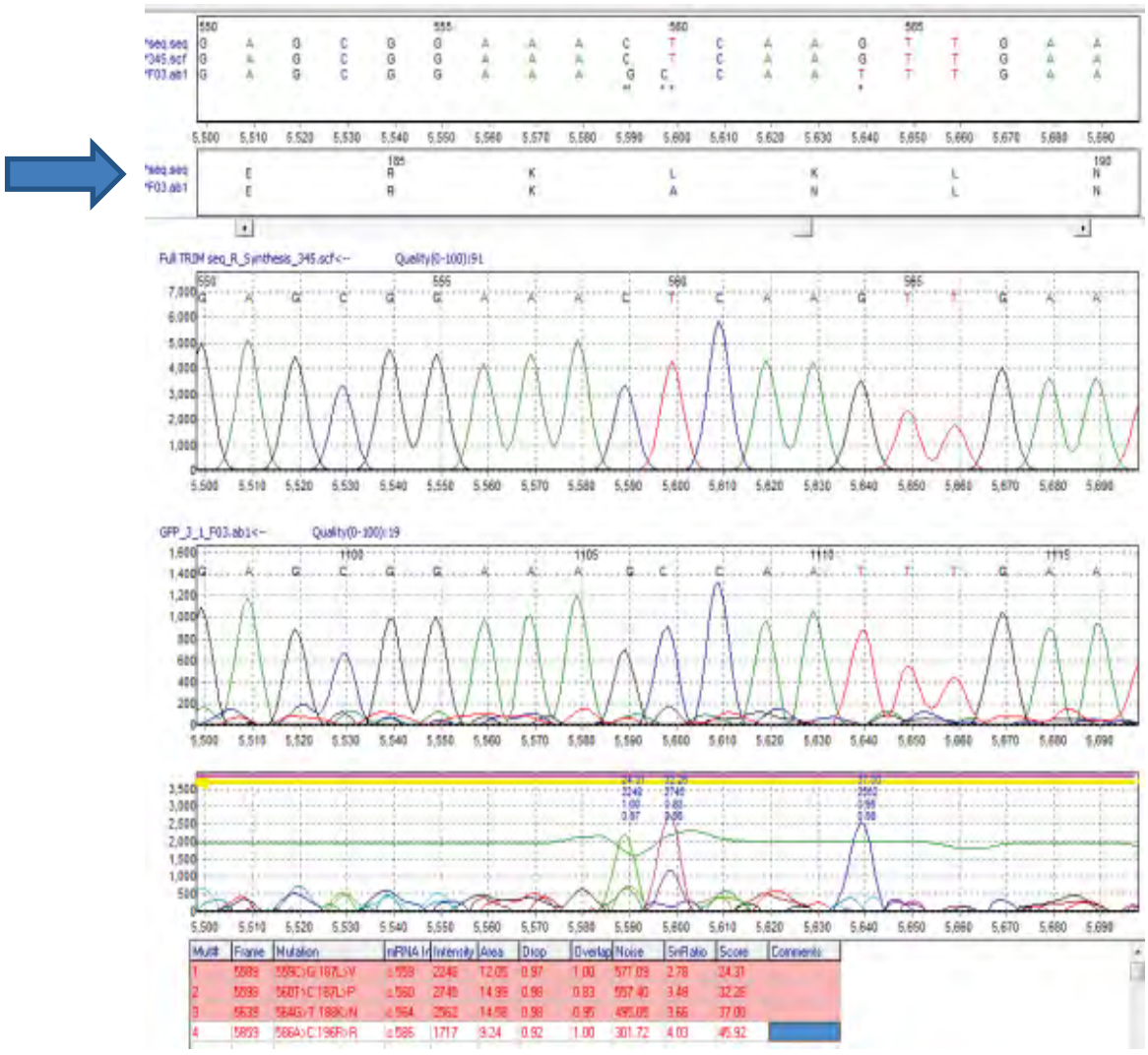

ΔNLSa–Clone 2.8

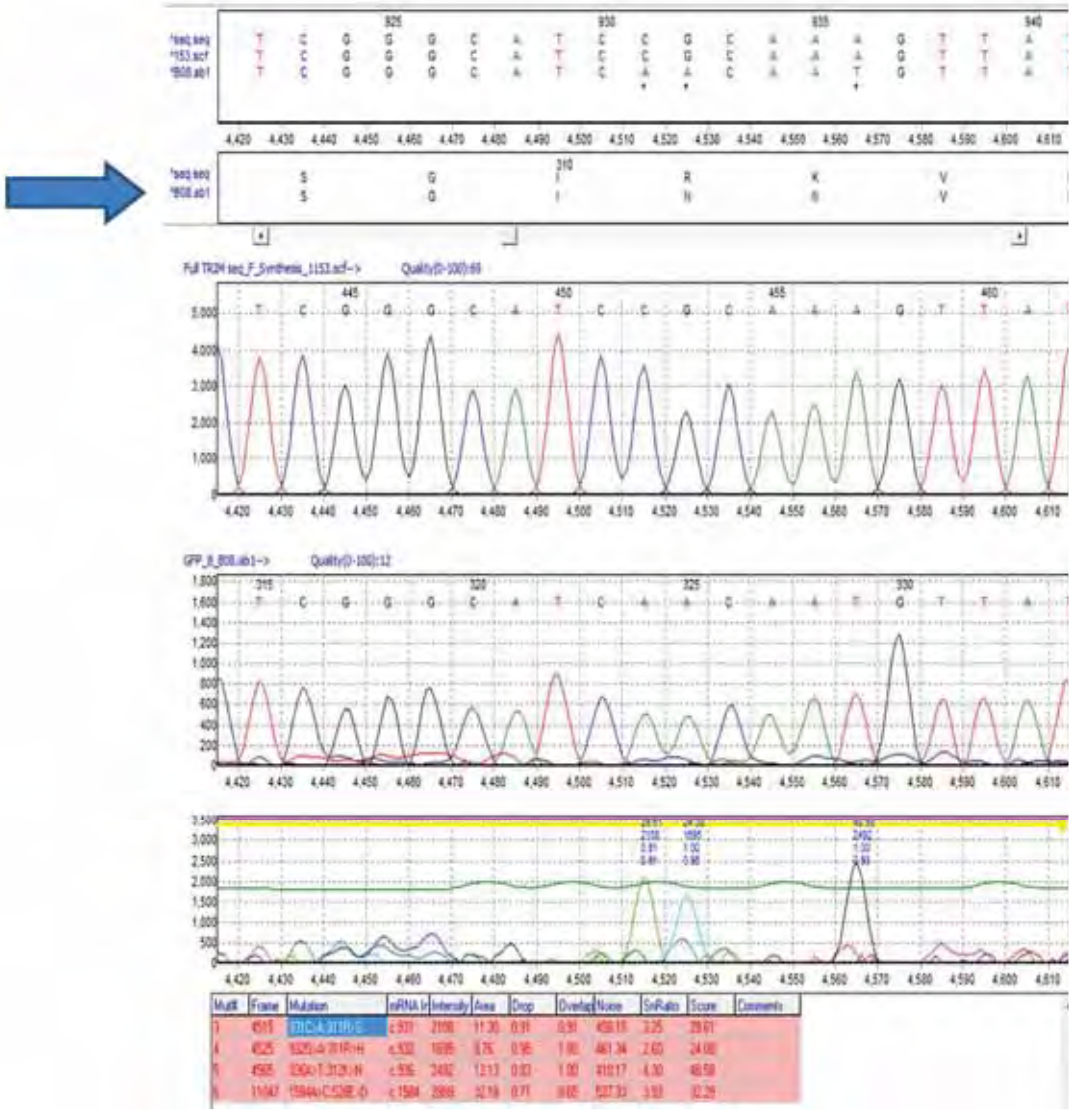

ΔNRBM–Clone 3.3

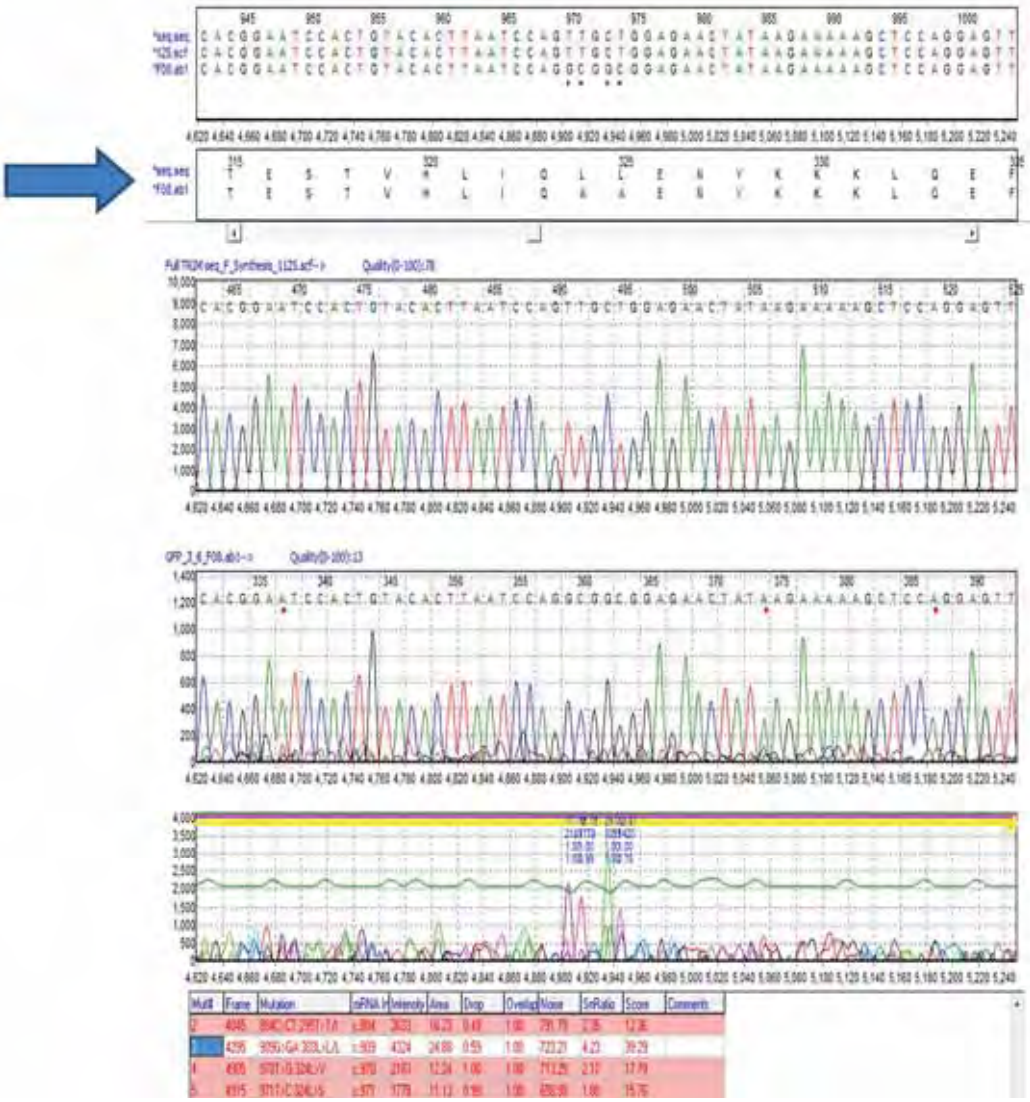

ΔNLSb–Clone 4.1

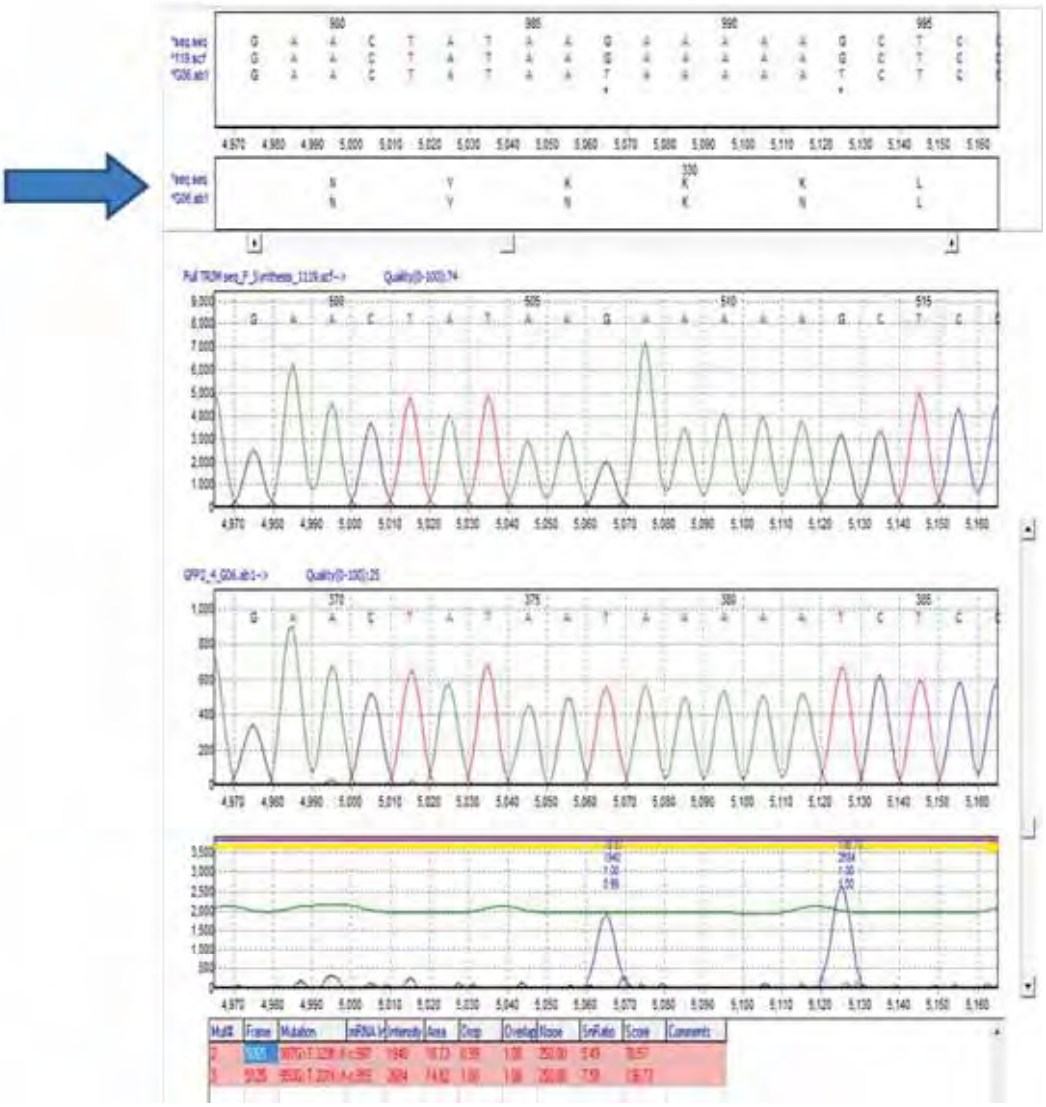

ΔSUMO–Clone 5.3

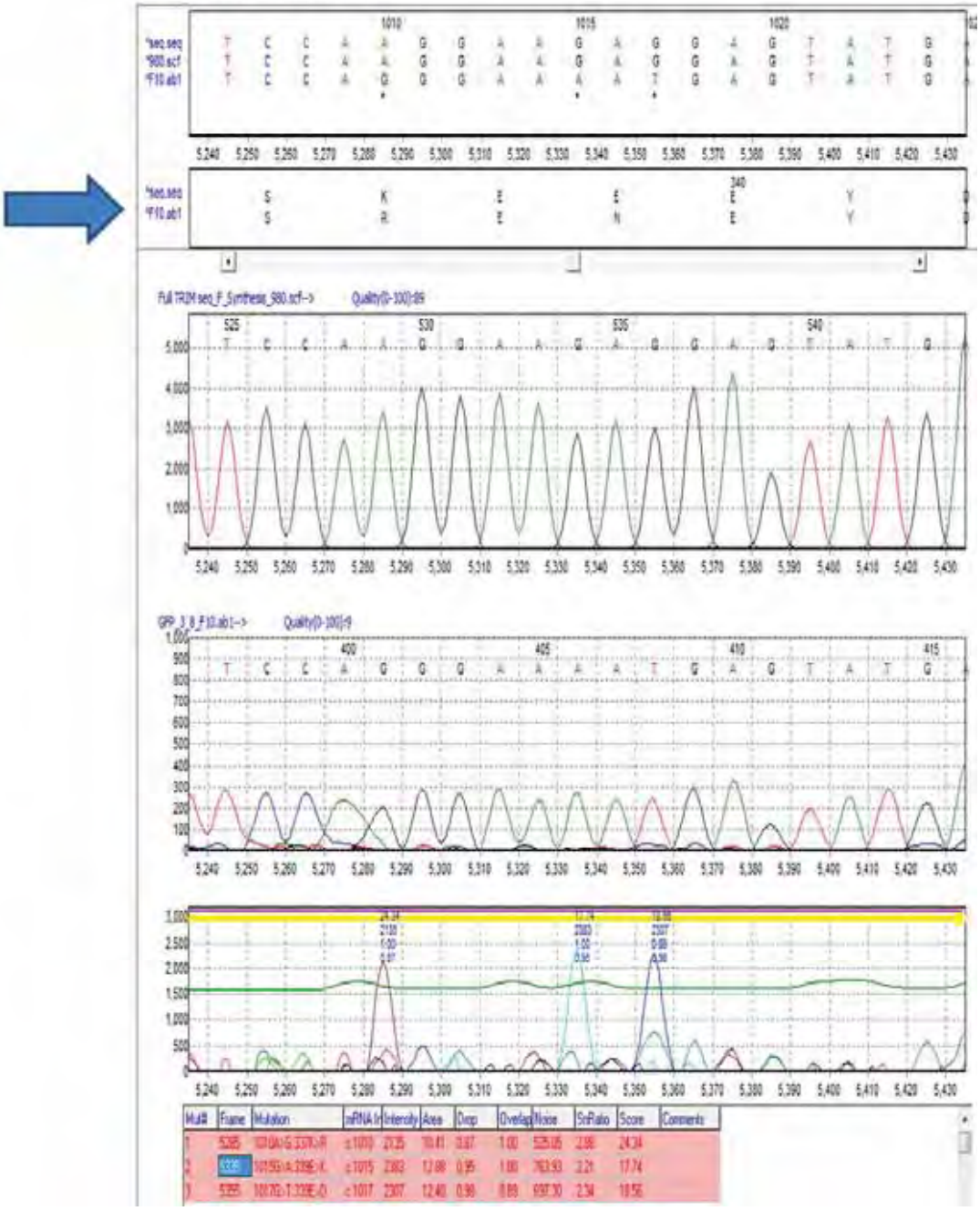

This is not the end, it’s just the beginning.